Metabolic engineering strategies for an increased PHB production in cyanobacteria

Dissertation

der Mathematisch-Naturwissenschaftlichen Fakultät

der Eberhard Karls Universität Tübingen

zur Erlangung des Grades eines

Doktors der Naturwissenschaften

(Dr. rer. nat.)

vorgelegt von

Moritz Koch

aus Bergisch Gladbach

Tübingen

2020

Gedruckt mit Genehmigung der Mathematisch-Naturwissenschaftlichen Fakultät der Eberhard Karls Universität Tübingen.

Tag der mündlichen Qualifikation: 16.09.2020

Dekan (stellvertretend):	Prof. Dr. Jozsef Fortagh
1. Berichterstatter:	Prof. Dr. Karl Forchhammer
2. Berichterstatter:	Prof. Dr. Dieter Jendrossek

Erklärung

Ich erkläre hiermit, dass ich die zur Promotion eingereichte Arbeit selbständig verfasst, nur die angegebenen Quellen und Hilfsmittel benutzt und Stellen, die wörtlich oder inhaltlich nach den Werken anderer Autoren entnommen sind, als solche gekennzeichnet habe. Eine detaillierte Abgrenzung meiner eigenen Leistungen von den Beiträgen meiner Kooperationspartner habe ich in „Declaration of author contribution" vorgenommen.

Tübingen, den _____

"If it is in our power to prevent something bad from happening, without thereby sacrificing anything of comparable moral importance, we ought, morally, to do it."

— Peter Singer

Table of contents

I. Abbreviations

I. Abbreviations

2-OG	2-oxoglutarate
3-PGA	3-phosphoglycerate
AC	Adenylate cyclase
ACC	Acetyl-CoA carboxylase
ADP	Adenosine diphosphate
AMP	Adenosine monophosphate
ATP	Adenosine triphosphate
BCCP	Biotin carboxyl carrier protein
BSA	Bovine serum albumin
CA	Carbonic anhydrase
cAMP	Cyclic AMP
CBB	Calvin–Benson–Bassham
CCM	CO_2-concentrating-mechanism
CDW	Cell dry weight
CoA	Coenzyme-A
ED	Entner-Doudoroff
EMP	Embden-Meyerhof-Parnas
FACS	fluorescence-activated cell sorting
FC	Flow cytometry
Gen	Gentamycine
GDH	Glutamate dehydrogenase
GOGAT	Glutamine 2-oxoglutarate aminotransferase
GS	Glutamine synthetase
h	hour
kDa	Kilo dalton
Kan	Kanamycine
LED	Light-emitting diode
MDA	Malondialdehyde
min	Minute
ml	Mililiter
NADPH	Nicotinamide adenine dinucleotide phosphate
NAGK	*N*-acetylglutamate kinase
OD_{750}	Optical density at 750nm
ORF	Open reading frame
PBS	Phosphate buffered saline
Pgam	Phosphoglyceratmutase
PHA	Polyhydroxyalkanoates
PHB	Poly-β-hydroxybutyrate
PPT1	PHB Prodcuer Tübingen 1
PTS	Phosphotransferase system
PS I	Photosystem I
PS II	Photosystem II
ROS	Reactive oxygen species
RubisCO	Ribulose-1,5-bisphosphate carboxylase/oxygenase
SDS	sodium-dodecylsulfate
TCA	Tricarboxylic acid
TEM	Transmission electron microscopy
V_{max}	Maximum reaction rate
w/v	Weight per volume
w/w	Weight per weight

II. Summary

Cyanobacteria constitute one of Earth's oldest and most diverse bacterial phyla. Due to their expansion all around the globe they are strongly influencing global carbon and nitrogen cycles. Although cyanobacteria are so important for the maintenance of these global cycles, many aspects of their metabolism are still poorly understood. One example is the metabolism of polyhydroxybutyrate (PHB), which is produced in many cyanobacteria like the model organism *Synechocystis* sp. PCC 6803. This intracellular biopolymer is mainly produced under conditions of nitrogen starvation when *Synechocystis* undergoes a transformation into a resting state termed chlorosis. However, the physiological function of PHB as well as corresponding factors influencing its biosynthesis are mostly unknown. In the present work, all these questions were investigated and comprehensively discussed.

To investigate the physiological function of PHB, a *Synechocystis* wildtype was compared to a PHB-free mutant strain. We could show that in *Synechocystis*, unlike in other bacteria, PHB is not used as a carbon storage and is furthermore not required for resuscitation from chlorosis. Factors influencing the formation of PHB are the aeration as well as the illumination regime, with more PHB being formed during day/night rhythm (compared to continuous light) and with high gas exchange in the culture. Interestingly, we could show that PHB is not degraded after resuscitation but is instead only disaggregated to smaller granules and distributed among dividing cells.

In other organisms, a variety of different proteins are involved in the PHB metabolism, including the formation, the maintenance as well as the degradation of the PHB granules. In this work we investigated several proteins, which are putatively involved in the PHB metabolism and discovered the novel regulator Slr0058, which is affecting the number and size of PHB granules. Different carbon pathways were analyzed for their impact on the PHB production, where the Embden Meyerhof Parnas pathway turned out to be the most important one. To analyze, where the carbon required for the formation of PHB is derived from, several knockout strains were analyzed for their ability to produce PHB. Whenever glycogen metabolism was disturbed, it negatively influenced the accumulation of PHB, indicating a direct link between both carbon-polymers. The carbon flux between both polymers was shown to be influenced by the protein Sll0944. This regulator is highly upregulated during chlorosis and inhibits the phosphoglycerate mutase, whereby it regulates the glycogen catabolism.

Since PHB exhibits similar material properties to polypropylene, PHB is often considered as a biobased and biodegradable plastic substitute, which is of high biotechnological interest. The ability of a Δ*sll0944* mutant strain to rapidly degrade glycogen was exploited to create a PHB overproduction strain. To achieve this, PHB biosynthesis genes were overexpressed in a Δ*sll0944* background to create the strain PPT1, which produced the highest rates of PHB ever achieved in a phototrophic bacterium. The results generated in this work deepen the understanding of the PHB metabolism in *Synechocystis* and lay the foundation for a sustainable, carbon neutral production of PHB.

III. Zusammenfassung

Cyanobakterien repräsentieren einen der ältesten bakteriellen Phyla der Welt. Aufgrund ihrer globalen Verbreitung besitzen sie einen starken Einfluss auf globale Kohlenstoff- und Stickstoffkreisläufe. Trotz dieser großen Relevanz sind viele Aspekte ihres Metabolismus bislang schlecht erforscht. Ein Beispiel dafür ist Polyhydroxybutyrat (PHB), welches in vielen Cyanobakterien (auch dem Modelorganismus *Synechocystis* sp. PCC 6803) gebildet wird. Dieses intrazelluläre Polymer wird vornehmlich unter Stickstoffmangel synthetisiert, während *Synechocystis* in einen Überdauerungszustand namens Chlorose übergeht. Bislang sind die physiologische Relevanz von PHB sowie Einflussfaktoren auf dessen Biosynthese größtenteils unbekannt. In der vorliegenden Arbeit werden all diese Fragen adressiert und umfassend diskutiert.

Um die physiologische Funktion des PHB zu erforschen wurde ein *Synechocystis* Wildtyp mit einer PHB-freien Mutante verglichen. Wir konnten zeigen, dass, im Gegensatz zu anderen Bakterien, PHB nicht als Kohlenstoffspeicher genutzt wird, und darüber hinaus keine Relevanz während der Recovery aus der Chlorose besitzt. Wichtige Faktoren für die PHB-Biosynthese sind sowohl die Beleuchtung als auch der Gasaustausch, wobei bei Tag/Nacht-Rhythmus (im Vergleich zu Dauerlicht), sowie bei hohem Gasaustausch mehr PHB gebildet wird. Interessanterweise wird PHB während der Recovery aus der Chlorose nicht abgebaut, sondern lediglich in kleinere Granula zerteilt und auf Tochterzellen verteilt.

In anderen Organismen sind viele verschiedene Proteine am PHB-Metabolismus beteiligt, etwa während der Bildung, der Instandhaltung oder der Degradation der PHB Granula. In dieser Arbeit wurden mehrere Proteine untersucht, die einen Einfluss auf den PHB Stoffwechsel haben könnten. Dabei wurde ein neuer Regulator entdeckt, Slr0058, welcher die Anzahl und Größe von PHB-Granula beeinflusst. Bei der Untersuchung verschiedener Kohlenstoffwege stellte sich heraus, dass der Embden Meyerhof Parnas Weg der wichtigste für die PHB Bildung ist. Um den intrazellulären Ursprung des PHB zu ermitteln wurde verschiedene Knock-Out Mutanten untersucht, wie sich die PHB Biosynthese durch die Mutation ändert. Dabei zeigte sich, dass eine Beeinträchtigung des Glykogen-Stoffwechsels sich negativ auf die PHB Bildung auswirkt, was auf eine Verknüpfung beider Polymere hindeutet. Dieser Stofffluss wird durch einen neu entdeckten Regulator, Slr0944, gesteuert. Dieser Regulator ist besonders abundant während der Chlorose, wo er die Phosphoglycerat-Mutase inhibiert und dadurch den Kohlenstofffluss reguliert.

Aufgrund der ähnlichen Materialeigenschaften zu Polypropylen wird PHB häufig als eine biobasierte und biologisch abbaubare Alternative angesehen, was von großer biotechnologischer Relevanz ist. Die Eigenschaft einer Δ*sll0944* Mutante, während der Chlorose vermehrt Glykogen abzubauen, wurde genutzt, um einen PHB Überproduktionsstamm zu erzeugen. Dazu wurden in einem Δ*sll0944* Stamm PHB-Biosynthese-Gene überexprimiert, wodurch der höchste jemals gemessen PHB Gehalt in einem phototrophen Organismus erzeugt wurde. Die Ergebnisse dieser Arbeit erweitern unser Verständnis vom PHB Metabolismus in *Synechocystis* und legen somit die Grundlage für eine nachhaltige, CO_2-neutrale PHB Produktion.

IV. Publications

1. Accepted Papers

1. Publication

Research Article

M. Koch, S. Doello, K. Gutekunst, K. Forchhammer (2019).

PHB is Produced from Glycogen Turn-over during Nitrogen Starvation in Synechocystis sp. PCC 6803.

International Journal of Molecular Sciences, 20, 1942.

2. Publication

Research Article

B. Watzer, P. Spaet, N. Neumann, **M. Koch**, O. Hennrich, K. Forchhammer (2019).

The central regulator PII controls nitrate and urea uptake in *Synechocystis* sp. PCC 6803.

Frontiers in Microbiology, 10: 1428.

3. Publication

Book chapter

M. Koch, K. Forchhammer (2020)

Storage polymers in cyanobacteria: friend or foe?

Cyanobacteria biotechnology, Wiley (book chapter)

4. Publication

Research Article

M. Koch, T. Orthwein, J. T. Alforth, K. Forchhammer (2020).

The Slr0058 protein from *Synechocystis* sp. PCC 6803 is a novel regulatory protein involved in PHB granule formation

Frontiers in Microbiology, 2020, 11:809

5. Publication

Research article

M. Koch, K. Berendzen, K. Forchhammer (2020).

On the role and production of PHB in the cyanobacterium *Synechocystis* sp. PCC 6803.

Life, 2020, 10, 47

2. Manuscripts in preparation

6. Publication

Research Article

M. Koch, Jonas Bruckmoser, Jörg Scholl, Waldemar Hauf, Bernhard Rieger, K. Forchhammer.

Maximizing PHB content in *Synechocystis* sp. PCC 6803: development of a new photosynthetic overproduction strain.

Microbial Cell Factories

7. Publication

Review

M. Koch and K. Forchhammer.

Polyhydroxybutyrate – a versatile biopolymer with more functions to be discovered.

Microbial Physiology

3. Declaration of personal contribution to the publications

1. Publication

PHB is Produced from Glycogen Turn-over during Nitrogen Starvation in Synechocystis sp. PCC 6803.

I have planned, conducted and interpreted all experiments shown in this publication except for the glycogen analysis and the experiments shown in figure 2. I prepared all figures except figure 2. The manuscript was written by me and Prof. Karl Forchhammer with input from all coauthors. I was responsible for the revision process, including submitting the paper and responding to the reviewer's comments. During the whole study I was under the supervision of Prof. Karl Forchhammer.

2. Publication

The central regulator PII controls nitrate and urea uptake in Synechocystis sp. PCC 6803.

I have constructed all 14 genetical constructs for the bacterial-two-hybrid assay and performed preliminary experiments for this study. Furthermore, I wrote the respective part of the methods section.

3. Publication

Storage polymers in cyanobacteria: friend or foe?

I have written the entire chapter about PHB and prepared all figures for this part. I was responsible for the revision process, including the correspondence to the editor and for including his comments to the entire publication. The entire writing process was supervised by Prof. Karl Forchhammer.

4. Publication

The Slr0058 protein from Synechocystis sp. PCC 6803 is a novel regulatory protein involved in PHB granule formation

I have planned, supervised and interpreted all experiments shown in this publication. I prepared or edited all figures in preparation for the manuscript. The manuscript was written by me and Prof. Karl Forchhammer. I was responsible for the revision process, including submitting the paper and

responding to the reviewer's comments. During the whole study I was under the supervision of Prof. Karl Forchhammer.

5. Publication

On the role and production of PHB in the cyanobacterium Synechocystis sp. PCC 6803.

I have planned, conducted and interpreted all experiments shown in this publication with technical support of Kenneth Berendzen for the FC/FACS experiments. I prepared all figures. The manuscript was written by me and Prof. Karl Forchhammer with input from Kenneth Berendzen. I was responsible for the revision process, including submitting the paper and responding to the reviewer's comments. During the whole study I was under the supervision of Prof. Karl Forchhammer.

6. Publication

Maximizing PHB content in Synechocystis sp. PCC 6803: development of a new photosynthetic overproduction strain.

I have planned, conducted and interpreted all experiments shown in this publication except the construct of the plasmid REphaAB and the qualitative analytic of PHB. I prepared all figures except the one about the qualitative analytic of PHB. The manuscript was written by me and Prof. Karl Forchhammer. During the whole study I was under the supervision of Prof. Karl Forchhammer.

7. Publication

Polyhydroxybutyrate – a versatile biopolymer with more functions to be discovered.

I have written the entire text and prepared all figures for this publication. The entire writing process was supervised by Prof. Karl Forchhammer.

V. Introduction

1. Cyanobacteria[1]

1.1 Classification, ecology and evolution

Cyanobacteria are a phylum of microorganisms, belonging to the kingdom of bacteria. They are gram negative prokaryotes and date back at least as early as 2.7 billion years ago (Sili et al., 2012). Within this time, they adapted to various environmental conditions, enabling them to survive on all light exposed parts of the earth, including extreme ecosystems, such as hot springs or the desert sand crust (Raanan et al., 2016, Papke et al., 2003).

Cyanobacteria can be categorized in five different sections, based on their morphology (Rippka et al., 1979). Section I comprises unicellular organisms, which reproduce by either binary fission or budding. Similarly, Section II cyanobacteria are also unicellular; unlike the previous Section though, these ones are able to reproduce by multiple fission. Section III comprises filamentous organisms, which show no specialized cells. In contrast, Section IV, which are also filamentous cyanobacteria, do have specialized cells within their filaments. These can be either heterocysts (nitrogen fixing cells), hormogonia (motile filaments) or akinetes (spore-like cells). While Section III and IV cells divide in only one plane, cyanobacteria of the Section V can divide in more than one plane. The members of this Section are also filamentous cyanobacteria, which do as well form specialized cells.

One unique feature about cyanobacteria is, that they are the only bacteria, which are able to perform oxygenic photosynthesis (Sánchez-Baracaldo and Cardona, 2020). This allows them to grow photoautotrophically, consume CO_2 while producing O_2. Due to this ability and their high abundance, cyanobacteria were responsible for a drastic change in the atmospheric composition during the paleoproterozoic era. In the so called "great oxygenation event", cyanobacteria started ~2.3 billion years ago to create the oxygen-enriched atmosphere of the world as we know it today (Schirrmeister et al., 2015)

1.2 *Synechocystis* sp. PCC 6803

Synechocystis sp. PCC 6803, hereafter *Synechocystis*, is a cyanobacterial model organism. In 1968 it was first isolated from a freshwater lake in Berkeley in 1968 (Stanier et al., 1971). Within the last decades, various laboratory sub-strains have evolved (Zavřel et al., 2017). They can be differentiated based on genotypic and phenotypic properties, such as their ability to grow on glucose or on their motility. Since it got first isolated, *Synechocystis* became a model organism for studying different aspects of photosynthetic lifestyle. One reason for this is its fully sequenced genome, which was the first ever-sequenced genome of a phototrophic microorganism (Kaneko et al., 1996). Furthermore, *Synechocystis* is capable of natural genetic transformation, making the organism accessible for genetic modification. This allows to easily create knockout strains and analyzing the function of its

[1] Parts of this introduction are quotes from KOCH, M. & FORCHHAMMER, K. 2020. Storage polymers in cyanobacteria: friend or foe? . *Cyanobacteria biotechnology,* Wiley.. Copyright Wiley-VCH Verlag GmbH & Co. KGaA. Reproduced with permission.

genes. Additionally, *Synechocystis* possesses a versatile metabolism, allowing them to generate energy from either sunlight or organic carbon sources. Due to these diverse metabolic lifestyles, namely phototrophic, mixotrophic or heterotrophic growth, *Synechocystis* possesses a variety of different carbon pathways and is therefore a model organisms for those as well (Chen et al., 2016). Unlike other cyanobacteria, *Synechocystis* is unable to fix atmospheric nitrogen, but instead takes up other sources of combined nitrogen, which is also intensively studied (Watzer et al., 2019). Finally, *Synechocystis* has the ability to produce a wide variety of biopolymers, such as glycogen, cyanophycin, polyhydroxybutyrate or polyphosphate, which are relevant for basic research as well as biotechnological applications. At the same time, the unicellular bacterium is easy to cultivate, since it grows planktonic, is relatively resistant to various stress and has a fast growth rate compared to other cyanobacteria (Branco Dos Santos et al., 2014). All of this makes *Synechocystis* a well-studied model-organism. In the following, the specificities of this cyanobacterium are further described.

2. Metabolism of *Synechocystis* sp. PCC 6803

2.1 Energy metabolism

2.1.1 Photosynthesis

Oxygenic photosynthesis can be divided in two processes: light-dependent reactions and the light-independent reactions. The light-dependent reactions are processes that harvest energy from sunlight and store it in energy-dense molecules, such as ATP or NADPH. In light-independent reactions, also known as Calvin-Benson-Bassham-Cycle, this energy is used to fix atmospheric CO_2 (described below under "CO_2 fixation"). The light-dependent reactions take place in the thylakoid membranes and are mediated by the Photosystem II and I complexes (PS II and I, respectively) (Lea-Smith et al., 2016) (Figure 1 A). In the first step, a light-harvesting complex, called phycobilisome, redirects absorbed light towards PS II. Here, a chlorophyll *a* molecule is excited by the absorption of one photon. As a consequence, one electron of chlorophyll *a* gets transferred through various electron acceptors, until it finally reaches plastoquinone, which gets reduced to plastoquinol. In this process, plastoquinone takes up two protons from the cytoplasmatic side of the thylakoid membrane. While plastoquinone diffuses through the thylakoid membrane, a series of redox reactions take place, where the electron gets passed to cytochrome *b6f* complexes. Simultaneously, plastoquinone releases the protons on the luminal side of the membrane, creating a proton gradient. In this process called the q-cycle, a total of two plastoquinone are reduced to two plastoquinol, before the latter are oxidized again at the luminal side of the membrane and 4 protons are released into the lumen. The electrons released in this process are passed on to a mobile, water soluble electron carrier, either plastocyanin or cytochrome c6, depending on the cupper concentration (Duran et al., 2004). When PSI is photooxidized by another photon, an electron is passed on to the next electron acceptor, ferredoxin. The oxidized chlorophyll *a* in the PSI reaction center is subsequently reduced by an electron from the plastocyanin / cytochrome c6 pool. The

ferredoxin can then be used in one of the two following ways. The first option is that ferredoxin serves as an electron donor for anabolic processes like nitrogen assimilation. In the second option, ferredoxin carries the electron to a ferredoxin NADP⁺ reductase, which oxidizes ferredoxin and reduces NADP⁺ to form NADPH. In some cases, reduced ferredoxin can also react with other enzymes like sulfite reductases or hydrogenases.

Right after the PS II lost one electron in the first step of this process described above, PS II is reduced again by deriving an electron from the oxygen evolution complex. The latter is attached to PS II and splits two molecules of water into 4 protons, 4 electrons and one molecule of oxygen. The electrons are then further transferred to the PS II complex, which channels them into the process described above. The four protons from this process, as well as the two protons transferred by the plastoquinone, create a proton gradient among the thylakoid membrane. This gradient can be utilized by the ATP synthase, which converts ADP to ATP (Lea-Smith et al., 2016).

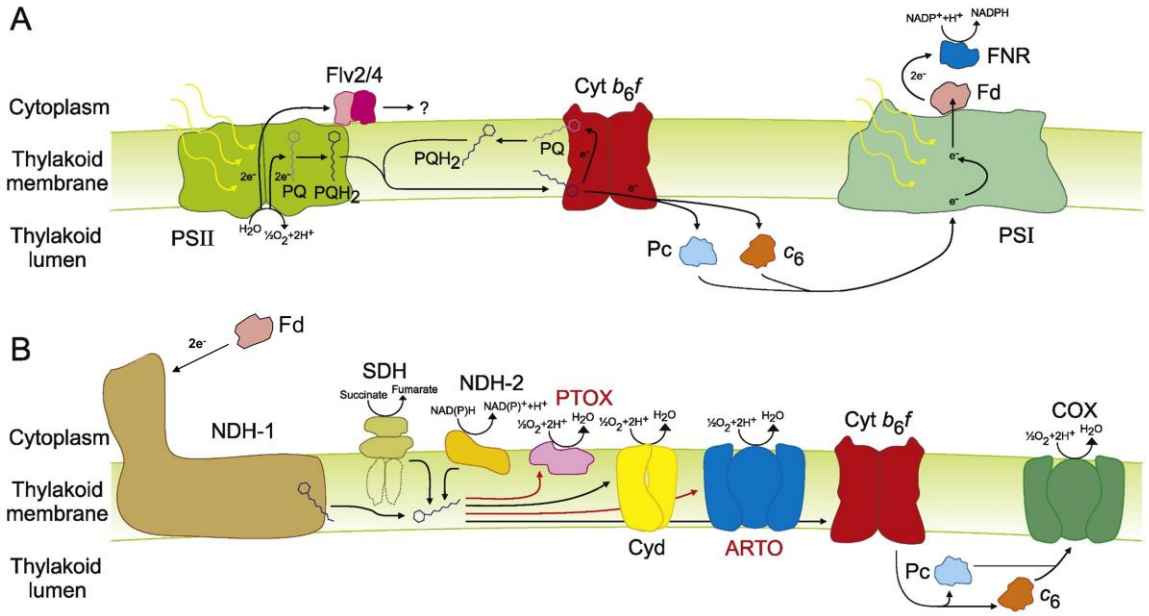

Figure 1. Schematic overview of important electron transport chains in cyanobacteria. A) photosynthetic and B) respiratory electron transport chains, both located at the thylakoid membrane. Red lines show pathways which are not present in *Synechocystis.* Broken lines indicate putative electron transport proteins or pathways, which are not yet experimentally confirmed. Modified from Lea-Smith *et al.* 2016. Abbreviations: ARTO—alternative respiratory terminal oxidase, COX—cytochrome-*c* oxidase, Cyd—*bd*-quinol oxidase, cyt b_6f—cytochrome b_6f , Cyt c_6—cytochrome c_6, Fd—ferredoxin, Flv2/4—Flavodiiron 2/4, FNR—ferredoxin-NADP⁺-reductase, NDH-1—NAD(P)H dehydrogenase 1, NDH-2—NAD(P)H dehydrogenase 2, Pc—plastocyanin, PQ—plastoquinone, PQH_2—plastoquinol, PS I—Photosystem I, PS II—Photosystem II, PTOX—plastid terminal oxidase, SDH—succinate dehydrogenase.

2.1.2 Respiration

The process of respiration is considered as the opposite of the photosynthetic electron flow. This process becomes necessary, when no energy can be produced via photosynthesis, for example

during the night. Then, energy-dense molecules and oxygen are converted to ATP and CO_2. This process is also often referred to as oxidative phosphorylation. Respiration takes mainly place in the thylakoid membrane and shares many components with the photosynthetic electron flow (Lea-Smith et al., 2016) (Figure 1 B). The first step is catalyzed by different kinds of dehydrogenases, which oxidize NADPH, NADH or succinate. Of those different dehydrogenases, in *Synechocystis* the succinate dehydrogenase appears to be the most import one (Cooley and Vermaas, 2001). The latter is part of the TCA cycle (tricarboxylic acid cycle), where succinate gets oxidized to fumarate. Alternatively, as a recent study has shown, the respiratory complex I uses ferredoxin derived from PS and thereby directly connects both complexes (Schuller et al., 2019). The electrons derived from NADPH, NADH or succinate are subsequently used to reduce the plastoquinone pool. From there, the electrons are transferred to the cytochrome *b6f* complex, similarly like in the photosynthetic electron flow. Another similarity between both processes is, that the electron from the cytochrome *b6f* complex get subsequently transferred to either cytochrome *c6* or plastocyanin, while generating proton motif force. From here, unlike in the photosynthetic electron flow, the electrons now get transferred to a terminal oxidase. Although there are several different ones present in cyanobacteria, the dominant one in *Synechocystis* is a cytochrome-c oxidase complex (Hart et al., 2005). These terminal oxidases transfer the electrons to the final electron acceptors oxygen and hydrogen, by which water is formed. The protons, which were pumped into the thylakoid lumen during the entire process described above, created a proton gradient, which is utilized by the ATP synthase to generate ATP. Another function of the terminal oxidases is the protection of the cell from oxidative stress during photobleaching. In times of fluctuating light intake, this prevents the cells from overreduction of the electron transport chain (Lea-Smith et al., 2013). Finally, although similar in their process, respiration and photosynthesis usually do not take place at the same time. This phenomenon is known as the Kok effect (Kok 1949).

2.2 Carbon metabolism

2.2.1 Carbon pathways

For carbon metabolism, there are three central pathways present in *Synechocystis*, namely the EMP (Embden Meyerhof Parnas) pathway, the ED (Entner Doudoroff) pathway and the OPP (oxidative pentose phosphate) pathway (Figure 2) (Makowka et al., 2020). The EMP pathway is also known as the classic glycolysis pathway and is important for carbon catabolism. This pathway utilizes a unique enzyme, a phosphofructokinase (Pfk), which converts fructose-6P to fructose-1,6-bisphosphate. Another carbon pathway is the ED, which has just recently been discovered to occur in cyanobacteria (Chen et al., 2016). A 2-keto3-deoxygluconate-6-phosphate aldolase (Eda) is the key enzyme, which is unique for the ED pathway. This pathway is important under mixotrophic growth and during day/night-autotrophic growth. Furthermore, the ED pathway was shown to supply anaplerotic intermediates, which is relevant during the onset of carbon fixation after a transition from dark to light (Makowka et al., 2020). Although the ED pathway generates less ATP than the EMP pathway, it has lower proteins costs. This trade-off can be beneficial under conditions of

mixotrophic conditions, where energy is plentiful available and cells are instead nutrient limited (Flamholz et al., 2013). Finally, the third main carbon route is the OPP pathway. Its unique enzyme is a 6-phosphogluconate dehydrogenase, which catalyses the reaction from 6P-gluconate to ribulose-5P. This pathway is most important during heterotrophic growth, where the EMP pathway plays also a minor role (Makowka et al., 2020). Additionally, the OPP pathway is channeling significant amounts of carbon during growth at alternating day/night rhythm, together with the ED pathway (Chen et al., 2016). Recent studies have furthermore suggested, that the OPP pathway is regulated via tricarboxylic acid (TCA) cycle intermediates (Ito and Osanai, 2020). Another remarkable feature of the OPP pathway is, that it can also run in reverse direction. For this it is known as the reductive pentose phosphate pathway or as the Calvin-Benson-Bassham (CBB) cycle. This pathway is important for carbon uptake and will be explained in the next chapter in more detail.

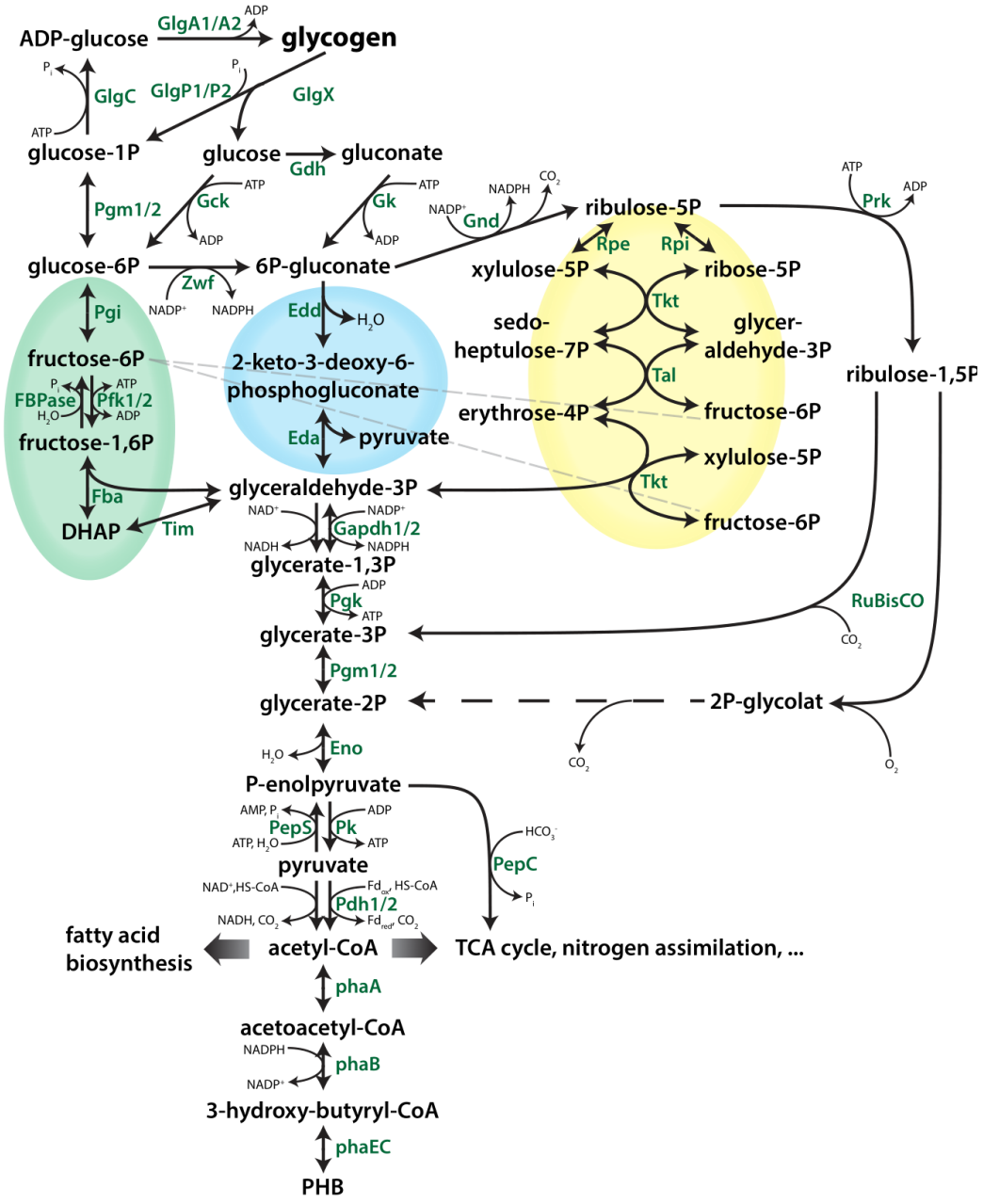

Figure 2. Central carbon metabolism *in Synechocystis* sp. PCC 6803. Important enzymes are shown in green. The EMP (Embden Meyerhof Parnas) pathway is highlighted in green, the ED (Entner Doudoroff) pathway in blue and the OPP (oxidative pentose phosphate) pathway in yellow.

Another less important pathway is the phosphoketolase pathway. Here the central enzyme is a phosphoketolase (Xfpk), which converts xylulose-5-phosphate (or fructose-6-phosphate) to acetyl phosphate and glyceraldehyde 3-phosphate (or erythrose 4-phosphate) (Xiong et al., 2015). Since the presence of this pathway has just recently been discovered in cyanobacteria, not much is known about its relevance during different growth conditions.

2.2.2 CO_2 fixation

Cyanobacteria can grow autotrophically and rely completely on inorganic carbon. To fix atmospheric carbon, cyanobacteria have developed different strategies. For the initial step, the transfer of carbon into the cell, *Synechocystis* possesses five different carbon uptake systems (Forchhammer and Selim, 2019, Burnap et al., 2015). Two of them are CO_2 uptake systems, while the three others are HCO_3- transporters. Once inside the cell, HCO_3^- gets transported to the carboxysomes, which are organelles where the carbon fixation takes place. The protein shell of the carboxysome represents a diffusion barrier and enables a high local carbon concentration (Rae et al., 2013). Here, a carbonic anhydrase dehydrates HCO_3- to CO_2 and thereby increases the local CO_2 concentration within the carboxysome. Inside the carboxysome, the enzyme ribulose-1,5-bisphosphate carboxylase/oxygenase (RuBisCO) is located. RuBisCO catalyzes the first step of the Calvin-Benson-Bassham (CBB) cycle, which serves as the main carbon fixing pathway in cyanobacteria. In the first step, RuBisCO carboxylates ribulose-1,5-bisphosphate with one molecule CO_2 to 2-carboxy 3-keto 1,5-biphosphoribotol. Since the latter is an unstable product, it immediately splits into two units of 3-phosphoglycerate. These molecules can than either continue through the CBB cycle to regenerate ribulose-1,5-bisphosphate or get used as central metabolites through various other carbon pathways. Here, newly fixed carbon can then either be used for anabolic reactions, such as the formation of amino acids, or stored in the form of glycogen.

One major disadvantage of the central enzyme RuBisCO is its low affinity and specificity for CO2, enabling it to also bind O_2 instead of CO_2. In this case, ribulose-1,5-bisphosphate is converted to one molecule of 3-phosphoglycerate and one molecule 2-phosphoglycolate. Since the latter is a toxic compound, *Synechocystis* has evolved various strategies to detoxify it (Eisenhut et al., 2008). However, since these detoxification steps require energy, losses of fixed carbon and liberates nitrogen, which has to be re-assimilated, this process called photorespiration is considered a tremendous waste of resources for the cell (Hagemann and Bauwe, 2016, Fernie and Bauwe, 2020).

Besides the CBB cycle, *Synechocystis* has evolved further strategies to improve the carbon uptake. One is a carbonic anhydrase module, which is attached to photosynthetic complex I. When reduced ferredoxin binds to complex I, its electrons can be used to pump protons inside the thylakoid lumen. Alternatively, this energy can be used to bind one molecule of CO_2 and convert it into $NaHCO_3$, which makes it part of the carbon-concentrating mechanism (Schuller et al., 2020). Furthermore, CO_2 can get fixed by the phosphoenolypyruvate carboxylase (PEPC). This enzyme carboxylates

phosphoenolpyruvate, leading to the formation of oxaloacetate (Scholl et al., 2020). However, a subsequent reaction of malic enzyme results in the loss of CO_2 again.

2.2.3 Carbon storage

While most of the fixed carbon is directly used for anabolic reactions, at certain times *Synechocystis* faces conditions of carbon excess. This can be the case during nutrient limitation, as well as during the day, when more carbon is fixed than directly needed. Under both conditions, carbon has to be stored. For this purpose, *Synechocystis* uses two different carbon storage polymers, namely glycogen and polyhydroxybutyrate (PHB). Since the latter has never been proven to truly serve as a carbon reservoir, it will not be considered in this paragraph. On the other hand, several studies have shown that glycogen is the most important carbon storage pool, heavily influencing the cell's metabolism (Damrow et al., 2016, Grundel et al., 2012)

Glycogen is built up of glucose 1-phosphate units, which first have to be activated by a glucose-1-phosphate adenylyltransferase (GlgC). This enzyme transfers an ADP residue from ATP to glucose 1-phosphate. ADP-glucose monomers are then polymerized by a glycogen synthase (GlgA), connecting the monomers via an α-1,4-glycosidic-linkage. Additionally, a branching enzyme (GlgB) adds α-1,6-glycosidic-linkages between growing glucan chains, resulting in a branched glycogen polymer (Preiss, 2006, Preiss, 1984).

During glycogen degradation, glycogen debranching enzymes (GlgX) hydrolyses the α-1,6-glycosidic-linkages to reduce the branching. The leftover glucan polymer, a chain of α-1,4-linked glucose units, is subsequently broken down into glucose 1-phosphate subunits via a glycogen phosphorylase (GlgP), which can be further catabolized via different metabolic routes (Doello et al., 2018).

Interestingly, *Synechocystis* possesses a pair of homologues versions of many enzymes involved in glycogen metabolism. This is the case for GlgA, GlgP, GlgX and potentially GlgB. While some of the enzymes can replace each other (for example GlgA1 and GlgA2) (Grundel et al., 2012), other show different activities and a deletion of one version cannot be compensated by the homologue variety (glgP1 and glgP2) (Doello et al., 2018). Interestingly, some of the homologue enzymes are contrary regulated on a transcriptional level. For example, GlgP2 is upregulated during the night, while GlgP1 is downregulated, indicating different physiological functions despite similar biochemical characteristics of the enzymes (Saha et al., 2016).

There are several studies demonstrating the importance of glycogen during unbalanced and stressful growth conditions. For example, glycogen free mutants with a deletion of *glgA1/A2* or *glgC* show slightly impaired growth when cultivated with continuous light (Grundel et al., 2012). However, when the same strains are grown under alternating day/night rhythm or nitrogen starvation, both cultures die within a few days (Grundel et al., 2012). This highlights the importance of glycogen as a storage polymer for balanced carbon and energy homeostasis.

2.3 Nitrogen metabolism

2.3.1 Nitrogen assimilation

The availability of nitrogen is an important and often limiting aspect for bacterial growth. *Synechocystis* as a non-diazotrophic cyanobacterium is unable to fix atmospheric nitrogen. Therefore, it relies completely on the uptake of combined nitrogen sources, such as urea, nitrate or ammonium. Ammonium is the preferred nitrogen source and its uptake mainly depends on the ammonium permesase Amt1 (Muro-Pastor et al., 2005). Other nitrogen sources like nitrate or urea are taken up by different transport systems including ABC-Transporters like NrtABCD for Nitrate/nitrite or UrtABCDE for urea (Ohashi et al., 2011, Valladares et al., 2002). Once inside the cell, inorganic nitrogen sources need to be converted to ammonium, which is the required molecule for nitrogen assimilation. In most habitats, nitrate represents the most common and abundant nitrogen source. For its assimilation, nitrate is converted to nitrite via a nitrate reductase. Subsequently, nitrite is reduced to ammonium via a nitrite reductase. For these reactions, the nitrate and nitrite reductase require reduced ferredoxin, which is provided by the photosynthetic reactions. Hence, a close connection between nitrogen assimilation and photosynthesis has been suggested (Esteves-Ferreira et al., 2018). The generated ammonium is incorporated into the intracellular nitrogen metabolism via the GS/GOGAT (glutamin synthetase / glutamine oxoglutarate aminotransferase) cycle. In a first step, the GS catalyzes an amidation of glutamate to form glutamine, while hydrolyzing ATP to ADP. In the next step, GOGAT transfers an amino group from glutamine to 2-oxoglutarate, resulting in two molecules glutamate, where one molecule glutamate remains the cycle to regenerate glutamine.

2.3.2 Chlorosis

When certain macronutrients are unavailable, *Synechocystis* undergoes a transformation into a resting state, a process known as chlorosis (Collier and Grossman, 1992). This process is best understood for nitrogen starvation and was intensively investigated in the strain *Synechococcus* sp. PCC 7942(Görl et al., 1998, Sauer et al., 2001) and later in *Synechocystis* (Klotz et al., 2016). In the following, this process is further described at the example of nitrogen depleted conditions. During chlorosis, the cell division stops, and the cells transform into a resting state, in which they maintain only a basal metabolic activity. While being in this phase, the cells are enabled to survive longer periods of nutrient starvation (Schwarz and Forchhammer, 2005). The chlorosis can be subdivided into three different phases (Görl et al., 1998): 1) the degradation of phycobilisomes, 2) cells degrade also chlorophyll *a* and 3) the cells reach a resting state, in which they can survive for prolonged times (Figure 3).

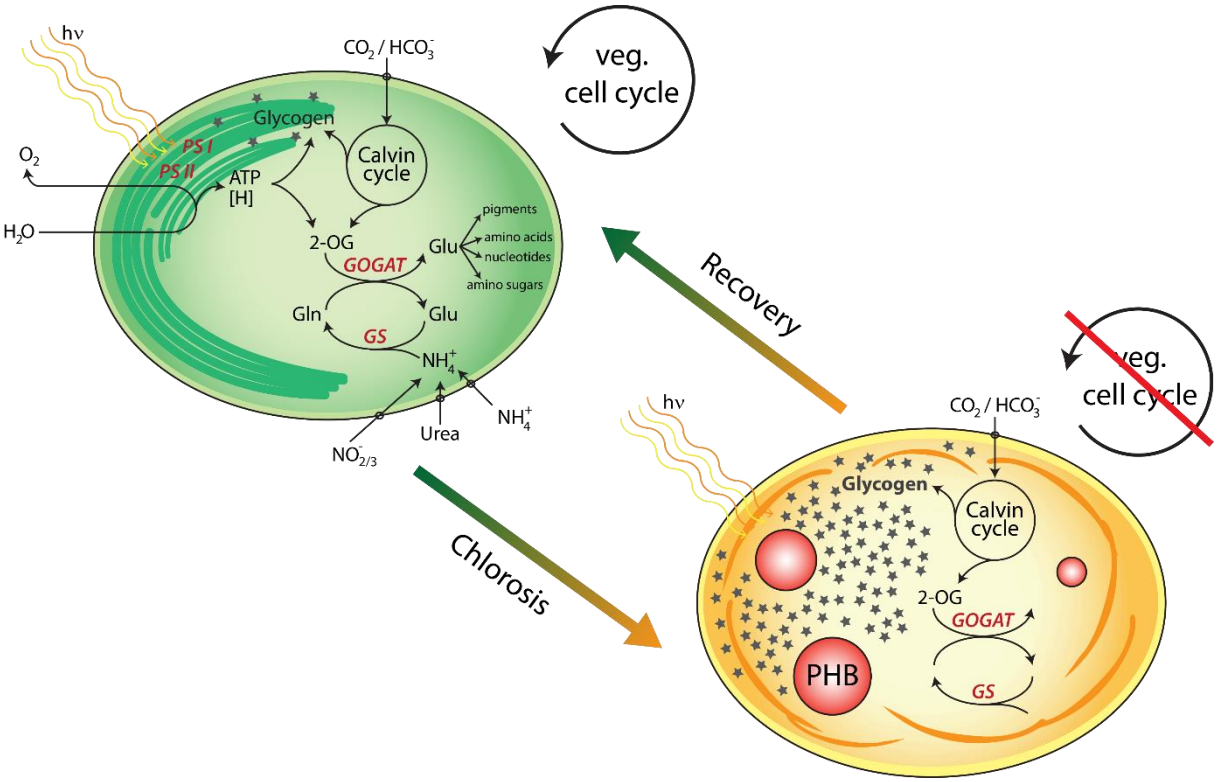

Figure 3. Schematic illustration of the chlorosis and recovery process in *Synechocystis* sp. PCC 6803 (Klotz *et al.* 2016). Shown are a vegetative cell (left) and a chlorotic one (right). Chlorosis can be induced by nitrogen starvation, which initiatives a transformation into a resting state.

At the beginning of chlorosis, the lack of nitrogen is detected via increased intracellular amounts of 2-oxoglutarate, which indicates a high carbon to nitrogen level (Muro-Pastor et al., 2005). In cyanobacteria the PII signal transduction Protein regulates the global nitrogen transcription factor NtcA through binding to its co-activator PipX. Under nitrogen excess conditions the sequestration of PipX by PII leads to a decreased NtcA-PipX complex formation. Under nitrogen depleted conditions, indicated by a high 2-oxogluterate level, the complex formation of PipX and PII is impaired. Free PipX can bind NtcA and activate the NtcA-regulon. While NtcA controls various different genes associated with the nitrogen metabolism, it also activates the expression of the adaptor protein NblA. The latter attaches to light harvesting complexes (phycobilisomes) and thereby initiatives their degradation (Karradt et al., 2008). Within a few days, the majority of the phycobilisomes are degraded, resulting in a strong decrease of photosynthetic activity of the cells. As a result of the degradation of photopigments, the color of the cultures change from green to yellow-green (Allen and Smith, 1969). Within the first day, the cells divide one last time, before they transition into a growth arrest. Besides the degradation of photopigments, the cells use the initial phase of chlorosis to build up intracellular carbon storage pools (glycogen). The synthesis peaks after two days and can reach amounts of up to ~40 % / cell dry weight (CDW) (Klotz and Forchhammer, 2017). In the second phase of chlorosis, the cells also degrade their remaining photopigments, mainly chlorophyll *a*. While doing so, the photosynthetic rate further decreases and the color of the culture changes to yellow-orange. At the same time, the synthesis of another biopolymer is initiated, polyhydroxybutyrate (PHB). In contrast to the glycogen accumulation, the PHB synthesis is significantly prolonged. The entire accumulation takes several weeks and reaches around 15 % /

CDW (Klotz et al., 2016). Finally, the cells reach the third and final phase of chlorosis. Here they perform only low level photosynthetic activity to keep the cells alive (Sauer et al., 2001). Regardless of the strong decay of metabolic activity, cells remain viable for long periods of time (Görl et al., 1998).

2.3.3 Resuscitation

Even after long periods within a chlorotic state, *Synechocystis* is able to recover in a few days upon the addition of nitrogen (Figure 3). The resuscitation from nitrogen starvation is a genetically determined program, by which the cells recover their photosynthetic pigments and turn into vegetative cells (Klotz et al., 2016). The entire process takes approximately two days and can be divided into two phases (Sawers, 2016). In the first step, cells start to degrade their intracellular glycogen reservoirs (Doello et al., 2018, Klotz and Forchhammer, 2017). This process releases energy and carbon, by which the cells are able to build up their translational machinery, such as ribosomes. In the second phase, which starts around 12-16 hours after the addition of nitrogen, cells start to rebuild their photopigments. This allows the cells to change from respiration to photosynthetic metabolism. The process is completed after 48 hours, when the cells have regained full photosynthetic capacity and start to divide again. Within two days, the dormant cells have been completely transformed into vegetative cells.

2.3.4 Sensing and regulation of nitrogen status via PII

PII is a homotrimeric signal transduction protein, which is widely spread among all domains of life (Forchhammer and Luddecke, 2016). It is important for sensing and regulating the intracellular carbon and nitrogen status. In cyanobacteria PII binds competitively two adenyl-nucleotides, ATP and ADP, and can thereby sense the intracellular energy level. Furthermore, PII has the ability to bind 2-oxoglutarate, a key intermediate during the nitrogen assimilation process. Since 2-oxoglutarte is part of the TCA cycle as well as the GS/GOGAT cycle, it directly links carbon and nitrogen metabolism. Hence, the interaction with 2-oxoglutarate allows PII to sense the intracellular nitrogen to carbon ratio. Besides binding different effector molecules and binding partners, the PII protein itself can also be post-translational modified. One well known modification of the cyanobacterial PII, is the phosphorylation of the Ser49, which occurs in dependence of nitrogen availability (Forchhammer and Tandeau de Marsac, 1995). Depending on these modifications, PII changes its interaction behavior with its binding partners.

Based on the signals derived from metabolite binding and post translational modification, PII can interact with various interaction partners. For this purpose, PII exhibits a large surface-exposed T-loop, which serves as an interaction module between PII and its binding partners. One example for potential interaction partners are nitrogen transporters / permeases, whereby PII could directly influence the uptake of different nitrogen sources. Furthermore, PII can also bind the small protein PipX. The latter is a co-activator of the global transcription factor NtcA, PII influences the regulation of genes related to the nitrogen metabolism (Espinosa et al., 2007). Finally, by interacting with the enzyme N-acetylglutamate kinase (NAGK), PII regulates the arginine biosynthesis (Fokina et al.,

2010) and thereby indirectly the biosynthesis of cyanophycin, a nitrogen storage polymer (Watzer and Forchhammer, 2018). It was furthermore shown that PII is able to interact with enzymes involved in carbon metabolism, such as the biotin carboxyl carrier protein BCCP of the acetyl-CoA carboxylase (ACC) (Hauf et al., 2016) or the phosphoenolpyruvate carboxylase (PEPC) (Scholl et al., 2020). This allows PII to directly influence the carbon flux within cyanobacterial cells. In summary, PII is able to regulate the carbon flux as well as the nitrogen metabolism.

3. PHB

3.1 Structure and physical properties

Polyhydroxybutyrate (PHB) was already discovered in *Bacillus megaterium* in 1926 (Lemoigne, 1926). PHB is composed of 3-hydroxy-butyrate monomers. This subunit has a simple structure, as it consists of the four carbon fatty acid butyrate with an hydroxy group at the third carbon atom. When several 3-hydroxybutyrate monomers are connected via an ester bond they form PHB (Jendrossek, 2009). The latter accumulates in the form of water insoluble inclusions within the cell. Contrary to a long-time belief, it was recently demonstrated that PHB granules do not contain phospholipids on their surface (Bresan et al., 2016). The general structure of PHB is shown in Figure 4.

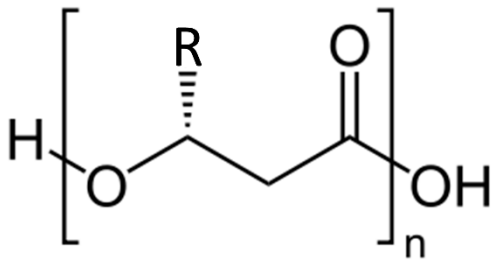

R-group	Carbon	Polymer
hydrogen	C_3	Poly(3-hydroxypropionate)
methyl	**C_4**	**Poly(3-hydroxybutyrate)**
ethyl	C_5	Poly(3-hydroxyvalerate)
propyl	C_6	Poly(3-hydroxyhexanoate)
pentyl	C_8	Poly(3-hydroxyoctanoate)
nonyl	C_{12}	Poly(3-hydroxydodecanoate)

Figure 4. General structure of PHA. Depending on the side chain R, several different types of PHA are formed. In the case of PHB, the side chain corresponds to a methyl group. The monomeric units (n) of PHAs are linked via an ester bond between the hydroxy- and the carboxyl groups, forming the respective PHA.

Six decades after PHB was first discovered, in 1983 researchers showed that when grown on long octan, *Pseudomonas oleovorans* produces poly-beta-hydroxyoctanoate granules (de Smet et al., 1983). This was the first time, that the microbial production of other polyhydroxyalkanoates (PHA) was discovered. PHAS are classified in three different groups, depending on the length of their side chain: short- (C_3-C_5), medium- (C_6-C_{16}) and long-chain-length PHA (scl, mcl and lcl, respectively) (Jendrossek, 2009). A selection of different PHA types is given in Figure 4.

Production of PHA is described from representatives from all three kingdoms of life: archaea, bacteria and eukaryotes. Just recently it has been reported, that also eukaryotic algae can naturally produce PHB, namely *Chlorella* (Cassuriaga et al., 2018) and *Botryococcus* (Kavitha et al., 2016). However, PHA production is best characterized in bacteria, such as *Pseudomonas putida* (Timm and Steinbüchel, 1990), *Cupriavidus necator* (formerly known as *Ralstonia eutropha*) (Wilde, 1962), *Bacillus megaterium* (Griebel et al., 1968), *Rhodococcus ruber* (Haywood et al., 1991), *Acinetobatcer*

sp. (Schembri et al., 1995). Besides a few exceptions, mcl PHAs are mainly produced by fluorescent *Pseudomonads* strains such as *P. putida* (Prieto et al., 2007). Hence, PHB is by far the most common PHA variant.

Due to its physical and chemical properties, PHB is often considered as a potential substitute for thermoplastic polymers, such as polypropylene. However, there are still strong differences compared to commonly used plastics. For example, its structure exhibits low elasticity but high rigidness, which are undesirable material properties for many applications (van der Walle et al., 2001). However, these physical properties vary strongly among the different PHAs. Depending on the length of the side chains, the material becomes more elastic and less brittle with longer side chains. Additionally, alternative side chains, such as aromatic groups, can further alter the properties of the PHA (Ishii-Hyakutake et al., 2018, Ward and O'Connor, 2005). Finally, heteropolymers, such as poly(3-hydroxybutyrate-co-3-hydroxyvalerate) (PHBV) further increase the range of physical properties of PHA based polymers (Rivera-Briso and Serrano-Aroca, 2018).

3.2 PHB biosynthesis

PHB synthesis starts with acetyl-CoA monomers. In the first step, an acetyl-CoA acetyltransferase, termed PhaA, catalyses the condensation of two units of acetyl-CoA to acetoacetyl-CoA. In the next step, an acetoacetyl-CoA reducatase (PhaB), reduces acetoacetyl-CoA to 3-hydroxyacetly-CoA, while oxidizing one molecule of NADPH to $NADP^+$. Finally, a PhaC polymerase connects a 3-hydroxyacetly-CoA to an elongated PHB polymer (Figure 5).

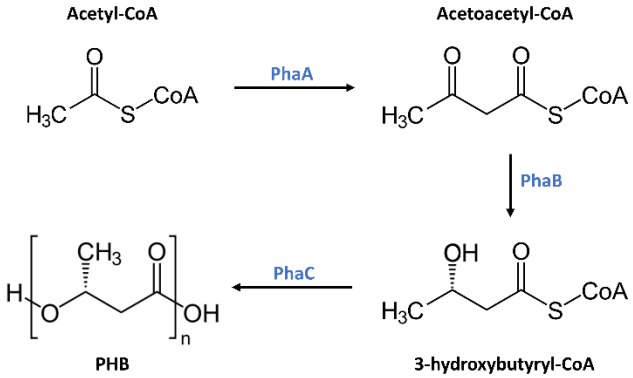

Figure 5. PHB synthesis pathway. Two units of acetyl-CoA are condensated to acetoacetyl-CoA via PhaA. Next, PhaB reduces it to 3-hydroxybutyryl-CoA. The latter serves as a monomer which gets polymerized to PHB by PhaC.

On the basis of primary sequences, substrate specificity and subunit composition, different classes of PHB polymerases can be distinguished (Rehm, 2003). The first class of PhaC comprises polymerases, which are PhaC homodimers and are present for example in *C. necator*. Similarly, class II, which contains PhaC1 and PhaC2 synthases and is present in *P. putida*, form also homodimers. In contrast to that, class III comprises heterodimers, such as PhaC-PhaE in *Synechcoystis* sp. PCC 6803. Also class IV synthases, which are for example present in *Bacillus* sp., are composed of two subunits. However, in the case of class IV, heterodimeric polymerases are composed of PhaC and PhaR. A

main difference between these four classes is that only class II is able to produce mcl PHA, while all other classes produce predominantly scl PHA, such as PHB (Jendrossek, 2009). It is known that the presence of certain metabolites, such as acetyl-phosphate, can alter the activity of PHB polymerase (Miyake et al., 1997).

The elongated polymer can subsequently be catabolized by PHA depolymerases, termed PhaZ. The latter can be either intra- or extracellular, depending on their purpose. In *C. necator*, there are seven different depolymerases annotated, indicating the importance of a regulated mobilization of PHB (Pohlmann et al., 2006).

Besides the enzymes mentioned above, some bacteria (like *P. putida*) possess further enzymes, which enable them to convert additional substrates into PHA. One enzyme is PhaJ, which converts enoyl-CoA into R-3-hydroxyacly-CoA and thereby connects the fatty acid ß-oxidation with the PHA synthesis (Fukui et al., 1998). PhaG, another enzyme found in *P. putida*, converts acyl-ACP to (R)-3-acyl-CoA and thereby links the fatty acid *de novo* synthesis to the PHA metabolism (Rehm et al., 1998). The fatty acid and PHA pathways are further interconnected by enzymes, which catalyze reactions in both pathways. For example, the enzyme FabG, which is actually part of the fatty acid biosynthesis, can also catalyze the same function as PhaB, but with a lower catalytic efficiency (Zhang et al., 2017). A complete model of the different pathways involved in the PHA metabolism is shown in Figure 6 (except the PHA depolymerization).

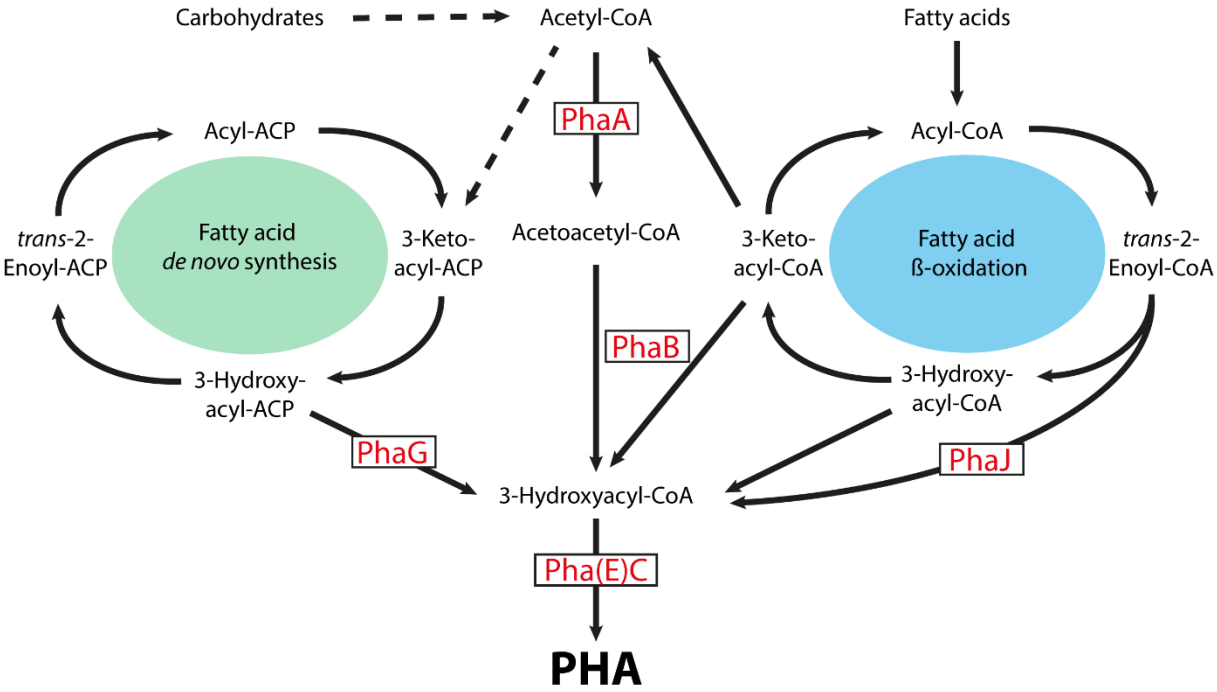

Figure 6. PHA metabolism and different metabolic pathways (Koch and Forchhammer, 2020). Important enzymes are highlighted in red. Not shown is the PHA depolymerization, which is utilized by PhaZ.

With all those enzymes in place, the entire PHA cycle is complete and acetyl-CoA can be completely metabolized to PHA and back again. Interestingly, some studies suggest that there could be a constant carbon flow of PHA synthesis and degradation. This way the cells could ensure that the right metabolic intermediates are available and could adapt the cell to environmental conditions. It was shown that PHA synthase and depolymerase are active at the same time, further supporting the initial hypothesis (Arias et al., 2013).

3.3 Proteins associated to PHB granules

Despite the simple structure of PHB, its granules are much more complex than just an accumulated polymer. Several proteins are located on the granule-surface or are involved in its metabolism and regulation. Due to this complexity, the name carbonosomes has been suggested to highlight that PHB granules are rather subcellular organelles and not just a prolonged chain of molecules (Jendrossek, 2009). In the following, the most important proteins, which are involved in PHB granule formation, maintenance and degradation, are described.

Phasins are low-molecular-weight proteins, which are directly attached to the surface of PHB granules (Mezzina and Pettinari, 2016). They are very abundant and serve various different purposes, such as structural, biosynthetic, catabolic and regulatory functions. Often these phasins are the predominant protein covering large parts of the granule-surface, whereby they also shield the cytoplasm from the hydrophobic PHB surface. A representative of such phasins is PhaP from *C. necator*. Here, several different kinds of PhaP are present, which cover the surface of the PHB granules. The amount of PhaP is tightly regulated and corresponds with the amount of intracellular PHB (York et al., 2001). A PhaP homologue was recently discovered in *Synechocystis* (Hauf et al., 2015). In *P. putida*, PhaF and PhaI are the main granule associated proteins (Prieto et al 1999).

Besides just covering the granules surface, phasins exhibit further functions. For example, PhaF from *P. putida* organizes PHA granules along the long-axis of the cell and ensures equal granule sharing upon cell division (Galán et al., 2011).When PhaF is not present, cells still produce PHA, but the entire cell population divides into cells with and other without PHA. PhaF is present as a homomeric tetramer, where the monomers possess an N-terminal helix and a short leucine zipper, potentially used for protein-protein interaction (Maestro et al 2013). With its DNA binding domain, PhaF furthermore serves as a regulator of the *pha* genes (Galán et al., 2011). The protein PhaI shares large similarities with the N-terminal region of PhaF, but without the leucine zipper. Although PhaI can be partially substituted by PhaF, both enzymes together are essential for a proper PHA metabolism.

Similarly to PhaF, in *C. necator,* PhaM has the function to bind to the PHB granulum as well as the DNA and thereby ensures equal distribution among the daughter cells. Additionally, PhaM activates the PHB synthase PhaC1 and thereby directly influences the PHB metabolism (Pfeiffer and Jendrossek, 2014). While PhaM regulates the PHB synthesis on the protein level, the regulators PhaR and PhaD regulate *pha* genes on a transcriptional level. In *C. necator*, PhaR binds upstream of *phaP* and thereby represses its transcription. Additionally, PhaR is also associated to PHB granules

(York et al., 2002). PhaD, on the other hand, serves as an activator in *P. putida*. Contrary to a long-time belief, it was recently demonstrated that PHB granules do not contain phospholipids on their surface (Bresan et al., 2016).

3.4 Physiological role of PHB in bacteria

The ability to produce PHB is widespread among different organisms. A phylogenetic analysis found the presence of the *phaC* gene in organisms from 40 different genera and within a wide range of taxonomical groups, highlighting how abundant the ability to produce PHB is (Kalia et al., 2007). This also demonstrates, how different the organisms are, which produce PHB, indicating different physiological functions of PHB based on the environment of the individual organism.

PHB are in general considered as carbon and energy storage, which are built up in time periods of carbon excess and which provide advantages in times of carbon shortage (Anderson and Dawes, 1990). This long-time belief still holds true for many bacteria, although more and more other physiological functions are recently discovered. Also, for some bacteria like cyanobacteria, no physiological relevance of PHB was yet discovered. The most important roles of PHB are described in the following.

In many organisms, PHB accumulates under conditions of nutrient limitation or unbalanced conditions, such as nitrogen limitation (Anderson and Dawes, 1990). However, there are also bacteria, like *C. necator*, which do accumulate PHB even during normal growth and under balanced conditions (Jendrossek and Pfeiffer, 2014). Nevertheless, the amount of accumulated PHB is usually higher when grown under nutrient limitation.

Another important aspect of PHB, besides serving as a storage polymer, is the ability to increase resistance against various kinds of stress. In *Azospirillum brasilense* for example, PHB deficient strains are more susceptible against abiotic stresses, such as UV irradiation, heat, desiccation, osmotic pressure and osmotic shock (Kadouri et al., 2003). In *Sinorhizobium* strains, an induced PHB accumulation after exposure to high salt concentrations was observed (Arora et al., 2006). In *Aeromonas hydrophila* the production of a poly(3HB-*co*-3HHx) copolymers results in increased resistance against a wide variety of abiotic stresses, including UV irradiation, hydrogen-peroxide, ethanol, heat and cold treatments and high osmotic pressure (Zhao et al., 2007). Interestingly, a study investigating *Pseudomonas oleovorans* showed that even the deletion of the PHA depolymyerase PhaZ was sufficient to increase the sensitivity towards hydrogen-peroxide and heat shock (Ruiz et al., 2004). This demonstrates that the entire PHB metabolism, including its mobilization, is important for providing stress tolerance to the PHB producing cells, rather than the sheer presence of the polymer (Castro-Sowinski et al., 2009). PHB was furthermore shown to increase the number of viable cells by protecting *C. necator* cells against cold stress (Nowroth et al., 2016). Additionally, in *Herbaspirillum seropedicae*, studies demonstrated that PHB reduces intracellular redoxstress, potentially by eliminate a surplus of reducing equivalents and thereby serving as an electron sink (Batista et al., 2018). In a similar way PHB is used in *Chromatium vinosum*, although here it rather serves as an electron storage than a sink. This anoxygenic phototrophic

bacterium converts glycogen to PHB under dark, anaerobic conditions. This provides the strain with the advantage over other fermenting organisms, which commonly secrete their fermentation products and thereby loose carbon (van Gemerden, 1968). Another example of the role of PHB can be found in *Bacillus cereus*: this bacterium produces most PHB just before the formation of spores and degrades it after sporulation, indicating the importance of PHB for surviving their dormant state (Valappil et al., 2007, Castro-Sowinski et al., 2009). Several studies also found an interconnection between PHB production and the formation of EPS (exopolysaccharides). Sometimes a mutant with impaired PHB production resulted in a higher EPS production (Wang et al., 2008), while in other strains, a lower PHB production correlated with lower EPS production. In the latter case, the authors suggest that the increased EPS production is attributable to the intracellular mobilization of carbon sources (PHB) (Kadouri et al., 2003).

Interestingly, PHB producing *Azospirillum brasilense* was able to endure long periods of starvation , but it also showed certain disadvantages compared to a PHB-free mutant, such as lower motility or impaired root adhesion and EPS production (Kadouri et al., 2002). This indicates that the ability to store PHB is not always an advantage but has to be balanced based on the environmental conditions. In a similar manner, *Sinorhizobium* bacteria were shown to use a bet-hedging strategy to produce offspring with higher or lower amounts of PHB. These offspring are better adapted for long or short period starvation, respectively (Ratcliff and Denison, 2010).

Another interesting function of PHB could be the provision of nutrients to a microbial community (Prieto et al., 2016). When a PHB producer, which converts inorganic carbon to a condensed carbon polymer, is decomposed for example by predatory bacteria, it releases its PHB granules to the environment (Jendrossek and Handrick, 2002). Thereby, the energy rich carbon polymer is made available to the microbial community. In coherence with this observation, most identified PHA depolymerases are those, which function extracellularly (Prieto et al., 2016). It was also shown, that predatory *Bdellovibrio* cells have a growth advantage when they were preying on PHA producing cells compared to a PHB-free mutant (Martínez et al., 2013). This further highlights the importance of PHB for the bacterial environment.

Since PHA producer, like some cyanobacterial strains, can convert inorganic carbon to an organic carbon polymer, degradation of these producer strains, for example by predatory bacteria, would release the granules into their environment. The released granules can then serve as potential substrate for other heterotrophic microorganisms (Jendrossek and Handrick, 2002). This fits well to the observation, that most identified PHA depolymerases are those, which function extracellularly (Prieto et al., 2016). It was also shown, that predatory *Bdellovibrio* cells have a growth advantage when they were preying on PHA producing cells compared to a PHB-free mutant (Martínez et al., 2013). This further highlights the importance of PHB for the microbial community.

Additional physiological functions of PHA in bacteria are summarized and further described in recent reviews (Castro-Sowinski et al., 2009, Obruca et al., 2020)

3.5 Physiological function in cyanobacteria

A large group of PHB producer are cyanobacteria. In a recent study, 137 different cyanobacterial strains were investigated for their ability to produce PHB. Out of these 137, 134 were PHB producers (Kaewbai-Ngam et al., 2016). Interestingly, a phylogenetic analysis revealed, that the full set of functional *phaABC* genes appeared for the first time in cyanobacteria, indicating its importance for cyanobacterial growth (Kalia et al., 2007). Although PHB appears to be very common in the phylum cyanobacteria, its physiological function is yet undiscovered. In recent years, several groups have tried to answer this question, for example by comparing a PHB-free Δ*phaEC* strain to a PHB-producing wildtype, the true function of PHB remains puzzling (Damrow et al., 2016, Klotz et al., 2016). Cyanobacteria produce PHB mostly under unbalanced growth conditions, for example when they are grown in a medium lacking either nitrogen, phosphate or potassium (Kaewbai-Ngam et al., 2016). Additional organic carbon sources, like acetate or fructose, can further increase the PHB production (Panda et al., 2006). PHB metabolism in cyanobacteria is best described during nitrogen starvation, which triggers a process called chlorosis (Koch et al., 2020, Troschl et al., 2017). PHB slowly accumulates during the course of several weeks; depending on the cyanobacterial strain, up to 25 % PHB per cell-dry-weight can be accumulated (Kaewbai-Ngam et al., 2016). PHB is commonly stored in a few granules, which are located in the middle of the cell (Hauf et al., 2015). Compared to other PHB producers, only relatively little is known about the proteins, which are involved in PHB metabolism. Although recently new proteins were found to play a role (for example the phasin PhaP) (Hauf et al., 2015), more proteins, like for example PHB degrading enzymes, are to be discovered. Most studies were performed in the strain *Synechocystis*, which serves as a well characterized model strain for cyanobacterial metabolism. In the following, the latest discoveries and hints towards PHB's physiological role are summarized.

3.5.1 The role of PHB during nutrient limitation

Cyanobacteria are known for producing a variety of different storage compounds, such as glycogen, cyanophycin or polyphosphate. In contrast to the unknown function of PHB, the polymers glycogen and cyanophycin can clearly be linked to carbon and nitrogen storage metabolism, respectively (Doello et al., 2018, Watzer and Forchhammer, 2018). As previous studies have shown, glycogen is the main carbon- and energy storage compound under conditions of nutrient limitation (Klotz et al., 2016, Doello et al., 2018) and its biosynthetic genes were found in all cyanobacterial genomes (Beck et al., 2012). It is remarkable that cyanobacteria produce two different carbon polymers, since most other microorganisms produce just one. This clearly indicates that the two carbon-polymers have different functions. Remarkable differences between PHB and glycogen are, that glycogen shows a higher solubility in water than PHB and that PHB forms much larger granules than glycogen. In contrast, glycogen shows a more complex branching pattern, making it potentially able to be sterically more condensed. It was already hypothesized, that the relatively small glycogen granules could serve as a quick-response carbon storage, due to its easier accessibility based on a larger surface to volume ratio, whereas PHB could instead form a long-term storage. However, under

conditions of nitrogen limitation, no physiological differences were ever discovered between WT and a PHB-free Δ*phaEC* mutant strain (Damrow et al., 2016).

3.5.2 Potential role of PHB in controlling the redox state

Besides conditions of nutrient limitation, glycogen is the essential energy and carbon storage during dark phases, where no photosynthesis can take place. Excess of energy gets stored in the form of glycogen during the day, while during the night, the polymer can be degraded during the night and generate energy and carbon to sustain the cyanobacterial metabolism. Although no studies so far have shown a PHB accumulation during conditions of balanced growth, there are several indicators that PHB might play a role during dark phases. Transcriptomic data from several studies have shown very clearly, that all PHB related genes are strongly upregulated at the beginning of the night and downregulated during the day (Saha et al., 2016, Kucho et al., 2005). It was furthermore shown, that PHB related genes are strictly controlled by the circadian clock (Köbler et al., 2018). Interestingly, the transcripts for PHB synthesis are countercyclically regulated to those of the glycogen metabolism. While the transcripts for glycogen synthesis are upregulated during the beginning of the day and downregulated during the beginning of the night, the PHB synthesizing genes are regulated in the exact opposite. This hints towards a conversion of both metabolites into each other. However, also during growth night, a PHB free mutant shows no growth phenotype, while the growth of glycogen free mutants is severely impaired (Damrow et al., 2016).

Fitting to these observations, PHB was already in the past considered to play a role as a potential electron sink, whereby PHB could store excess of electrons, since the formation of one PHB subunit requires one NADPH (De Philippis et al., 1992). This hypothesis, that PHB formation in cyanobacteria is involved in redox homeostasis, was further corroborated in studies by Schlebusch and Forchhammer (2010) and Hauf et al., (2013). A *Synechocystis* mutant, unable to accumulate PHB during nitrogen starvation, was characterized in detail (Schlebusch and Forchhammer, 2010). In this mutant, the gene *sll0783,* which belongs to the most strongly induced genes during nitrogen starvation, was knocked out. This gene is the first gene of the Nit1C operon, a highly conversed gene cluster present in cyanobacteria and many other bacterial species (including proteobacteria and actinobacteria), enabling the utilization of cyanide (Jones et al., 2018). Many heterotrophic bacteria possessing this gene cluster are able to produce PHB and to fix nitrogen. Since the entire operon was highly upregulated in *Synechocystis* during nitrogen starvation, a role during nitrogen-chlorosis was suspected. Further analysis revealed, that the Δ*sll0783* mutant showed a strong decrease in its PHB synthase activity (Schlebusch and Forchhammer, 2010). Induction of expression of the PHB synthesis genes (*phaAB* and *phaEC*) was delayed as compared to the WT. However, in contrast to the expression of the *phaCE* genes, the activity of PHB synthase decayed in the mutant following an initial transient increase. Interestingly, the Δ*sll0783* mutant showed an impairment in its recovery from nitrogen starvation, which implied that that this could be due to decreased amounts of PHB in the sll0783 mutant. However, subsequent work showed that the ability to produce PHB *per se* is not relevant for resuscitation from nitrogen starvation (Damrow et al., 2016, Klotz et al., 2016). The inability of the Δ*sll0783* mutant to sustain PHB synthesis could finally be attributed to the redox-

state of the cells: during nitrogen-starvation, the NADPH/NADP$^+$ ratio steadily increased in wild-type cells, whereas in the Δ*sll0783* mutant it remained constant. Treatment of the mutant cells with the protonophore CCCP or the ATPase inhibitor DCCD restored PHB synthase activity and PHB synthesis due to a compensatory increase in the NADPH/NADP$^+$ ratio (Hauf et al., 2013). Inhibition in ATP synthesis arrests anabolic reactions that consume NADPH. This highlights that the increased levels of NADPH trigger synthesis of PHB. Hence, the formation of PHB would be particularly beneficial whenever a surplus of NADPH cannot be metabolized, for example because respiration is not possible and anaerobic processes are required. In this scenario, PHB would serve as an intracellular electron sink with the advantage to sustain all intracellular carbon, instead of secreting it like other fermentation products, such as acetate. Since this is advantageous under conditions of electron excess, such as anaerobic growth, the EMP pathway is also the most relevant during fermentation processes (Stal and Moezelaar, 1997).

Another role of PHB could be a storage to prevent intracellular acidification: it was shown that a PHB free *C. necator* secretes pyruvate into its medium (Raberg et al., 2014). This fits to a previous observation, where *Synechocystis* mutants unable to synthesize glycogen secrete pyruvate and 2-oxoglutarate under conditions of carbon excess such as growth with additional glucose or during nitrogen starvation (Grundel et al., 2012). Here the authors argue that it is extremely important for the cells to have a carbon sink to control their carbon homeostasis or to avoid energy spilling. Potentially PHB could here serve as an additional buffer for storing excess carbon, particularly because it is metabolically closer to pyruvate than glycogen. However, in contrast to the glycogen-deficient mutants, no studies have reported secreted organic acids in the supernatant of a PHB-free mutant. To further investigate this, future studies should investigate secreted metabolites under different growth conditions in a Δ*phaEC* mutant and compare it to a WT.

Interestingly, it was shown that the formation of PHB sometimes shows a phenotypical heterogeneity. This indicates that the formation of PHB is not always beneficial, but rather a bet-hedging strategy of the cells to be prepared for different potential outcomes (Ratcliff and Denison, 2010). This further highlights that the ability to possess PHB might be relevant under only very specific scenarios, hence making the physiological function hard to discover.

3.6 Biotechnological applications

Nowadays, most industrially produced PHB comes from heterotrophic bacteria, like *C. necator*. This organism comes with many advantages, as it is fast growing and shows high accumulation of PHB (~90% / CDW) (Anderson and Dawes, 1990). However, one of its limitations is the organic carbon source, which *C. necator* requires for high PHB accumulation (Reis et al., 2003, Mudliar et al., 2007). Additionally, these organic carbon sources are usually produced from plants like maize, which requires valuable cropland. Especially in the future, when the degradation of arable farmland is progressing due to climate change, using food crops for the production of plastics would become more of an ethical problem (Harding et al., 2007, Issa et al., 2019, Posen et al., 2016). Hence, a more sustainable way of producing PHB, especially on a large scale, is urgently needed. As cyanobacteria

could be helpful organisms to achieve this goal, their potential and obstacles for an industrial production of PHB are described in the following sub-chapters.

3.7 Genetical engineering of cyanobacteria for PHB production

Besides introducing pathways to provide more PHB precursors, several other strategies have been applied to genetically alter *Synechocystis.* Detailed lists about created strains and their produced yield have been previously reviewed in several publications (Kamravamanesh et al., 2018b, Singh and Mallick, 2017, Vieira et al., 2018).

The most common approach was to overexpress native or heterologous PHB synthesis genes (Khetkorn et al., 2016, Hondo et al., 2015, Takahashi et al., 1998, Sudesh et al., 2002). Often the genes *phaABC* of *C. necator* were used, since this species can natively reach values of up to 80% PHB / CDW. These genes were then coupled to strong promotors, like psbA2, which originally sits in front of the gene which encodes for the D1 protein of the Photosystem II and shows very high expression levels (Khetkorn et al., 2016, Englund et al., 2016).

Another interesting approach has been suggested by Osanai *et al.*, when they overexpressed the response regulator *rre37* (Osanai et al., 2014). This caused an acceleration of the glycogen catabolism. As shown recently, the intracellular pools of PHB and glycogen are connected (Velmurugan and Incharoensakdi, 2018). Hence, a degradation of the latter causes an increase of the former. A similar effect was observed when the sigma factor *sigE* was overexpressed (Osanai et al., 2013). Again, an increase of glycogen degradation and PHB synthesis genes was observed, leading to higher overall values of PHB. However, the effects of upregulated glycogen/PHB metabolism genes appeared to be rather transient, since they are changing during the course of chlorosis (Nakaya et al., 2015).

With the emergence of new technologies, genetic alterations could be achieved even faster. The discovery of CRISPR Cas allows markerless genome editing (Wendt et al., 2016), while CRISPRi allows to specifically tune down the gene expression (Yao et al., 2016b). However, the efficiency of this relatively new technique has to be further optimized (Behler et al., 2018, Ungerer and Pakrasi, 2016).

Some of the highest intracellular PHB values have been achieved in a random mutagenesis approach. By applying UV light, random mutations were introduced, which were then screened for strains with high PHB production rates (Kamrava et al., 2018). In one of these screenings, a mutant was discovered which produces 2.5 times more PHB compared to the WT.

4. Research questions

The ability to produce PHB is widespread among different forms of life. Particularly, a wide range of bacteria produce PHB and its derivatives for various reasons. At the same time, PHB is of high biotechnological relevance, due to its similar properties to conventionally used plastics. Therefore, gaining deeper insights into PHB metabolism is of high relevance for basic- as well as for applied research. The following research questions were investigated in this work:

1. PHB is particularly common among organisms belonging to the phylum cyanobacteria. Despite its abundancy, its physiological function in cyanobacteria remain unknown (Damrow et al., 2016). Furthermore, only very little knowledge is available about which conditions influence PHB formation.

2. The enzymes involved in the biosynthesis of PHB were discovered long ago. However, in the recent years it became clear, that PHB granules are highly structured organelles ("carbonosomes"). Although the metabolism is intensively studied in organisms like *C. necator*, only very little knowledge is available about how PHB is metabolized in cyanobacteria. This involves fundamental questions such as where the carbon, which is the most important element in PHB, is derived from. Recent ^{13}C analyses have only revealed that the carbon present in PHB is based on intracellular recycling (Dutt and Srivastava, 2018), but it remained unclear, from where within the cell the carbon is derived.

3. Furthermore, gaining deeper insights into which carbon pathways are involved in the PHB metabolism might elucidate more knowledge about its physiological function.

4. So far, only very few proteins involved in the PHB formation and degradation are known in cyanobacteria. Foremost, the PHB depolymerase, an essential enzyme for PHB mobilization, has not yet been found. Additionally, only one phasin, PhaP, has recently been discovered (Hauf et al., 2015). It is very likely that, like in other bacteria, more proteins and phasins are involved in the PHB metabolism.

5. So far, the distribution of PHB within a homogeneous culture has not been investigated.

6. As mentioned before, PHB has been in the focus of biotechnological industry for years, due to its good material properties as well as its biodegradability. However, PHB is usually produced from heterotrophic organisms, requiring an organic carbon source for the production. One great advantage of the natural PHB producer *Synechocystis* is that its photosynthesis enables it to produce PHB carbon neutral by fixing the CO_2 required for the PHB synthesis directly from the atmosphere. However, so far, the market potential of cyanobacterial PHB is still rather limited, especially due to low prediction yields. Although several groups tried to further increase the amount of accumulated PHB, most of them barely increased the intracellular contents. Hence, creating PHB overproduction strains would be desirable.

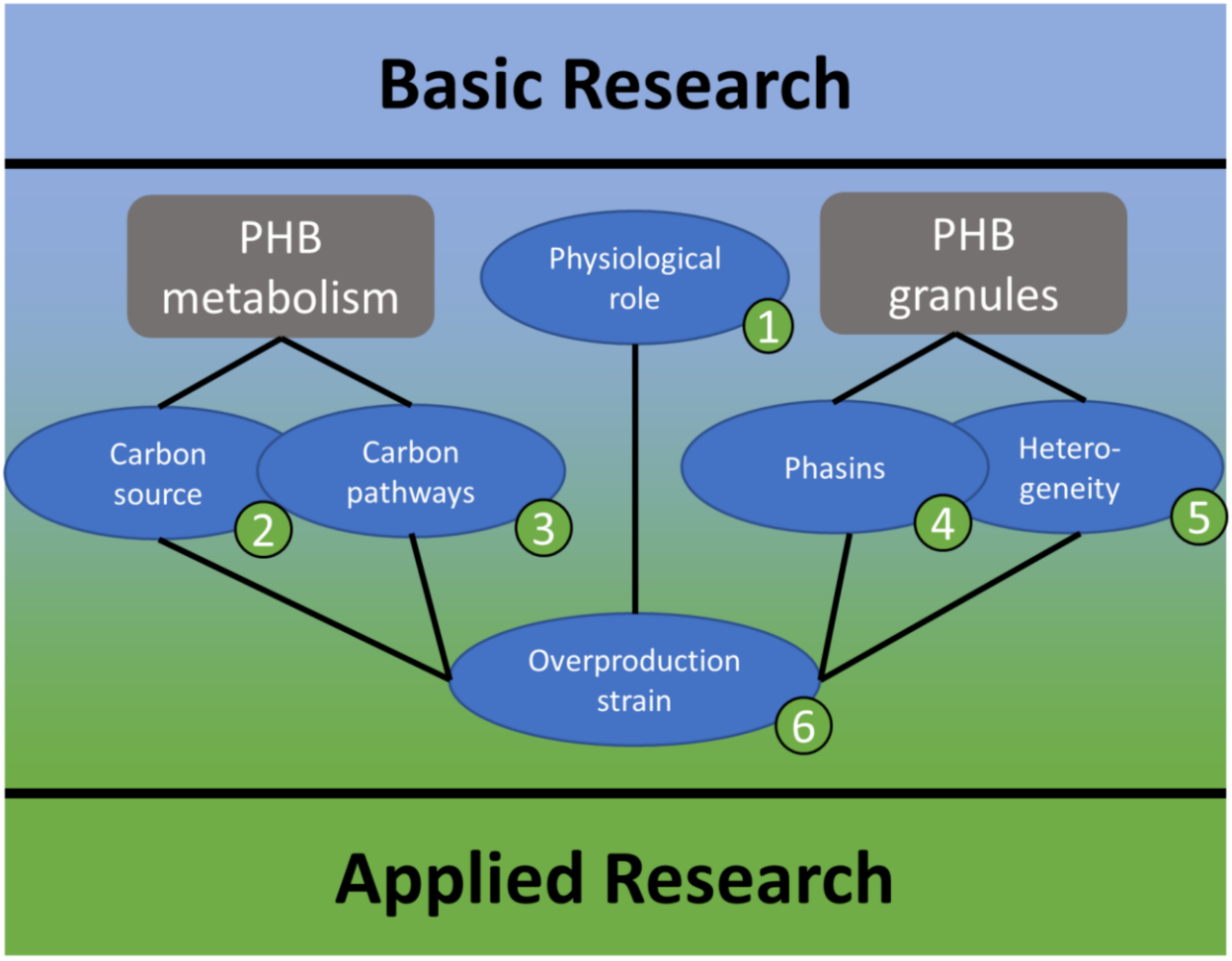
Basic Research
PHB metabolism
Physiological role
PHB granules
1
Carbon source
Carbon pathways
2
3
Phasins
Hetero-geneity
4
5
Overproduction strain
6
Applied Research

VI. Results

The main results of the following publications are summarized in section VI "Results". Section VI also provides non-published, additional results related to the publications.

- **M. Koch,** S. Doello, K. Gutekunst, K. Forchhammer (2019).
  PHB is Produced from Glycogen Turn-over during Nitrogen Starvation in Synechocystis sp. PCC 6803.
  International Journal of Molecular Sciences, 20, 1942.

- **M. Koch**, T. Orthwein, J. T. Alforth, K. Forchhammer (2020).
  Investigation of PHB related proteins in Synechocystis sp. PCC 6803 revealed novel phasin Slr0058.
  Frontiers in Microbiology, 2020, 11:809

- **M. Koch**, K. Berendzen, K. Forchhammer (2020).
  On the role and production of PHB in the cyanobacterium *Synechocystis* sp. PCC 6803.
  Life, 2020, 10, 47

- **M. Koch**, Jonas Bruckmoser, Jörg Scholl, Waldemar Hauf, Bernhard Rieger, K. Forchhammer.
  Maximizing PHB content in *Synechocystis* sp. PCC 6803: development of a new photosynthetic overproduction strain.
  Microbial Cell Factories (Manuscript in preparation)

1. The physiological role of PHB

The presence of PHB in cyanobacteria is known for a long time (Carr, 1966) and it is very abundant among various cyanobacterial species (Kaewbai-Ngam et al., 2016). However, only little is known about the physiological role of PHB in cyanobacteria, as well as the conditions which influence the formation of PHB.

1.1 Heterogeneity

One interesting phenomenon about the PHB formation is the unequal distribution of granules per cell. When a population of nitrogen starved *Synechocystis* cells is investigated under a microscope, a strong heterogeneity in the amount of PHB granules per cell can be observed (Figure 7 A). To further investigate this phenomenon, we analyzed the intracellular PHB content of individual cells within a *Synechocystis* cultures applying flow-cytometry (FC). For this, intracellular PHB granules were stained via a fluorescent dye (Bodipy) to detect the granules with FC. Interestingly, the FC analysis revealed that there is no Gauss distribution of PHB within the cells. Instead, most cells contained mediocre amounts of PHB, while a smaller part of the population accumulated larger quantities (Figure 7 B).

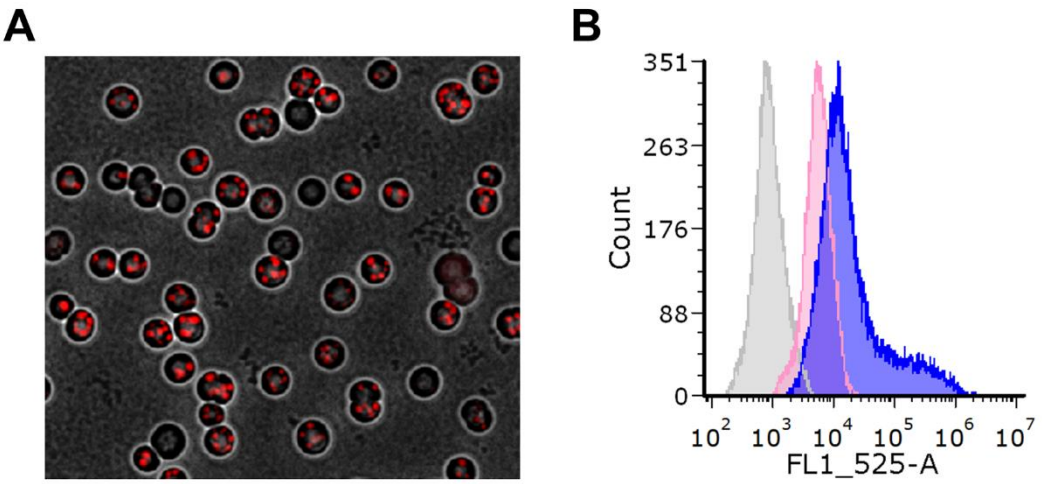

Figure 7. Heterogeneity in PHB content among nitrogen starved *Synechocystis* cells. (A) Analysis via fluorescence microscopy of cells which were starved from nitrogen for 14 days. The PHB granules were stained with Nile red to visualize them. (B) Flow-cytometry analysis of intracellular PHB content in *Synechocystis* cells stained with bodipy. The y axis shows the number of cells, while the x axis shows Nile red fluorescence to indicate PHB content. Blue curve: *Synechocystis* WT cells. Grey curve: unstained WT cells. Red: Stained Δ*phaEC* mutant (PHB-free) cells (Publication 5).

To test whether this distribution was based on an inheritable effect, chlorotic cells were separated into two groups (low and high PHB producer) based on their PHB content, by applying a fluorescence-activated cell sorter (FACS). The results showed that cells from both groups established the same distribution pattern as in the initial experiment (Figure 7 B, Publication 5 Figure 7) . This demonstrates that the decision, if a cell becomes a low- or high-PHB-producer, does not depend on a heritable trait, but much rather on a probabilistic genetic program. Similar bet-

hedging strategies have already been observed in other PHB producers before (Ratcliff and Denison, 2010). The results indicate that the PHB production is only relevant under specialized conditions, since only a small fraction of the entire population exhibited a high PHB content.

1.2 Conditions affecting PHB synthesis

In order to gain deeper insights into the conditions, under which PHB has a physiological relevance, nitrogen starved *Synechocystis* cells were cultivated under different growth conditions. As a control, a PHB free Δ*phaEC* mutant was grown under the same conditions.

In confirmation with previous studies, the results show that PHB has no impact on the ability to survive and resuscitate from nitrogen starvation (Publication 5, Figure 3). This was demonstrated by monitoring the reappearance of photosynthetic pigments as well as the photosynthetic activity of photosystem II. In both cases, no difference between the WT and the Δ*phaEC* mutant were observed. To see how different cultivation conditions influence the PHB production, nitrogen starved cells were cultivated at different aeration and illumination (Publication 5, Figure 1). Here it became apparent that growth under dark/light regime intensified the PHB production, while an impaired gas exchange (caused by a non-shaking treatment) reduced the PHB production.

When the same set of cultivation conditions were applied to nitrogen starved mutants of the central carbon metabolism (lacking either the EMP pathway or the OPP pathway, Δ*pfk* or Δ*zwf*, respectively), it became clear that the EMP pathway is the most relevant for the formation of PHB, while the OPP plays only a minor role (Publication 5, Figure 2).

Finally, several abiotic stress conditions were applied to nitrogen starved chlorotic WT cells and their viability was compared to a Δ*phaEC* mutant. Although more than 30 different conditions were tested (including different temperatures, salt concentrations etc.), under none of them the PHB containing WT showed a growth advantage compared to the PHB free Δ*phaEC* mutant (Publication 5, Table 1). This indicates that the conditions, under which PHB-containing cells exhibit a growth advantage over non-PHB producers, have still to be found.

1.3 Additional results: Δ*phaEC* mutant characterization

To find conditions, where the ability to produce PHB is advantageous, the differences between WT and Δ*phaEC* were further characterized under a variety of cultivation conditions. In order to see, if there are differences during vegetative growth, the combination of four different parameters were compared: growth at continuous light or growth during dark/light regime, as well as growth during continuous shaking or growth in a standing flask. Over the course of four days, OD_{750} was monitored. While both strains grew comparably under most conditions, strong differences were observed during standing+day/night rhythm conditions. Here, the growth of the Δ*phaEC* mutant strain was drastically impaired compared to the WT (Figure 8).

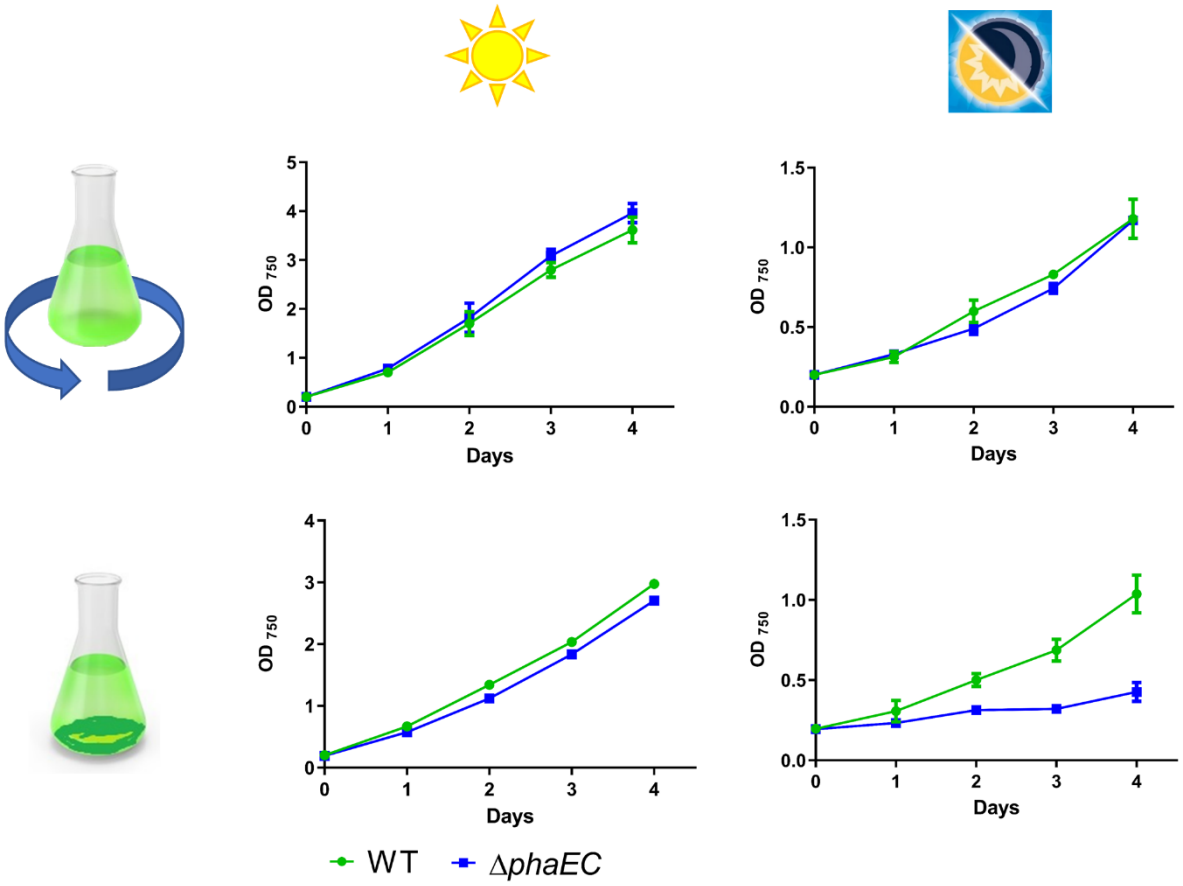

Figure 8. Growth curves of vegetative *Synechocystis* WT and Δ*phaEC* mutant cultures under different growth conditions. Top row: continuous shaking. Bottom row: standing. Left column: continuous illumination. Right column: 12/12 hour dark/light cycles. Each point represents a mean of three independent biological replicates.

The results showed that the combination of both, dark phases and limitation of gas-exchange, caused a growth deficiency in the Δ*phaEC* strain, although growth occurred in BG_{11} medium with all nutrients provided. To further understand what limits the growth of the Δ*phaEC* strain during the standing/light-dark conditions, further experiments were performed. For this, all following experiments were performed under the same standing and dark/light conditions as the experiment shown in Figure 8.

To validate if limited supply CO_2 was the cause for the impaired growth, WT and Δ*phaEC* cells were grown in BG_{11} medium, which was supplemented with 100 mM $NaHCO_3$ (Figure 9 A). However, the additional carbon source could not restore the mutant's phenotype, suggesting that carbon appears not to be the limiting factor.

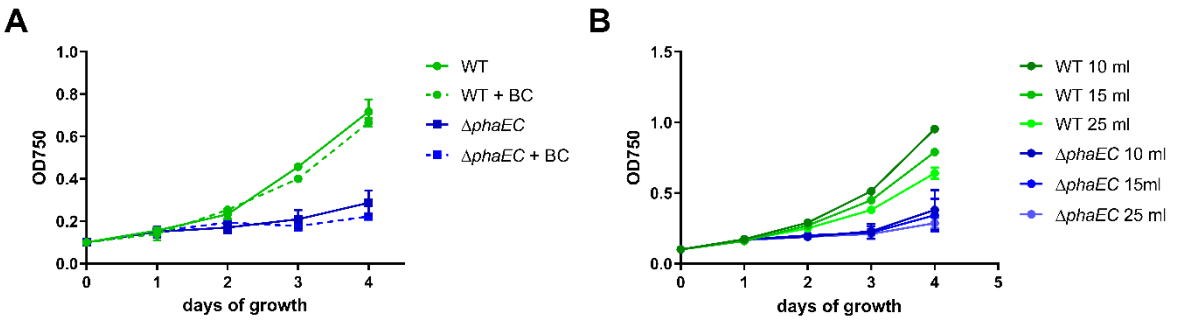

Figure 9. Growth comparison between WT and Δ*phaEC* strain under different growth conditions. All cultures were incubated at standing conditions and dark/light regime. (A) Cultures were grown with 100 mM bicarbonate (dotted line) or without (solid line). (B) Different culture volumes were used and incubated in identical containers (25 ml Erlenmeyer flask) to simulate different water columns. Each point represents a mean of three independent biological replicates.

To test, whether a larger water column above the standing cells could intensify the limitation of gas exchange, cells were grown in different culture volumes. Additionally to the original conditions, cells were grown in 10, 15 and 25 ml medium. However, a higher water column decreased the growth rates of both, the WT and the Δ*phaEC* strain. Hence, the largest difference was observed at growth in 10 ml medium, since the WT grew relatively fast under these conditions (Figure 9 B).

Besides CO_2, the other major gas which is relevant for cyanobacterial growth is oxygen, particularly when cultivated in dark phases, where cells perform respiration. To see if the oxygen availability was sinking to a level, where anaerobic conditions occur, the oxygen levels within standing WT and Δ*phaEC* cultures were monitored online over several consecutive days. To finally test, how the oxygen levels change during prolonged phases of darkness, the cells were kept in the dark for the last two days at the end of the experiment (Figure 10).

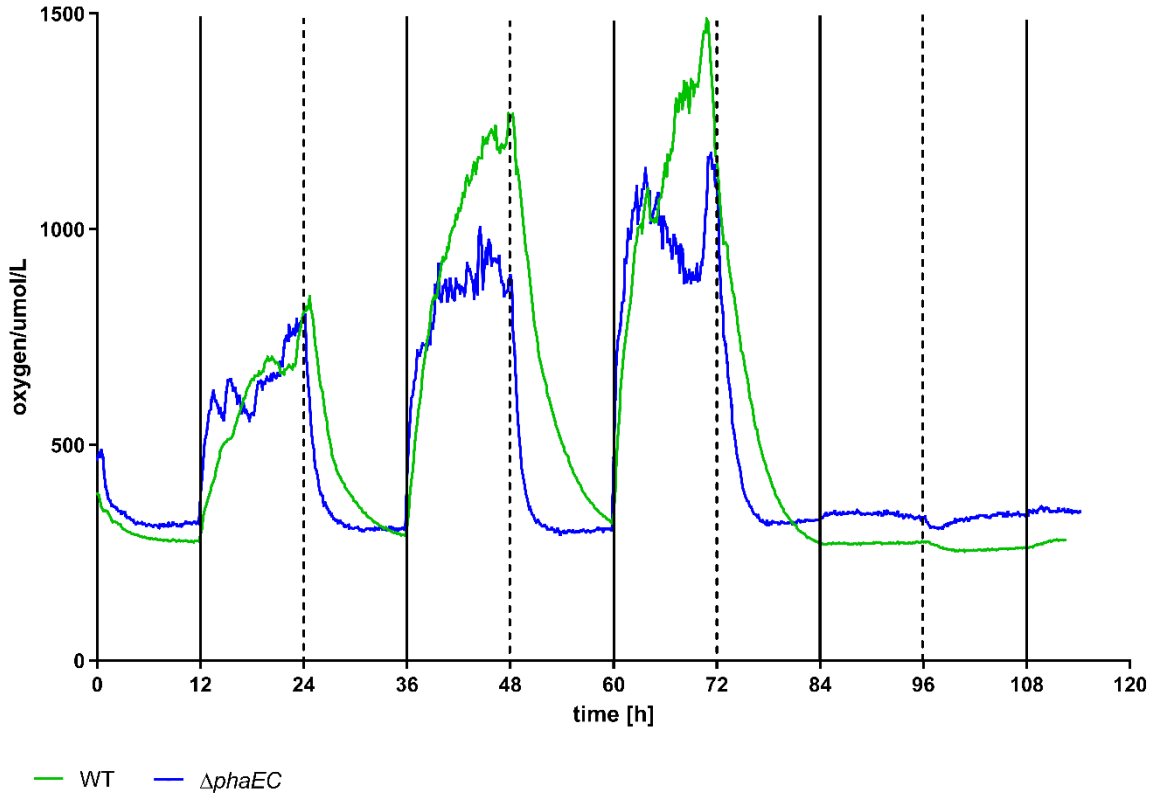

Figure 10. Oxygen measurements of standing WT and Δ*phaEC* cultures at 12/12 hours dark/light regime. The measurement was started at the beginning of the night. Solid vertical lines indicate the beginning of the light phase, while dotted lines show the start of the dark phases. After 72 hours, the cells were kept in the dark. Oxygen was detected via an oxygen sensor placed at the bottom of the incubation flask. The equilibrium level was determined at~390µmol/l.

Although the oxygen levels never reached fully anoxic conditions, during dark phases they were diminished to ~80 % of the equilibrium levels. Interestingly, the Δ*phaEC* strain showed a slightly different oxygen production and consumption pattern compared to the WT. During the day, the Δ*phaEC* strain produced less oxygen and in a more fluctuating way, while during the night the mutant strain consumed the oxygen more rapidly. During the prolonged dark phases at the end of the experiment, both strains still consumed small amounts of oxygen, which matched the circadian rhythm.

To test if PHB could play a role in buffering excess electrons or reducing redox stress caused by reactive oxygen species, WT and Δ*phaEC* strains were grown under conditions of different light intensities. Under low light (10 µE), the WT strain grew only slightly faster than the mutant strain. Interestingly, under high light conditions (70 µE), the Δ*phaEC* strain grew slower than under low light, while the growth rate of the WT drastically increased (Figure 11 A).

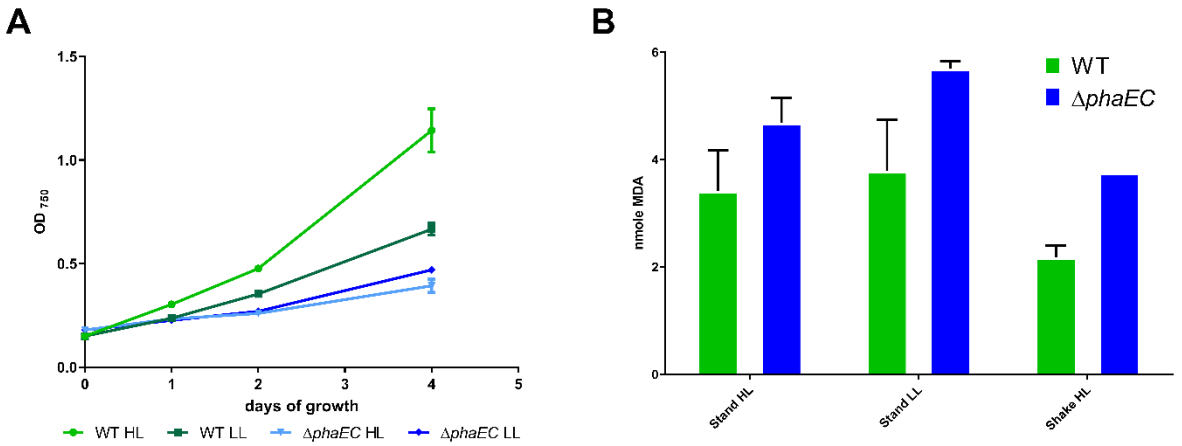

Figure 11. Effect of different light intensities on growth and redox stress of WT and Δ*phaEC* cultures. All cultures were cultivated at dark/light regime. (A) Growth curve of standing cultures cultivated at low light (10 µE) and high light (70 µE). (B) Intracellular accumulation of MDA (malondialdehyde), a lipid peroxidation marker. Samples were taken from cultures which were either standing or shaken. HL = high light, 70 µE; LL = low light, 10 µE.

During incubation at high light, the occurrence of ROS (radical oxygen species) is increased. To test how different illumination influence the creation of ROS within WT and Δ*phaEC* cultures, the intracellular amount of MDA (malondialdehyde) was measured (Figure 11 B). MDA serves as a marker for lipid peroxidation, which are caused by intracellular redox species. The MDA content was measured under different light intensities and aeration conditions. In these experiments, the overall amounts of MDA were lower in cultures, which were shaken compared to standing cultures. Furthermore, the Δ*phaEC* strain always exhibited higher MDA levels than the WT, indicating increased levels of redox stress.

To validate that the observed phenotypes are directly caused by the absence of the *phaEC* genes, the mutant was complemented with the *phaEC* operon on a plasmid. Furthermore, the Δ*phaEC* deletion was also introduced to a different background (a glucose tolerant (GT) WT strain). All strains were grown under standing and dark/light conditions.

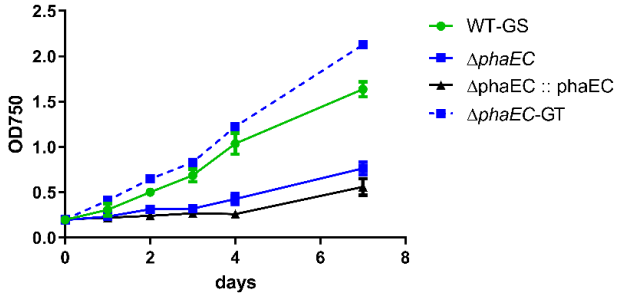

Figure 12. Growth curves of different strains at standing, dark/light conditions. Each point represents a mean of three independent biological replicates.

Surprisingly, the complementation was unable to recover the WT phenotype and the complemented strain still showed an impaired-growth phenotype. Although microscopic analysis revealed that the complemented strain regained its ability to produce PHB, the impaired growth phenotype

remained. This could be explained by the design of the mutant strains: While the Δ*phaEC* strain lacked the entire annotated transcriptional unit TU946, the complementation reintroduced only both deleted genes, *slr1829* and *slr1830*. In addition to these two genes, the TU946 harbors a downstream sequence of several hundred basepairs, which overlap with a gene of unknown function on the antisense DNA strand (*sll1736*). Bioinformatic analysis revealed, that the gene product of *sll1736* could serve as a protein, which is relevant for the respiratory chain. Furthermore, when the Δ*phaEC* mutation was introduced in the GT background, no impaired growth was observed.

2. PHB metabolism in *Synechocystis*

2.1 PHB is derived from intracellular glycogen pools

Despite the growing interest in cyanobacterial PHB, only very little knowledge is available about molecular details of PHB metabolism. One open question is where the carbon required for PHB formation is derived from. While it is known, that most of it comes from intracellular sources (Dutt and Srivastava, 2018), its exact origin remained puzzling. To test whether the intracellular glycogen and PHB pools are interconnected, enzymes involved in the glycogen synthesis were deleted (Publication 1). The resulting strains (Δ*glgA1*, Δ*glgA2* and Δ*glgC*) were analyzed for their intracellular glycogen and PHB accumulation during three weeks of nitrogen starvation. The experiments revealed that two strains (Δ*glgA2* and Δ*glgC*) showed only mild decreases in their intracellular PHB production. The Δ*glgA1* strain on the other hand exhibited drastically decreased PHB levels (Publication 1, Figure 3).

In another experiment, strains which were impaired in the degradation of glycogen (strains (Δ*glgP1*, Δ*glgP2* and the double knockout strain Δ*glgP1/2*) were also investigated (Figure 13). Similar to the glycogen synthase mutants Δ*glgA1* and Δ*glgA2*, only one of the two glycogen phosphorylase strains showed a difference compared to the WT. In this case, the Δ*glgP2* produced drastically less PHB, which was also the case for the double knockout strain Δ*glgP1/P2*. Furthermore, these two strains showed also a decelerated glycogen mobilization over the course of the chlorosis (Figure 13).

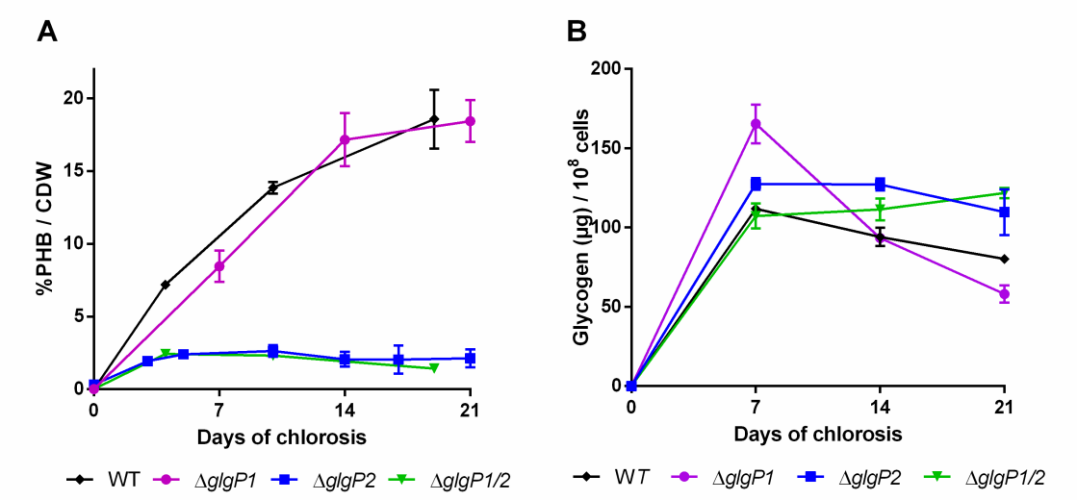

Figure 13. PHB content in percentage of cell dry weight (CDW) (A) and glycogen content (B) of mutants impaired in the glycogen degradation. Cultures were shifted to nitrogen free medium at day 0 and were subsequently cultivated for 21 days. Each point represents a mean of three independent biological replicates (Publication 1).

2.2 The EMP pathway is the most relevant pathway for PHB production

To identify the relevance of the three main carbon catabolic pathways for PHB production during chlorosis, knockout strains of the EMP, the ED and the OPP pathway were investigated (Δ*pfk,* Δ*eda* and Δ*gnd*, respectively) (Publication 1, Figure 6). It turned out, that the Δ*eda* strain produced similar amounts of PHB as the WT, while the Δ*gnd* strain produced slightly less. Most strikingly, the Δ*pfk* strain showed a drastic reduction in its PHB production, suggestion an important role of the EMP pathway for the PHB metabolism.

2.3 Slr0058 is a new regulator of PHB granule number

Compared to other PHB producing bacteria, such as *C. necator*, relatively little is known about the cyanobacterial proteins which are involved in the PHB metabolism. Besides the enzymes, which are directly involved in the PHB production (PhaABEC), only one more phasin, PhaP, is known. Bioinformatic analyses were performed to identify further genes, which are putatively involved in PHB metabolism. It turned out that one operon, containing the genes *slr0058-slr0061*, harbors two genes, which show similarities to known PHB-related proteins. The gene product of *slr0058* shows structural similarities to a motive found in PhaF, a phasin known from *P. putida.* Furthermore, the protein Slr0060 shows similarities to an esterase (patatin-like phospholipase family), indicating a potential function as a putative PHB depolymerase (Sznajder et al., 2015).

To further investigate the function of these genes, knockout strains of both genes were generated and fully characterized (Δ*slr0058* and Δ*slr0060*, respectively). During vegetative growth, chlorosis and resuscitation, no distinct differences were observed between the WT and Δ*slr0060.* Δ*slr0058* on the other hand showed a change in pigmentation during vegetative growth as well as during chlorosis (more blueish or paler than the WT, respectively) (Publication 4, Figure 3 A + B). Interestingly, the Δ*slr0058* mutant produced small amounts of PHB during vegetative growth (up to

2 %), which could further be linked to decreased growth rate of this mutant. Most strikingly, Δ*slr0058* cells accumulated much more PHB granules during chlorosis, more than twice as much compared to the WT (Figure 14). At the same time, the overall amount of produced PHB remained similar to the WT. Studies with fluorescently labeled proteins could not show a direct co-localization of Slr0058 to the PHB granules. Instead, Slr0058 aggregated in a small number of foci during vegetative growth, which disappeared during the course of chlorosis.

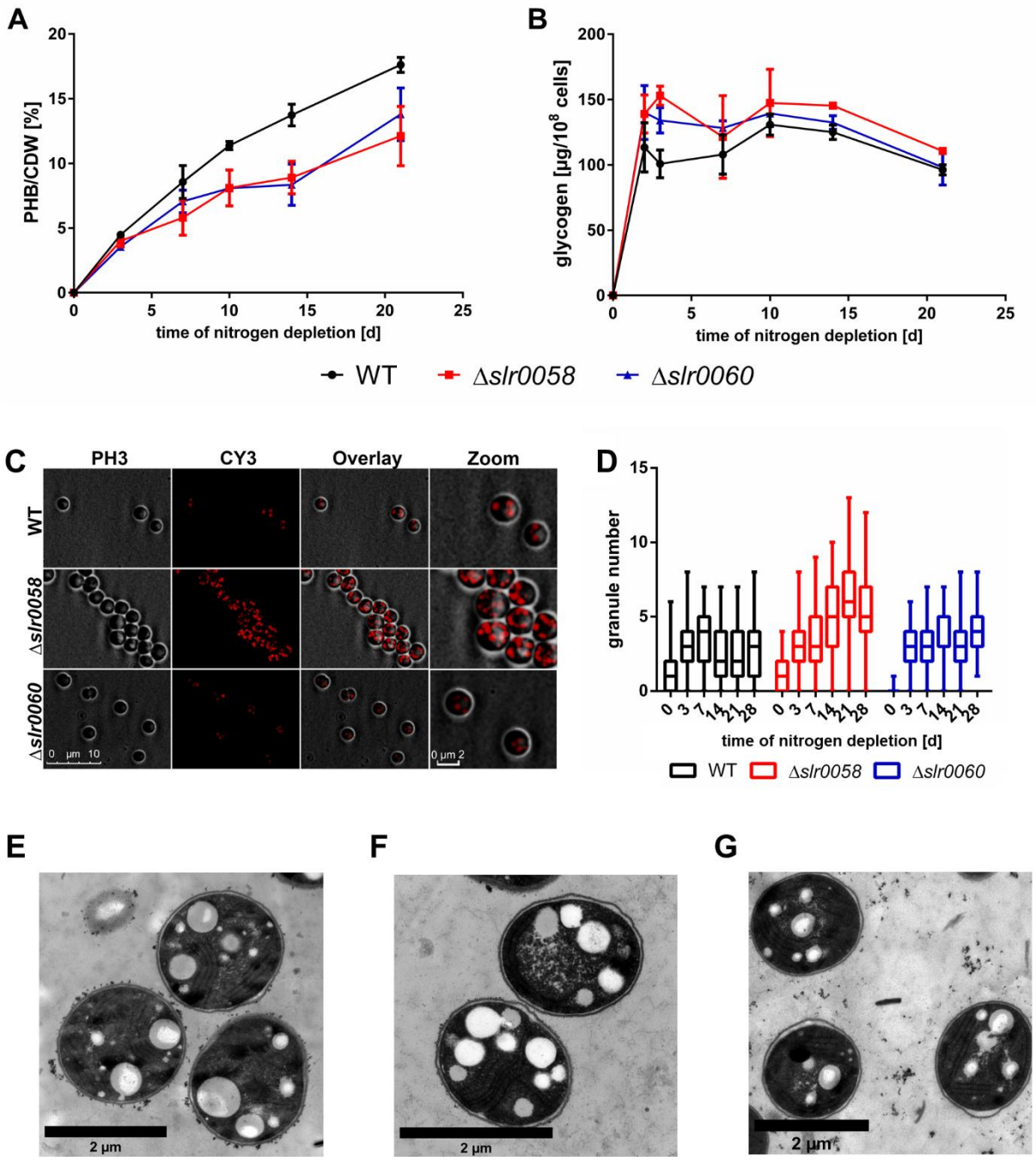

Figure 14. Phenotypical analysis of WT, Δ*slr0058* and Δ*slr0060* during chlorosis. (A) Accumulation of PHB per cell dry weight (CDW) during 21 days of chlorosis. (B) Accumulation of glycogen normalized to OD_{750} during 21 days of chlorosis. Each point represents a mean of three independent biological replicates. (C) 3-D deconvoluted microscopic images of 21-day nitrogen depleted cultures of all three strains. The cells were stained with Nile red to visualize PHB granules. From left to right: image of the phase contrast channel; image

of the Cy3 channel with Nile-red stained PHB granules; overlay of both channels. (D) Box plot of the granule number per cell at different time points of chlorosis. Each time point represents the count of 70 cells in three independent cultures. The line within the boxes represents the median. (E–G) Electron microscopic pictures of WT (E), Δ*slr0058* (F), and Δ*slr0060* (G) cells after 17 days of nitrogen starvation. PHB granules are visible as white inclusions inside the cell (Publication 4).

3. Metabolic engineering for PHB overproducers

Today, due to a huge environmental plastic pollution, a growing interest in the production of biodegradable plastics has developed. *Synechocystis* could serve as a potential production host for biodegradable PHB, particularly because of its carbon neutral lifestyle. However, *Synechocystis* naturally produces only small amounts of intracellular PHB. Hence, overproduction strains ought to be developed.

3.1 Sllo944 is causing metabolic flow towards PHB

In a recent transcriptomic analysis, the gene *sllo944* has been discovered as one of the strongest up-regulated genes during nitrogen starvation in *Synechocystis* (Klotz et al., 2016). Bioinformatic analysis did not reveal any known homologues. Interestingly, the gene product of *sllo944* was found to be an interaction partner of PII, a central regulatory protein in cyanobacteria. It was furthermore confirmed that Sllo944 has the ability to bind the enzyme phosphoglycerate mutase (PGAM) (Publication 6). The latter has an important regulatory function in the central metabolism, as it converts glycerate-3P to glycerate-2P. This reaction marks an important branching point, as it connects metabolites coming from either the upper glycolysis or the CBB cycle to the lower glycolysis. The newly formed glycerate-3P marks the first stable product from the RuBisCO, which can be either used for the gluconeogenesis or catabolized in the lower glycolysis. Interestingly, a *sllo944* deletion mutant (Δ*sllo944*) showed a rapid degradation of its glycogen pool during nitrogen starvation. Simultaneously, a strong increase of its intracellular PHB pools occurred (Figure 15).

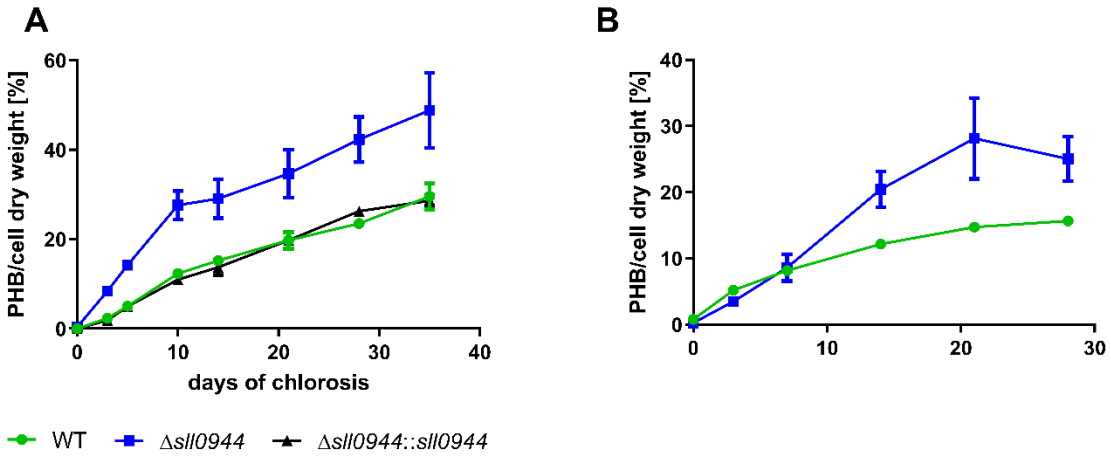

Figure 15. PHB content in percentage of cell dry weight (CDW) in WT and Δ*sllo944* cultures at (A) dark/light regime or (B) continuous light. Cultures were shifted to nitrogen free medium at day 0 and were subsequently cultivated for 28 or 35 days, respectively. Each point represents a mean of three independent biological replicates.

While the Δ*sllo944* mutant produced around 30 % PHB / CDW when cultivated at continuous light, the accumulation went up to more than 40 % PHB / CDW in case of dark/light regimes. The WT produced roughly half of these amounts under the same conditions.

3.2 Overproducer strain PPT1

It was previously shown, that the intracellular PHB accumulation in *Synechocystis* can be increased by the overexpression of the biosynthetic genes *phaAB* (Khetkorn et al., 2016). To combine this effect with the phenotype of the Δ*sllo944* mutant, the genes *phaAB* of the strain *C. necator* were cloned on a heterologous pVZ322 plasmid under the regime of a strong psbA2 promotor. By introducing this plasmid into the Δ*sllo944* mutant, the new strain Δ*sllo944*RE*phaAB* was created. For simplifications, this strain was termed "PPT1" (for "PHB Producer Tübingen 1").

When vegetative growth was compared between the *Synechocystis* WT and PPT1, no differences were observed, neither during continuous light, dark/light regime, in liquid cultures nor on solid agar plates. During exponential growth, PPT1 produced minor amounts of PHB (~ 0.4 % / CDW). When cultivated for three weeks under conditions of nitrogen starvation and dark/light regime, PPT1 produced 45 % PHB / CDW, which was more than strains harboring the individual mutations produced at the same time (Δ*sllo944* and RE*phaAB* contained 32 % and 31 %, respectively). While PPT1 produced similar amounts of PHB during continuous light (48 % PHB / CDW), its initial production rates were lower. Hence, the subsequent experiments were performed with incubation at dark/light regime. To test how the medium composition influences the PHB production, WT and PPT1 were cultivated in medium lacking either sulphur, phosphorus or nitrogen and phosphorus combined. While the first two media resulted in only low accumulations of PHB, the combined nitrogen/phosphorus free medium produced 63 % PHB / CDW. When additional $NaHCO_3$ was added to the nitrogen/phosphorus free medium, the maximum reached PHB values were similar, but the initial production rates went up to 46 % PHB / CDW after one week. When instead 10 mM acetate were added, the overall values further increased to 81 % PHB / CDW (Figure 16). A qualitative analysis of the accumulated PHB revealed that the polymers consists of only PHB and no other PHA.

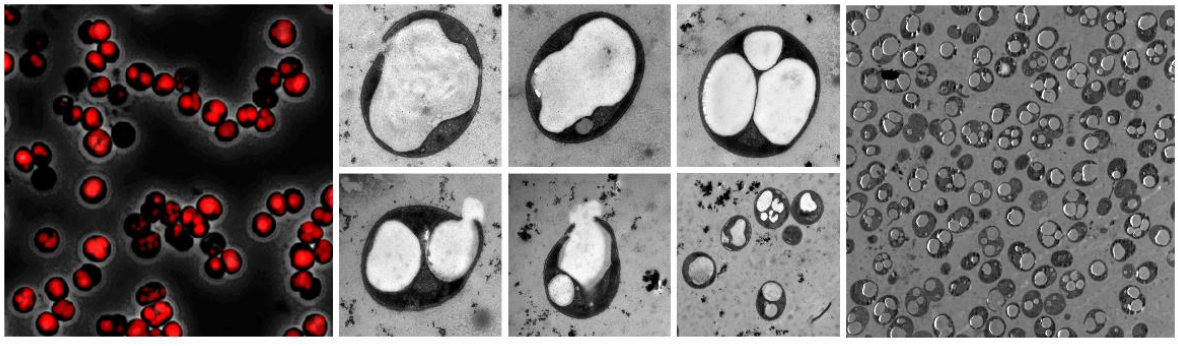

Figure 16. PPT1 cells after 21 days of nitrogen-phosphorus-starvation with 10 mM acetate grown under alternating light/dark regime. Left: Fluorescence microscopic picture. PHB granules are visualized as red inclusions after staining with Nile red. Top row: TEM images of cells harbouring large PHB granules. Bottom row: cells exhibiting a fractured cell wall. Right: overview of multiple cells.

3.3 Additional research: creation and characterization of overproduction strains

3.3.1 Cyanophycin production in the Δ*sll0944* mutant

When the PPT1 strain was cultivated in phosphorus free medium, it accumulated large intracellular granules (Figure 17). These granules were not stainable with Nile red or Bodipy, indicating an absence of a hydrophobic surface like is known from PHB.

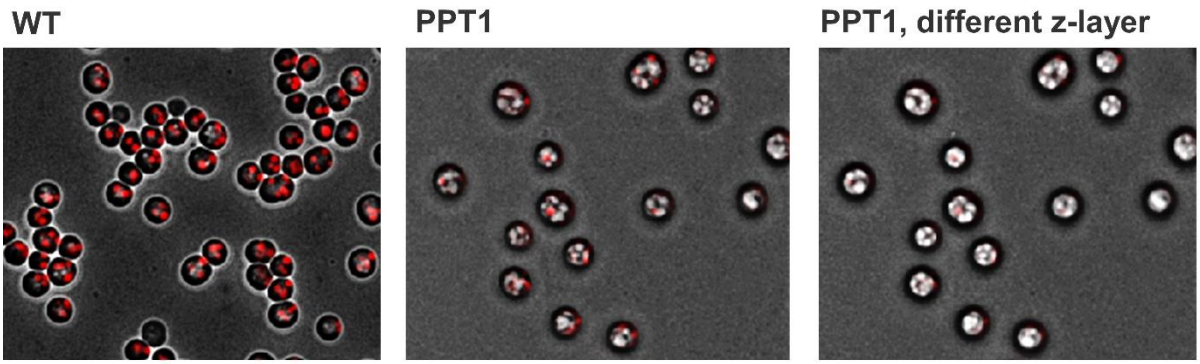

Figure 17. Fluorescence microscopic pictures of WT and PPT1 cells after 12 days of phosphorus starvation. Cells are stained with Nile red to visualize PHB granules. Pictures shown are an overlay of phase contrast and Cy3 fluorescence channel.

Since the granules were too large for being glycogen, it has been hypothesized that it could be cyanophycin instead. To verify this, the amount of intracellular PHB and cyanophycin was determined in the WT, Δ*sll0944* and PPT1 strains after 12 days of incubation in phosphorus free medium at dark/light regime (Figure 18).

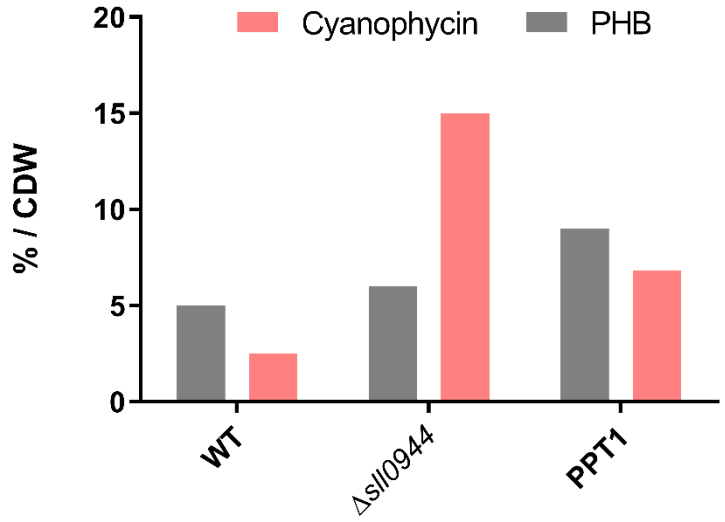

Figure 18. Quantification of the biopolymers cyanophycin and PHB in percentage of cell dry weight (CDW). Cells were incubated for 12 days at dark/light regime in a phosphorus depleted medium.

While the WT produced small amounts of both, PHB and cyanophycin (5 and 2 % /CDW, respectively), the Δ*sll0944* mutant accumulated similar amounts of PHB, but drastically increased amounts of cyanophycin (15 % / CDW). In contrast, the PPT1 strain produced much less cyanophycin, but more PHB instead.

To validate these results, the same cells, which were used for the previous experiment, were stained via the Sakaguchi method, which stains cyanophycin granules. Here, the previous observation was confirmed, as it showed that the WT and PPT1 produced only small amounts of cyanophycin, while the Δ*sllo944* mutant accumulated large quantities (Figure 19).

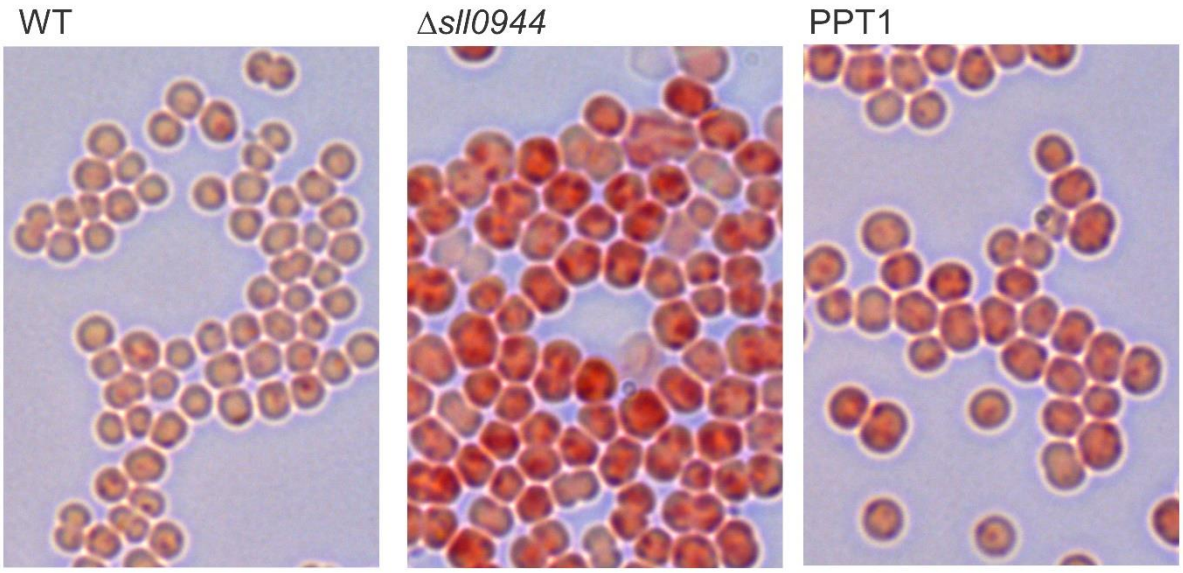

Figure 19. *Synechocystis* cultures stained with Sakaguchi staining to visualize cyanophycin granules. The intensity of red colour indicates the amount of arginine. Dark red dots are cyanophycin granules. Cells were incubated for 12 days at dark/light regime in a phosphorus depleted medium.

3.3.2 Overexpression of *phaG*

In organisms like *P. putida*, the enzyme PhaG connects the fatty acid biosynthesis with the PHB metabolism by providing more precursors for the PHB production. Since *Synechocystis* does not produce this enzyme naturally, a new overexpression plasmid was created, where *phaG* was under the control of a strong psbA2 promotor on a pVZ322 plasmid. The plasmid was transformed into a glucose sensitive *Synechocystis* WT, which was then transferred to nitrogen depleted medium (Figure 20 A). Here, the newly generated strain produced similar amounts of PHB as the WT within the first two weeks. Interestingly, after three weeks the cells strongly increased their PHB production to over 60 % PHB / CDW.

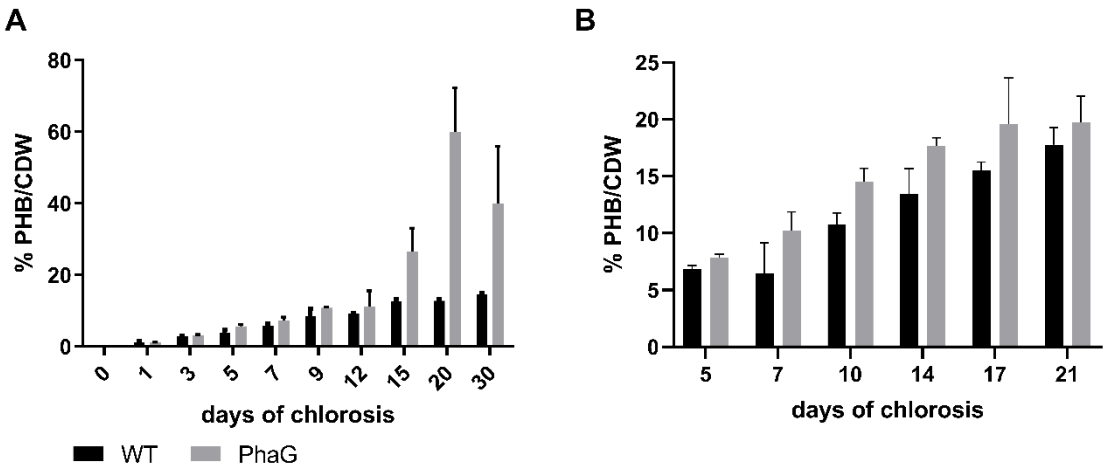

Figure 20. PHB content in percentage of cell dry weight (CDW) of WT and PhaG mutant. (A) Initial experiment, (B) repetition of the experiment. Cultures were shifted to nitrogen free medium at day 0 and were subsequently grown for 30 or 21 days, respectively. Each point represents a mean of three independent biological replicates.

Although the experiment was repeated five times, the high production rates of the initial experiment were never reached again. However, the PhaG mutant strain always exhibited higher intracellular PHB contents than the WT (Figure 20 B)

Since PhaG provides precursor from the fatty acid biosynthesis, a mutant overexpressing this enzyme might also produce mcl PHA. To test this, the produced polymers of WT and the PhaG mutant were analyzed via gas chromatography. However, the only polymer found in both strains was PHB.

4. PII regulates nitrogen transporter

The regulation of the intracellular nitrogen homeostasis is of crucial importance for cyanobacteria. One important protein involved in this is the central regulator PII. There are several strategies, how PII influences the intracellular nitrogen levels. One strategy is to regulate the uptake of combined nitrogen sources. Various P_{II} pull-down analyses in our lab indicated an involvement of PII in the regulation of the nitrogen influx, potentially by directly interacting with the respective transporters and permeases.

A bacterial-two-hybrid assay was applied to verify the interactions between PII and the ABC-type transporters NrtABCD (nitrate/nitrite transporter), UrtABCDE (urea transporter), as well as the permease Amt1 (ammonium channel) (Publication 2, Figure 5). Of those ABC transporters, only the cytoplasmic localized ATP-binding proteins (NrtCD and UrtDE, respectively) were tested.

The bacterial-two-hybrid assays revealed an interaction between PII and Amt1. Furthermore, the interaction with NrtC and NrtD as well as UrtE subunit could be confirmed, while no interaction with UrtD was detected. Some interactions, like between PII and NrtD, depended strongly on whether

the NrtD was N- or C-terminally tagged with the subunit of the adenylate cyclase, demonstrating how specific the interactions are. Furthermore, different PII variants (PII(I86N), PII(S49D), and PII(R9L)) were tested. While PII(S49D) exhibits a phosphomimetic T-loop, PII(I86N) shows a change in its T-loop conformation and PII(R9L) exhibits changed effector binding properties. In contrast to the WT, the PII variants showed only weak or no interaction with the permease Amt1. PII(S49D) and PII(I86N) showed weak interactions with the Nrt-proteins, while PII(R9L) showed no interaction at all. In contrast to the WT, none of the PII variants interacted with the C-terminally tagged UrtE.

5. Materials and Methods of the additional results

5.1 Cultivation of Synechocystis

Unless stated differently, *Synechocystis* cultures were grown at constant light (50µE), 28 °C and shaking at 120 rpm. Erlenmeyer flasks (100 ml) were used and filled with 50 ml of cyanobacterial culture. For the mutant characterization experiments of Δ*phaEC*, 10 ml of culture was incubated in 25 ml flasks. Depending on the experiment, cultures were either constantly shaken at 120 rpm or incubated at standing conditions. Whenever a dark/light regime was applied, 12/12 hour rhythms were used. For growth, standard BG11 medium was used (Rippka et al., 1979). Antibiotics were added when required.

5.2 Construction of genetically modified organisms

For the construction of the PhaG mutant, the *phaG* sequence of *P. putida* gene was used and codon optimized for *Synechocystis.* The synthetic gene was synthesized by IDT (Iowa, USA). A pVZ322 plasmid (Wolk et al., 1984) was linearized by double digestion with SalI and PstI. Both fragments, the opened plasmid and the gBlock, were combined using Gibson cloning (Gibson et al., 2009). The correct assembly was confirmed by sequencing the resulting plasmid. Correct plasmids were transformed into Synechocystis and transferred to Kan/Gen agar plates. After colonies have formed, successful segregation was confirmed via colony PCR.

5.3 Oxygen measurements

To continuously measure the oxygen concentration during vegetative growth, 10 ml *Synechocystis* culture of an OD_{750} = 0.2 were incubated in a 25 ml Erlenmeyer flask. The culture was incubated alternating dark/light cycle and under standing conditions without shaking. An oxygen sensor was placed at the bottom at the inside of the flask. A FiBox from PreSens (Regensburg, Germany) was used to determine the dissolved oxygen concentration within the medium. The equilibrium concentration was determined at 360 µM dissolved oxygen under our measured conditions.

5.4 MDA assay

MDA (malondialdehyde) was measured as an indicator for intracellular redox stress. For this, *Synechocystis* cultures were grown in standing or shaking conditions and different light intensities at a dark/light regime. Samples were taken 2 hours after the transition to the light phase. Cells corresponding to 1 ml at an OD_{750} of 1 were harvested by centrifugation and ruptured by FastPrep-24 (MP Biomedicals, Illkirch-Graffenstaden, France). The Lipid Peroxidation (MDA) Assay Kit from MERCK (Darmstadt, Germany) was used according to the manufacturer protocol.

5.5 Cyanophycin quantification

For the quantification of cyanophycin, 50 ml of *Synechocystis* culture were used. For the determination of the cell dry weight, 10 ml were centrifuged and the pellet transferred into a pre-cradled reaction tube. The pellet was dried in a vacuum concentrator and the weight determined.

The remaining 40 ml were also harvested via centrifugation and resuspended in 100 % acetone, where the cells are incubated for 30 min while being constantly shaken. The sample is centrifuged once more for 15 min at 25 000 *g*. The resulting pellet is resuspended in 0.1 M HCl (1.5 ml) and incubated at 60°C and constant shaking for 1 h. During this incubation, cyanophycin is solubilized. Remaining cell debris are removed by for 15 min at 25 000 *g*. To precipitate cyanophycin from the supernatant, 300 µl of 1 M Trs/HCl (ph 8.0) is added and incubated at 4°C for 40 min. The solution is centrifuged once more at 25 000 *g* for 15 min at 4 °C. The pellet is resuspended in 500 µl 0.1 HCl. The final amount of cyanophycin is quantified by determination of arginine (Messineo, 1966).

5.6 Sakaguchi staining

To stain intracellular cyanophycin granules, *Synechocystis* cells were stained with Sakaguchi staining as previously described (Watzer et al., 2015). In short, 500 µl culture were centrifuged (3 min at 10 000 *g*). The pellet was resuspended in 500 µl PBS and with 2.5 % glutaraldehyde. The samples were incubated at 4°C for 30 min, before they were washed with 1 ml PBS. Cells were centrifuged for 8 min at 3 000 *g* at 4 °C. Next, 80 µl 5 M KOH followed by 10 µl of 1 % (w/v) 2,4-dichloro-1-naphthol dissolved in absolute ethanol were used to resuspend the pelleted cells. Cells were incubated for 2 min at room temperature. Finally, the cells were centrifuged (5 min at 3 000 *g*), resuspended in 100 µl PBS and examined using a Leica DM 2500 microscope.

VII. Discussion

1. Physiological function of PHB in cyanobacteria

Although PHB is very abundant within the phylum of cyanobacteria, no physiological function has yet been discovered. The results shown in this work shed further light on the conditions under which PHB is relevant, although no clear function could be assigned to the polymer. Unlike previously believed, the formation of PHB is not only linked to phases of nutrient limitation. Additionally, experiments showed that the formation if PHB is also linked to dark phases and controlled by a diurnal rhythm.

1.1 The role of PHB during nutrient limitation

In many bacteria, PHB is known as a storage compound for carbon and energy, which accumulates in times of nutrient depletion. Additionally, PHB can increase the tolerance against various stresses. However, when a *Synechocystis* WT was exposed to these conditions, it never showed any growth advantage compared to a PHB free mutant Δ*phaEC.* One potential explanation for the undetectable phenotype could be a compensation by other mechanisms.

During billions of years, cyanobacteria evolved various resistance mechanisms against different stresses. A common stress is the availability of too much or too little light and energy availability. While it is important to get sufficient energy in times of low light, the opposite, i.e. exposure to high light, can also be dangerous. Therefore, cyanobacteria have evolved sophisticated mechanisms to cope with conditions of high light stress. Furthermore, particularly at times of high light and low carbon, an excess of energy can lead to the formation of reactive oxygen species (ROS), which are byproducts of aerobic metabolism, which can damage the cells (Latifi et al., 2009). To increase their resilience against such threats, cyanobacteria have evolved numerous strategies, while some of them serve as a backup for one another. One hypothesis is that PHB serves as a buffer against redox stress or for excess of electrons. However, a growth deficiency could only become visible when other factors, which serve for the same purpose, are unavailable. For example, *Synechocystis* produces lactate, acetate and succinate, which also required electrons for their formation. Under dark, anerobic conditions, when cells are exposed to a surplus of electrons, a secretion of succinate and lactate was observed (Ueda et al., 2016). It was furthermore observed, that the deletion of an acetate kinase increases the amount of secreted succinate, indicating that different metabolites can substitute each other in their function as buffers of excess electrons (Osanai et al., 2015). Since the production of these metabolites (acetate, succinate, lactate) could compensate the unavailability of PHB in a Δ*phaEC* strain, a deletion of enzymes, which are relevant for fermentation pathways could provide interesting insights. One potential gene to be deleted could be the lactate dehydrogenase (Ddh), which converts pyruvate and NADH to lactate and NAD^+. For the production of acetate, two different genes are relevant. An acetate kinase (Acs), which converts acetyl-P to acetate, or an acetyl-CoA synthase (Acs), which converts acetyl-CoA to acetate. While a mutant which is unable to produce succinate is probably not viable, a temporary knock-down using CRISPRi could be a realistic possibility (Yao et al., 2016a). In general, fermentation is only poorly studied in *Synechocystis* and could therefore be an interesting research topic. Comparing the secreted metabolites during

nitrogen starvation between a WT and a Δ*phaEC* mutant could further reveal the importance of PHB as an electron sink.

This potential role of PHB is further supported by the observation that the EMP pathway was shown to be the most important pathway for PHB biosynthesis (Publication 1, Figure 6 and Publication 5, Figure 2). During the catabolism of one glucose residue via the EMP pathway the only energy rich metabolites generated are ATP and NADH. When the ED or the OPP pathways are utilized for glucose catabolism instead, also NADPH is generated. At times where the cell interior has a surplus of reduced compounds, no further NADPH generation would be desirable. The observation that under conditions, where PHB is formed, most carbon is channeled through the EMP pathway, shows that these are conditions where the cells have an excess of intracellular reduction equivalents in the form of NADPH.

In comparison to other PHB producing bacteria, the PHB biosynthesis are located on two different operons (*slr1993/1994* for *phaAB* and *slr1829/1830* for *phaEC*, respectively). This peculiarity could indicate a unique role of PHB in cyanobacteria. While in most other PHB producing bacteria the biosynthetic genes are transcribed simultaneously, *Synechocystis* has the ability to finetune the PHB synthesis. This could be relevant since the unregulated production of PHB was shown to be harmful (Publication 4, Figure 2 + 3), hence the formation of PHB has to be tightly regulated. The formation of complex PHB granules require energy from the cell, and if PHB is not properly regulated, it can even be harmful for the cells. The fact that *Synechocystis* nevertheless produces PHB underlines that PHB has to provide an evolutionary advantage for the cells.

Another hint towards the physiological function of PHB is that the polymer was not metabolized, even when the cells were transferred to nutrient rich medium (Publication 4, Figure 6). Instead, the granules were only disaggregated and distributed among the newly formed daughter cells during the resuscitation from nitrogen starvation. This indicates that PHB could serve rather as a disposal for undesired products, which are formed during chlorosis. However, in this scenario it remains puzzling why the cells would not simply secrete the undesired reduction potential in form of metabolites, such as acetate.

Another remarkable feature about the PHB formation is its heterogeneity (Publication 5, Figure 6). The strong diversity of cells with low or high amounts of PHB indicates that PHB formation is not necessary or beneficial under all environmental conditions. Only ~10 % of cells were assigned as high-PHB-producers, while most other cells contained only small to moderate amounts of PHB. This indicates that the accumulation of large amounts of PHB is potentially only relevant under rare and unpredictable occurring situations, since only a minority of cells produced high amounts of it. Future experiments could try to further investigate this phenomenon by separating low and high producing PHB cells and test how they are able to withstand different stress conditions.

1.2 The role of PHB during dark phases

Although it was previously believed that PHB in cyanobacteria is only produced during conditions of nutrient limitation, several experiments indicate an additional role during dark phases, even in the presence of all required nutrients. For instance, all PHB related genes are strictly regulated by a diurnal rhythm (Publication 5, Figure A3) (Köbler et al., 2018). Interestingly, the genes are strongly upregulated at the beginning of the night, while they are downregulated during the day (Figure 21). This further suggests an involvement of PHB during dark phases.

Preliminary results showed a small PHB accumulation during the night under conditions of limited gas exchange. However, the detected amounts of PHB were close to the detection limit and only observed in a glucose sensitive substrain of *Synechocystis*. Since it was not possible to complement the Δ*phaEC* mutant strain used in this study, not all differences to the WT strain can be clearly linked to the absence of PHB. However, the observed phenotypes of this mutant strain could provide hints about the physiological function of PHB, which could be confirmed with a complementable Δ*phaEC* strain.

Another hypothesis is the involvement of PHB for an increased resistance against redox stress. In experiments, where cells were exposed to high light stress, a PHB free mutant grew worse compared to low light, while the WT strain grew better during high light conditions. Furthermore showed the analysis of intracellular MDA increased redox stress in a Δ*phaEC* mutant, regardless of the light intensity (Figure 11). It has to be mentioned though, that both experiments were performed with a Δ*phaEC* mutant strain, which was unable to produce PHB, but might have also acquired additional mutations, since it was impossible to restore the WT phenotype by a complementation with a plasmid encoding the *phaEC* genes. However, also experiments in other strains have found a connection between PHB and the intracellular redox potential. A mutant which was lacking the protein Sll0783 showed decreased NADPH levels (Hauf et al., 2013). Furthermore, this mutant barely produced any PHB anymore, indicating a connection between intracellular redox status and PHB formation (Schlebusch and Forchhammer, 2010). Another publication showed 1.85 times higher NADPH levels in a PHB free *Synechocystis* mutant compared to the WT (Xie et al., 2011).

Interestingly, growth comparisons showed the strongest disadvantage of a Δ*phaEC* strain during dark phases combined with limited gas exchange (Figure 8). The gas exchange limitation was caused by growth at standing conditions, which simulates the conditions present in a natural occurring habitat, like for example a pond. Due to the gas exchange barrier of a water column above the cells, respiration during the night was causing a decline in oxygen levels within the medium. Although the conditions where never completely anoxic, oxygen-limited conditions were reached during the late-night phases. Further investigation of this phenomena, for example with higher water columns, could be interesting, to test if this creates even higher oxygen limitations. To the best of our knowledge, experiments investigating these natural occurring conditions of a slight gas exchange limitation (in contrast to continuous shaking or strict anerobic conditions) where never tested so far. Foremost, for further investigations the creation of a Δ*phaEC* mutant without downstream effects is

necessary. In the current Δ*phaEC* mutant the entire *phaEC* operon is deleted, which also affects a short UTR downstream of *phaEC,* as well as a gene located on the antisense DNA strand (*sll1736*). The latter encodes for a protein of unknown function and is located adjacent to genes of the respiratory chain (NADH dehydrogenase subunits). Hence, a mutant affecting these genetical reasons could explain the growth phenotype under conditions of reduced gas exchange. In a newly generated mutant, an antibiotic resistance cassette should be inserted into the gene *phaE*, instead of replacing *phaEC* with the cassette. Additionally, further analysis of this downstream region, as well as the anti-sense strain, could be interesting to investigate, since it could have caused the strong growth phenotype during dark/standing conditions (Figure 8).

2. Interconnection between different carbon pools

Several experiments have shown a connection between the PHB and glycogen pools (Publication 1). Interestingly, the biosynthesis of PHB starts slightly delayed after the induction of nitrogen starvation, while glycogen formation starts immediately upon N-downshift. This further indicates, that PHB is likely not a storage polymer, otherwise it would be more likely to be formed immediately after the onset of chlorosis. Since the intracellular accumulation of PHB continuous throughout the chlorosis it is likely that PHB is formed from products produced during phase II of chlorosis. Additionally, a recent publication has found a potential connection between PHB and lipopolysaccharides (Matsuhashi et al 2015). Based on this observation, further experiments investigating the potential involvement of degraded thylakoid membranes for the formation of PHB would be interesting to investigate.

Interestingly, a Δ*glgC* mutant is still able to produce PHB, while a Δ*glgP* mutant is strongly impaired, although both strains cannot metabolize glycogen. While the Δ*glgC* strain probably accumulates glucose-1P, Δ*glgP* stores carbon as glycogen. Hence, it makes a big difference which metabolite accumulates for the ability to produce PHB. Furthermore, the specific kind of glycogen which is produces plays an important role: While a Δ*glgA1* mutant was strongly impaired in its PHB production, a Δ*glgA2* mutant produced similar amounts as the WT (Publication 1, Figure 3). This further highlights the importance of the two different kinds of glycogen and their varying ability to get metabolized (Yoo et al., 2014). Finally, the relationships between PHB and glycogen can also be seen in transcriptomic data of cultures grown in alternating day/night rhythm. While the glycogen synthesizing genes were upregulated during the day and downregulated during the night, genes which are involved in the glycogen degradation where regulated in an opposite manner. Interestingly, the regulation of PHB biosynthesis genes behaved as the glycogen-degrading enzymes (downregulated during the day and upregulated during the night). This further indicates a potential conversion of the two polymers into each other (Figure 21).

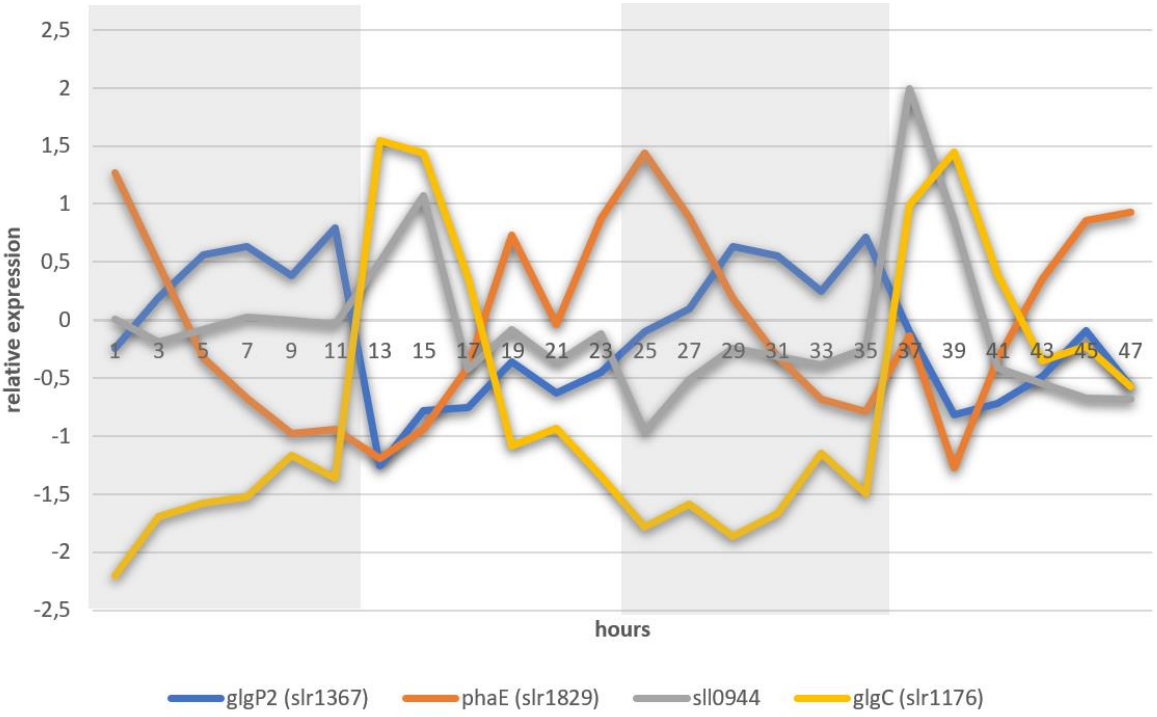

Figure 21. Transcriptome of representative genes of the glycogen anabolism (glgC, yellow), glycogen catabolism (*glgP2*, blue), PHB biosynthesis (*phaE*, orange) and *sllo944*. The transcriptomic data are derived from Saha *et al*. 2016. Shown are two consecutive days of *Synechocystis* cells grown at a dark/light regime, where a grey background indicates a night phase.

Interestingly, the *sllo944* transcript shows a strong up-regulation at the beginning of the day (Figure 21). It has not been investigated so far, what the role of Sllo944 during vegetative growth is and how this influences the potential PHB metabolism und balanced conditions.

3. Proteins associated to PHB metabolism

In the past years, several new proteins involved in the PHB metabolism have been identified (Hauf et al., 2015) (Publication 4). Although the physiological relevance of Slroo6o has not been fully understood, the fact that it has been found in a PHB-granule pulldown supports its involvement in the PHB metabolism (Schlebusch, 2012). Additionally, the localization of *slroo6o* on the same operon as *slroo58*, which was shown to influence the number of PHB granules, makes it likely that both genes are involved in PHB metabolism. Future studies could investigate *slroo59* and *slroo61*, two genes located on the same operon, but with no predicted function. Additionally, a transcriptomic analysis revealed that during day/night rhythm the gene *sllooo62*, which is located adjacent to *slroo58* on the antisense DNA strand, shows the same transcriptomic pattern (Kucho et al., 2005). This could also indicate an involvement of *sllooo62* in the PHB metabolism.

Since the deletion of *slroo6o* did not cause a drastic change in the intracellular amount of PHB, the PHB depolymerase is most likely still to be found. Since the absolute amount of PHB remains the same even after the resuscitation from nitrogen starvation (Publication 4, Figure 6), it is questionable if *Synechocystis* possesses a PHB depolymerase at all. However, it is assumed that all

organisms, which produce PHB, should also have a PHB depolymerase in order to mobilize the PHB again. One potential candidate for a depolymerase is encoded by the gene *slr1916*. A bioinformatical analysis of all *Synechocystis* genes revealed that *slr1916* shows the strongest structural similarity to other intracellular PHB depolymerases. Interestingly, a recent study, where a mutant library of the entire *Synechocystis* genome was created using CRISPRi, showed that the knock-down of *slr1916* caused a strong increase in its growth rate by 13 % (Yao et al., 2020). Besides a depolymerase, more phasins might still to be discovered. While in organisms like *C. necator* 7 different phasins are known (Pfeiffer and Jendrossek, 2012), there is only one described in *Synechocystis* so far, PhaP. Although Slr0058 influences the number and size of PHB granules in *Synechocystis*, it is probably not directly located to mature PHB granules (only during the early phases) and can thereby not considered a classical phasin (Figure 22). Another promising candidate is encoded by *slr0455*, which shows predicted structural similarities to a phasin. Further studies are needed to investigate this topic.

Some of the major findings of this work, including a proposed model for the role of Slr0058, are shown in Figure 22.

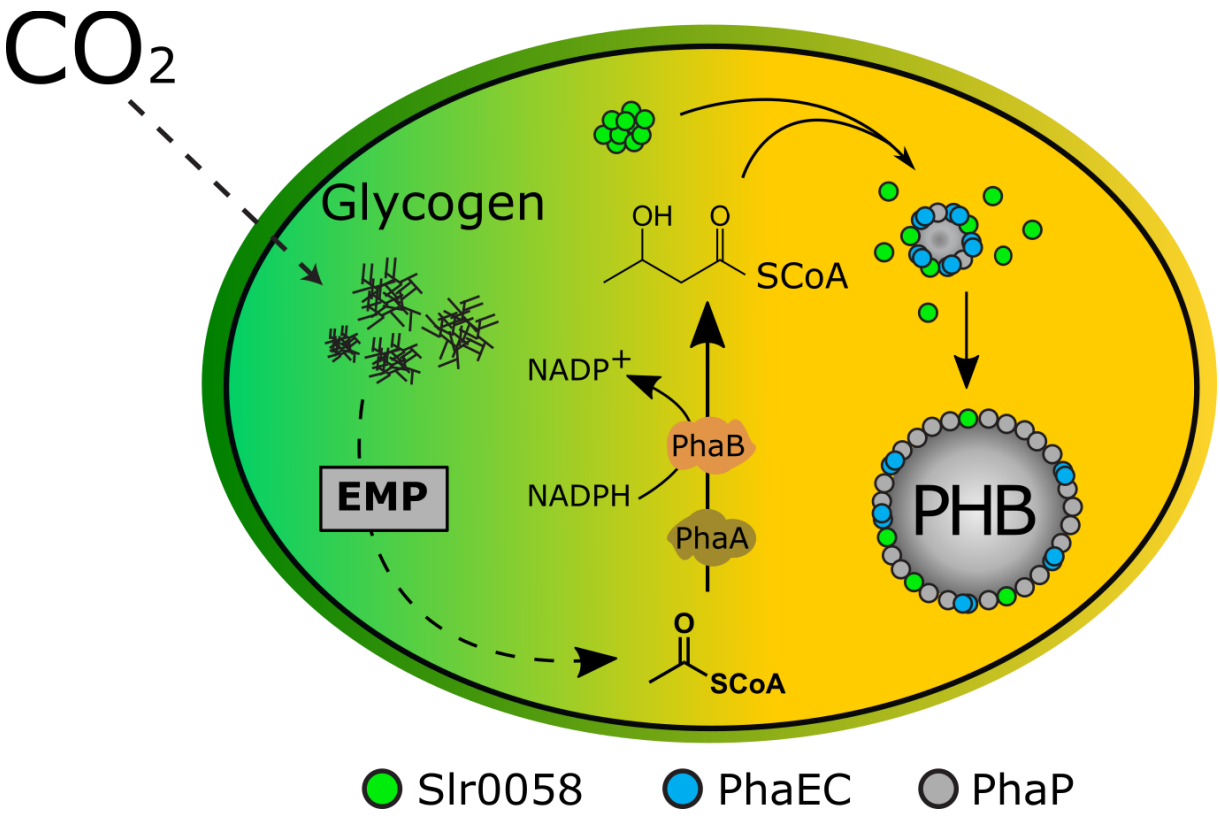

Figure 22. Schematic overview of the PHB metabolism in *Synechocystis*. During early chlorosis, CO_2 is taken up into the cell and is stored in the form of glycogen granules. During the later stages of chlorosis, glycogen is slowly degraded and metabolized via the EMP pathway, where Sll0944 regulates the flux from glycerate-3P (3-PG) to glycerate-2P (2-PG). The latter is subsequently converted to acetyl-CoA, which serves as the building block for PHB. Slr0058 acts as an initiation point for the PHB synthesis and slowly detaches from the granules. Instead, more PHB synthases and phasins cover the granule surface.

4. Metabolic engineering for increased PHB production

In the past decades, numerous approaches have tried to generate genetically engineered cyanobacteria with increased PHB production. However, most approaches resulted in only small amounts of accumulated polymer. This is partially due to different *Synechocystis* WT strains being used, which produce as little as 1 % PHB / CDW, even during nitrogen starvation (Osanai et al., 2013). In contrast, the Tübingen *Synechocystis* WT produced up to 20 % PHB / CDW. Hence, this strain serves as a good basis for the construction of PHB overproduction mutants.

4.1 Δ*sll0944* as a chassis for metabolic engineering

As previously shown exhibits the Δ*sll0944* mutant strain a rapid mobilization of glycogen during nitrogen starvation. Much of the carbon derived from glycogen was channeled into the formation of PHB, resulting in a massive accumulation of more than 40 % PHB / CDW. Interestingly, when cultivated in phosphorus deficient medium, the Δ*sll0944* strain still produced more PHB than the WT, but more remarkably, it also accumulates large quantities of cyanophycin. When the flux towards PHB was increased by the overexpression of RE*phaAB* (strain PPT1), the strain still produced more cyanophycin than the WT, but additionally redirected more carbon towards PHB (Figure 18). This indicates that in the WT under phosphorus limited conditions, the formation of PHB is probably constrained by the enzymatic activity of PhaAB. The fact that *Synechocystis* WT prefers to produce cyanophycin over PHB indicates that cyanophycin might have a larger physiological relevance during phosphate starvation.

Although the Δ*sll0944* strain is an overproducer of PHB, its metabolism could be exploited to produce other high value products. Since many metabolites are based on the production of acetyl-CoA, a Δ*sll0944*/Δ*phaAB* strain could serve as a chassis, where the introduction of synthetic pathways could redirect the metabolic flux from acetyl-CoA to a desired product. Examples for such acetyl-CoA derived products are 1-butanol, 3-hydroxypropionate or isoprenoids, which could be used as biofuels, flavors, biofuels, vitamins or pharmaceuticals (Zhang et al., 2019).

4.2 Optimization of PPT1

To further increase the intracellular PHB accumulation, the genes *phaAB* from *C. necator* were introduced into the Δ*sll0944* strain. The resulting PHB content was so large that it might have caused cell rupture. However, the achieved time-space-yield is still rather low, due to slow growth rates, long incubation time in chlorosis as well as small overall biomass. In the following, several approaches to increase the overall amount of PHB by using the PPT1 strain are discussed.

Cultivation medium. The highest intracellular amounts of PHB were reached when the cells were cultivated in BG_{11} medium without nitrogen and phosphorus, as well as with the addition of 10 mM acetate. However, this medium might still be further optimized. Previous studies have shown that the growth rates of *Synechocystis* in BG_{11} are limited by sulfate, which causes ROS formation and thereby rapid bleaching of pigments when depleted (van Alphen et al., 2018). Another limiting factor

was iron, particularly when cells are grown under continuous mode. Studies have shown that when these two factors are considered, *Synechocystis* was enabled to grow at a doubling time of 4.3 h, which is twice as fast as the common textbook knowledge. A growth medium could be further optimized with the addition of potassium, which was shown to result in higher PHB production during dark cultivation (Ueda et al., 2016). Finally, the addition of acetate to the growth medium is an additional cost factor. Replacing acetate with waste water or fish pond discharge are alternative sources of organic carbon, which are available at no cost and where shown to successfully replace synthetic carbon sources such as acetate (Panda et al., 2006).

Aeration. While some groups have found that sealing samples during nutrient limitation could further boost the PHB production (Panda et al., 2006), our experiments have shown the opposite: When incubated in closed containers, which eliminated any gas exchange, the PHB production was drastically diminished (Publication 7, Figure S5). This is in line with other studies (Kamravamanesh et al., 2017) (Publication 5, Figure 1). Hence it can be concluded, that for future experiments, sufficient gas exchange should be ensured, for example by rigorous shaking. Furthermore, supplying gas with enriched CO_2 content could be tested to further boost the PHB production. When 100 mM $NaHCO_3$ were added to PHB producing *Synechocystis* cultures, no increase in the maximum PHB content was achieved. However, the initial production rates were strongly increased, with one replicate reaching >60 % PHB / CDW after one week. These results indicate that the pace of PHB production could be further accelerated by an elevated CO_2 supply.

Illumination. In our experiments, cultivation at alternating dark/light phases proved to be superior for PHB production, due to higher PHB contents per CDW, as well as higher initial production rates. However, it should be considered that growth and also chlorosis during dark/light regime leads to lower overall biomass compared to cultivation at continuous light. The benefit of dark/light cycles is that this would allow cultivation using natural light and no artificial light source. Furthermore, the process of chlorosis can be accelerated with increased light intensity. When supplied with sufficient CO_2, cyanobacterial cells are able to tolerate higher light intensities (Lippi et al., 2018). Further experiments investigating different combinations of light/CO_2 supply could help to accelerate the PHB accumulation.

Reactor design. Studies have shown that optimized pH and temperature can further increase the PHB production (Panda et al., 2006). A more controlled environment, for example via a temperature control or pH control, could be tested to optimize the conditions for PPT1. Alternatively to the cultivation in a shake flask, the usage of optimized growth chambers, such as the CellDEG system, could be considered. These systems have already been demonstrated to be suitable for high density productions in a short time with high yields of cyanophycin (Lippi et al., 2018) or sesquiterpenoid (Dienst et al., 2020). Although this system can provide very high time-space yields, the ability to be up-scaled are limited. Instead, cultivation in larger pilot plants could be of interest. First examples of *Synechocystis* sp. cultivation for the production of PHB have already been demonstrated in a 200 l pilot plant, which was attached to the exhaust of a coal power plant (Troschl et al., 2018). In another

approach, three 11 000 l photobioreactors were successfully used to cultivate wastewater born cyanobacteria for the production of PHB (Rueda et al., 2020).

4.3 Design of PPT2

Although PPT1 has already achieved high PHB values, the metabolic design could be further engineered ("PPT2") to achieve desirable properties, such as a faster PHB accumulation. However, since these values of >80 % PHB / CDW were only reached after the addition of acetate and after three weeks of incubation, further improvements are necessary for a more cost- and time-efficient production. Since *Synechocystis* cells are able to produce 50% glycogen within 2 days during the early stage of chlorosis, they should in principle be able to produce PHB at similar rates, demonstrating the room for improvements.

TEM pictures have shown numerous cells with ruptured cell walls, indicating that the PHB contents reached in PPT1 were already close to the maximal possible content. Furthermore, since cells always contain a certain amount of intracellular structures, such as remaining thylakoid membranes, it seems unlikely that much more than 80 % PHB / CDW can be reached. One potential strategy to overcome this limiting cell wall could be the disruption of Z-ring formation by deleting ftsZ or by deleting the actin-like protein MreB to create longer cell. The same strategy has already been successfully implemented in *Halomonas*, resulting in large cells with high PHB contents (Jiang et al., 2017).

For the construction of PPT1, the genes RE*phaAB* were introduced together with a strong psbA2 promotor on the self-replicating plasmid pVZ322. To ensure a stable expression, an integration into the genome would be desirable. This could be achieved by using the pEERM1 plasmid, which integrates a gene of interest together with a strong ribosomal binding site downstream of the psbA2 promotor (Englund et al., 2015). However, previous attempts using this plasmid to introduce RE*phaAB* or RE*phaC* into the genome have not been successful (Orthwein, 2019). Furthermore, the PPT1 strain uses the original genes from *C. necator*. Instead, codon optimized genes could lead to a higher expression of these genes. Although it was previously shown that the additional expression of *phaC* (in combination with *phaAB*) could decrease the overall PHB productivity in *Synechocystis* (Khetkorn et al., 2016), this does not have to be the case with PPT1. The very high PHB amounts reached in PPT1 could lead to a situation where the amount of PHB- synthase is limiting. Hence, designing a new construct, which includes *phaC* from *C. necator* in addition to *phaAB* could be desirable. Alternatively, the usage of a different PHA synthase could provide PHA with improved material properties. A recent study has discovered a cyanobacterium (*Anabaena spiroides* TISTR 8075) which is able to produce PHBV under phototrophic conditions (Tarawat et al., 2020). This would allow the production of PHBV instead of mere PHB.

Besides improving the expression of the main biosynthetic PHB genes *phaAB(E)C*, the insertion of additional genes could help to redirect the carbon flux more towards PHB, for example by increasing the availability of the precursor acetyl-CoA. As a background, a strain overexpressing *phaABC*

should be used to ensure a rapid conversion of acetyl-CoA to PHB. Furthermore, a PHB overproduction chassis should include the Δ*sll0944* phenotype.

Reduction of side-products. An increased flux towards a product of interest can be achieved by the elimination of undesired side-products. One approach would be the deletion of *glgC* to stop the glycogen synthesis. Although it is known that a Δ*glgC* mutant is unable to survive longer periods of nitrogen starvation, the initial chlorosis phase could be long enough for the strain to survive and to redirect most of its fixed carbon into PHB. Additionally, previous studies have shown that the unavailability of a carbon sink (like in the case of a Δ*glgC* strain) can result in growth impairment. This leads in the Δ*glgC* strain to an overflow metabolism, where it secretes metabolites like 2-oxoglutarate or pyruvate (Grundel et al., 2012). Another study showed that after the introduction of an alternative sink (in this case the biosynthesis genes for isobutanol) the Δ*glgC* mutant recovered the original growth rate of the WT (Li et al., 2014). Hence, the increased flux towards PHB in a *phaABC* overexpressing background could ensure continuous carbon flow and avoid the undesired accumulation of metabolites, which could cause the growth impairment in a Δ*glgC* strain. Additionally, a recent study showed that when no carbon sink is available during chlorosis (like in the case of a Δ*glgA1/2* strain), metabolites like ADP-glucose accumulate, which are toxic for the cells. However, upon the addition of NaCl, cells started to produce glucosylglycerol to cope with the osmotic stress. Since glucosylglycerol is produced from ADP-glcose, the metabolic stress is relived and the cells can grow normally (Díaz-Troya et al., 2019). This phenomenon could be exploited to design strains which are glycogen deficient (like the Δ*glgA1/2* strain), which are otherwise difficult to cultivate. To ensure that the carbon is not ending up in downstream metabolites, alternative carbon sink pathways, like towards the TCA cycle, could be down-regulated, for example by using CRISPRi for an inducible reduction of the phosphoenolpyruvate carboxylase (PepC) or the citrate synthase (GltA).

Intensification of catabolism. During the first two days of chlorosis, *Synechocystis* accumulates large quantities of glycogen. Tapping this carbon storage could strongly increase the precursor availability for PHB production. One way could be the overexpression of glycogen phosphorylases *glgP1/2*. Since the posttranslational regulation of both enzymes is unknown, using heterologous enzymes could be more efficient. The downside of this strategy is the uncertainty, if the product of GlgP, glucose-1P, would be further metabolized or if other enzymes of the upper glycolysis function as additional bottlenecks. A more promising approach could be to increase the overall carbon catabolism. For this, the overexpression of two central regulators, Rre37 and SigE, was shown to be successful (Nakaya et al., 2015, Osanai et al., 2014). Expressing both regulators under a NtcA dependent promotor could ensure the specific transcription during chlorosis. If PHB should take place during vegetative growth, coupling its formation to the day/night rhythm could be beneficial. This approach was already successfully demonstrated for the production of fumarate, where the constructed strain produced fumarate constantly during the day as well as during the night (Du et al., 2019). Finally, the introduction of a specific point mutation in the phosphate-specific transport system integral membrane protein A (PstA) showed to strongly upregulated the carbon flow towards PHB (Kamravamanesh et al., 2018a).

Increased precursor supply by additional pathways. The deletion of the *sllo944* has shown, that an increased supply of precursors is a limiting factor for the PHB biosynthesis. Rerouting the intracellular carbon flux could increase the carbon supply from other internal sources. One example is the expression of *phaG.* This 3-hydroxyacyl-CoA-acyl carrier protein transferase connects the fatty acid *de novo* synthesis with the PHB biosynthesis in *P. putida* (Rehm et al., 1998). Although the mere overexpression of *phaG* did not lead to a strong increase in accumulated PHB (Figure 20), an insertion into the PPT1 strain could be more successful. Another alternative pathway is catabolized by the phosphoketolase Xfpk (Anfelt et al., 2015). This enzyme produces acetyl phosphate from xylulose 5-phosphate or fructose 6-phosphate. Thereby this pathway connects metabolites of the glycolysis and the OPP directly with the production of acetyl-phosphate, which can be easily converted to acetyl-CoA in a single enzymatic reaction. The usage of a phosphoketolase for the production of PHB has already been successfully demonstrated before (Carpine et al., 2017). Finally, the enzyme NphT7 could be exploited. In *Streptomyces* sp. it converts acetyl-CoA and malonyl-CoA to acetoacetyl-CoA and CoA (Okamura et al., 2010). Since this reaction involves the hydrolysis of ATP to ADP it is energetically favorable (Lan and Liao, 2012). This approach has already been demonstrated to increase the PHB production (Lau et al., 2014) (Weiß, 2018). In addition to the improved precursor supply, increased NADPH availability could be necessary for PHB biosynthesis. Since more NADPH is generated via the OPP than the EMP pathway, blocking the latter could increase the PHB production. Although a blockage of the EMP pathway was shown to drastically decrease the PHB production, this could have been resulted from the surplus of NADPH within the cells. In the background of an additional sink for NADPH (the reaction catalyzed by the overexpressed PhaB), which is the case in the strain PPT1, the blockage of the EMP pathway could be beneficial.

Decrease heterogeneity. When *Synechocystis* WT cells produce PHB, a strong heterogeneity of the accumulated polymer was reported within a population. Even in the overproduction strain PPT1, a certain variety in the PHB content was observed (Figure 16). The mechanistic program behind this phenomenon is unknown. From other strains like *C. necator* or *P. putida* it is known, that PHB formation follows a complex regulation (Velázquez-Sánchez et al., 2020). PHB accumulation is regulated on different levels including transcriptional or translational regulation and potentially factors such as quorum sensing. Further investigation of the heterogeneity phenotype is necessary to understand the mechanism behind it and to create a population of homogeneous PHB overproducer cells. In previous experiments, FACS was used to analyze the inheritability of the low and high PHB phenotypes (Publication 5, Figure 6). Although it was shown that the heterogeneity is not based on genetic differences, the FACS method could be used to identify and separate natural occurring mutants with high PHB phenotypes. A recent publication applied a double-staining for FACS separation, using BODIPY 493/503 for PHA staining and SYTO 62 for DNA staining. It resulted in a fast and reliable quantification of PHB biosynthesis (Karmann et al., 2016). This technique could be used to identify natural occurring variants and high-producer cells within a PPT1 population.

New background strain. Although *Synechocystis* is a well-studied model organism, it also has several disadvantages compared to other cyanobacterial strains. One example is its relatively high

doubling time of around 8 hours. Other cyanobacterial strains can grow much faster, for example the recently discovered strain *Synechococcus* UTEX 2973, which is closely related to *Synechococcus elongatus* PCC 7942. This strain can be cultivated at 41°C under continuous 500 µE, where it exhibits a doubling time of only 1.9 hours. Introducing the PPT1 genetical setup (*Δsllo944*RE*phaABC*) could combine fast growth with high PHB production yields. An alternative strain with interesting properties is *Chlorogloea fritschii* TISTR 8527. This strain was shown to be self sedimenting (Monshupanee et al., 2016), which could help to reduce downstream processing cost, an important factor determining the final price of the product (Panuschka et al., 2019).

Altered growth behavior. *Synechocystis* is known to produce PHB specifically under conditions of nutrient limitation. However, coupling PHB production to growth could lead to a faster and direct conversion of CO_2 to PHB. The factors determining why PHB is not produced during vegetative growth have yet to be discovered. Once this would be achieved, growth could be slowed down in order to redirect all carbon and energy towards PHB. In a recent study the authors have repressed all genes in *E.coli* via CRISPRi to find genes, which can be down-regulated to have more metabolic flux towards a desired product (Li et al., 2020). Another study tried a similar approach in *Synechocystis*, where they used CRISPRi to down-regulate growth for an increased biofuel production. One of the most promising candidates was the down-regulation of *gltA* (citrate synthase), which increased carbon partitioning to n-butanol 5-fold compared to the WT (Shabestary et al., 2018). Such experiments will become easier once a library of *Synechocystis* knockout strains is available, which is currently under development (Mills et al., 2020, Gale et al., 2019).

5. Final conclusions

With the results presented in this work we significantly contributed to the knowledge about PHB metabolism in cyanobacteria. We discovered the intracellular carbon sources where PHB is derived from and showed which pathways are relevant for its formation; we could show which environmental conditions favor PHB production; and we discovered new regulatory factors controlling the formation of PHB. All this knowledge can now be applied to develop robust PHB production strains for industrial applications. A first example has been set by the creation of PPT1, a strain which exhibited the highest PHB content ever achieved in any phototrophic organism.

However, all these results were based on laboratory conditions and still have to be transferred to large-scale bioreactors. At the same time, environmental problems are pressing and issues like the global plastic pollution are becoming more dramatic (World Economic Forum, 2016). Technological solutions might take too long to adequately address all those challenges. Hence, a more holistic approach, including social and humanitarian sciences, are necessary to conduct a societal transformation towards more sustainability. Recent studies have shown that a safe and just life within our planetary boundaries is possible (O'Neill et al., 2018). It is up to us researchers to step out of our ivory towers, actively engage with civil society and take responsibility (Barnosky et al., 2016) - to guide our world towards a sustainable future.

VIII.References

ALLEN, M. M. & SMITH, A. J. 1969. Nitrogen chlorosis in blue-green algae. *Archives of Microbiology,* 69**,** 114-20.

ANDERSON, A. J. & DAWES, E. A. 1990. Occurrence, Metabolism, Metabolic Role, and Industrial Uses of Bacterial Polyhydroxyalkanoates. *Microbiological Reviews,* 54**,** 450-472.

ANFELT, J., KACZMARZYK, D., SHABESTARY, K., RENBERG, B., ROCKBERG, J., NIELSEN, J., UHLÉN, M. & HUDSON, E. P. 2015. Genetic and nutrient modulation of acetyl-CoA levels in Synechocystis for n-butanol production. *Microbial Cell Factories,* 14**,** 167.

ARIAS, S., BASSAS-GALIA, M., MOLINARI, G. & TIMMIS, K. N. 2013. Tight coupling of polymerization and depolymerization of polyhydroxyalkanoates ensures efficient management of carbon resources in Pseudomonas putida. *Microbial Biotechnology,* 6**,** 551-563.

ARORA, N. K., SINGHAL, V. & MAHESHWARI, D. K. 2006. Salinity-induced accumulation of poly-β-hydroxybutyrate in rhizobia indicating its role in cell protection. *World Journal of Microbiology and Biotechnology,* 22**,** 603-606.

BARNOSKY, A., EHRLICH, P. & HADLY, E. 2016. Avoiding collapse: Grand challenges for science and society to solve by 2050. *Elementa: Science of the Anthropocene,* 4**,** 000094.

BATISTA, M. B., TEIXEIRA, C. S., SFEIR, M. Z. T., ALVES, L. P. S., VALDAMERI, G., PEDROSA, F. D., SASSAKI, G. L., STEFFENS, M. B. R., DE SOUZA, E. M., DIXON, R. & MULLER-SANTOS, M. 2018. PHB Biosynthesis Counteracts Redox Stress in Herbaspirillum seropedicae. *Frontiers in Microbiology,* 9.

BECK, C., KNOOP, H., AXMANN, I. M. & STEUER, R. 2012. The diversity of cyanobacterial metabolism: genome analysis of multiple phototrophic microorganisms. *BMC genomics,* 13**,** 56-56.

BEHLER, J., VIJAY, D., HESS, W. R. & AKHTAR, M. K. 2018. CRISPR-Based Technologies for Metabolic Engineering in Cyanobacteria. *Trends in Biotechnology,* 36**,** 996-1010.

BRANCO DOS SANTOS, F., DU, W. & HELLINGWERF, K. J. 2014. Synechocystis: Not Just a Plug-Bug for CO2, but a Green E. coli. *Frontiers in bioengineering and biotechnology,* 2**,** 36-36.

BRESAN, S., SZNAJDER, A., HAUF, W., FORCHHAMMER, K., PFEIFFER, D. & JENDROSSEK, D. 2016. Polyhydroxyalkanoate (PHA) Granules Have no Phospholipids. *Scientific Reports,* 6**,** 26612.

BURNAP, R., HAGEMANN, M. & KAPLAN, A. 2015. Regulation of CO2 Concentrating Mechanism in Cyanobacteria. *Life,* 5**,** 348-371.

CARPINE, R., DU, W., OLIVIERI, G., POLLIO, A., HELLINGWERF, K. J., MARZOCCHELLA, A. & BRANCO DOS SANTOS, F. 2017. Genetic engineering of Synechocystis sp. PCC6803 for poly-β-hydroxybutyrate overproduction. *Algal Research,* 25**,** 117-127.

CARR, N. G. 1966. The occurrence of poly-beta-hydroxybutyrate in the blue-green alga, Chlorogloea fritschii. *Biochimica et Biophysica Acta,* 120**,** 308-10.

CASSURIAGA, A. P. A., FREITAS, B. C. B., MORAIS, M. G. & COSTA, J. A. V. 2018. Innovative polyhydroxybutyrate production by Chlorella fusca grown with pentoses. *Bioresource Technology,* 265**,** 456-463.

CASTRO-SOWINSKI, S., BURDMAN, S., MATAN, O. & OKON, Y. 2009. Natural Functions of Bacterial Polyhydroxyalkanoates.

CHEN, X., SCHREIBER, K., APPEL, J., MAKOWKA, A., FÄHNRICH, B., ROETTGER, M., HAJIREZAEI, M., SÖNNICHSEN, F., SCHÖNHEIT, P., MARTIN, W. & GUTEKUNST, K. 2016. The Entner–Doudoroff pathway is an overlooked glycolytic route in cyanobacteria and plants. *Proceedings of the National Academy of Sciences,* 113**,** 201521916.

COLLIER, J. L. & GROSSMAN, A. R. 1992. Chlorosis induced by nutrient deprivation in Synechococcus sp. strain PCC 7942: not all bleaching is the same. *Journal of Bacteriology,* 174**,** 4718-26.

COOLEY, J. W. & VERMAAS, W. F. J. 2001. Succinate Dehydrogenase and Other Respiratory Pathways in Thylakoid Membranes of Synechocystis sp. Strain PCC 6803: Capacity Comparisons and Physiological Function. *Journal of Bacteriology,* 183**,** 4251-4258.

DAMROW, R., MALDENER, I. & ZILLIGES, Y. 2016. The Multiple Functions of Common Microbial Carbon Polymers, Glycogen and PHB, during Stress Responses in the Non-Diazotrophic Cyanobacterium Synechocystis sp. PCC 6803. *Frontiers in microbiology,* 7**,** 966-966.

DE PHILIPPIS, R., ENA, A., GUASTIINI, M., SILI, C. & VINCENZINI, M. 1992. Factors affecting poly-β-hydroxybutyrate accumulation in cyanobacteria and in purple non-sulfur bacteria. *FEMS Microbiology Letters,* 103**,** 187-194.

DE SMET, M. J., EGGINK, G., WITHOLT, B., KINGMA, J. & WYNBERG, H. 1983. Characterization of intracellular inclusions formed by Pseudomonas oleovorans during growth on octane. *Journal of bacteriology,* 154**,** 870-878.

DÍAZ-TROYA, S., ROLDÁN, M., MALLÉN-PONCE, M. J., ORTEGA-MARTÍNEZ, P. & FLORENCIO, F. J. 2019. Lethality caused by ADP-glucose accumulation is suppressed by salt-induced carbon flux redirection in cyanobacteria. *Journal of Experimental Botany,* 71**,** 2005-2017.

DIENST, D., WICHMANN, J., MANTOVANI, O., RODRIGUES, J. S. & LINDBERG, P. 2020. High density cultivation for efficient sesquiterpenoid biosynthesis in Synechocystis sp. PCC 6803. *Scientific Reports,* 10**,** 5932.

DOELLO, S., KLOTZ, A., MAKOWKA, A., GUTEKUNST, K. & FORCHHAMMER, K. 2018. A Specific Glycogen Mobilization Strategy Enables Rapid Awakening of Dormant Cyanobacteria from Chlorosis. *Plant Physiology,* 177**,** 594-603.

DU, W., JONGBLOETS, J. A., GUILLAUME, M., VAN DE PUTTE, B., BATTAGLINO, B., HELLINGWERF, K. J. & BRANCO DOS SANTOS, F. 2019. Exploiting Day- and Night-Time Metabolism of Synechocystis sp. PCC 6803 for Fitness-Coupled Fumarate Production around the Clock. *ACS synthetic biology,* 8**,** 2263-2269.

DURAN, R. V., HERVAS, M., DE LA ROSA, M. A. & NAVARRO, J. A. 2004. The efficient functioning of photosynthesis and respiration in Synechocystis sp. PCC 6803 strictly requires the presence of either cytochrome c6 or plastocyanin. *Journal of Biological Chemistry,* 279**,** 7229-33.

DUTT, V. & SRIVASTAVA, S. 2018. Novel quantitative insights into carbon sources for synthesis of poly hydroxybutyrate in Synechocystis PCC 6803. *Photosynthesis Research,* 136**,** 303-314.

EISENHUT, M., RUTH, W., HAIMOVICH, M., BAUWE, H., KAPLAN, A. & HAGEMANN, M. 2008. The photorespiratory glycolate metabolism is essential for cyanobacteria and

might have been conveyed endosymbiontically to plants. *Proceedings of the National Academy of Sciences,* 105**,** 17199-17204.

ENGLUND, E., ANDERSEN-RANBERG, J., MIAO, R., HAMBERGER, B. & LINDBERG, P. 2015. Metabolic Engineering of Synechocystis sp. PCC 6803 for Production of the Plant Diterpenoid Manoyl Oxide. *ACS synthetic biology,* 4**,** 1270-1278.

ENGLUND, E., LIANG, F. & LINDBERG, P. 2016. Evaluation of promoters and ribosome binding sites for biotechnological applications in the unicellular cyanobacterium Synechocystis sp. PCC 6803. *Scientific Reports,* 6**,** 36640.

ESPINOSA, J., FORCHHAMMER, K. & CONTRERAS, A. 2007. Role of the Synechococcus PCC 7942 nitrogen regulator protein PipX in NtcA-controlled processes. *Microbiology,* 153**,** 711-718.

ESTEVES-FERREIRA, A. A., INABA, M., FORT, A., ARAUJO, W. L. & SULPICE, R. 2018. Nitrogen metabolism in cyanobacteria: metabolic and molecular control, growth consequences and biotechnological applications. *Critical Reviews in Microbiology,* 44**,** 541-560.

FERNIE, A. R. & BAUWE, H. 2020. Wasteful, essential, evolutionary stepping stone? The multiple personalities of the photorespiratory pathway. *The Plant Journal*.

FLAMHOLZ, A., NOOR, E., BAR-EVEN, A., LIEBERMEISTER, W. & MILO, R. 2013. Glycolytic strategy as a tradeoff between energy yield and protein cost. *Proceedings of the National Academy of Sciences U S A,* 110**,** 10039-44.

FOKINA, O., CHELLAMUTHU, V.-R., ZETH, K. & FORCHHAMMER, K. 2010. A Novel Signal Transduction Protein PII Variant from Synechococcus elongatus PCC 7942 Indicates a Two-Step Process for NAGK–PII Complex Formation. *Journal of Molecular Biology,* 399**,** 410-421.

FORCHHAMMER, K. & LUDDECKE, J. 2016. Sensory properties of the PII signalling protein family. *Febs journal,* 283**,** 425-37.

FORCHHAMMER, K. & SELIM, K. 2019. Carbon/Nitrogen Homeostasis Control in Cyanobacteria. *FEMS microbiology reviews,* 44.

FORCHHAMMER, K. & TANDEAU DE MARSAC, N. 1995. Phosphorylation of the PII protein (glnB gene product) in the cyanobacterium Synechococcus sp. strain PCC 7942: analysis of in vitro kinase activity. *Journal of Bacteriology,* 177**,** 5812-5817.

FUKUI, T., SHIOMI, N. & DOI, Y. 1998. Expression and characterization of (R)-specific enoyl coenzyme A hydratase involved in polyhydroxyalkanoate biosynthesis by Aeromonas caviae. *Journal of Bacteriology,* 180**,** 667-73.

GALE, G. A. R., SCHIAVON OSORIO, A. A., MILLS, L. A., WANG, B., LEA-SMITH, D. J. & MCCORMICK, A. J. 2019. Emerging Species and Genome Editing Tools: Future Prospects in Cyanobacterial Synthetic Biology. *Microorganisms,* 7.

GIBSON, D. G., YOUNG, L., CHUANG, R. Y., VENTER, J. C., HUTCHISON, C. A., 3RD & SMITH, H. O. 2009. Enzymatic assembly of DNA molecules up to several hundred kilobases. *Nature Methods,* 6**,** 343-5.

GÖRL, M., SAUER, J., BAIER, T. & FORCHHAMMER, K. 1998. Nitrogen-starvation-induced chlorosis in Synechococcus PCC 7942: adaptation to long-term survival. 144**,** 2449-2458.

GRIEBEL, R., SMITH, Z. & MERRICK, J. M. 1968. Metabolism of poly(β-hydroxybutyrate). I. Purification, composition, and properties of native poly(β-hydroxybutyrate) granules from Bacillus megaterium. *Biochemistry,* 7**,** 3676-3681.

GRUNDEL, M., SCHEUNEMANN, R., LOCKAU, W. & ZILLIGES, Y. 2012. Impaired glycogen synthesis causes metabolic overflow reactions and affects stress responses in the cyanobacterium Synechocystis sp PCC 6803. *Microbiology-Sgm,* 158**,** 3032-3043.

HAGEMANN, M. & BAUWE, H. 2016. Photorespiration and the potential to improve photosynthesis. *Current Opinion Chemical Biology,* 35**,** 109-116.

HARDING, K. G., DENNIS, J. S., VON BLOTTNITZ, H. & HARRISON, S. T. L. 2007. Environmental analysis of plastic production processes: Comparing petroleum-based polypropylene and polyethylene with biologically-based poly-β-hydroxybutyric acid using life cycle analysis. *Journal of Biotechnology,* 130**,** 57-66.

HART, S. E., SCHLARB-RIDLEY, B. G., BENDALL, D. S. & HOWE, C. J. 2005. Terminal oxidases of cyanobacteria. *Biochemical Society Transactions,* 33**,** 832-835.

HAUF, W., SCHLEBUSCH, M., HUGE, J., KOPKA, J., HAGEMANN, M. & FORCHHAMMER, K. 2013. Metabolic Changes in Synechocystis PCC6803 upon Nitrogen-Starvation: Excess NADPH Sustains Polyhydroxybutyrate Accumulation. *Metabolites,* 3**,** 101-18.

HAUF, W., SCHMID, K., GERHARDT, E. C., HUERGO, L. F. & FORCHHAMMER, K. 2016. Interaction of the Nitrogen Regulatory Protein GlnB (PII) with Biotin Carboxyl Carrier Protein (BCCP) Controls Acetyl-CoA Levels in the Cyanobacterium Synechocystis sp. PCC 6803. *Frontires of Microbiology,* 7**,** 1700.

HAUF, W., WATZER, B., ROOS, N., KLOTZ, A. & FORCHHAMMER, K. 2015. Photoautotrophic Polyhydroxybutyrate Granule Formation Is Regulated by Cyanobacterial Phasin PhaP in Synechocystis sp. Strain PCC 6803. *Applied Environmental Microbiology,* 81**,** 4411-22.

HAYWOOD, G., ANDERSON, A., WILLIAMS, D., DAWES, E. & EWING, D. 1991. Accumulation of a Poly(hydroxyalkanoate) copolymer containing primarily 3-hydroxyvalerate from simple carbohydrate substrates by Rhodococcus sp. NCIMB 40126. *International journal of biological macromolecules,* 13**,** 83-8.

HONDO, S., TAKAHASHI, M., OSANAI, T., MATSUDA, M., HASUNUMA, T., TAZUKE, A., NAKAHIRA, Y., CHOHNAN, S., HASEGAWA, M. & ASAYAMA, M. 2015. Genetic engineering and metabolite profiling for overproduction of polyhydroxybutyrate in cyanobacteria. *Journal of Bioscience and Bioengineering,* 120**,** 510-7.

ISHII-HYAKUTAKE, M., MIZUNO, S. & TSUGE, T. 2018. Biosynthesis and Characteristics of Aromatic Polyhydroxyalkanoates. *Polymers,* 10**,** 1267.

ISSA, I., DELBRUCK, S. & HAMM, U. 2019. Bioeconomy from experts' perspectives - Results of a global expert survey. *PLoS One,* 14**,** e0215917.

ITO, S. & OSANAI, T. 2020. Unconventional biochemical regulation of the oxidative pentose phosphate pathway in the model cyanobacterium Synechocystis sp. PCC 6803. *Biochemical Journal,* 477**,** 1309-1321.

JENDROSSEK, D. 2009. Polyhydroxyalkanoate granules are complex subcellular organelles (carbonosomes). *Journal of Bacteriology,* 191**,** 3195-202.

JENDROSSEK, D. & HANDRICK, R. 2002. Microbial degradation of polyhydroxyalkanoates. *Annual Review of Microbiologyl,* 56**,** 403-32.

JENDROSSEK, D. & PFEIFFER, D. 2014. New insights in the formation of polyhydroxyalkanoate granules (carbonosomes) and novel functions of poly(3-hydroxybutyrate). *Environmental Microbiology,* 16**,** 2357-2373.

JIANG, X.-R., YAO, Z.-H. & CHEN, G.-Q. 2017. Controlling cell volume for efficient PHB production by Halomonas. *Metabolic Engineering,* 44**,** 30-37.

JONES, L. B., GHOSH, P., LEE, J. H., CHOU, C. N. & KUNZ, D. A. 2018. Linkage of the Nit1C gene cluster to bacterial cyanide assimilation as a nitrogen source. *Microbiology,* 164**,** 956-968.

KADOURI, D., BURDMAN, S., JURKEVITCH, E. & OKON, Y. 2002. Identification and isolation of genes involved in poly(beta-hydroxybutyrate) biosynthesis in Azospirillum brasilense and characterization of a phbC mutant. *Applied Environmental Microbiology,* 68**,** 2943-9.

KADOURI, D., JURKEVITCH, E. & OKON, Y. 2003. Poly β-hydroxybutyrate depolymerase (PhaZ) in Azospirillum brasilense and characterization of a phaZ mutant. *Archives of Microbiology,* 180**,** 309-318.

KAEWBAI-NGAM, A., INCHAROENSAKDI, A. & MONSHUPANEE, T. 2016. Increased accumulation of polyhydroxybutyrate in divergent cyanobacteria under nutrient-deprived photoautotrophy: An efficient conversion of solar energy and carbon dioxide to polyhydroxybutyrate by Calothrix scytonemicola TISTR 8095. *Bioresource Technology,* 212**,** 342-347.

KALIA, V. C., LAL, S. & CHEEMA, S. 2007. Insight in to the phylogeny of polyhydroxyalkanoate biosynthesis: horizontal gene transfer. *Gene,* 389**,** 19-26.

KAMRAVA, D., KOVÁCS, T., PFLÜGL, S., DRUZHININA, I., KROLL, P., LACKNER, M. & HERWIG, C. 2018. *Increased poly-B-hydroxybutyrate production from carbon dioxide in randomly mutated cells of cyanobacterial strain Synechocystis sp. PCC 6714: Mutant generation and Characterization*.

KAMRAVAMANESH, D., KOVACS, T., PFLUGL, S., DRUZHININA, I., KROLL, P., LACKNER, M. & HERWIG, C. 2018a. Increased poly-beta-hydroxybutyrate production from carbon dioxide in randomly mutated cells of cyanobacterial strain Synechocystis sp. PCC 6714: Mutant generation and characterization. *Bioresource Technology,* 266**,** 34-44.

KAMRAVAMANESH, D., LACKNER, M. & HERWIG, C. 2018b. Bioprocess Engineering Aspects of Sustainable Polyhydroxyalkanoate Production in Cyanobacteria. *Bioengineering (Basel, Switzerland),* 5**,** 111.

KAMRAVAMANESH, D., PFLÜGL, S., NISCHKAUER, W., LIMBECK, A., LACKNER, M. & HERWIG, C. 2017. Photosynthetic poly-β-hydroxybutyrate accumulation in unicellular cyanobacterium Synechocystis sp. PCC 6714. *AMB Express,* 7**,** 143-143.

KANEKO, T., SATO, S., KOTANI, H., TANAKA, A., ASAMIZU, E., NAKAMURA, Y., MIYAJIMA, N., HIROSAWA, M., SUGIURA, M., SASAMOTO, S., KIMURA, T., HOSOUCHI, T., MATSUNO, A., MURAKI, A., NAKAZAKI, N., NARUO, K., OKUMURA, S., SHIMPO, S., TAKEUCHI, C., WADA, T., WATANABE, A., YAMADA, M., YASUDA, M. & TABATA, S. 1996. Sequence analysis of the genome of the unicellular cyanobacterium Synechocystis sp. strain PCC6803. II. Sequence determination of the entire genome and assignment of potential protein-coding regions. *DNA Research,* 3**,** 109-36.

KARMANN, S., FOLLONIER, S., BASSAS-GALIA, M., PANKE, S. & ZINN, M. 2016. Robust at-line quantification of poly(3-hydroxyalkanoate) biosynthesis by flow cytometry using a BODIPY 493/503-SYTO 62 double-staining. *Journal of Microbiological Methods,* 131**,** 166-171.

KARRADT, A., SOBANSKI, J., MATTOW, J., LOCKAU, W. & BAIER, K. 2008. NblA, a key protein of phycobilisome degradation, interacts with ClpC, a HSP100 chaperone partner of a cyanobacterial Clp protease. *Journal of Biological Chemistry,* 283**,** 32394-403.

KAVITHA, G., KURINJIMALAR, C., SIVAKUMAR, K., PALANI, P. & RENGASAMY, R. 2016. Biosynthesis, purification and characterization of polyhydroxybutyrate from Botryococcus braunii kutz. *International Journal of Biological Macromolecules,* 89**,** 700-6.

KHETKORN, W., INCHAROENSAKDI, A., LINDBLAD, P. & JANTARO, S. 2016. Enhancement of poly-3-hydroxybutyrate production in Synechocystis sp. PCC 6803 by overexpression of its native biosynthetic genes. *Bioresource Technology,* 214**,** 761-8.

KLOTZ, A. & FORCHHAMMER, K. 2017. Glycogen, a major player for bacterial survival and awakening from dormancy. *Future microbiology,* 12.

KLOTZ, A., GEORG, J., BUČINSKÁ, L., WATANABE, S., REIMANN, V., JANUSZEWSKI, W., SOBOTKA, R., JENDROSSEK, D., HESS, WOLFGANG R. & FORCHHAMMER, K. 2016. Awakening of a Dormant Cyanobacterium from Nitrogen Chlorosis Reveals a Genetically Determined Program. *Current Biology,* 26**,** 2862-2872.

KÖBLER, C., SCHULTZ, S.-J., KOPP, D., VOIGT, K. & WILDE, A. 2018. The role of the Synechocystis sp. PCC 6803 homolog of the circadian clock output regulator RpaA in day–night transitions. *Molecular Microbiology,* 110**,** 847-861.

KOCH, M., BERENDZEN, K. W. & FORCHHAMMER, A. K. 2020. On the Role and Production of Polyhydroxybutyrate (PHB) in the Cyanobacterium Synechocystis sp. PCC 6803. *Life (Basel),* 10.

KOCH, M. & FORCHHAMMER, K. 2020. Storage polymers in cyanobacteria: friend or foe? . *Cyanobacteria biotechnology,* Wiley.

KUCHO, K., OKAMOTO, K., TSUCHIYA, Y., NOMURA, S., NANGO, M., KANEHISA, M. & ISHIURA, M. 2005. Global analysis of circadian expression in the cyanobacterium Synechocystis sp. strain PCC 6803. *Journal of Bacteriology,* 187**,** 2190-9.

LAN, E. I. & LIAO, J. C. 2012. ATP drives direct photosynthetic production of 1-butanol in cyanobacteria. *Proceedings of the National Academy of Sciences of the United States of America,* 109**,** 6018-6023.

LATIFI, A., RUIZ, M. & ZHANG, C.-C. 2009. Oxidative stress in cyanobacteria. *FEMS Microbiology Reviews,* 33**,** 258-278.

LAU, N.-S., FOONG, C. P., KURIHARA, Y., SUDESH, K. & MATSUI, M. 2014. RNA-Seq Analysis Provides Insights for Understanding Photoautotrophic Polyhydroxyalkanoate Production in Recombinant Synechocystis Sp. *PLOS ONE,* 9**,** e86368.

LEA-SMITH, D. J., BOMBELLI, P., VASUDEVAN, R. & HOWE, C. J. 2016. Photosynthetic, respiratory and extracellular electron transport pathways in cyanobacteria. *Biochimica et Biophysica Acta (BBA) - Bioenergetics,* 1857**,** 247-255.

LEA-SMITH, D. J., ROSS, N., ZORI, M., BENDALL, D. S., DENNIS, J. S., SCOTT, S. A., SMITH, A. G. & HOWE, C. J. 2013. Thylakoid Terminal Oxidases Are Essential for the Cyanobacterium Synechocystis sp. PCC 6803 to Survive Rapidly Changing Light Intensities. *Plant Physiology,* 162**,** 484-495.

LEMOIGNE, M. 1926. Produit de déshydratation et de polymérisation de l'acide b-oxybutyrique. *Bull. Soc. Chim. Biol.,* 8:770-782.

LI, S., JENDRESEN, C. B., LANDBERG, J., PEDERSEN, L. E., SONNENSCHEIN, N., JENSEN, S. I. & NIELSEN, A. T. 2020. Genome-Wide CRISPRi-Based Identification of Targets for Decoupling Growth from Production. *ACS Synthetic Biology*.

LI, X., SHEN, C. R. & LIAO, J. C. 2014. Isobutanol production as an alternative metabolic sink to rescue the growth deficiency of the glycogen mutant of Synechococcus elongatus PCC 7942. *Photosynthesis Research,* 120**,** 301-10.

LIPPI, L., BÄHR, L., WÜSTENBERG, A., WILDE, A. & STEUER, R. 2018. Exploring the potential of high-density cultivation of cyanobacteria for the production of cyanophycin. *Algal Research,* 31**,** 363-366.

MAKOWKA, A., NICHELMANN, L., SCHULZE, D., SPENGLER, K., WITTMANN, C., FORCHHAMMER, K. & GUTEKUNST, K. 2020. Glycolytic Shunts Replenish the Calvin-Benson-Bassham Cycle as Anaplerotic Reactions in Cyanobacteria. *Molecular Plant,* 13.

MARTÍNEZ, V., JURKEVITCH, E., GARCÍA, J. L. & PRIETO, M. A. 2013. Reward for Bdellovibrio bacteriovorus for preying on a polyhydroxyalkanoate producer. *Environmental Microbiology,* 15**,** 1204-1215.

MESSINEO, L. 1966. Modification of the Sakaguchi reaction: Spectrophotometric determination of arginine in proteins without previous hydrolysis. *Archives of Biochemistry and Biophysics,* 117**,** 534-540.

MEZZINA, M. P. & PETTINARI, M. J. 2016. Phasins, Multifaceted Polyhydroxyalkanoate Granule-Associated Proteins. *Applied and Environmental Microbiology,* 82**,** 5060-5067.

MILLS, L. A., MCCORMICK, A. J. & LEA-SMITH, D. J. 2020. Current knowledge and recent advances in understanding metabolism of the model cyanobacterium Synechocystis sp. PCC 6803. *Bioscience Reportsp,* 40.

MIYAKE, M., KATAOKA, K., SHIRAI, M. & ASADA, Y. 1997. Control of poly-beta-hydroxybutyrate synthase mediated by acetyl phosphate in cyanobacteria. *Journal of Bacteriology,* 179**,** 5009-5013.

MONSHUPANEE, T., NIMDACH, P. & INCHAROENSAKDI, A. 2016. Two-stage (photoautotrophy and heterotrophy) cultivation enables efficient production of bioplastic poly-3-hydroxybutyrate in auto-sedimenting cyanobacterium. *Scientific Reports,* 6**,** 37121.

MUDLIAR, S. N., VAIDYA, A. N., SURESH KUMAR, M., DAHIKAR, S. & CHAKRABARTI, T. 2007. Techno-economic evaluation of PHB production from activated sludge. *Clean Technologies and Environmental Policy,* 10**,** 255.

MURO-PASTOR, M. I., REYES, J. C. & FLORENCIO, F. J. 2005. Ammonium assimilation in cyanobacteria. *Photosynthesis Research,* 83**,** 135-50.

NAKAYA, Y., IIJIMA, H., TAKANOBU, J., WATANABE, A., HIRAI, M. Y. & OSANAI, T. 2015. One day of nitrogen starvation reveals the effect of sigE and rre37 overexpression on the expression of genes related to carbon and nitrogen metabolism in Synechocystis sp. PCC 6803. *Journal of Bioscience and Bioengineering,* 120**,** 128-34.

NOWROTH, V., MARQUART, L. & JENDROSSEK, D. 2016. Low temperature-induced viable but not culturable state of Ralstonia eutropha and its relationship to accumulated polyhydroxybutyrate. *FEMS microbiology letters,* 363**,** fnw249.

O'NEILL, D. W., FANNING, A. L., LAMB, W. F. & STEINBERGER, J. K. 2018. A good life for all within planetary boundaries. *Nature Sustainability,* 1**,** 88-95.

OBRUCA, S., SEDLACEK, P., SLANINOVA, E., FRITZ, I., DAFFERT, C., MEIXNER, K., SEDRLOVA, Z. & KOLLER, M. 2020. Novel unexpected functions of PHA granules. *Applied Microbiology and Biotechnology*.

OHASHI, Y., SHI, W., TAKATANI, N., AICHI, M., MAEDA, S., WATANABE, S., YOSHIKAWA, H. & OMATA, T. 2011. Regulation of nitrate assimilation in cyanobacteria. *Journal of Experimental Botany,* 62**,** 1411-24.

OKAMURA, E., TOMITA, T., SAWA, R., NISHIYAMA, M. & KUZUYAMA, T. 2010. Unprecedented acetoacetyl-coenzyme A synthesizing enzyme of the thiolase superfamily involved in the mevalonate pathway. *Proceedings of the National Academy of Sciences,* 107**,** 11265-11270.

ORTHWEIN, T. 2019. Investigation of Putative PHB Associated Proteins and Metabolic Engineering of the PHB Synthesis in Synechocystis sp. PCC 6803. *Master thesis*

OSANAI, T., NUMATA, K., OIKAWA, A., KUWAHARA, A., IIJIMA, H., DOI, Y., TANAKA, K., SAITO, K. & HIRAI, M. Y. 2013. Increased bioplastic production with an RNA polymerase sigma factor SigE during nitrogen starvation in Synechocystis sp. PCC 6803. *DNA Research,* 20**,** 525-35.

OSANAI, T., OIKAWA, A., NUMATA, K., KUWAHARA, A., IIJIMA, H., DOI, Y., SAITO, K. & HIRAI, M. 2014. Pathway-Level Acceleration of Glycogen Catabolism by Response Regulator Rre37 in the Cyanobacterium Synechocystis sp. PCC 6803. *Plant physiology,* 164.

OSANAI, T., SHIRAI, T., IIJIMA, H., NAKAYA, Y., OKAMOTO, M., KONDO, A. & HIRAI, M. Y. 2015. Genetic manipulation of a metabolic enzyme and a transcriptional regulator increasing succinate excretion from unicellular cyanobacterium. *Frontiers in Microbiology,* 6**,** 1064.

PANDA, B., JAIN, P., SHARMA, L. & MALLICK, N. 2006. Optimization of cultural and nutritional conditions for accumulation of poly-beta-hydroxybutyrate in Synechocystis sp. PCC 6803. *Bioresource Technology,* 97**,** 1296-301.

PANUSCHKA, S., DROSG, B., ELLERSDORFER, M., MEIXNER, K. & FRITZ, I. 2019. Photoautotrophic production of poly-hydroxybutyrate – First detailed cost estimations. *Algal Research,* 41**,** 101558.

PAPKE, R. T., RAMSING, N. B., BATESON, M. M. & WARD, D. M. 2003. Geographical isolation in hot spring cyanobacteria. *Environmental Microbiology,* 5**,** 650-9.

PFEIFFER, D. & JENDROSSEK, D. 2012. Localization of poly(3-hydroxybutyrate) (PHB) granule-associated proteins during PHB granule formation and identification of two new phasins, PhaP6 and PhaP7, in Ralstonia eutropha H16. *Journal of bacteriology,* 194**,** 5909-5921.

PFEIFFER, D. & JENDROSSEK, D. 2014. PhaM Is the Physiological Activator of Poly(3-Hydroxybutyrate) (PHB) Synthase (PhaC1) in Ralstonia eutropha. *Applied and Environmental Microbiology,* 80**,** 555-563.

POHLMANN, A., FRICKE, W. F., REINECKE, F., KUSIAN, B., LIESEGANG, H., CRAMM, R., EITINGER, T., EWERING, C., PÖTTER, M., SCHWARTZ, E., STRITTMATTER, A., VOß, I., GOTTSCHALK, G., STEINBÜCHEL, A., FRIEDRICH, B. & BOWIEN, B. 2006. Genome sequence of the bioplastic-producing "Knallgas" bacterium Ralstonia eutropha H16. *Nature Biotechnology,* 24**,** 1257-1262.

POSEN, I. D., JARAMILLO, P. & GRIFFIN, W. M. 2016. Uncertainty in the Life Cycle Greenhouse Gas Emissions from U.S. Production of Three Biobased Polymer Families. *Environmental Science & Technology,* 50**,** 2846-58.

PREISS, J. 1984. Bacterial glycogen synthesis and its regulation. *Annual Review of Microbiology,* 38**,** 419-58.

PREISS, J. 2006. Bacterial Glycogen Inclusions: Enzymology and Regulation of Synthesis. *Inclusions in Prokaryotes*, 71-108.

PRIETO, A., DE EUGENIO, L., GALÁN, B., LUENGO, J. & WITHOLT, B. 2007. Synthesis and Degradation of Polyhydroxyalkanoates. *Pseudomonas,* 397-428.

PRIETO, A., ESCAPA, I. F., MARTINEZ, V., DINJASKI, N., HERENCIAS, C., DE LA PENA, F., TARAZONA, N. & REVELLES, O. 2016. A holistic view of polyhydroxyalkanoate metabolism in Pseudomonas putida. *Environmental Microbiology,* 18**,** 341-57.

RAANAN, H., OREN, N., TREVES, H., KEREN, N., OHAD, I., BERKOWICZ, S. M., HAGEMANN, M., KOCH, M., SHOTLAND, Y. & KAPLAN, A. 2016. Towards clarifying what distinguishes cyanobacteria able to resurrect after desiccation from those that cannot: The photosynthetic aspect. *Biochimica et Biophysica Acta,* 1857**,** 715-22.

RABERG, M., VOIGT, B., HECKER, M. & STEINBÜCHEL, A. 2014. A Closer Look on the Polyhydroxybutyrate- (PHB-) Negative Phenotype of Ralstonia eutropha PHB-4. *PLOS ONE,* 9**,** e95907.

RAE, B. D., LONG, B. M., WHITEHEAD, L. F., FORSTER, B., BADGER, M. R. & PRICE, G. D. 2013. Cyanobacterial carboxysomes: microcompartments that facilitate CO2 fixation. *Journal of Molecular Microbiology and Biotechnology,* 23**,** 300-7.

RATCLIFF, W. C. & DENISON, R. F. 2010. Individual-level bet hedging in the bacterium Sinorhizobium meliloti. *Current Biology,* 20**,** 1740-4.

REHM, B. H., KRUGER, N. & STEINBUCHEL, A. 1998. A new metabolic link between fatty acid de novo synthesis and polyhydroxyalkanoic acid synthesis. The PHAG gene from Pseudomonas putida KT2440 encodes a 3-hydroxyacyl-acyl carrier protein-coenzyme a transferase. *Journal of Biological Chemistry,* 273**,** 24044-51.

REHM, B. H. A. 2003. Polyester synthases: natural catalysts for plastics. *Biochemical Journal,* 376**,** 15-33.

REIS, M. A. M., SERAFIM, L. S., LEMOS, P. C., RAMOS, A. M., AGUIAR, F. R. & VAN LOOSDRECHT, M. C. M. 2003. Production of polyhydroxyalkanoates by mixed microbial cultures. *Bioprocess and Biosystems Engineering,* 25**,** 377-385.

RIPPKA, R., DERUELLES, J., WATERBURY, J. B., HERDMAN, M. & STANIER, R. Y. 1979. Generic Assignments, Strain Histories and Properties of Pure Cultures of Cyanobacteria. *Microbiology,* 111**,** 1-61.

RIVERA-BRISO, A. L. & SERRANO-AROCA, Á. 2018. Poly(3-Hydroxybutyrate-co-3-Hydroxyvalerate): Enhancement Strategies for Advanced Applications. *Polymers,* 10**,** 732.

RUEDA, E., GARCÍA-GALÁN, M. J., ORTIZ, A., UGGETTI, E., CARRETERO, J., GARCÍA, J. & DÍEZ-MONTERO, R. 2020. Bioremediation of agricultural runoff and biopolymers production from cyanobacteria cultured in demonstrative full-scale photobioreactors. *Process Safety and Environmental Protection,* 139**,** 241-250.

RUIZ, J. A., LOPEZ, N. I. & MENDEZ, B. S. 2004. rpoS gene expression in carbon-starved cultures of the Polyhydroxyalkanoate-accumulating species Pseudomonas oleovorans. *Current Microbiology,* 48**,** 396-400.

SAHA, R., LIU, D., HOYNES-O'CONNOR, A., LIBERTON, M., YU, J., BHATTACHARYYA-PAKRASI, M., BALASSY, A., ZHANG, F., MOON, T. S., MARANAS, C. D. & PAKRASI, H. B. 2016. Diurnal Regulation of Cellular Processes in the Cyanobacterium Synechocystis sp. Strain PCC 6803: Insights from Transcriptomic, Fluxomic, and Physiological Analyses. *mBio,* 7.

SÁNCHEZ-BARACALDO, P. & CARDONA, T. 2020. On the origin of oxygenic photosynthesis and Cyanobacteria. *New Phytologist,* 225**,** 1440-1446.

SAUER, J., SCHREIBER, U., SCHMID, R., VÖLKER, U. & FORCHHAMMER, K. 2001. Nitrogen starvation-induced chlorosis in Synechococcus PCC 7942. Low-level photosynthesis as a mechanism of long-term survival. *Plant physiology,* 126**,** 233-243.

SAWERS, G. 2016. Dormancy: Illuminating How a Microbial Sleeping Beauty Awakens. *Current Biology,* 26**,** R1139-R1141.

SCHEMBRI, M. A., WOODS, A. A., BAYLY, R. C. & DAVIES, J. K. 1995. Identification of a 13-kDa protein associated with the polyhydroxyalkanoic acid granules from Acinetobacter spp. *FEMS Microbiol Lett,* 133**,** 277-83.

SCHIRRMEISTER, B. E., GUGGER, M. & DONOGHUE, P. C. J. 2015. Cyanobacteria and the Great Oxidation Event: evidence from genes and fossils. *Palaeontology,* 58**,** 769-785.

SCHLEBUSCH, M. 2012. Analysis of the Sll0783 Function in PHB Synthesis in Synechocystis PCC 6803: a Crucial Role of NADPH in N-Starvation. *Dissertation*.

SCHLEBUSCH, M. & FORCHHAMMER, K. 2010. Requirement of the nitrogen starvation-induced protein Sll0783 for polyhydroxybutyrate accumulation in Synechocystis sp. strain PCC 6803. *Applied Environmental Microbiology,* 76**,** 6101-7.

SCHOLL, J., DENGLER, L., BADER, L. & FORCHHAMMER, K. 2020. Phosphoenolpyruvate Carboxylase from the Cyanobacterium Synechocystis sp. PCC 6803 is under Global Metabolic Control by PII Signaling. *Molecular Microbiology*.

SCHULLER, J., SAURA, P., THIEMANN, J., SCHULLER, S., GAMIZ-HERNANDEZ, A., KURISU, G., NOWACZYK, M. & KAILA, V. 2020. Redox-coupled proton pumping drives carbon concentration in the photosynthetic complex I. *Nature Communications,* 11**,** 494.

SCHULLER, J. M., BIRRELL, J. A., TANAKA, H., KONUMA, T., WULFHORST, H., COX, N., SCHULLER, S. K., THIEMANN, J., LUBITZ, W., SÉTIF, P., IKEGAMI, T., ENGEL, B. D., KURISU, G. & NOWACZYK, M. M. 2019. Structural adaptations of photosynthetic complex I enable ferredoxin-dependent electron transfer. *Science,* 363**,** 257-260.

SCHWARZ, R. & FORCHHAMMER, K. 2005. Acclimation of unicellular cyanobacteria to macronutrient deficiency: emergence of a complex network of cellular responses. 151**,** 2503-2514.

SHABESTARY, K., ANFELT, J., LJUNGQVIST, E., JAHN, M., YAO, L. & HUDSON, E. P. 2018. Targeted Repression of Essential Genes To Arrest Growth and Increase Carbon Partitioning and Biofuel Titers in Cyanobacteria. *ACS Synth Biol,* 7**,** 1669-1675.

SILI, C., TORZILLO, G. & VONSHAK, A. 2012. Ecology of Cyanobacteria II.

SINGH, A. K. & MALLICK, N. 2017. Advances in cyanobacterial polyhydroxyalkanoates production. *FEMS Microbiol Lett,* 364.

STAL, L. J. & MOEZELAAR, R. 1997. Fermentation in cyanobacteria1. *FEMS Microbiology Reviews,* 21**,** 179-211.

STANIER, R. Y., KUNISAWA, R., MANDEL, M. & COHEN-BAZIRE, G. 1971. Purification and properties of unicellular blue-green algae (order Chroococcales). *Bacteriological Reviews,* 35**,** 171-205.

SUDESH, K., TAGUCHI, K. & DOI, Y. 2002. Effect of increased PHA synthase activity on polyhydroxyalkanoates biosynthesis in Synechocystis sp. PCC6803. *International Journal of Biological Macromolecules,* 30**,** 97-104.

SZNAJDER, A., PFEIFFER, D. & JENDROSSEK, D. 2015. Comparative Proteome Analysis Reveals Four Novel Polyhydroxybutyrate (PHB) Granule-Associated Proteins in Ralstonia eutropha H16. *Applied and Environmental Microbiology,* 81**,** 1847-1858.

TAKAHASHI, H., MIYAKE, M., TOKIWA, Y. & ASADA, Y. 1998. Improved accumulation of poly-3- hydroxybutyrate by a recombinant cyanobacterium. *Biotechnology Letters,* 20**,** 183-186.

TARAWAT, S., INCHAROENSAKDI, A. & MONSHUPANEE, T. 2020. Cyanobacterial production of poly(3-hydroxybutyrate-co-3-hydroxyvalerate) from carbon dioxide or a single organic substrate: improved polymer elongation with an extremely high 3-hydroxyvalerate mole proportion. *Journal of Applied Phycology*.

TIMM, A. & STEINBÜCHEL, A. 1990. Formation of polyesters consisting of medium-chain-length 3-hydroxyalkanoic acids from gluconate by Pseudomonas aeruginosa and other fluorescent pseudomonads. *Applied and Environmental Microbiology,* 56**,** 3360-3367.

TROSCHL, C., MEIXNER, K. & DROSG, B. 2017. Cyanobacterial PHA Production-Review of Recent Advances and a Summary of Three Years' Working Experience Running a Pilot Plant. *Bioengineering (Basel, Switzerland),* 4**,** 26.

TROSCHL, C., MEIXNER, K., FRITZ, I., LECHNER, K., ROMERO, A., KOVALCIK, A., SEDLACEK, P. & DROSG, B. 2018. Pilot-scale production of poly-β-hydroxybutyrate with the cyanobacterium Synechocytis sp. CCALA192 in a non-sterile tubular photobioreactor. *Algal Research,* 34**,** 116-125.

UEDA, S., KAWAMURA, Y., IIJIMA, H., NAKAJIMA, M., SHIRAI, T., OKAMOTO, M., KONDO, A., HIRAI, M. Y. & OSANAI, T. 2016. Anionic metabolite biosynthesis enhanced by potassium under dark, anaerobic conditions in cyanobacteria. *Scientific Reports,* 6**,** 32354.

UNGERER, J. & PAKRASI, H. B. 2016. Cpf1 Is A Versatile Tool for CRISPR Genome Editing Across Diverse Species of Cyanobacteria. *Scientific Reports,* 6**,** 39681.

VALAPPIL, S. P., MISRA, S. K., BOCCACCINI, A. R., KESHAVARZ, T., BUCKE, C. & ROY, I. 2007. Large-scale production and efficient recovery of PHB with desirable material properties, from the newly characterised Bacillus cereus SPV. *Journal of Biotechnology,* 132**,** 251-8.

VALLADARES, A., MONTESINOS, M. L., HERRERO, A. & FLORES, E. 2002. An ABC-type, high-affinity urea permease identified in cyanobacteria. *Molecular Microbiology,* 43**,** 703-15.

VAN ALPHEN, P., ABEDINI NAJAFABADI, H., BRANCO DOS SANTOS, F. & HELLINGWERF, K. J. 2018. Increasing the Photoautotrophic Growth Rate of Synechocystis sp. PCC 6803 by Identifying the Limitations of Its Cultivation. *Biotechnol Journal,* 13**,** e1700764.

VAN DER WALLE, G. A., DE KONING, G. J., WEUSTHUIS, R. A. & EGGINK, G. 2001. Properties, modifications and applications of biopolyesters. *Advances in Biochemical Engineering / Biotechnologyl,* 71**,** 263-91.

VAN GEMERDEN, H. 1968. On the ATP generation by Chromatium in darkness. *Archives of Microbiology,* 64**,** 118-24.

VELÁZQUEZ-SÁNCHEZ, C., ESPÍN, G., PEÑA, C. & SEGURA, D. 2020. The Modification of Regulatory Circuits Involved in the Control of Polyhydroxyalkanoates Metabolism to Improve Their Production. *Frontiers in Bioengineering and Biotechnology,* 8**,** 386.

VELMURUGAN, R. & INCHAROENSAKDI, A. 2018. Disruption of Polyhydroxybutyrate Synthesis Redirects Carbon Flow towards Glycogen Synthesis in Synechocystis sp. PCC 6803 Overexpressing glgC/glgA. *Plant Cell Physiology,* 59**,** 2020-2029.

VIEIRA, C. J. A., BOTELHO, M. J., FRANCO, L. B., SILVA, B. V. D., AGUIAR, C. A. P. & DE, M. M. G. 2018. Recent Advances and Future Perspectives of PHB Production by Cyanobacteria. *Industrial Biotechnology,* 14**,** 249-256.

WANG, C., SHENG, X., EQUI, R., TRAINER, M., CHARLES, T. & SOBRAL, B. 2008. Influence of the Poly-3-Hydroxybutyrate (PHB) Granule-Associated Proteins (PhaP1 and PhaP2) on PHB Accumulation and Symbiotic Nitrogen Fixation in Sinorhizobium meliloti Rm1021. *Journal of bacteriology,* 189**,** 9050-6.

WARD, P. G. & O'CONNOR, K. E. 2005. Bacterial synthesis of polyhydroxyalkanoates containing aromatic and aliphatic monomers by Pseudomonas putida CA-3. *International Journal of Biological Macromoleculesl,* 35**,** 127-33.

WATZER, B., ENGELBRECHT, A., HAUF, W., STAHL, M., MALDENER, I. & FORCHHAMMER, K. 2015. Metabolic pathway engineering using the central signal processor PII. *Microbial Cell Factories,* 14**,** 192.

WATZER, B. & FORCHHAMMER, K. 2018. Cyanophycin Synthesis Optimizes Nitrogen Utilization in the Unicellular Cyanobacterium Synechocystis sp. Strain PCC 6803. *Applied Environmental Microbiology,* 84.

WATZER, B., SPÄT, P., NEUMANN, N., KOCH, M., SOBOTKA, R., MACEK, B., HENNRICH, O. & FORCHHAMMER, K. 2019. The Signal Transduction Protein PII Controls Ammonium, Nitrate and Urea Uptake in Cyanobacteria. *Frontiers in Microbiology,* 10.

WEIß, A.-L. 2018. Identifikation und Expression verschiedener PHP assoziierter Proteine in Synechocystis sp. PCC 6803. *Bachelor thesis*

WENDT, K. E., UNGERER, J., COBB, R. E., ZHAO, H. & PAKRASI, H. B. 2016. CRISPR/Cas9 mediated targeted mutagenesis of the fast growing cyanobacterium Synechococcus elongatus UTEX 2973. *Microbial Cell Factories,* 15**,** 115.

WILDE, E. 1962. Untersuchungen über Wachstum und Speicherstoffsynthese von Hydrogenomonas. *Archiv für Mikrobiologie,* 43**,** 109-137.

WOLK, C. P., VONSHAK, A., KEHOE, P. & ELHAI, J. 1984. Construction of shuttle vectors capable of conjugative transfer from Escherichia coli to nitrogen-fixing filamentous cyanobacteria. *Proceedings of the National Academy of Sciences U S A,* 81**,** 1561-5.

WORLD ECONOMIC FORUM, E. M. F. A. M. C. 2016. The New Plastics Economy — Rethinking the future of plastics. *Report*.

XIE, J., ZHOU, J., ZHANG, H. & LI, Y. 2011. [Increasing reductant NADPH content via metabolic engineering of PHB synthesis pathway in Synechocystis sp. PCC 6803]. *Sheng Wu Gong Cheng Xue Bao,* 27**,** 998-1004.

XIONG, W., LEE, T., ROMMELFANGER, S., GJERSING, E., CANO, M., MANESS, P.-C., GHIRARDI, M. & YU, J. 2015. Phosphoketolase pathway contributes to carbon metabolism in cyanobacteria. *Nature Plants,* 1**,** 15187.

YAO, L., CENGIC, I., ANFELT, J. & HUDSON, E. P. 2016a. Multiple Gene Repression in Cyanobacteria Using CRISPRi. *ACS Synthetic Biology,* 5**,** 207-212.

YAO, L., CENGIC, I., ANFELT, J. & HUDSON, E. P. 2016b. Multiple Gene Repression in Cyanobacteria Using CRISPRi. *ACS Synth Biol,* 5**,** 207-12.

YAO, L., SHABESTARY, K., BJÖRK, S., ASPLUND-SAMUELSSON, J., JOENSSON, H., JAHN, M. & HUDSON, E. 2020. Pooled CRISPRi screening of the cyanobacterium

Synechocystis sp PCC 6803 for enhanced industrial phenotypes. *Nature Communications,* 11.

YOO, S.-H., LEE, B.-H., MOON, Y., SPALDING, M. H. & JANE, J.-L. 2014. Glycogen Synthase Isoforms in Synechocystis sp. PCC6803: Identification of Different Roles to Produce Glycogen by Targeted Mutagenesis. *PLOS ONE,* 9**,** e91524.

YORK, G. M., STUBBE, J. & SINSKEY, A. J. 2001. New Insight into the Role of the PhaP Phasin of Ralstonia eutropha in Promoting Synthesis of Polyhydroxybutyrate. *Journal of Bacteriology,* 183**,** 2394-2397.

YORK, G. M., STUBBE, J. & SINSKEY, A. J. 2002. The Ralstonia eutropha PhaR Protein Couples Synthesis of the PhaP Phasin to the Presence of Polyhydroxybutyrate in Cells and Promotes Polyhydroxybutyrate Production. *Journal of Bacteriology,* 184**,** 59-66.

ZAVŘEL, T., OČENÁŠOVÁ, P. & ČERVENÝ, J. 2017. Phenotypic characterization of Synechocystis sp. PCC 6803 substrains reveals differences in sensitivity to abiotic stress. *PloS one,* 12**,** e0189130-e0189130.

ZHANG, H., LIU, Y., YAO, C., CAO, X., TIAN, J. & XUE, S. 2017. FabG can function as PhaB for poly-3-hydroxybutyrate biosynthesis in photosynthetic cyanobacteria Synechocystis sp. PCC 6803. *Bioengineered,* 8**,** 707-715.

ZHANG, S., YANG, W., CHEN, H., LIU, B., LIN, B. & TAO, Y. 2019. Metabolic engineering for efficient supply of acetyl-CoA from different carbon sources in Escherichia coli. *Microbial Cell Factories,* 18**,** 130.

ZHAO, Y., LI, H., QIN, L., WANG, H. & CHEN, G.-Q. 2007. Disruption of the polyhydroxyalkanoate synthase gene in Aeromonas hydrophila reduces its survival ability under stress conditions. *FEMS microbiology letters,* 276**,** 34-41.

IX. Appendix

1. Accepted publication

M. Koch, S. Doello, K. Gutekunst, K. Forchhammer (2019).

PHB is Produced from Glycogen Turn-over during Nitrogen Starvation in Synechocystis sp. PCC 6803.

International Journal of Molecular Sciences, 20, 1942.

International Journal of
Molecular Sciences

MDPI

Article

PHB is Produced from Glycogen Turn-over during Nitrogen Starvation in *Synechocystis* sp. PCC 6803

Moritz Koch [1], Sofía Doello [1], Kirstin Gutekunst [2] and Karl Forchhammer [1,*]

[1] Interfaculty Institute of Microbiology and Infection Medicine Tübingen, Eberhard-Karls-Universität Tübingen, 72076 Tübingen, Germany; moritz.koch@uni-tuebingen.de (M.K.); sofia.doello@gmail.com (S.D.)
[2] Department of Biology, Botanical Institute, Christian-Albrechts-University, 24118 Kiel, Germany; kgutekunst@bot.uni-kiel.de
* Correspondence: karl.forchhammer@uni-tuebingen.de; Tel.: +49-7071-29-72096

Received: 4 April 2019; Accepted: 18 April 2019; Published: 20 April 2019

Abstract: Polyhydroxybutyrate (PHB) is a polymer of great interest as a substitute for conventional plastics, which are becoming an enormous environmental problem. PHB can be produced directly from CO_2 in photoautotrophic cyanobacteria. The model cyanobacterium *Synechocystis* sp. PCC 6803 produces PHB under conditions of nitrogen starvation. However, it is so far unclear which metabolic pathways provide the precursor molecules for PHB synthesis during nitrogen starvation. In this study, we investigated if PHB could be derived from the main intracellular carbon pool, glycogen. A mutant of the major glycogen phosphorylase, GlgP2 (*slr1367* product), was almost completely impaired in PHB synthesis. Conversely, in the absence of glycogen synthase GlgA1 (*sll0945* product), cells not only produced less PHB, but were also impaired in acclimation to nitrogen depletion. To analyze the role of the various carbon catabolic pathways (EMP, ED and OPP pathways) for PHB production, mutants of key enzymes of these pathways were analyzed, showing different impact on PHB synthesis. Together, this study clearly indicates that PHB in glycogen-producing *Synechocystis* sp. PCC 6803 cells is produced from this carbon-pool during nitrogen starvation periods. This knowledge can be used for metabolic engineering to get closer to the overall goal of a sustainable, carbon-neutral bioplastic production.

Keywords: cyanobacteria; bioplastic; PHB; sustainable; glycogen; metabolic engineering; Synechocystis

1. Introduction

Cyanobacteria are among the most widespread organisms on our planet. Their ability to perform oxygenic photosynthesis allows them to grow autotrophically with CO_2 as the sole carbon source [1]. Additionally, many cyanobacteria acquired the ability to fix nitrogen, one of the most limiting nutrients [2]. However, many others are not able to fix nitrogen, one of them being the well-studied model organism *Synechocystis* sp. PCC 6803 (hereafter: *Synechocystis*) [3]. Nitrogen starvation starts a well-orchestrated survival process in *Synechocystis*, called chlorosis [4]. During chlorosis, *Synechocystis* degrades not only its photosynthetic machinery, but also accumulates large quantities of biopolymers, namely glycogen and poly-hydroxy-butyrate (PHB) [5]. Glycogen synthesis following the onset of nitrogen starvation serves transiently as a major sink for newly fixed CO_2 [6] before CO_2 fixation is tuned down during prolonged nitrogen starvation. During resuscitation from chlorosis, a specific glycogen catabolic metabolism supports the re-greening of chlorotic cells [7]. By contrast to the pivotal role of glycogen, the function of the polymer PHB remains puzzling, since mutants impaired in PHB synthesis survived and recovered from chlorosis as awild-type [8,9]. Nevertheless, many different cyanobacterial species produce PHB, implying a hitherto unrecognized functional importance [10].

In other microorganisms PHB fulfills various functions during conditions of unbalanced nutrient availability and can also protect cells against low temperatures or redox stress [11–13]. Understanding the intracellular mechanisms that lead to PHB production could help to elucidate the physiological role of this polymer. Regardless of the physiological significance of PHB, this polymer has been recognized as a promising alternative for current plastics, which contaminate terrestrial and aquatic ecosystems [14]. PHB can serve as a basis for completely biodegradable plastics, with properties comparable to petroleum-derived plastics [15,16]. Since *Synechocystis* produces PHB only under nutrient limiting conditions, this phenomenon can be exploited to temporally separate the initial biomass production from PHB production induced by shifting cells to nitrogen limiting conditions [10].

One of the biggest obstacles preventing economic PHB production in cyanobacteria remains the low level of intracellular PHB accumulation [17]. While chemotrophic bacteria are capable of producing more than 80% PHB of their cell dry mass, (e.g., *Cupriavidus necator*), most cyanobacteria naturally produce less than 20% of their cell dry mass [15]. Additionally, their growth rate is too slow to compete with the PHB production in chemotrophic bacteria. There have been many attempts in the past to further improve the intracellular PHB production, often with limited [1] success [18–20]. One of the most successful approaches has been achieved by random mutagenesis, leading to up to 37% PHB of the cell dry mass [21]. However, more directed approaches involving genetic engineering are often limited by a lack of knowledge about how the cells' metabolism works in detail. For example, until today, it was still unknown from which carbon metabolites PHB was derived. There have been several different studies analyzing the intracellular fluxes in cyanobacteria [22]. However, most of them did not analyze the carbon flow during prolonged nitrogen starvation. One of these studies showed that in nitrogen-starved photosynthetically grown cyanobacteria up to 87% of the carbon in PHB is derived from intracellular carbon sources rather than from newly fixed CO_2 [23]. However, until now, it was not clearly resolved which metabolic routes provide the precursors for PHB synthesis. This knowledge would lay the foundation for future metabolic engineering approaches to create overproduction strains. Hence, the goal of this study was to find out where the carbon for the PHB production is coming from and which pathways it is taking until it reaches PHB.

It has been shown that disruption of PHB synthesis results in an increased production of glycogen; however, an overproduction of glycogen did not lead to higher amounts of PHB [24]. Another study that also investigated the accumulation of glycogen in a PHB-free mutant Δ*phaC*, could not detect any differences in growth or glycogen accumulation [8].

An important aspect in the issue concerning the relation between glycogen and PHB metabolism deals with the contribution of various carbon metabolic pathways for the production of precursors for PHB under conditions of nitrogen limitation. *Synechocystis* is able to catabolize glucose via three parallel operating glycolytic pathways [25] (Figure 1): the Embden-Meyerhof-Parnas (EMP) pathway, the oxidative pentose phosphate (OPP) pathway [26], and the Entner Doudoroff (ED) pathway [25]. When nitrogen-starved cells recover from chlorosis, they require the parallel operating OPP and ED pathways, whereas the EMP pathway seems dispensable [7]. Metabolic analysis of mutants overexpressing the transcriptional regulator *rre37* showed a correlated upregulation of PHB synthesis and EMP pathway genes (*phaAB* and *pfkA*, respectively) [27]. However, so far is has not been investigated, how important these pathways for the production of PHB during nitrogen starvation.

This work started with the initial aim to define whether PHB synthesis depends on the metabolism of glycogen. Since the initial results implied that PHB is strongly affected by glycogen catabolism, we further investigated the importance of the different carbon pathways EMP, ED and OPP for the production of PHB. These findings shall help to further understand the intracellular PHB metabolism in cyanobacteria, which can be used to create more efficient PHB overproduction strains, making the production of PHB as a bioplastic more cost efficient.

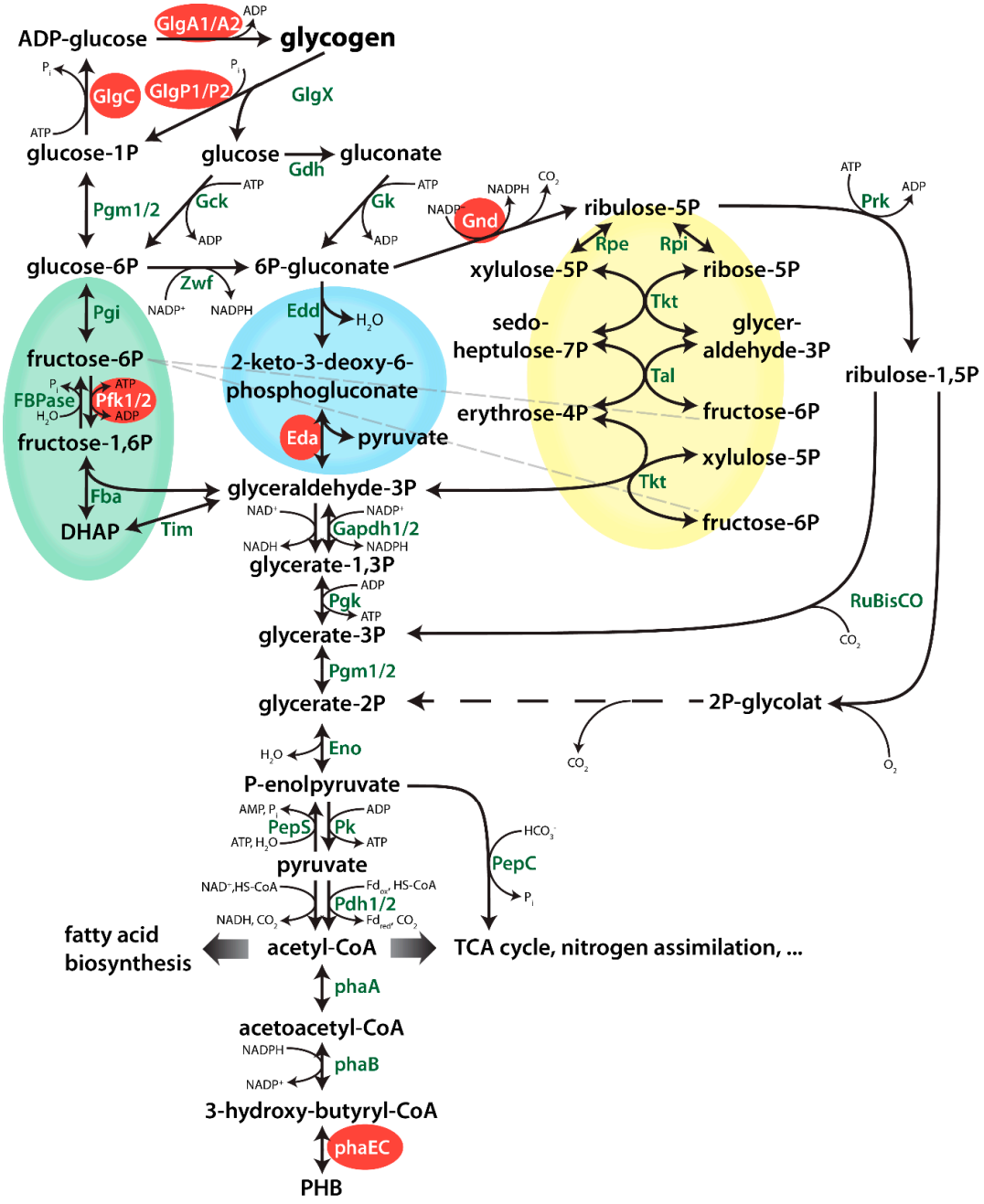

Figure 1. Overview of central metabolism of Synechocystis. Genes which were deleted in this study are highlighted in with a red background. Dotted lines represent several enzymatic reactions. The EMP, ED and OPP (Embden-Meyerhof-Parnas, Entner-Doudoroff, Oxidative Pentose Phosphate) pathways are highlighted in green, blue and yellow, respectively.

2. Results

Following the onset of nitrogen-starvation, large quantities of fixed carbon are stored in *Synechocystis* cells as glycogen granules. Long-term starvation experiments of *Synechocystis* cultures have shown that, while cells are chlorotic, glycogen is slowly degraded, following its initial rapid accumulation but PHB is slowly and steadily accumulating [9]. Considering that chlorotic cells are photosynthetically inactive, these data could indicate a potential correlation between the turn-over of glycogen and the synthesis of PHB. An overview of the metabolic pathways connecting the glycogen pool with PHB is shown in Figure 1. To substantiate the hypothesis that PHB might be derived from

glycogen turn-over, we investigated PHB accumulation in various mutant strains, in which key steps in different pathways are interrupted. The respective mutations are shown in Figure 1. All strains used in this work were characterized previously, with their phenotypes, including growth behaviours, described in the respective publications (see Table A1). Furthermore, all mutants used in these studies were fully segregated to ensure clear phenotypes.

2.1. Impact of Glycogen Synthesis on PHB Production

To analyze the role of glycogen synthesis on the production of PHB, we first analyzed the accumulation of these biopolymers during nitrogen starvation in mutants with defects in glycogen synthesis. The double mutant of the two glycogen synthase genes *glgA1* (*sll0945*) and *glgA2* (*sll1393*) is unable to acclimate to nitrogen deprivation and rapidly dies upon shifting cells to nitrogen free $BG11^0$ medium [8] and, therefore, could not be analyzed. Instead, we used a knockout mutant of the glucose-1-phosphate adenylyltransferase (*glgC*, *slr1176*) and two knockout strains of each of the isoforms of the glycogen synthase, *glgA1* (*sll0945*) and *glgA2* (*sll1393*). Yoo et al. [28] reported that the single *glgA1* and *glgA2* mutants were still able to produce similar amounts of glycogen as the wild-type (WT), since one glycogen synthase is still present, and this seems to be sufficient to reach the wild-type levels of glycogen. However, the structure of the glycogen produced by the two isoforms seemed to slightly differ in chain-length distribution [28]. In that study, no distinguishing phenotype of the two mutant strains had been reported. In the present study, the cultures were shifted to nitrogen free medium $BG11^0$ and further incubated under constant illumination of 40 µmol photons m^{-2} s^{-1}. Under these experimental conditions, the Δ*glgA1* mutant showed an impaired chlorosis reaction, whereas the Δ*glgA2* mutant performed chlorosis as the wild-type strain (Figure 2A). To further determine the viability of two weeks nitrogen-starved cells, serial dilutions were dropped on nitrate-supplemented BG11 plates. As shown in Figure 2B, the Δ*glgA1* mutant was severely impaired in recovering from nitrogen starvation, whereas Δ*glgA2* could recover from chlorosis with the same efficiency as the wild-type (Figure 2B).

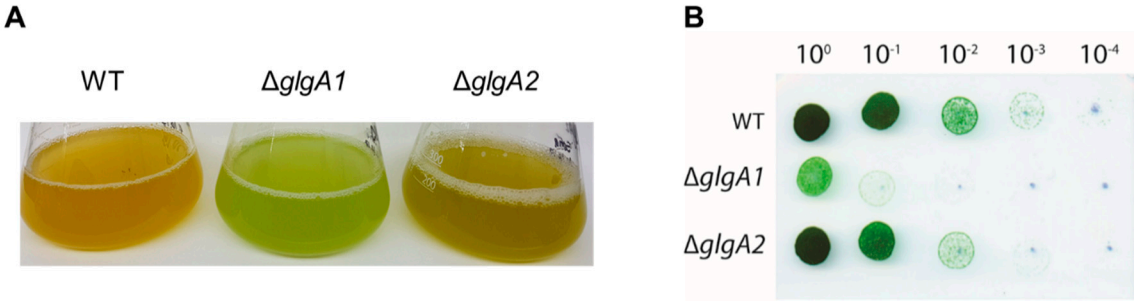

Figure 2. Characterization of the glycogen synthase mutants, Δ*glgA1* and Δ*glgA2*. (**A**) Cultures after five days of nitrogen starvation. (**B**) Recovery assay of chlorotic wild-type (WT) and mutants Δ*glgA1* and Δ*glgA2*, using the drop agar method. Cultures that were nitrogen-starved for 14 days were serially diluted from 1 to 1:10,000 and from each dilution, a drop of 5 µL was plated on BG11 agar and grown for seven days.

During the course of three weeks of nitrogen starvation, the quantities of PHB and glycogen that accumulate in the cells were determined (Figure 3A,B).

In the wild-type, the amount of glycogen already peaked after the first week and slowly decreased in the following two weeks (Figure 3B). As previously reported by Yoo et al. [28], the single Δ*glgA1* and Δ*glgA2* mutants initially accumulated similar amounts of glycogen to the wild-type, but in contrast to the wild-type, the level of glycogen remained high. The PHB content in the *glgA2* mutant was similar to the wild-type for the first seven days of nitrogen starvation, but PHB accumulation slowed down afterwards (Figure 3B). By contrast, the *glgA1* mutant was strongly impaired in PHB production. Together, the phenotype of the *glgA1* and *glgA2* mutants indicates that glycogen synthase GlgA1 plays

a much more important role in nitrogen starvation acclimation than GlgA2, although the amount of glycogen produced by these two strains is almost the same. One explanation could be that the subtle differences in the glycogen produced form the two isoenzymes might result in different functions, with GlgA1-produced glycogen being much more relevant for the maintenance metabolism in chlorotic cells and for the resuscitation from chlorosis than glycogen produced by GlgA2. In clear correlation with the redundant role of GlgA2, the *glgA2* mutant was not impaired in PHB synthesis, whereas mutation of the functionally important *glgA1* gene resulted in strongly impaired PHB synthesis.

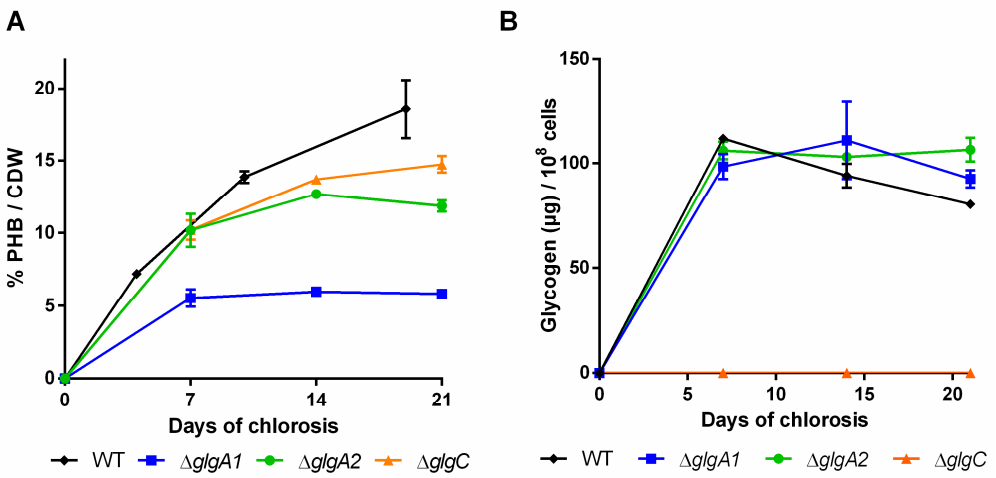

Figure 3. Polyhydroxybutyrate (PHB) content in percentage of cell dry weight (CDW) (**A**) and cellular glycogen content (**B**) of mutants impaired in the glycogen synthesis. Cultures were shifted to nitrogen free medium at day 0 and were subsequently grown for 21 days. Each point represents a mean of three independent biological replicates.

The *glgC* mutant was previously characterized by Grundel et al. [6]. They showed that Δ*glgC* is not able to perform a proper nitrogen-starvation acclimation response: it maintains its pigments while it loses viability, which was also observed in our experiments. Namakoshi et al. [29] showed that this mutant is unable to synthesize glycogen, which is also in line with our results. Under our conditions, unlike previously described by Damrow et al. [8], the *glgC* mutant did not show an increased amount of PHB compared to the WT, but seemed to accumulate less PHB instead (Figure 3A). It has to be noted though that Damrow et al. [8] investigated only one single timepoint, after seven days of nitrogen starvation. In addition, these results should be treated with care, since PHB content is normalized to cell dry weight, which shrinks in the *glgC* mutant due to progressive cell lysis. Consequently, the cell density was severely diminished at the end of the experiment (OD_{750} of 0.51, compared to ~1.15 of other mutants and the wild-type). The differences between our study and that of Damrow et al. [8] thus may result from differences in cell lysis rather than from differences in PHB synthesis. When the relatively low cell density of the *glgC* mutant is considered, it produces much less PHB per volume compared to the wild-type.

2.2. Impact of Glycogen Degradation on PHB Production

If glycogen turn-over would result in PHB accumulation during chlorosis, synthesis of PHB should be abrogated when glycogen degradation is impaired. To test this assumption, mutants in catabolic glycogen phosphorylase genes (*glgP*) were investigated with the same methods as described above. Glycogen can be degraded by the two glycogen phosphorylase isoenzymes, encoded by *glgP1* (slr1356) and *glgP2* (slr1367) [7]. A detailed study by Doello et al. [7] showed that GlgP2 is the main enzyme responsible for glycogen degradation during resuscitation from nitrogen chlorosis. Knocking out GlgP1 (Δ*glgP1*) does not affect the efficiency of recovery, whereas knocking out GlgP2 (Δ*glgP2*) or both phosphorylases (Δ*glgP1/2*) completely impairs the ability to degrade glycogen [7]. Here, we

investigated glycogen and PHB accumulation during three weeks of nitrogen starvation in these glycogen phosphorylases mutants.

Although the initial amount of glycogen was higher in the *glgP1* mutant compared to the WT (Figure 4B), the amount decreased during the course of the experiment. By contrast, no glycogen degradation occurred in the Δ*glgP2* and Δ*glgP1/2* double mutant. This correlates with the specific requirement of chlorotic cells for GlgP2 for resuscitation from nitrogen starvation, as it has been previously described [7].

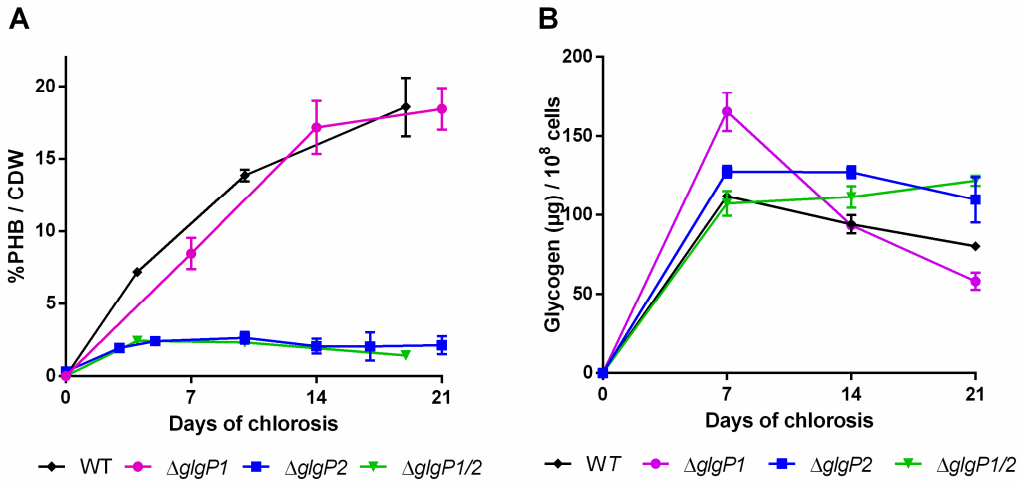

Figure 4. PHB content in percentage of cell dry weight (CDW) (**A**) and glycogen content (**B**) of mutants impaired in the glycogen degradation. Cultures were shifted to nitrogen free medium at day 0 and were subsequently grown for 21 days. Each point represents a mean of three independent biological replicates.

Intriguingly, the different mutants showed a drastic difference in the amounts of PHB being produced (Figure 4A): While the Δ*glgP1* strain produced similar amounts of PHB as the wild-type, a strong decrease was observed for the Δ*glgP2* strain. The same phenotype was observed for the double knockout mutant, indicating that origin of the effect is based on the absence of *glgP2*. The PHB synthesis phenotypes were further confirmed by fluorescence microscopy after staining PHB with Nile red (Figure 5). PHB granules appear as bright red fluorescing intracellular granular structures. In agreement with the results from PHB quantification by HPLC analysis, the Δ*glgP1* strain showed similar amounts and distribution of PHB granules than the wild-type. By contrast, only very small granules, if at all visible, could be detected in the strains Δ*glgP2* and Δ*glgP1/2*.

Altogether, the inability of the mutants Δ*glgP2* and Δ*glgP1/2* to accumulate PHB demonstrates unequivocally that glycogen catabolism through GlgP2 is required for the ongoing PHB synthesis during prolonged nitrogen starvation.

2.3. Impact of Mutations in Carbon Catabolic Pathway on PHB Production

The experiments outlined above revealed that specific glycogen synthesizing or degrading enzymes have a strong effect on the amounts of PHB being produced and that glycogen turn-over via GlgP2 provides the carbon skeletons for PHB synthesis. To investigate how the released glucose phosphate molecules are metabolized downstream of glycogen, knockouts of the three most important glycolytic routes [25] were checked for their PHB and glycogen production during chlorosis. While the strain Δ*eda* (*sll0107*) lacks the ability to metabolize molecules via the ED pathway, Δ*gnd* is not able to use the OPP pathway. Additionally, the strain Δ*pfk1/2* lacks both phosphofructokinases, which causes an interruption of the EMP pathway. Also, the individual knockouts of both isoforms, Δ*pfk1* and Δ*pfk2*, were investigated.

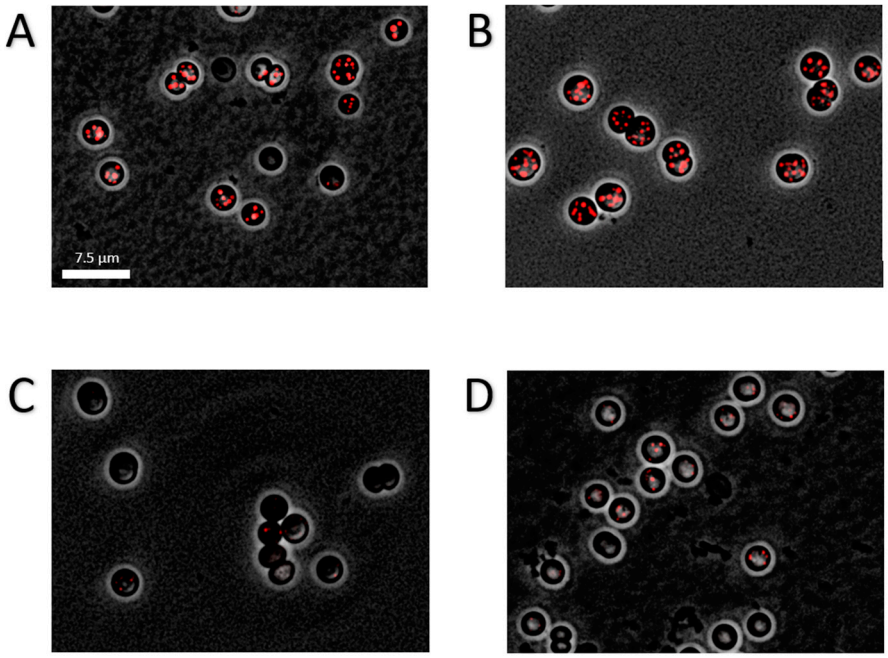

Figure 5. Fluorescence microscopic picture of Nile-red stained PHB granules in chlorotic cells. Cultures where grown for 14 days in nitrogen depleted medium $BG11^0$. Shown is an overlay of phase contrast with a CY3 channel of the WT (**A**), Δ*glgP1* (**B**), Δ*glgP2* (**C**) and Δ*glgP1/2* (**D**). Scale bar corresponds to 7.5 µm.

Again, the different mutant strains and a WT control were grown for three weeks under nitrogen deprived conditions and PHB and glycogen content was quantified (Figure 6).

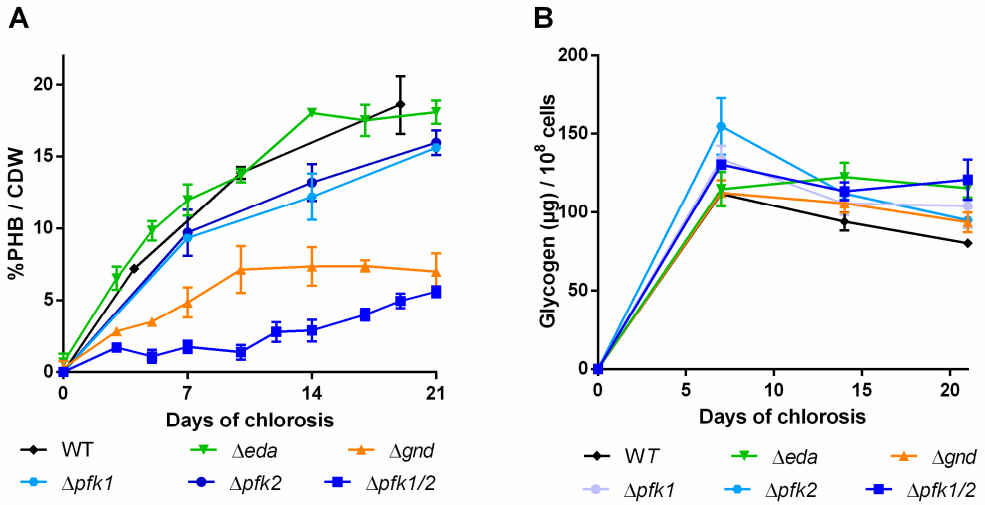

Figure 6. PHB content in percentage of cell dry weight (CDW) (**A**) and glycogen content (**B**) of mutants with disrupted carbon pathway. Cultures were shifted to nitrogen free medium at day 0 and were subsequently grown for 21 days. Each point represents a mean of three independent biological replicates.

Distortion of the ED pathway (Δ*eda*) did not result in any PHB phenotype different from the WT and the glycogen content remained high during the course of the experiment. In the Δ*gnd* mutant, a slower increase of PHB than in the WT was observed within the first ten days (Figure 6A) and PHB accumulation subsequently ceased. When the EMP pathway was blocked (Δ*pfk1/2*), only very little PHB was produced in the first two weeks of the chlorosis. Thereafter though, PHB production slightly

increased and finally reached similar levels as in the Δ*gnd* mutant. The total amount of glycogen over the time of chlorosis did not decrease in this mutant. The single Δ*pfk* mutants showed PHB contents similar to the WT, indicating that the two isoenzymes are able to replace each other's function. Taken together, it appears that EMP and OPP pathways contribute to PHB production, whereas the ED pathway does not play a role.

2.4. Impact of PHB Formation on Glycogen Synthesis

In order to check how the PHB production affects the accumulation of glycogen, a PHB-free mutant, namely Δ*phaEC*, was checked for its production of carbon polymers (Figure 7).

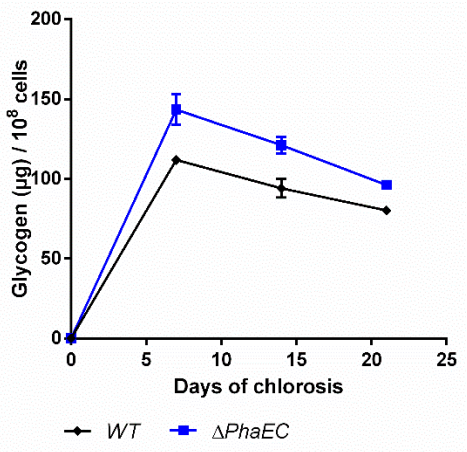

Figure 7. Glycogen content of wild-type and mutant lacking the PHB synthase genes (*PhaEC*). Cultures were shifted to nitrogen free medium at day 0 and were subsequently grown for 21 days. Each point represents a mean of three independent biological replicates.

As expected, the mutant was unable to synthesize PHB (data not shown [8]). Compared to the WT, the mutant produced moderately higher amounts of glycogen and degrades it slightly faster, so that at the end of the experiments, the glycogen levels were quite similar.

3. Discussion

As recently shown by isotope labeling experiments [23], the majority of the carbon from PHB is coming from intracellular metabolites, which contribute around 74% to the carbon within PHB. Additionally, a random mutagenized strain, which is an overproducer of PHB, shows also a strongly accelerated decay of glycogen [30]. Here, we provide clear evidence that the intracellular glycogen pool and its products provide the carbon metabolites for PHB synthesis during nitrogen starvation. In the absence of glycogen degradation, as it is the case in the Δ*glgP2* and the Δ*glgP1/2* double mutant, PHB synthesis is almost completely abrogated. In the Δ*glgP2* mutant, the remaining GlgP1 enzyme is apparently not efficiently catabolizing glycogen, which agrees with its lack of function for the resuscitation from chlorosis. By contrast, GlgP2 is required for glycogen catabolism and resuscitation from chlorosis [7]. From these data, it is reasonable to hypothesize that during chlorosis, GlgP2 slowly degrades glycogen, and the degradation products end up in the PHB pool.

Like the two glycogen phosphorylase isoenzymes, the two glycogen synthase isoenzymes GlgA1 and GlgA2 appear to have specialized functions. Even though both Δ*glgA1* and Δ*glgA2* synthesized similar amounts of glycogen, deletion of *glgA1* resulted in a mutant with reduced bleaching, viability and PHB content whereas Δ*glgA2* was less affected. This indicates that glycogen produced by GlgA1 is important for resuscitation and growth. On the other hand, GlgA2 produced glycogen appeared less important or its function is yet unknown. Previous publications did not see such a difference, which may be explained by a much shorter time of nitrogen starvation used in their study [6]. Taken together, those mutants (*glgP2* and Δ*glgA1*) that were less viable under nitrogen starvation, did also

synthesize less PHB. It remains to be demonstrated, if the different impact that GlgA1 and GlgA2 exert on viability and PHB synthesis originates from the slightly different branching patterns [28] of the glycogen, that they synthesize.

In the Δ*glgC* mutant, PHB is formed, although no glycogen is produced (Figure 3), which seems to contradict the hypothesis of glycogen-derived PHB [8,28]. Taking into account the above results, it appears likely that the carbon metabolites used for PHB can under certain conditions bypass the glycogen pool. When *glgC* is knocked out, glucose-1P (and its precursor, glucose-6P) cannot be further converted into ADP-glucose and may accumulate. The glucose-phosphates could then be downstream metabolized to glyceraldehyde-3P and further converted into PHB. By contrast, when *glgA1* is mutated, the newly fixed carbon can be converted by GlgC to ADP-glucose and subsequently enters the GlgA2-synthesized inactive glycogen pool, where it cannot be further metabolized into PHB. A similar connection between PHB and glycogen has already been described in other organisms (*Sinorhizobium meliloti*), where PHB levels were lower in a mutant lacking *glgA1* [31]. Since the GlgA1/GlgA2 double mutant rapidly dies upon nitrogen starvation [6], the impact of the complete absence of glycogen due to glycogen synthase deficiency on PHB synthesis cannot be experimentally tested.

Furthermore, we observed that a slower degradation of glycogen often correlates with a low-PHB-phenotype, as seen in the case of Δ*glgA1*, Δ*glgP2*, Δ*glgP1/2* and Δ*pfk1/2* (Figures 3, 4 and 6, respectively). This further supports the hypothesis, that only when glycogen gets degraded during the process of chlorosis, PHB is formed. In two cases, Δ*glgP1/2* and Δ*pfk1/2*, the amount of glycogen was even increasing during the later course of nitrogen starvation. This hints towards an ongoing glycogen formation during nitrogen chlorosis, which gets only visible once glycogen degradation is disturbed. Apparently, glycogen metabolism is much more dynamic than presumed from the relative static pool size observed in the wild-type. A steady glycogen synthesis may be counterbalanced by ongoing degradation, together resulting in only a slow net change of its pool size.

The residual metabolism in nitrogen starved chlorotic cells [9,32] is probably required to ensure long-term survival through repair of essential biomolecules such as proteins, DNA and RNA, osmoregulation, regulated shifts in metabolic pathways and the preparation for a quick response as soon as nutrients are available again [33,34]. According to these needs, non-growing starved cells still require a constant supply of ATP, reduction equivalents and the ability to produce cellular building blocks for survival. In line with this, we observed that PHB production was mainly achieved via the EMP pathway, which has the highest ATP yield among the three main carbon catalytic pathways (EMP, OPP, ED). In addition, we found that the OPP pathway is involved in PHB synthesis as well. This pathway provides metabolites for biosynthetic purposes as the repair of biomolecules for maintenance. By contrast, deletion of the ED pathway, which has a lower ATP yield in comparison to the EMP pathway and is physiologically probably most important in connection with photosynthesis and the Calvin–Benson cycle [7,25], did not impair PHB production under nitrogen starvation. Nevertheless, the glycogen levels did not decrease in the Δ*gnd* mutant, implying that mutation of the ED pathway affects the dynamics of glycogen turn-over discussed above.

Finally, we observed that the various carbon catabolic pathways have different functional importance for PHB production, in a time-dependent manner: While the mutant Δ*gnd* (blocking the OPP pathway) produced PHB in the first phase of the experiment but later stopped its synthesis, the Δ*pfk1/2* mutant (impaired in the EMP pathway) was initially blocked in PHB accumulation but later started to produce it (Figure 4). Interestingly, the time point, at which the Δ*gnd* mutant stopped PHB production matched its start in the Δ*pfk1/2* mutant. This could indicate a consecutive role of EMP and OPP pathway during nitrogen chlorosis. Although the exact function of the EMP pathway remains unknown, we show here for the first time a phenotype of a cyanobacterial mutant lacking this pathway. This suggested to also investigate the deletion of the individual knockouts. Deletion of only one of the Pfk isoenzymes (*pfk1*: sll1196 and *pfk2*: sll0745) resulted in mutants that produced about 80% of the PHB of WT cells, whereas the PHB production of the double mutant Δ*pfk1/2* was severely reduced. Pfk1 and Pfk2 can thus obviously compensate for the loss of the respective other, even though PHB

production is highest if both enzymes are present. This observation is well in line with transcriptomic studies, which detected an increase in expression of both Pfk isoenzymes during nitrogen starvation [5]. The observation that both EMP and OPP pathway are of importance during arrested growth under nitrogen starvation is in agreement with earlier investigations that reported the upregulation of the sugar catabolic genes *pfk1*, *pfk2*, *zwf*, *gnd* and *gap1* concomitantly with glycogen accumulation [5,35]. EMP and OPP pathway thus support PHB production in non-growing, nitrogen-starved cells, whereas ED and OPP pathway are most important during resuscitation form nitrogen chlorosis after feeding the cells with nitrate [7].

The mutant Δ*phaEC* did not produce any PHB and degraded glycogen similarly to the WT (Figure 7). This indicates that there is no direct feedback between these two polymer pools. In the absence of PHB synthesis, metabolites form glycogen degradation could be leaked by overflow reactions. Under unbalanced metabolic situations, it has been shown that cyanobacteria can excrete metabolites into the medium to control their intracellular energy status [6,36,37]. In any case, this result demonstrates that PHB and glycogen do not compete for CO_2 fixation products, but glycogen is epistatic over PHB synthesis.

Previous studies showed that, under nitrogen starvation, certain genes are upregulated, which are under the regulation of SigE, a group 2 σ factor [38]. Among these genes are glycogen degrading enzymes like *glgP1* and *glgP2* and *glgX*, but also the key enzymes for the pathways further downstream, namely *pfk* and *gnd*. The fact that all these genes are expressed simultaneously with the genes of the PHB synthesis [9], demonstrate that all relevant transcripts of the key enzymes required for the conversion from glycogen to PHB are present during nitrogen starvation. Our finding that PHB is mainly synthesized from glycogen degradation during nitrogen chlorosis is supported by a recent study, where a *Synechocystis* sp. PCC 6714 strain with enhanced PHB accumulation was created by random mutagenesis. Transcriptome analysis revealed that this strain exhibits an increased expression of glycogen phosphorylase [21]. This indicates that manipulation of glycogen metabolism may be a key for improved PHB synthesis.

Gaining further insights into the intracellular carbon fluxes could provide more information on how PHB production is regulated. Once the regulation is understood, this knowledge could be used to redirect the large quantities of glycogen towards PHB. This knowledge could be used in metabolic engineering approaches to either completely reroute the carbon from glycogen (making up more than 60% of the CDW) to PHB, for example by overexpression of glycogen degrading enzymes, or even from inorganic carbon to PHB directly. Therefore, the new insights from this work can be exploited for biotechnological applications to further increase the amounts of PHB being produced in cyanobacteria.

4. Materials and Methods

4.1. Cyanobacterial Cultivation Conditions

For standard cultivation, *Synechocystis* sp. PCC 6803 cells were grown in 200 mL BG_{11} medium, supplemented with 5 mM $NaHCO_3$ [39]. A list of the used strains of this study is provided in Table A1. Two different wild-type strains, a Glc sensitive and a Glc tolerant one, were used. Both strains showed the same behavior during normal growth as well as during chlorosis. Appropriate antibiotics were added to the different mutants to ensure the continuity of the mutation. The cells were cultivated at 28 °C, shaking at 120 rpm and constant illumination of 40–50 µmol photons m^{-2} s^{-1}. Nitrogen starvation was induced as described previously [40]. In short, exponentially growing cells (OD 0.4–0.8) were centrifuged for 10 min at 4000× *g*. The cells were washed in 100 mL of BG_0 (BG_{11} medium without $NaNO_3$) before they were centrifuged again. The resulting pellet was resuspended in BG_0 until it reached an OD of 0.4.

4.2. Microscopy and Staining Procedures

To observe PHB granules within the cells, 100 µL of cyanobacterial cells were centrifuged (1 min at 10,000× *g*) and 80 µL of the supernatant discarded. Nile Red (10 µL) was added and used to resuspend the pellet in the remaining 20 µL of the supernatant. From these mixtures, 10 µL were taken and applied on an agarose coated microscope slide to immobilize the cells. The Leica DM5500B microscope (Leica, Wetzlar, Germany) was used with a 100× /1.3 oil objective for fluorescence microscopy. To detect Nile red stained PHB granules, an excitation filter BP 535/50 was used, together with a suppression filter BP 610/75. A Leica DFC360FX (Leica, Wetzlar, Germany)) was used for image acquisition.

4.3. PHB Quantification

PHB content within the cells was determined as described previously [41]. Roughly 15 mL of cells were harvested and centrifuged at 4000× *g* for 10 min at 25 °C. The resulting pellet was dried for 3 h at 60 °C in a speed-vac (Christ, Osterode, Germany), before 1 mL of concentrated H_2SO_4 was added and boiled for 1 h at 100 °C to break up the cells and to convert PHB to crotonic acid. From this, 100 µL were taken and diluted in 900 µL 0.014 M H_2SO_4. To remove cell debris, the samples were centrifuged for 10 min at 10,000× *g*, before 500 µL of the supernatant were transferred to 500 µL 0.014 M H_2SO_4. After an additional centrifugation step with the same conditions as above, the supernatant was used for HPLC analysis on a Nucleosil 100 C 18 column (Agilent, Santa Clara, CA, USA) (125 by 3 mm). As a liquid phase, 20 mM phosphate buffer (pH 2.5) was used. Commercially available crotonic acids was used as a standard with a conversion ratio of 0.893. The amount of crotonic acid was detected at 250 nm.

4.4. Glycogen Quantification

Intracellular glycogen content was measured by harvesting 2 mL of cyanobacterial culture. The cells were washed twice with 1 mL of ddH_2O. Afterwards the pellet was resuspended in 400 µL KOH (30% *w/v*) and incubated for 2 h at 95 °C. For the subsequent glycogen precipitation, 1200 µL ice cold ethanol (final concentration of 70%) were added. The mixture was incubated at –20 °C for 2–24 h. Next, the solution was centrifuged at 4 °C for 10 min at 10,000× *g*. The pellet was washed twice with 70% and 98% ethanol and dried in a speed-vac for 20 min at 60 °C. Next, the pellet was resuspended in 1 mL of 100 mM sodium acetate (pH 4.5) and 8 µL of an amyloglucosidase solution (4.4 U/µL) were added. For the enzymatic digest, the cells were incubated at 60 °C for 2 h. For the spectrometical glycogen determination, 200 µL of the digested mixture was used and added to 1 mL of O-toluidine-reagent (6% O-toluidine in 100% acetic acid). The tubes were incubated for 10 min at 100 °C. The samples were cooled down on ice for 3 min, before the OD_{635} was measured. The final result was normalized to the cell density at OD_{750}, where OD_{750} = 1 represents 10^8 cells. A glucose standard curve was used to calculate the glucose contents in the sample from their OD540.

4.5. Drop Agar Method

Serial dilutions of chlorotic cultures were prepared (10^0, 10^{-1}, 10^{-2}, 10^{-3}, 10^{-4} and 10^{-5}) starting with an OD_{750} of 1. Five microliters of these dilutions were dropped on solid BG_{11} agar plates and cultivated at 50 µmol photons m^{-2} s^{-1} and 27 °C for 7 days.

Author Contributions: Conceptualization, M.K. and K.F.; Methodology, M.K., S.D. and K.F.; Investigation, M.K. and S.D.; Writing-Original Draft Preparation, M.K., S.D. and K.F.; Writing-Review & Editing, M.K., S.D., K.G. and K.F.; Supervision, K.F.; Project Administration, M.K. and K.F.

Funding: This research was funded by the Studienstiftung des Deutschen Volkes and the RTG 1708 "Molecular principles of bacterial survival strategies". We acknowledge support by Deutsche Forschungsgemeinschaft and Open Access Publishing Fund of University of Tübingen.

Acknowledgments: We would like to thank Yvonne Zilliges for providing the mutants Δ*glgA1*, Δ*glgA2* and Δ*glgC*. Furthermore, we thank Eva Nussbaum for maintaining the strain collection and Andreas Kulick for assistance with HPLC analysis.

Conflicts of Interest: The authors declare no conflict of interest.

Appendix A

Table A1. List of used strains.

Strain	Background	Relevant Marker of Genotype	Reference
Synechocystis sp. PCC 6803 GS	GS	-	Pasteur culture collection
Synechocystis sp. PCC 6803 GT	GT	-	Chen et al. 2016
Δ*glgA1*	GT	*sll0945::kmR*	Gründel et al. 2012
Δ*glgA2*	GT	*sll1393::cmR*	Gründel et al. 2012
Δ*glgC*	GT	*slr1176::cmR*	Damrow et al. 2012
Δ*glgP1*	GS	*sll1356::kmR*	Doello et al. 2018
Δ*glgP2*	GS	*slr1367::spR*	Doello et al. 2018
Δ*glgP1/2*	GS	*sll1356::kmR*, *slr1367::spR*	Doello et al. 2018
Δ*eda*	GT	*sll0107::gmR*	Chen et al. 2016
Δ*gnd*	GT	*sll0329::gmR*	Chen et al. 2016
Δ*pfkB1/2*	GT	*sll1196::kmR*, *sll0745::spR*	Chen et al. 2016
Δ*phaEC*	GS	*slr1829*, *slr1830::kmR*	Klotz et al. 2016

References

1. Soo, R.M.; Hemp, J.; Parks, D.H.; Fischer, W.W.; Hugenholtz, P. On the origins of oxygenic photosynthesis and aerobic respiration in Cyanobacteria. *Science* **2017**, *355*, 1436–1440. [CrossRef] [PubMed]
2. Vitousek, P.M.; Howarth, R.W. Nitrogen Limitation on Land and in the Sea—How Can. It Occur. *Biogeochemistry* **1991**, *13*, 87–115. [CrossRef]
3. Kaneko, T.; Tanaka, A.; Sato, S.; Kotani, H.; Sazuka, T.; Miyajima, N.; Sugiura, M.; Tabata, S. Sequence analysis of the genome of the unicellular cyanobacterium *Synechocystis* sp. strain PCC6803. I. Sequence features in the 1 Mb region from map positions 64% to 92% of the genome. *DNA Res.* **1995**, *2*, 153–166. [CrossRef]
4. Forchhammer, K.; Schwarz, R. Nitrogen chlorosis in unicellular cyanobacteria—a developmental program for surviving nitrogen deprivation. *Environ. Microbiol.* **2018**. [CrossRef] [PubMed]
5. Osanai, T.; Oikawa, A.; Shirai, T.; Kuwahara, A.; Iijima, H.; Tanaka, K.; Ikeuchi, M.; Kondo, A.; Saito, K.; Hirai, M.Y. Capillary electrophoresis-mass spectrometry reveals the distribution of carbon metabolites during nitrogen starvation in *Synechocystis* sp. PCC 6803. *Environ. Microbiol.* **2014**, *16*, 512–524. [CrossRef] [PubMed]
6. Grundel, M.; Scheunemann, R.; Lockau, W.; Zilliges, Y. Impaired glycogen synthesis causes metabolic overflow reactions and affects stress responses in the cyanobacterium *Synechocystis* sp. PCC 6803. *Microbiology* **2012**, *158*, 3032–3043. [CrossRef] [PubMed]
7. Doello, S.; Klotz, A.; Makowka, A.; Gutekunst, K.; Forchhammer, K. A Specific Glycogen Mobilization Strategy Enables Rapid Awakening of Dormant Cyanobacteria from Chlorosis. *Plant Physiol.* **2018**, *177*, 594–603. [CrossRef]
8. Damrow, R.; Maldener, I.; Zilliges, Y. The Multiple Functions of Common Microbial Carbon Polymers, Glycogen and PHB, during Stress Responses in the Non-Diazotrophic Cyanobacterium *Synechocystis* sp. PCC 6803. *Front. Microbiol.* **2016**, *7*, 966. [CrossRef]
9. Klotz, A.; Georg, J.; Bučinská, L.; Watanabe, S.; Reimann, V.; Januszewski, W.; Sobotka, R.; Jendrossek, D.; Hess, W.R.; Forchhammer, K. Awakening of a Dormant Cyanobacterium from Nitrogen Chlorosis Reveals a Genetically Determined Program. *Curr. Biol.* **2016**, *26*, 2862–2872. [CrossRef]
10. Ansari, S.; Fatma, T. Cyanobacterial Polyhydroxybutyrate (PHB): Screening, Optimization and Characterization. *PLoS ONE* **2016**, *11*, e0158168. [CrossRef]
11. Nowroth, V.; Marquart, L.; Jendrossek, D. Low temperature-induced viable but not culturable state of Ralstonia eutropha and its relationship to accumulated polyhydroxybutyrate. *FEMS Microbiol. Lett.* **2016**, *363*, fnw249. [CrossRef]

12. Batista, M.B.; Teixeira, C.S.; Sfeir, M.Z.T.; Alves, L.P.S.; Valdameri, G.; Pedrosa, F.O.; Sassaki, G.L.; Steffens, M.B.R.; de Souza, E.M.; Dixon, R.; et al. PHB Biosynthesis Counteracts Redox Stress in Herbaspirillum seropedicae. *Front. Microbiol.* **2018**, *9*, 472. [CrossRef] [PubMed]
13. Urtuvia, V.; Villegas, P.; González, M.; Seeger, M. Bacterial production of the biodegradable plastics polyhydroxyalkanoates. *Int. J. Biol. Macromol.* **2014**, *70*, 208–213. [CrossRef] [PubMed]
14. Li, W.C.; Tse, H.F.; Fok, L. Plastic waste in the marine environment: A review of sources, occurrence and effects. *Sci. Total Environ.* **2016**, *566*, 333–349. [CrossRef] [PubMed]
15. Drosg, B.; Gattermayr, F.; Silvestrini, L. Photo-autotrophic Production of Poly(hydroxyalkanoates) in Cyanobacteria. *Chem. Biochem. Eng. Q.* **2015**, *29*, 145–156. [CrossRef]
16. Martin, K.; Lukas, M. Cyanobacterial Polyhydroxyalkanoate Production: Status Quo and Quo Vadis? *Curr. Biotechnol.* **2015**, *4*, 464–480.
17. Singh, A.; Sharma, L.; Mallick, N.; Mala, J. Progress and challenges in producing polyhydroxyalkanoate biopolymers from cyanobacteria. *J. Appl. Phycol.* **2017**, *29*, 1213–1232.
18. Lau, N.S.; Foong, C.P.; Kurihara, Y.; Sudesh, K.; Matsui, M. RNA-Seq Analysis Provides Insights for Understanding Photoautotrophic Polyhydroxyalkanoate Production in Recombinant *Synechocystis* sp. *PLoS ONE* **2014**, *9*, e86368. [CrossRef]
19. Khetkorn, W.; Incharoensakdi, A.; Lindblad, P.; Jantaro, S. Enhancement of poly-3-hydroxybutyrate production in *Synechocystis* sp. PCC 6803 by overexpression of its native biosynthetic genes. *Bioresour. Technol.* **2016**, *214*, 761–768. [CrossRef]
20. Carpine, R. Genetic engineering of *Synechocystis* sp. PCC6803 for poly-β-hydroxybutyrate overproduction. *Algal Res. Biomass Biofuels Bioprod.* **2017**, *25*, 117–127. [CrossRef]
21. Kamravamanesh, D.; Kovacs, T.; Pflügl, S.; Druzhinina, I.; Kroll, P.; Lackner, M.; Herwig, C. Increased poly-beta-hydroxybutyrate production from carbon dioxide in randomly mutated cells of cyanobacterial strain *Synechocystis* sp. PCC 6714: Mutant generation and characterization. *Bioresour. Technol.* **2018**, *266*, 34–44. [CrossRef]
22. Steuer, R.; Knoop, H.; Machné, R. Modelling cyanobacteria: From metabolism to integrative models of phototrophic growth. *J. Exp. Bot.* **2012**, *63*, 2259–2274. [CrossRef]
23. Dutt, V.; Srivastava, S. Novel quantitative insights into carbon sources for synthesis of poly hydroxybutyrate in Synechocystis PCC 6803. *Photosynth. Res.* **2018**, *136*, 303–314. [CrossRef]
24. Rajendran, V.; Incharoensakdi, A. Disruption of polyhydroxybutyrate synthesis redirects carbon flow towards glycogen synthesis in *Synechocystis* sp. PCC 6803 overexpressing glgC/glgA. *Plant Cell Physiol.* **2018**, *59*, 2020–2029.
25. Chen, X.; Schreiber, S.; Appel, J.; Makowka, A.; Fähnrich, B.; Roettger, M.; Hajirezaei, M.R.; Sönnichsen, F.D. The Entner-Doudoroff pathway is an overlooked glycolytic route in cyanobacteria and plants. *Proc. Natl. Acad. Sci. USA* **2016**, *113*, 5441–5446. [CrossRef]
26. Yu, J.; Liberton, M.; Cliften, P.F.; Head, R.D.; Jacobs, J.M.; Smith, R.D.; Koppenaal, D.W.; Brand, J.J.; Pakrasi, H.B. Synechococcus elongatus UTEX 2973, a fast growing cyanobacterial chassis for biosynthesis using light and CO2. *Sci. Rep.* **2015**, *5*, 8132. [CrossRef] [PubMed]
27. Osanai, T.; Oikawa, A.; Numata, K.; Kuwahara, A.; Iijima, H.; Doi, Y.; Saito, K.; Hirai, M.Y. Pathway-level acceleration of glycogen catabolism by a response regulator in the cyanobacterium Synechocystis species PCC 6803. *Plant Physiol.* **2014**, *164*, 1831–1841. [CrossRef] [PubMed]
28. Yoo, S.H.; Lee, B.H.; Moon, Y.; Spalding, M.H.; Jane, J.L. Glycogen Synthase Isoforms in *Synechocystis* sp. PCC6803: Identification of Different Roles to Produce Glycogen by Targeted Mutagenesis. *PLoS ONE* **2014**, *9*, e91524. [CrossRef]
29. Namakoshi, K.; Nakajima, T.; Yoshikawa, K.; Toya, Y.; Shimizu, H. Combinatorial deletions of glgC and phaCE enhance ethanol production in *Synechocystis* sp. PCC 6803. *J. Biotechnol.* **2016**, *239*, 13–19. [CrossRef]
30. Kamravamanesh, D.; Slouka, C.; Limbeck, A.; Lackner, M.; Herwig, C. Increased carbohydrate production from carbon dioxide in randomly mutated cells of cyanobacterial strain *Synechocystis* sp. PCC 6714: Bioprocess. understanding and evaluation of productivities. *Bioresour. Technol.* **2019**, *273*, 277–287. [CrossRef] [PubMed]
31. Wang, C.X.; Saldanha, M.; Sheng, X.; Shelswell, K.J.; Walsh, K.T.; Sobral, B.W.; Charles, T.C. Roles of poly-3-hydroxybutyrate (PHB) and glycogen in symbiosis of Sinorhizobium meliloti with *Medicago* sp. *Microbiology* **2007**, *153*, 388–398. [CrossRef] [PubMed]

32. Sauer, J.; Schreiber, U.; Schmid, R.; Völker, U.; Forchhammer, K. Nitrogen starvation-induced chlorosis in Synechococcus PCC 7942. Low-level photosynthesis as a mechanism of long-term survival. *Plant Physiol.* **2001**, *126*, 233–243. [CrossRef] [PubMed]
33. Lever, M.A.; Rogers, K.L.; Lloyd, K.G.; Overmann, J.; Schink, B.; Thauer, R.K.; Hoehler, T.M.; Jørgensen, B.B. Life under extreme energy limitation: A synthesis of laboratory- and field-based investigations. *FEMS Microbiol. Rev.* **2015**, *39*, 688–728. [CrossRef]
34. Kempes, C.P.; van Bodegom, P.M.; Wolpert, D.; Libby, E.; Amend, J.; Hoehler, T. Drivers of Bacterial Maintenance and Minimal Energy Requirements. *Front. Microbiol.* **2017**, *8*, 31. [CrossRef]
35. Osanai, T.; Azuma, M.; Tanaka, K. Sugar catabolism regulated by light- and nitrogen-status in the cyanobacterium *Synechocystis* sp. PCC 6803. *Photochem. Photobiol. Sci.* **2007**, *6*, 508–514. [CrossRef] [PubMed]
36. Cano, M.; Holland, S.C.; Artier, J.; Burnap, R.L.; Ghirardi, M.; Morgan, J.A.; Yu, J. Glycogen Synthesis and Metabolite Overflow Contribute to Energy Balancing in Cyanobacteria. *Cell Rep.* **2018**, *23*, 667–672. [CrossRef]
37. Benson, P.J.; Purcell-Meyerink, D.; Hocart, C.H.; Truong, T.T.; James, G.O.; Rourke, L.; Djordjevic, M.A.; Blackburn, S.I.; Price, G.D. Factors Altering Pyruvate Excretion in a Glycogen Storage Mutant of the Cyanobacterium, Synechococcus PCC7942. *Front. Microbiol.* **2016**, *7*, 475. [CrossRef]
38. Osanai, T.; Kanesaki, Y.; Nakano, T.; Takahashi, H.; Asayama, M.; Shirai, M.; Kanehisa, M.; Suzuki, I.; Murata, N.; Tanaka, K. Positive regulation of sugar catabolic pathways in the cyanobacterium *Synechocystis* sp. PCC 6803 by the group 2 sigma factor sigE. *J. Biol. Chem.* **2005**, *280*, 30653–30659. [CrossRef]
39. Rippka, R.; Deruelles, D.; Waterbury, J.B.; Herdman, M.; Stanier, R.Y. Generic Assignments, Strain Histories and Properties of Pure Cultures of Cyanobacteria. *J. Gen. Microbiol.* **1979**, *111*, 1–61. [CrossRef]
40. Schlebusch, M.; Forchhammer, K. Requirement of the Nitrogen Starvation-Induced Protein Sll0783 for Polyhydroxybutyrate Accumulation in *Synechocystis* sp. Strain PCC 6803. *Appl. Environ. Microbiol.* **2010**, *76*, 6101–6107. [CrossRef]
41. Taroncher-Oldenburg, G.; Nishina, K.; Stephanopoulos, G. Identification and analysis of the polyhydroxyalkanoate-specific beta-ketothiolase and acetoacetyl coenzyme A reductase genes in the cyanobacterium *Synechocystis* sp. strain PCC6803. *Appl. Environ. Microbiol.* **2000**, *66*, 4440–4448. [CrossRef] [PubMed]

2. Accepted publication

B. Watzer, P. Spaet, N. Neumann, **M. Koch**, O. Hennrich, K. Forchhammer (2019).

The central regulator PII controls nitrate and urea uptake in *Synechocystis* sp. PCC 6803.

Frontiers in Microbiology, 10: 1428.

frontiers in Microbiology

ORIGINAL RESEARCH
published: 25 June 2019
doi: 10.3389/fmicb.2019.01428

The Signal Transduction Protein P_{II} Controls Ammonium, Nitrate and Urea Uptake in Cyanobacteria

*Björn Watzer[1†], Philipp Spät[1,2†], Niels Neumann[1], Moritz Koch[1], Roman Sobotka[3], Boris Macek[2], Oliver Hennrich[1] and Karl Forchhammer[1]**

[1] Interfaculty Institute of Microbiology and Infection Medicine Tübingen, Department of Organismic Interactions, University of Tübingen, Tübingen, Germany, [2] Interfaculty Institute for Cell Biology, Department of Quantitative Proteomics, University of Tübingen, Tübingen, Germany, [3] Centre Algatech, Institute of Microbiology, Academy of Sciences of the Czech Republic, Třeboň, Czechia

P_{II} signal transduction proteins are widely spread among all domains of life where they regulate a multitude of carbon and nitrogen metabolism related processes. Non-diazotrophic cyanobacteria can utilize a high variety of organic and inorganic nitrogen sources. In recent years, several physiological studies indicated an involvement of the cyanobacterial P_{II} protein in regulation of ammonium, nitrate/nitrite, and cyanate uptake. However, direct interaction of P_{II} has not been demonstrated so far. In this study, we used biochemical, molecular genetic and physiological approaches to demonstrate that P_{II} regulates all relevant nitrogen uptake systems in *Synechocystis* sp. strain PCC 6803: P_{II} controls ammonium uptake by interacting with the Amt1 ammonium permease, probably similar to the known regulation of *E. coli* ammonium permease AmtB by the P_{II} homolog GlnK. We could further clarify that P_{II} mediates the ammonium- and dark-induced inhibition of nitrate uptake by interacting with the NrtC and NrtD subunits of the nitrate/nitrite transporter NrtABCD. We further identified the ABC-type urea transporter UrtABCDE as novel P_{II} target. P_{II} interacts with the UrtE subunit without involving the standard interaction surface of P_{II} interactions. The deregulation of urea uptake in a P_{II} deletion mutant causes ammonium excretion when urea is provided as nitrogen source. Furthermore, the urea hydrolyzing urease enzyme complex appears to be coupled to urea uptake. Overall, this study underlines the great importance of the P_{II} signal transduction protein in the regulation of nitrogen utilization in cyanobacteria.

Keywords: P_{II} signaling protein, GlnB, cyanobacteria, nitrogen regulation, nitrate uptake, ammonium uptake, urea uptake, ABC transporters

OPEN ACCESS

Edited by:
Jörg Stülke,
University of Göttingen, Germany

Reviewed by:
Wolfgang R. Hess,
University of Freiburg, Germany
Andreas Burkovski,
University of Erlangen-Nuremberg, Germany

****Correspondence:***
Karl Forchhammer
karl.forchhammer@uni-tuebingen.de

† These authors have contributed equally to this work

Specialty section:
This article was submitted to Microbial Physiology and Metabolism, a section of the journal Frontiers in Microbiology

Received: *09 April 2019*
Accepted: *05 June 2019*
Published: *25 June 2019*

Citation:
Watzer B, Spät P, Neumann N, Koch M, Sobotka R, Macek B, Hennrich O and Forchhammer K (2019) The Signal Transduction Protein P_{II} Controls Ammonium, Nitrate and Urea Uptake in Cyanobacteria. Front. Microbiol. 10:1428. doi: 10.3389/fmicb.2019.01428

INTRODUCTION

The emergence of the oxygenic photosynthesis by ancestors of present cyanobacteria (Soo et al., 2017) laid the ground for the evolution of present days life on planet earth. Until today, cyanobacteria occupy a high variety of illuminated habitats, where they represent one of the most abundant primary producers (Whitton, 2012). Accordingly, cyanobacteria are essential contributors to the global carbon cycle. Many cyanobacterial strains have acquired the ability to fix atmospheric nitrogen, making them key players in the global nitrogen turnover

(Herrero and Flores, 2008). Nitrogen represents a necessary macronutrient for all living organisms and therefore constitutes an important growth-limiting factor in most ecosystems (Vitousek and Howarth, 1991). The regulation of nitrogen metabolism in cyanobacteria mainly depends on the fine-tuned network of the signal transduction protein P_{II}, the global nitrogen transcription factor NtcA and the NtcA co-activator PipX (Vegapalas et al., 1992; Espinosa et al., 2006, 2007, 2014; Forchhammer, 2008; Luque and Forchhammer, 2008; Forcada-Nadal et al., 2018).

P_{II} signal-transduction proteins are widespread in all three domains of life, where they represent one of the largest and most ancient families of signaling proteins (Chellamuthu et al., 2013; Forchhammer and Luddecke, 2016). P_{II} proteins are involved in the regulation of various nitrogen- and carbon-anabolic processes (Forchhammer, 2004, 2008). Canonical P_{II} proteins are homo-trimeric with three characteristic loop regions, designated as B-, C-, and T-loops, which compose the effector molecule binding sites (Cheah et al., 1994; Xu et al., 2003; Forchhammer, 2004, 2008; Llacer et al., 2007; Fokina et al., 2010a; Zhao et al., 2010; Zeth et al., 2014). The large surface exposed T-loop is the prevailing protein interaction module of P_{II}. The P_{II} proteins sense the energy status of the cell by the competitive binding of ADP or ATP (Zeth et al., 2014). Binding of ATP and synergistic binding of 2-oxoglutarate (2-OG) allows P_{II} to sense the current carbon/nitrogen status of the cell (Fokina et al., 2010a). 2-OG is an intermediate of the TCA-cycle that provides the carbon skeleton for inorganic nitrogen incorporation by the glutamine synthetase/glutamate synthase (GS/GOGAT) cycle. Due to this, 2-OG links carbon and nitrogen metabolism and acts as an indicator for the intracellular carbon/nitrogen balance (Muro-Pastor et al., 2001; Fokina et al., 2010a). Besides effector molecule binding, post-translational modification of P_{II} represents a second level of regulation (Forchhammer et al., 2004; Merrick, 2014). Depending on nitrogen availability, cyanobacterial P_{II} can be phosphorylated at the apex of the T-loop at position Ser49 (Forchhammer and Tandeau de Marsac, 1995; Forchhammer and Hedler, 1997). In other prokaryotes, like *E. coli*, P_{II} is modified by uridylylation in response to nitrogen availability instead of phosphorylation (Jiang et al., 1998). Binding of effector molecules as well as post-translational modifications lead to various P_{II} conformations. Depending on the conformational state, P_{II} can interact with a variety of interaction partners and thereby regulate the cellular C/N balance (Radchenko and Merrick, 2011; Forchhammer and Luddecke, 2016). In cyanobacteria, P_{II} indirectly regulates the global nitrogen control transcriptional factor NtcA through binding of the NtcA co-activator PipX (Espinosa et al., 2007). In common with other bacteria, the cyanobacterial P_{II} protein can control the acetyl-CoA levels by interacting with the biotin carboxyl carrier protein (BCCP) of acetyl-CoA carboxylase (ACC) (Hauf et al., 2016). Furthermore, P_{II} regulates arginine biosynthesis by interacting with the enzyme *N*-acetylglutamate kinase (NAGK), which catalyzes the rate-limiting step of this pathway (Caldovic and Tuchman, 2003; Heinrich et al., 2004; Llacer et al., 2007; Watzer et al., 2015). If sufficient energy and nitrogen is available, indicated by a high intracellular ATP and low 2-OG level, non-phosphorylated P_{II} interacts with NAGK, enhancing its catalytic efficiency and relieving it from feedback inhibition by arginine (Heinrich et al., 2004; Maheswaran et al., 2004; Llacer et al., 2007). At high intracellular arginine levels, the carbon/nitrogen storage polymer cyanophycin (multi-L-arginyl-poly-L-aspartate) accumulates in *Synechocystis* sp. strain PCC 6803 (hereafter *Synechocystis*) (Maheswaran et al., 2006; Watzer et al., 2015). A P_{II} variant was identified with a single amino acid substitution, Ile86 to Asn86 [thereafter referred as P_{II}(I86N)], which constitutively binds NAGK *in vitro* (Fokina et al., 2010b). Replacing the wild-type P_{II} with a I86N variant in *Synechocystis* generated a mutant strain, which strongly overproduced arginine and cyanophycin (Watzer et al., 2015). On the other hand, the P_{II}(I86N) strain showed a growth defect in ammonium-supplemented medium (Watzer et al., 2015).

Cyanobacteria use nitrogen sources in a hierarchical order, with ammonium being the preferred nitrogen source. As a consequence, when ammonium is provided together with other suitable nitrogen sources, ammonium will be utilized first (Muro-Pastor et al., 2005). In most natural habitats, the ammonium availability is low, so that high affinity ammonium permeases are required for efficient ammonium uptake (Rees et al., 2006). In *Synechocystis,* the Amt1 permease is mainly responsible for ammonium uptake (Montesinos et al., 1998). However, elevated intracellular ammonium concentrations are toxic to the cells (Drath et al., 2008; Dai et al., 2014), and therefore, ammonium transport must be tightly controlled. The ammonium transporter family (Amt) is widespread among all domains of life (Wirén and Merrick, 2004). In *E. coli*, the P_{II} homolog GlnK regulates the ammonium permease AmtB by direct protein–protein interaction. Under ammonium excess conditions, ADP-complexed GlnK blocks an uncontrolled influx of ammonium by inserting the apex of the T-loop into the cytoplasmic exit pores of AmtB (Conroy et al., 2007).

For the assimilation of nitrate, an active nitrate transporter, a nitrate reductase (NR) and a nitrite reductase (NiR) are required (Ohashi et al., 2011). Two types of nitrate transporter systems have been found among cyanobacteria, a high-affinity nitrate/nitrite permease NrtP and the ABC-type transporter NrtABCD (NRT) (Omata et al., 1993; Luque et al., 1994; Sakamoto et al., 1999; Ohashi et al., 2011). NRT is a bispecific nitrate/nitrite transporter showing high affinity for both substrates (Maeda and Omata, 1997). Intracellular nitrate is first reduced to nitrite by NR and subsequently reduced to ammonium by NiR. Subsequently, ammonium is assimilated in the GS/GOGAT cycle (Flores and Herrero, 1994). Both, NR and NiR, use photosystem I reduced ferredoxin as an electron donor, indicating a coupling of photosynthesis and nitrate assimilation (Manzano et al., 1976; Flores and Herrero, 1994). Addition of ammonium to nitrate adapted cells results in an immediate inhibition of nitrate uptake and a repression of proteins involved in nitrate assimilation (NR and NiR). The ammonium-induced inhibition of NRT is regulated by the P_{II} protein and the C-terminal domain of NrtC (Kobayashi et al., 1997; Lee et al., 1998). Phosphomimetic variants of P_{II} and a P_{II} phosphatase (PphA) deletion mutant, in which P_{II} is constitutively phosphorylated, showed

ammonium promoted inhibition of nitrate uptake like the wild-type (Lee et al., 2000; Kloft and Forchhammer, 2005). However, this response was abolished in a P_{II} deficient mutant (Kloft and Forchhammer, 2005).

The ability to utilize urea as nitrogen source is widely distributed among bacteria, fungi and algae (Baker et al., 2009; Solomon et al., 2010; Esteves-Ferreira et al., 2018). In common with other bacteria, the cyanobacteria *Synechocystis* and *Anabaena* sp. PCC 7120 possess a high affinity urea ABC-type transporter, which is capable of urea import at concentrations lower than 1 μM (Valladares et al., 2002). The gene cluster *urtABCDE*, encoding all subunits of this ABC-type urea transporter, is transcriptionally controlled by the global transcription factor NtcA (Valladares et al., 2002).

The present study was inspired by the phenotype of the cyanophycin-accumulating strain variant *Synechocystis* P_{II}(I86N), which was impaired in ammonium utilization. Starting with analyzing a possible regulation of the cyanobacterial Amt1 permease by P_{II}, we found additional evidence for a direct regulation of the nitrate/nitrite transporter NrtABCD and the urea transporter UrtABCDE by the P_{II} signaling protein during this study.

MATERIALS AND METHODS

Cultivation Conditions

Standard cloning procedures were performed in *Escherichia coli* NEB 10-beta (NEB). Strains were grown in LB-medium at 37°C with constant shaking at 300 rpm.

Synechocystis strains were grown photoautotrophically in BG-11 medium supplemented with 5 mM $NaHCO_3$ and nitrate, ammonium, or urea as nitrogen source (Rippka et al., 1979). BG-11 agar plates were produced by adding 1.5% (w/v) Bacto-agar (Difco), 0.3% (w/v) sodium thiosulfate pentahydrate and 10 mM TES-NaOH pH 8 (Roth) to liquid BG-11 medium. Antibiotics were added when required. Cultivation of liquid cultures for physiological experiments occurred in 50, 100, or 500 mL Erlenmeyer flasks, at 28°C and with constant shaking of 120 rpm. Cultures were continuously illuminated with a photon flux rate of 40–50 μE. Growth rates were determined by measuring the optical density at 750 nm (OD_{750}).

For induction of nitrogen starvation conditions, exponentially growing cells (OD_{750} 0.4–0.8) were harvested by centrifugation (3,000 × *g* for 10 min at room temperature), washed and resuspended in BG-11 medium lacking a suitable nitrogen source (BG-11^0).

For spot assays (drop plate method), *Synechocystis* cultures were adjusted to an OD_{750} of 1. A dilution series to the power of 10 was made using BG-11^0. Then, 5 μL of every dilution step (10^0–10^{-4}) were dropped on BG-11 agar plates. Plates were cultivated at 28°C with constant illumination of 40 μmol of photons s^{-1} m^{-2}.

Bacterial Two-Hybrid Assay

Plasmids were constructed by PCR amplification using high-fidelity Q5 polymerase (NEB) and oligonucleotides with overlapping regions. Genomic *Synechocystis* DNA or plasmids served as templates. PCR fragments were inserted in linearized bacterial two-hybrid vectors pUT18 and pKT25 containing the genes for either the T18 or T25 subunit of the adenylate cyclase CyaA (Karimova et al., 2001) by isothermal, single-reaction DNA assembly according to Gibson et al. (2009). Since the multiple cloning site of pKT25 is located downstream of the T25 subunit, allowing only N-terminal localization of the tag, we constructed plasmid pKT25n (**Table 1**; pKT25n_fw and pKT25n_rev) to achieve a C-terminal fusion of the tag to the gene of interest. Therefore, plasmid pKT25 was linearized using PCR and the gene of interest was fused upstream of the T25 subunit. Primers, plasmids, and strains used in this study are listed in **Tables 1–3**, respectively.

Escherichia coli BTH101 cells were co-transformed with plasmid pUT18 and plasmid pKT25 or pKT25n (**Table 2**). Plasmids pKT25 or pKT25n contained the possible P_{II} interaction partner fused N- or C-terminal to the T25 subunit. Plasmid pUT18 contains a gene-fusion of the P_{II}-encoding *gln*B gene or a genetically modified *gln*B gene containing the I86N mutation [Ile (5′ATC) at codon position 86 to Asn (5′AAC)] (Watzer et al., 2015), the R9L mutation [Arg (5′CGC) at codon position 9 to Leu (5′CTG)] (Fokina et al., 2010a) or the S49D mutation [Ser (5′TCG) at codon position 49 to Asp (5′GAT)] (Lee et al., 2000) with the T18 subunit. The *gln*B gene and the modified *gln*B genes were always fused N-terminal with the T18 subunit. Co-transformants were plated on LB-plates (supplemented with 100 μg mL^{-1} ampicillin and 50 μg mL^{-1} kanamycin) and cultivated for 2 days at 30°C.

To reduce the level of heterogeneity, five clones from each plate were picked to inoculate 5 mL LB-medium (containing 100 μg mL^{-1} ampicillin and 50 μg mL^{-1} kanamycin). Cultures were cultivated overnight at 37°C. Overnight cultures were diluted 1:100 in 3 mL of fresh LB-medium (containing 100 μg mL^{-1} ampicillin and 50 μg mL^{-1} kanamycin) and grown to an OD_{600} of 0.7. Three μL of each culture were plated on X-Gal (containing 100 μg mL^{-1} ampicillin, 50 μg mL^{-1} kanamycin, 1 mM IPTG, 40 μg mL^{-1} X-Gal) and MacConkey (containing 100 μg mL^{-1} ampicillin, 50 μg mL^{-1} kanamycin, 1 mM IPTG, 1% maltose) reporter plates. Reporter plates were incubated for 3–4 days at 25°C.

Construction and Cultivation of *Synechocystis* P_{II}-3xFLAG Tag Strains

The previously described pPD-*N*FLAG and pPD-*C*FLAG plasmids were used to construct *Synechocystis* P_{II} (GlnB) fusion proteins with an N- or C-terminal 3xFLAG tag, respectively (Hollingshead et al., 2012; Chidgey et al., 2014). Together with a kanamycin resistance cassette, this construct was inserted in the *Synechocystis* wild-type genome by homologous recombination, replacing the *psbAII* gene (Chidgey et al., 2014). Transformants were selected and segregated by kanamycin resistance. For pull-down experiments, 2 L batch cultures were inoculated at OD_{750} = 0.2 in BG-11 medium and propagated as described above, with magnetic stirring at 120 rpm and bubbling with 2% CO_2 (v/v) supplemented ambient air. Cell harvesting was

TABLE 1 | Oligonucleotides used in this study.

Primer	Sequence (5′–3′ direction)
pKT25n_fw	ACCATGCAGCAATCGCATCAG
pKT25n_rev	CATAGCTGTTTCCTGTGTGAAATTG
glnB_fw	TGTGTGGAATTGTGAGCGGATAACAATTTCACACAGGAAACAGCTATGAAAAAAGTAGAAGCGATTATTC
glnB_rev	CTCGCTGGCGGCTGAATTCGAGCTCGGTACCCGGGGATCAATAGCTTCGGTATCCTTTTC
pipX_fw	TTCACACAGGAAACAGCTATGAGTAACGAAATTTACCTTAAC
pipX_rev	GATGCGATTGCTGCATGGTAAAAGTGTTTTTATGTAACTTTG
pipX_pKT25n_fw	AAGTTACATAAAAACACTTTTACCATGCAGCAATCGCATCAG
pipX_pKT25n_rev	TAAGGTAAATTTCGTTACTCATAGCTGTTTCCTGTGTGAAATTG
amt1_pKT25_fw	CTGGCGCGCACGCGGCGGGCTGCAGGGTCGACTCTAGAGATGTCTAATTCGATATTGTCTAAAC
amt1_pKT25_rev	AAAACGACGGCCGAATTCTTAGTTACTTAGGTACCCGGGGATCTTATTCAGGGACAGTGG
amt1_fw	AACAATTTCACACAGGAAACAGCTATGTCTAATTCGATATTGTCTAAAC
amt1_rev	TGATGCGATTGCTGCATGGTTTCAGGGACAGTGGCACCG
amt1_pKT25n_fw	TCTCCGGTGCCACTGTCCCTGAAACCATGCAGCAATCGCATC
amt1_pKT25n_rev	ACAATATCGAATTAGACATAGCTGTTTCCTGTGTGAAATTGTTATCCGC
nrtC_pKT25_fw	CGCGCACGCGGCGGGCTGCAGGGTCGACTCTAGAGGATCCCCCCTTCATTGAAATTGATCATGTTG
nrtC_pKT25_rev	AGTCACGACGTTGTAAAACGACGGCCGAATTCTTAGTTATTGATTAACTTGATCAATTTGGTCGATGAG
nrtC_fw	AATTTCACACAGGAAACAGCTATGCCCTTCATTGAAATTGATCATG
nrtC_rev	CTGATGCGATTGCTGCATGGTTTGATTAACTTGATCAATTTGG
nrtC_pKT25n_fw	AAATTGATCAAGTTAATCAAACCATGCAGCAATCGCATCAG
nrtC_pKT25n_rev	TCAATTTCAATGAAGGGCATAGCTGTTTCCTGTGTGAAATTG
nrtD_pKT25_fw	CGCACGCGGCGGGCTGCAGGGTCGACTCTAGAGGATCCCCAAACAATGAATGTCAATGACCCTATCC
ntrD_pKT25_rev	CCCAGTCACGACGTTGTAAAACGACGGCCGAATTCTTAGTTAAGACCCTTCCATGGATTCCACTGAGGGGGTAG
nrtD_fw	AATTTCACACAGGAAACAGCTATGCAAACAATGAATGTCAATGACCCTATC
nrtD_rev	CTGATGCGATTGCTGCATGGTAGACCCTTCCATGGATTCCACTGAG
nrtD_pKT25n_fw	TGGAATCCATGGAAGGGTCTACCATGCAGCAATCGCATCAG
nrtD_pKT25n_rev	ATTGACATTCATTGTTTGCATAGCTGTTTCCTGTGTGAAATTG
urtD_pKT25_fw	CGCACGCGGCGGGCTGCAGGGTCGACTCTAGAGGATCCCACCAGCAAAATCTTAGAAATTCAAG
urtD_pKT25_rev	CCCAGTCACGACGTTGTAAAACGACGGCCGAATTCTTAGCTAATCTCCATCCTCATCAAC
urtD_fw	ACACAGGAAACAGCTATGACCAGCAAAATCTTAGAAATTCAAGAC
urtD_rev	GATGCGATTGCTGCATGGTATCTCCATCCTCATCAACACTG
urtD_pKT25n_fw	AGTGTTGATGAGGATGGAGATACCATGCAGCAATCGCATCAG
urtD_pKT25n_rev	TTCTAAGATTTTGCTGGTCATAGCTGTTTCCTGTGTGAAATTG
urtE_fw	GCGCGCACGCGGCGGGCTGCAGGGTCGACTCTAGAGGATGCTATGTTATCCTTTCCCCCATTCTTG
urtE_rev	CCCAGTCACGACGTTGTAAAACGACGGCCGAATTCTTAGTTATACTGCCAAAAATTTTTGGATAAC
urtE_fw	ACAATTTCACACAGGAAACAGCTATGGCTATGTTATCCTTTCCC
urtE_rev	TGATGCGATTGCTGCATGGTTACTGCCAAAAATTTTTGGATAACC
urtE_pKT25n_fw	TATCCAAAAATTTTTGGCAGTAACCATGCAGCAATCGCATCAG
urtE_pKT25n_rev	GGGAAAGGATAACATAGCCATAGCTGTTTCCTGTGTGAAATTG

performed at OD_{750} = 0.6 by mixing the cultures with ice in a 2:1 ratio (w/w) for rapid metabolic inactivation, and centrifugation at 7,477 × *g* for 10 min. Cell pellets were subsequently washed with nitrogen-free BG-11^0 at 4°C and snap frozen in liquid nitrogen. For experimental controls, the wild-type strain was similarly cultivated and subjected to pull-down assays followed by mass spectrometry analyses as described below. Two independent replicates were prepared per condition.

Preparation of Cell Extracts and Anti-FLAG Pull-Down

Frozen cell pellets were washed with 5 mL IP buffer, containing 25 mM MES/NaOH; pH 6.5, 5 mM $CaCl_2$, 10 mM $MgCl_2$, and 20% (v/v) glycerol and subsequently resuspended in 3 mL IP buffer, including protease inhibitors (complete EDTA-free; Roche) for cell lysis. Therefore, an equal volume of glass beads (0.1–0.15 mm diameter) was added and cells were disrupted using a FastPrep-24 Ribolyser (MP Biomedicals) with five cycles of 20 s at 6.5 m s^{-1} and 4°C. After centrifugation for 5 min at 3,314 × *g* and 4°C, the supernatant was transferred and adjusted with IP buffer to a final volume of 6 mL. For membrane protein solubilization, 1.5% (w/v) dodecyl-β-D-maltoside (DDM; Carl Roth) was added and incubated under agitation for 1 h at 4°C, before insoluble cell debris was removed by centrifugation for 20 min at 20,000 × *g* and 4°C. The soluble cell extracts (from 2 L cultures) were subjected to the P_{II}-FLAG pull-down procedure: for this, 400 μL of resuspended anti-FLAG-M2-agarose (Sigma) was added into empty SPE-columns and washed twice with each 1 mL IP buffer, supplemented with 0.04% (w/v) DDM, before

TABLE 2 | Plasmids used in this study.

Plasmid	Tag localization	Description	References
pPD-*N*FLAG	N-terminal	Encoding the N-terminal 3xFLAG tag	Hollingshead et al., 2012
pPD-*C*FLAG	C-terminal	Encoding the C-terminal 3xFLAG tag	Chidgey et al., 2014
pKT25		Encoding T25 fragment of adenylate cyclase CyaA (amino acids 1–224)	Karimova et al., 2001
pKT25n		Derived from pKT25. Upstream of the T25 fragment	This study
pUT18		Encoding T18 fragment of adenylate cyclase CyaA (amino acids 225–399)	Karimova et al., 2001
pUT18 *gln*B	N-terminal	Derived from pUT18. Encoding *gln*B	This study
pUT18 *gln*B (I86N)	N-terminal	Derived from pUT18. Encoding *gln*B containing the I86N mutation	This study
pKT25n *pip*X	C-terminal	Derived from pKT25. Sequence encoding *pip*X. Positive control	This study
pKT25 *pip*X	N-terminal	Derived from pKT25. Sequence encoding *pip*X. Positive control	This study
pKT25n *amt*1	C-terminal	Derived from pKT25. Sequence encoding *amt*1	This study
pKT25 *amt*1	N-terminal	Derived from pKT25. Sequence encoding *amt*1	This study
pKT25n *nrt*C	C-terminal	Derived from pKT25. Sequence encoding *nrt*C	This study
pKT25 *nrt*C	N-terminal	Derived from pKT25. Sequence encoding *nrt*C	This study
pKT25n *nrt*D	C-terminal	Derived from pKT25. Sequence encoding *nrt*D	This study
pKT25 *nrt*D	N-terminal	Derived from pKT25. Sequence encoding *nrt*D	This study
pKT25n *urt*D	C-terminal	Derived from pKT25. Sequence encoding *urt*D	This study
pKT25 *urt*D	N-terminal	Derived from pKT25. Sequence encoding *urt*D	This study
pKT25n *urt*E	C-terminal	Derived from pKT25. Sequence encoding *urt*E	This study
pKT25 *urt*E	N-terminal	Derived from pKT25. Sequence encoding *urt*E	This study

the supernatants were incubated for 5 min and removed by gravity flow. Repeated washing steps with each 5 mL DDM supplemented IP buffer were performed similarly, until the flow through appeared colorless. Elution of coupled proteins from the anti-FLAG resin was performed by incubation in 600 μL DDM supplemented IP buffer containing 0.3 μg/mL 3xFLAG^{TM} peptide (Sigma-Aldrich) for 40 min.

Proteomics Workflow, NanoLC-MS/MS Analysis, and Data Processing

Eluates from the pull-down workflow were subjected to acetone/methanol precipitation and resulting protein pellets were resuspended in denaturation buffer for subsequent tryptic digestion as described elsewhere (Spät et al., 2015). Resulting peptide mixtures were subjected to stage tip purification (Rappsilber et al., 2007). Protein detection by mass spectrometry (MS) was performed as described previously (Spät et al., 2015): in brief, peptide mixtures were loaded onto a 15 cm reversed-phase C_{18} nanoHPLC column on an EASY-LC system (Proxeon Biosystems) and separated in a 90 min segmented linear gradient. Eluted peptides were ionized by the on-line coupled ESI source and injected in a LTQ Orbitrap XL mass spectrometer (Thermo Scientific). MS spectra were acquired in the positive-ion mode. Per scan cycle, one initial full (MS) scan was followed by fragmentation of the 15 most intense multiply charged ions by collision induced dissociation (CID) for MS/MS scans. The scan range was 300–2,000 m/z for precursor ions at resolution 60,000 and sequenced precursors were dynamically excluded for fragmentation for 90 s. The lock mass option was enabled for real time mass recalibration (Olsen et al., 2005). All raw spectra were processed with the MaxQuant software (version 1.5.2.8) (Cox and Mann, 2008) at default settings. Peak lists were searched against a target-decoy database of *Synechocystis* sp. PCC 6803 with 3,671 protein sequences, retrieved from Cyanobase (Nakao et al., 2010) (July 2014), plus the sequence of the N- or C-terminal 3xFLAG tagged P_{II} fusion protein (MDYKDDDDKDYKDDDDKDYKDDDDKAAAKKVEAIIRPF KLDEVKIALVNAGIVGMTVSEVRGFGRQKGQTERYRGSEYT VEFLQKLKIEIVVDEGQVDMVVDKLVSAARTGEIGDGKIFIS PVDSVVRIRTGEKDTEAI or MKKVEAIIRPFKLDEVKIALVN AGIVGMTVSEVRGFGRQKGQTERYRGSEYTVEFLQKLKIEIV VDEGQVDMVVDKLVSAARTGEIGDGKIFISPVDSVVRIRTG EKDTEAIASYKDDDDKDYKDDDDKDYKDDDDK), respectively, as well as 245 common contaminants with the following database search criteria: trypsin was defined as a cleaving enzyme and up to two missed cleavages were allowed; carbamidomethylation of cysteines was defined as a fixed modification

TABLE 3 | Strains used in this study.

Strains	Description	References
E. coli NEB 10-beta	Cloning strain	NEB
E. coli BTH101	Bacterial two-hybrid host strain	Euromedex
Synechocystis sp. PCC 6803	Wild type	Pasteur Culture Collection
Synechocystis sp. P_{II}(I86N)	Genomic P_{II}(I86N) mutant	Watzer et al., 2015
Synechocystis sp. ΔP_{II}	Chromosomal deletion of *glnB*	Hisbergues et al., 1999
Synechocystis sp. ΔP_{II} + P_{II}-Venus	*Synechocystis* sp. ΔP_{II} transformed with pVZ322 encoding a P_{II}-Venus fusion	Hauf et al., 2016

and methionine oxidation and protein N-terminal acetylation as variable modifications. Peptide and protein false discovery rates retrieved from MaxQuant were limited to 1%, each. Raw data acquired by mass spectrometry was deposited at the ProteomeXchange Consortium via the Pride partner repository (Vizcaino et al., 2013) under the identifier PXD013411.

Determination of Nitrate, Nitrite, Ammonium, and Urea in Cell-Free Culture Medium

To determine the nitrate, ammonium, or urea uptake, exponentially growing cells (OD_{750} = 0.4–0.8) were harvested by centrifugation (3,000 × *g* for 10 min at room temperature) and washed twice with BG-11^0 medium lacking combined nitrogen sources. Subsequently, the cultures were adjusted to OD_{750} = 1 with BG-11^0 medium. The assays were started by adding either 200 μM $NaNO_3$, 200 μM NH_4^+ or 150 μM urea, respectively. Cells were cultivated under constant shaking of 120 rpm and illumination of 40–50 μE. 1 mL aliquots of the cell suspensions were taken and subsequently centrifuged (13,000 × *g* for 5 min at room temperature) to remove the cells.

For nitrate quantification, the absorbance at 210 nm was measured in the cell-free medium. Since both nitrate and nitrite absorb at 210 nm, the apparent nitrate values were corrected for the presence of nitrite (Kloft and Forchhammer, 2005). Nitrite concentration of the cell-free medium was determined using the modified Griess reaction according to Fiddler (1977).

The ammonium concentration of cell-free medium was measured by using the Nessler reaction (Vogel et al., 1989). Urea was quantified by using the urea nitrogen (BUN) colorimetric detection kit (Invitrogen).

Microscopy Procedures and Image Evaluation

Fluorescence microscopy was performed using a Leica DM5500B microscope with a 100×/1.3 oil objective. For the detection of Venus fluorescence, an ET500/20× excitation filter and an ET535/30m emission filter were used referred as YFP-channel. To detect cyanobacterial autofluorescence, an excitation filter BP 535/50 and a suppression filter BP 610/75 were used. Image acquisition was done with a Leica DFC360FX black-and-white camera. Captured images were colored with the Leica Application Suite Software (LAS AF) provided by Leica Microsystems. Bright-field images were exposed for 6 ms, Venus fluorescence images for 150 ms and autofluorescence images for 100 ms. Microscope slides covered with dried 2% (w/v) agarose solution were used to immobilize the cells during all microscopical examinations.

Quantitative image evaluation by fluorescence intensity measurements was performed using the open-source software ImageJ (Fiji) (Schindelin et al., 2012). To estimate the fluorescence intensities in different cell compartments, a linear profile of the gray values across the cells through the plasma membrane and cytoplasm was determined. The average gray level of the cytoplasm was subtracted from the maximum gray level of the plasma membrane signal to yield the "Δ fluorescence" value, which indicates the cytoplasmic membrane-localized signal. An example of this profile data quantification is given in **Supplementary Figure 1**.

RESULTS

P_{II} Signaling Mutants Show Increased Sensitivity to Ammonium

P_{II} homologs of the GlnK subfamily from heterotrophic bacteria are known to regulate cellular ammonium influx by direct protein–protein interaction with the ammonium permease AmtB (Huergo et al., 2012). The observation of impaired ammonium utilization in the *Synechocystis* strain, which harbors the P_{II}(I86N) variant, suggested that this P_{II} variant either blocked ammonium uptake or abolished proper ammonium uptake regulation with consequent ammonium sensitivity. The Ile 86 to Asn point mutation in this P_{II} variant causes a specific alteration of the T-loop conformation, which facilitates interaction with NAGK and thus, results in an over-activation of this P_{II} target (Fokina et al., 2010b). Conversely, other P_{II} targets might by negatively affected by the altered T-loop conformation. To gain further insights into the role of P_{II} in ammonium uptake, we tested ammonium utilization of a P_{II} deletion mutant (ΔP_{II}) (Hisbergues et al., 1999) and of the ΔP_{II} strain complemented with P_{II}-Venus (P_{II}-Venus-comp.) (Hauf et al., 2016). The complementation strain was previously generated by introducing a shuttle vector (pVZ322), encoding a P_{II}-Venus fusion under control of the native *gln*B promoter into the *Synechocystis* ΔP_{II} mutant (Hauf et al., 2016). The Venus fluorescent protein was fused to the C-terminus of P_{II} to avoid sterical hindrance of the T-loop.

When grown in presence of 5 mM ammonium in liquid medium, the *Synechocystis* wild-type, the ΔP_{II} and the P_{II}-Venus-comp. strains showed similar growth rates and ammonium consumption (**Figures 1A,B**). However, with an elevated ammonium concentration of 10 mM, only the wild-type and P_{II}-Venus-comp. strains could maintain normal growth, while the ΔP_{II} mutant arrested growth (**Figure 1C**). Ammonium utilization of wild-type and P_{II}-Venus-comp. were similar under this condition (**Figure 1D**) while the ΔP_{II} strain ceased ammonium utilization (**Figure 1D**). The ammonium-sensitive phenotype of the ΔP_{II} strain, in particular the response toward 10 mM ammonium, resembled the previously reported phenotype of the *Synechocystis* P_{II}(I86N) strain (Watzer et al., 2015). One possibility to explain the inability of the P_{II} mutant strains to grow in 10 mM ammonium-supplemented medium is an increased sensitivity toward toxic effects of ammonium. Although ammonium represents the preferred nitrogen source, it becomes toxic for many photosynthetic organisms at higher concentrations (Drath et al., 2008). To find out whether the reduced growth and impaired ammonium utilization results from ammonium intoxication, we assayed the growth of the various strains in the presence of increasing concentrations of ammonium using the spot assay method (**Figure 2**). Over a range from 5 to 40 mM ammonium, the wild-type and P_{II}-Venus-comp. strains showed a similar growth

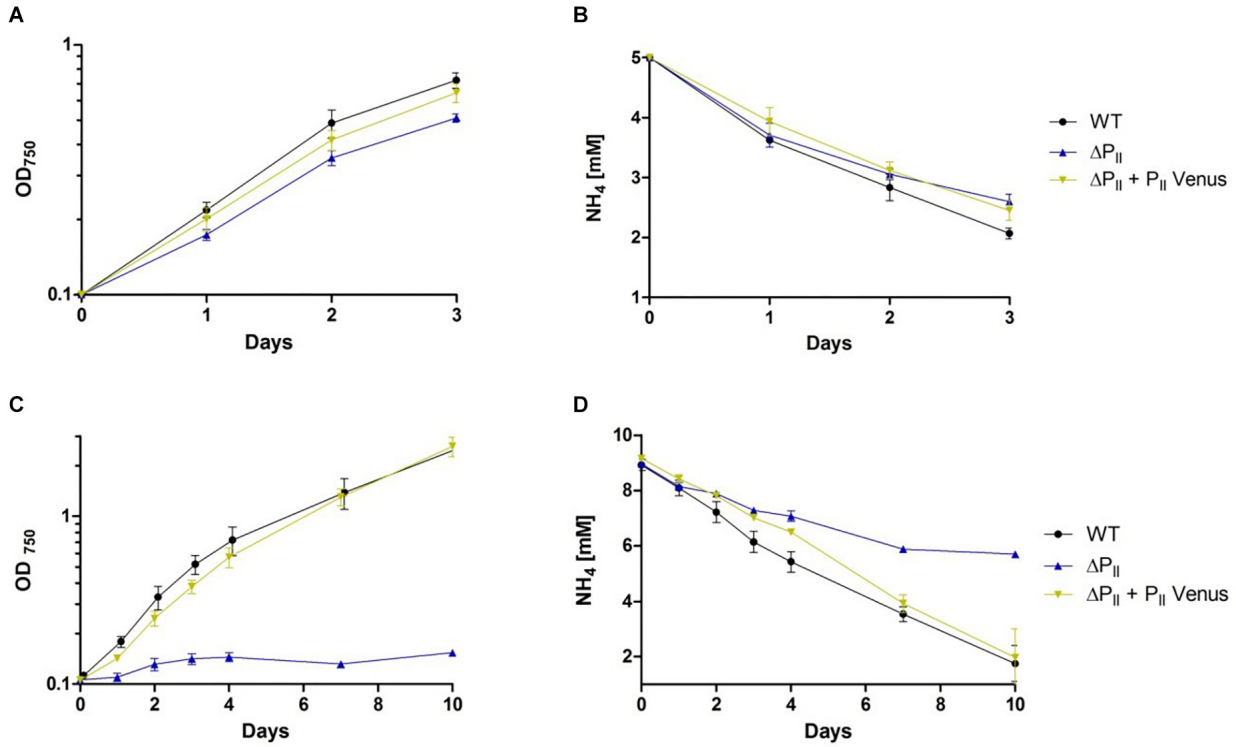

FIGURE 1 | Ammonium supplemented growth and ammonium utilization of *Synechocystis* sp. wild-type, ΔP_{II} and P_{II}-Venus-comp. (ΔP_{II} + P_{II}-Venus) strains. Values are the means of three biological replicates. **(A)** Growth curve in presence of 5 mM ammonium. **(B)** Ammonium concentration in culture supernatants of the various *Synechocystis* strains grown in BG-11 medium with 5 mM ammonium. **(C)** Growth curve in presence of 10 mM ammonium. **(D)** Ammonium concentration in culture supernatants of the various *Synechocystis* strains grown in BG-11 medium with 10 mM ammonium.

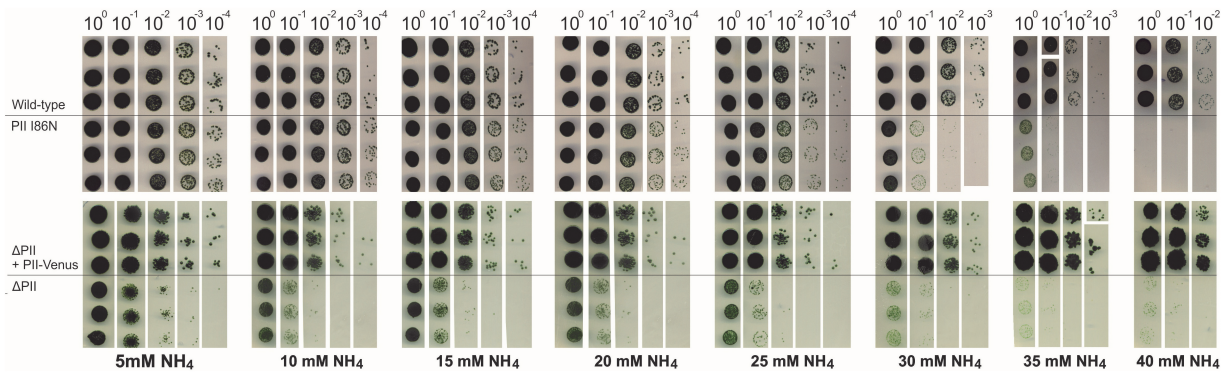

FIGURE 2 | Ammonium sensitivity of the various *Synechocystis* strains (as in **Figure 1**) as determined by the drop plate method with three biological replicates per strain. Starved cultures were adjusted to an OD_{750} of 1.0 and diluted tenfold in series. The dilutions were dropped onto BG-11 agar plates containing increasing concentrations of ammonia (5–40 mM).

and ammonium tolerance. However, the P_{II}(I86N) mutant showed impaired growth at 25 mM while the ΔP_{II} mutant was already strongly affected at a concentration of 10 mM ammonium (**Figure 2**). This demonstrated that P_{II} is indeed required to cope with elevated ammonium concentrations. The P_{II}(I86N) mutant can only partially replace the wild-type P_{II} protein, whereas P_{II}-Venus perfectly complemented the ΔP_{II} strain.

Identification of Novel P_{II} Interaction Partners by FLAG-Tag P_{II} Pull-Down Assays

Uncontrolled influx of ammonium and resulting intoxication of *Synechocystis* ΔP_{II} and P_{II}(I86N) mutants is likely a cause for the elevated ammonium sensitivity in these strains. This suggested the involvement of P_{II} in the regulation of

Synechocystis ammonium permeases. In order to verify such an interaction, we performed pull-down assays using a C-terminal 3xFLAG-tagged P_{II} fusion protein that was expressed in *Synechocystis* under control of the strong *psbA* promoter. Protein extracts were prepared in presence of detergent, to solubilize membrane-bound proteins, and were subjected to anti-FLAG-tag immunoprecipitation. The proteome composition of the immunoprecipitate was subsequently analyzed by MS to reveal the proteins that co-purify with FLAG-tag P_{II}. As an initial experiment, the immunoprecipitation was performed with cells grown in BG-11 medium, containing nitrate as unique nitrogen source. To discriminate between P_{II} interaction partners and unspecific background proteins, the non-transformed wild-type strain was used as an experimental control. Each experiment was further validated by an independent replicate.

As a proof of concept, we were able to identify P_{II} as the most abundant protein in the P_{II} 3xFLAG pull-down (thereafter P_{II} pull-down). Furthermore, some reported interaction partners, such as PipX, were either exclusively identified in the P_{II} pull-down, or, as in the case of the P_{II} phosphatase PphA, were strongly enriched compared to the background control (**Supplementary Figure 2**) (Kloft and Forchhammer, 2005; Espinosa et al., 2007; Forcada-Nadal et al., 2014). The identification of a large number of background proteins in the experiments depends on the wash-stringency, the abundance of individual proteins and the high sensitivity of MS-detection. To distinguish between specific P_{II}-enriched interaction partners and background, we determined relative protein abundance ratios between the P_{II} and control experiments by using label free quantification (LFQ) (Cox et al., 2014). Proteins with a significantly higher abundance in the P_{II} pull-down were identified by significance analysis (p-value = 0.01). Since both independent replicates from nitrate-grown cultures yielded very similar results, we correlated the data (**Figure 3**). Using this approach, the major ammonium permease Amt1 (Montesinos et al., 1998) indeed appeared among the significantly enriched proteins, supporting our suggestion that Amt1 represents a P_{II} binding target in cyanobacteria. Surprisingly, we could also identify subunits of other nitrogen import complexes besides Amt1 among the

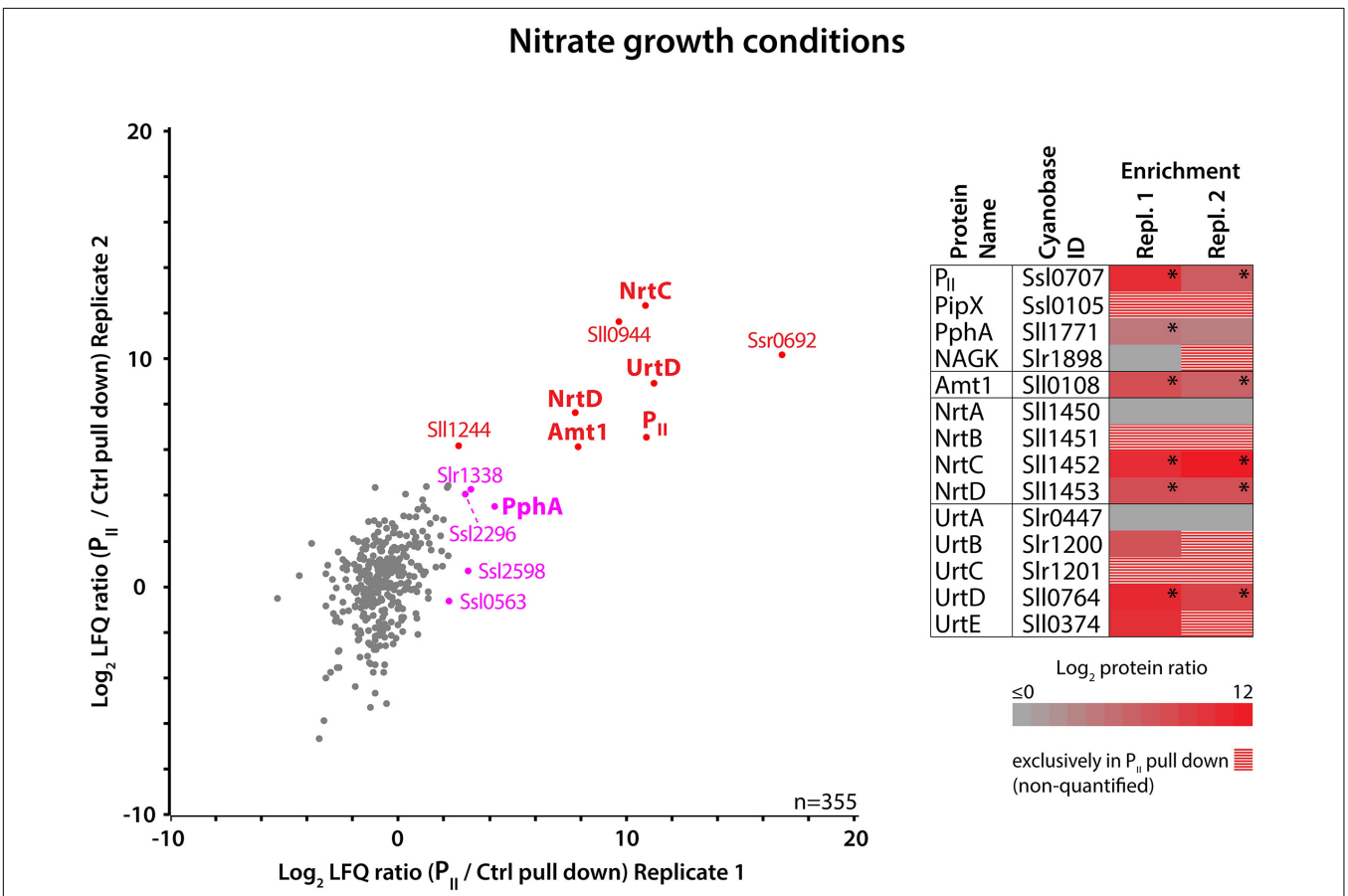

FIGURE 3 | Proteins enriched in anti-FLAG-tag P_{II} immunoprecipitates from nitrate growth conditions. **(Left)** Scatterplot of the $\log_2$ transformed LFQ protein ratios (P_{II}/control pull-down experiment) of 355 quantified proteins detected in two independent replicates. P_{II} pull-down specific outliers which are significantly enriched in both replicates are indicated in red, and significant outliers enriched only in Replicate 1 are indicated in magenta (p-value = 0.01). **(Right)** Heat map representation of the P_{II}-specific enrichment of nitrogen metabolism related proteins. Log_2 transformed LFQ protein ratios from both replicates are color coded and stars indicate significance. Proteins with missing LFQ ratios, detected exclusively in the P_{II} but not in the control pull-down, are striped in red/gray.

significantly enriched proteins, in particular subunits of the bispecific NrtABCD nitrate/nitrite and the UrtABCDE urea transporter complexes. For the NRT and URT transporters, all subunits except the periplasmic substrate binding proteins NrtA and UrtA were either exclusively present or strongly enriched in the P_{II} pull-downs. This suggests that the cytoplasmic components of the transporters together with the pore forming subunit are still associated in a complex, detached from the loosely associated periplasmic binding proteins (NrtA or UrtA).

To further validate a potential interaction between P_{II} and the URT transporter complex, we repeated the experiment with cells grown in urea-supplemented medium. In agreement with the results from the P_{II} pull-down at nitrate growth conditions, we detected an enrichment of the P_{II} target PipX, the ammonium permease Amt1, subunits of the NRT nitrate/nitrite transporter, and most prominent, subunits of the URT urea transporter (**Supplementary Figure 3**). By correlating the data from both independent replicates (**Figure 4**), it became evident that UrtD and UrtE are the strongest enriched proteins under this condition besides P_{II}. This suggests that the presence of urea in the medium influences the interaction of the URT transporter complex with P_{II}.

Besides proteins associated with nitrogen import, we also identified two small hypothetical proteins to be significantly enriched in all experiments, Sll0944 and Ssr0692. Interestingly, both proteins are under transcriptional control of the global nitrogen regulator NtcA (Giner-Lamia et al., 2017), and reveal opposed dynamics in response to nitrogen availability. Under nitrogen-limiting conditions, Sll0944 was found to be strongly up-regulated at transcriptome and proteome levels, whereas Ssr0692 was strongly down-regulated (Spät et al., 2015; Giner-Lamia et al., 2017). Intriguingly, Ssr0692 seems to be up-regulated under carbon limitation (Battchikova et al., 2010) and might be associated to carbon fixation, as it was identified as a potential interactor of NdhH (Sato et al., 2007). The protein Sll0944 is highly conserved in cyanobacteria and possesses a domain of unknown function (DUF1830). Overall, our results imply a direct linkage of Sll0944 and Ssr0692 to nitrogen metabolism with a regulatory involvement of P_{II}. Both proteins are currently under investigation to validate a potential interaction with P_{II} and to determine their function.

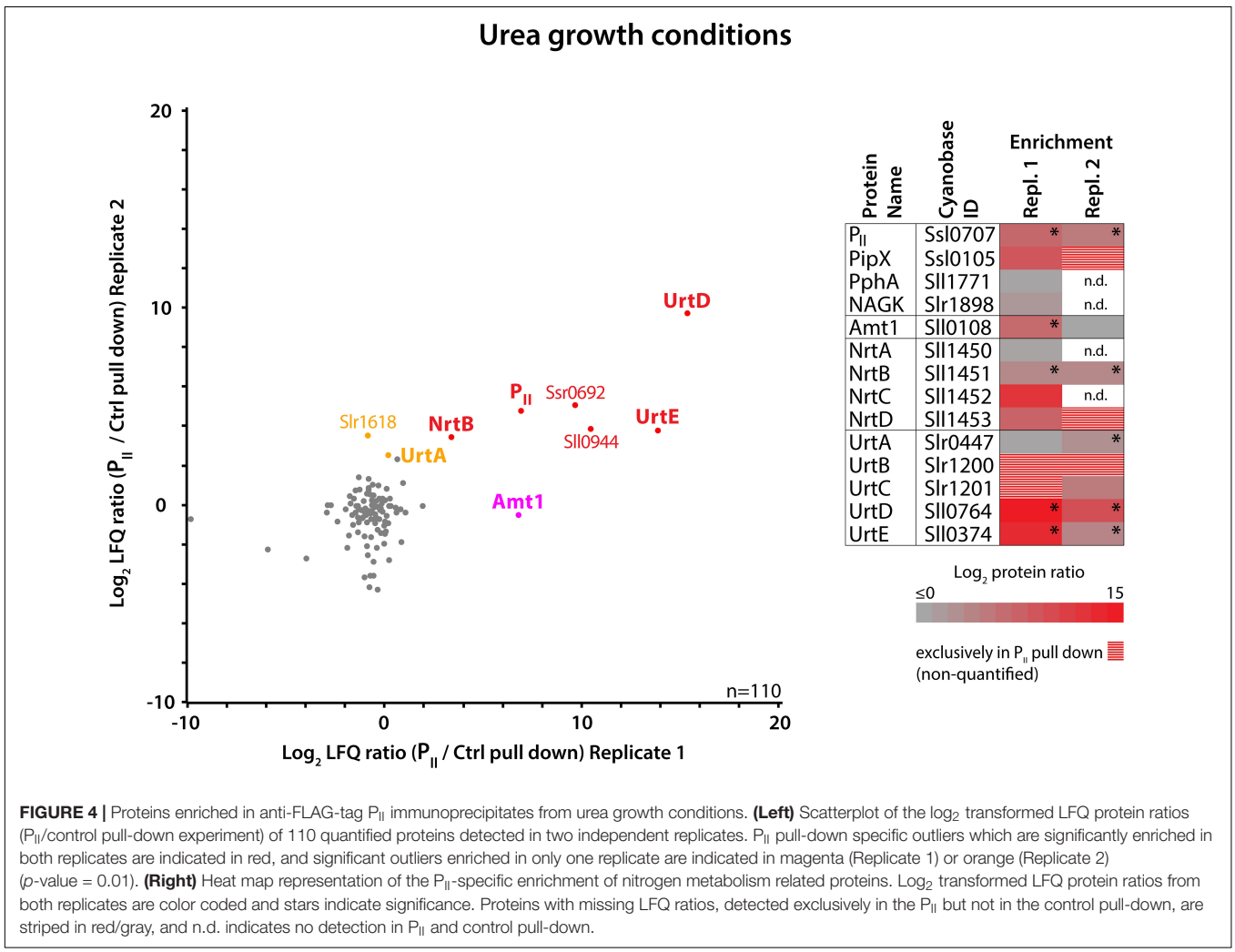

FIGURE 4 | Proteins enriched in anti-FLAG-tag P_{II} immunoprecipitates from urea growth conditions. **(Left)** Scatterplot of the log_2 transformed LFQ protein ratios (P_{II}/control pull-down experiment) of 110 quantified proteins detected in two independent replicates. P_{II} pull-down specific outliers which are significantly enriched in both replicates are indicated in red, and significant outliers enriched in only one replicate are indicated in magenta (Replicate 1) or orange (Replicate 2) (*p*-value = 0.01). **(Right)** Heat map representation of the P_{II}-specific enrichment of nitrogen metabolism related proteins. Log_2 transformed LFQ protein ratios from both replicates are color coded and stars indicate significance. Proteins with missing LFQ ratios, detected exclusively in the P_{II} but not in the control pull-down, are striped in red/gray, and n.d. indicates no detection in P_{II} and control pull-down.

Surprisingly, the well-studied P_{II} interactor NAGK was not clearly enriched in these experiments. A low percentage of P_{II}-NAGK complexes was expected to be present under nitrate or urea growth conditions (Burillo et al., 2004), although the strongest interaction occurs under conditions of nitrogen oversupply. Possibly, the C-terminal 3xFLAG-tag fusion of this P_{II} variant could negatively affect complex formation with NAGK. Therefore, pull-down experiments were also performed with an N-terminal 3xFLAG-tag fusion to P_{II}. There, we could clearly identify NAGK in the pull-down of nitrate grown cells in two independent replicates (**Table 4**). The identification of NAGK in both N-terminal P_{II}-fusion pull-down replicates implies that the localization of the 3xFLAG-tag has an influence on the interaction between P_{II} and its targets. Comparing the results from N- or C-terminal FLAG-tag fused P_{II} pull-down experiments can give additional information to identify potential P_{II} interaction partners. In contrast to the experiments utilizing the C-terminal FLAG-tag, where subunits of the heterotrimeric urease complex UreABC were not enriched, to our surprise, the N-terminal FLAG-tagged P_{II} protein co-purified the entire urease-complex including associated urease accessory proteins D, F, and G. This remarkable finding implies a possible direct interaction between the urease transport complex and the succeeding enzymatic machinery urea metabolism, indicating possible metabolic channeling of urea (Sweetlove and Fernie, 2018).

TABLE 4 | Identified proteins in pull-down experiments at nitrate growth conditions utilizing the N-terminal 3xFLAG-tagged P_{II} fusion protein: Displayed are the identified proteins from two independent replicates (Repl. I and Repl. II).

Protein name/ complex	Cyanobase ID	Mol. weight (kDa)	iBAQ intensity	
			Repl. I	Repl. II
P_{II}/N-3xFLAG P_{II}	Ssl0707	15.43	$4.2*10^7$	$1.1*10^9$
PipX	Ssl0105	10.45	$3.1*10^6$	$9.1*10^7$
PphA	Sll1771	28.47	$4.2*10^4$	$9.1*10^5$
NAGK	Slr1898	31.53	$9.4*10^4$	$6.5*10^5$
Amt1	Sll0108	53.58	$1.2*10^8$	$2.9*10^8$
NrtA	Sll1450	48.97	$1.1*10^5$	$1.4*10^6$
NrtB	Sll1451	29.72	$8.8*10^5$	$5.1*10^6$
NrtC	Sll1452	75.10	$1.4*10^6$	$6.1*10^6$
NrtD	Sll1453	36.56	$1.9*10^5$	$2.9*10^6$
UrtA	Slr0447	48.36	$1.0*10^5$	$2.6*10^5$
UrtB	Slr1200	41.68	$2.4*10^5$	$1.6*10^6$
UrtC	Slr1201	45.08	$3.5*10^5$	$4.9*10^6$
UrtD	Sll0764	41.19	$8.1*10^5$	$3.9*10^6$
UrtE	Sll0374	27.42	$6.5*10^5$	$6.4*10^6$
UreA	Slr1256	11.06	–	$4.9*10^5$
UreB	Sll0420	11.38	$2.0*10^5$	$5.2*10^7$
UreC	Sll1750	61.04	$9.9*10^6$	$3.5*10^7$
UreD	Sll1639	27.16	$1.2*10^5$	$6.4*10^5$
UreF	Slr1899	20.23	$3.1*10^4$	$5.2*10^5$
UreG	Sll0643	22.01	$1.3*10^5$	$1.2*10^6$
Sll0944	Sll0944	18.15	$8.4*10^5$	$9.8*10^7$
Ssr0692	Ssr0692	5.85	$2.8*10^5$	$9.3*10^6$

Protein intensities were calculated using the MaxQuant iBAQ algorithm (Schwanhausser et al., 2011).

Bacterial Two-Hybrid Assay

To further confirm the interaction of P_{II} with the identified nitrogen transporters, we performed bacterial two-hybrid assays using the *Bordetella pertussis* adenylate cyclase two-hybrid system (BACTH) (Battesti and Bouveret, 2012). We tested the cytoplasmic localized ATP-binding proteins of the ABC-type transporters NrtC, NrtD, UrtD, UrtE (Omata et al., 1993; Valladares et al., 2002) as well as Amt1 for possible interactions with various P_{II} proteins. For each interaction candidate, an N- and a C-terminal fusion to the T25 fragment was constructed. In case of a positive interaction with a P_{II}-T18 fusion, cAMP is formed within a cAMP deficient *E. coli* host cell. The interactions were tested by plate assays on X-Gal and MacConkey reporter plates for highest detection sensitivity. The P_{II} – PipX and leucine zipper interactions were used as positive controls. P_{II}-T18 fusions with an empty pKT25 vector were used as negative controls. Next to wild-type P_{II}-T18 fusion, we also included T18 fusions of the P_{II}(I86N), P_{II}(S49D), and P_{II}(R9L) variants to find out how these different P_{II} variants, including a phosphomimetic T-loop variant and variants with different effector binding properties would differ in potential P_{II} interactions. **Figure 5** shows the observed interactions on X-Gal plates in the bacterial two-hybrid assays.

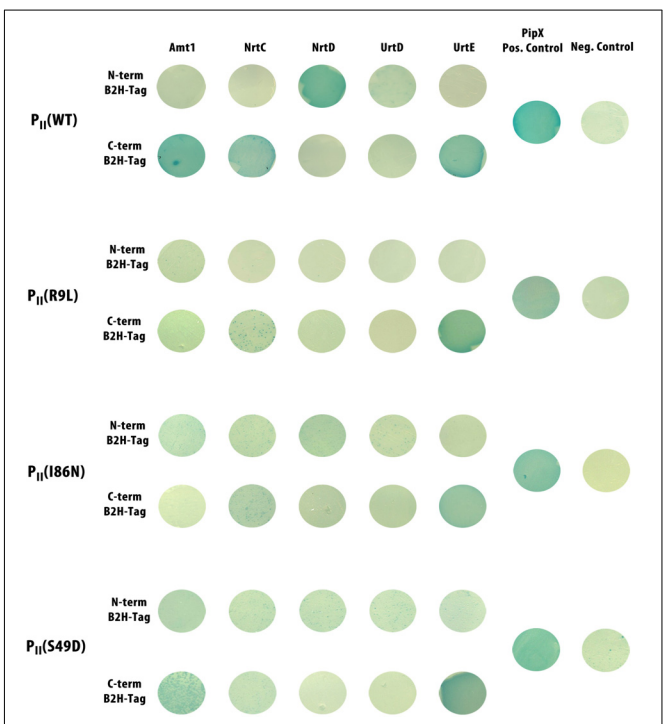

FIGURE 5 | Bacterial-two-hybrid interactions on X-Gal plates of wild-type P_{II} and the P_{II} variants P_{II}(R9L), P_{II}(I86N), P_{II}(S49D) with different transporter subunits. Interaction of P_{II} with C-terminal tagged PipX was used as a positive control. P_{II} with an empty pKT25 vector was used as negative control. Positive interactions are indicated by a blue coloration of the colonies.

All P_{II} variants showed interaction with the known P_{II} interaction partner PipX. Wild-type P_{II} showed clear interaction with Amt1 C-terminally fused to the T25 fragment, while the variants P_{II}(I86N) and P_{II}(R9L) did not interact. The loss of interaction of P_{II}(I86N) is in agreement with our previous conclusions regarding the impaired ammonium utilization of *Synechocystis* sp. strain P_{II}(I86N). The phosphomimetic variant P_{II}(S49D) showed weak interaction with Amt1. In case of the nitrate transport ATP-binding subunits NrtC and NrtD, the BACTH assay revealed clear interaction of wild-type P_{II} with both subunits. Intriguingly, P_{II} interacted only with NrtC when it was fused at its C-terminus with T25, whereas in the case of NrtD, P_{II} interacted with the N-terminal fusion. In contrast to wild-type P_{II}, the P_{II}(R9L) variant was completely unable to interact with any of the Nrt-proteins, while weak interactions were observed with variants P_{II}(S49D) and P_{II}(I86N). With the ATP-binding subunits of the urea transporter, no interaction was observed with the UrtD protein, neither with wild-type P_{II} nor with any of the tested variants. By contrast, the C-terminal T25 fusion of UrtE showed clear interaction with wild-type and all P_{II} variants. The fact that positive interactions only occurred with selective combinations of P_{II} variants and N-or C-terminal T25 fusions of target proteins supports the conclusion that the observed interactions are indeed specific.

P_{II} Deletion Mutant and P_{II}(I86N) Mutant Excrete Nitrite

The pull-down and BACTH assays shown above clearly indicated interaction of wild-type P_{II} protein with components of the uptake systems for ammonium, nitrate, and urea. The interaction with Amt1 likely resembles the known interaction of the P_{II} protein GlnK from heterotrophic bacteria with AmtB (Conroy et al., 2007; Gruswitz et al., 2007) and perfectly explains the physiological response of *Synechococcus* PCC 7942 (hereafter *Synechococcus*) and *Synechocystis* P_{II} mutants toward ammonium. Interaction of P_{II} with components of the NrtABCD nitrate/nitrite transporter had in fact been suggested previously by several physiological studies, which documented altered nitrate utilization properties in various *Synechococcus* and *Synechocystis* P_{II} mutants (Kobayashi et al., 1997; Lee et al., 1998, 2000; Kloft and Forchhammer, 2005). A characteristic phenotype of a P_{II} deletion mutant grown in the presence of nitrate is the uncontrolled uptake of nitrate and subsequent excretion of nitrite into the medium (Kloft and Forchhammer, 2005). Reduction of nitrate requires two electrons whereas six electrons are needed for the reduction of nitrite to ammonium. Because of the lower electron demand for nitrate reduction, nitrite reduction becomes limiting when insufficient reductant is available. Therefore, when nitrate uptake is uncontrolled, nitrite accumulates and is excreted. We wondered if the *Synechocystis* P_{II}(I86N) strain shows a similar nitrite excretion phenotype than the P_{II} deficient mutant when grown on nitrate and if P_{II}-Venus complements the nitrite excretion phenotype of the P_{II}-deficient mutant.

To answer this question, *Synechocystis* wild-type strain, P_{II}(I86N), ΔP_{II} and the P_{II}-Venus comp. strains were grown with nitrate as sole nitrogen source under constant illumination (40 μmol photons m^{-2} s^{-1}) and samples were removed for nitrite determination. Under these conditions, the various strains showed similar growth rates (**Figure 6**). Both mutant strains expected to be impaired in proper control of the NRT complex, the ΔP_{II} mutant and the P_{II}(I86N) strain, indeed excreted nitrite into the medium. Notably, the P_{II}(I86N) mutant excreted much lower nitrite amounts than the P_{II} deletion mutant, in agreement with the partial interaction of the P_{II}(I86N) variant observed in the BACTH assays with NrtC and NrtD subunits. By contrast, P_{II}-Venus perfectly complemented the nitrite excretion phenotype. Together, these results indicated that the BACTH interactions of P_{II} with the NrtC and NtcD subunits are physiologically meaningful.

P_{II} Is Responsible for Inhibition of Nitrate Uptake

To gain further insights in the P_{II}-dependent regulation of nitrate uptake, we measured nitrate consumption rates of the various P_{II}-mutants under different conditions. For this purpose, cells from exponential phase of growth in standard BG-11 medium were washed and subsequently incubated in BG-11^0 medium containing 200 μM NO_3 as nitrogen source. Nitrate utilization was quantified by measuring the nitrate concentration in the culture supernatant over time. Under constant illumination of 40 μmol photons m^{-2} s^{-1}, *Synechocystis* wild-type and the P_{II}-Venus comp. strain showed lower nitrate consumption rates, while both, the P_{II}(I86N) and ΔP_{II} mutant, showed higher nitrate removal (**Figure 7A**). In agreement with our previous results, we observed excretion of nitrite by the P_{II}(I86N) and ΔP_{II} mutants (**Figure 7B**). Interestingly, while the nitrate utilization rate of the P_{II}(I86N) and ΔP_{II} mutant appeared almost identical, the two mutants differed in their rate of nitrite excretion. While nitrite excretion of the ΔP_{II} mutant accelerated over time, the P_{II}(I86N) initially excreted nitrite faster but then slowed it down over time, explaining the lower amounts of nitrite in the exponentially growing culture (**Figure 6**) as compared to the ΔP_{II} mutant.

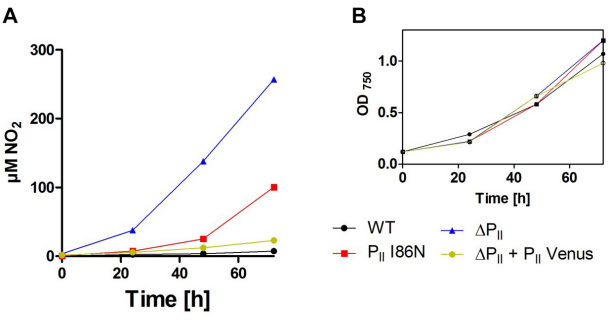

FIGURE 6 | (A) Nitrite excretion of *Synechocystis* sp. wild-type, P_{II}(I86N), ΔP_{II} and P_{II}-Venus-comp. (ΔP_{II} + P_{II}-Venus) complementation grown in BG11 medium supplemented with nitrate. **(B)** Corresponding growth curve to the experiment shown in panel **(A)**.

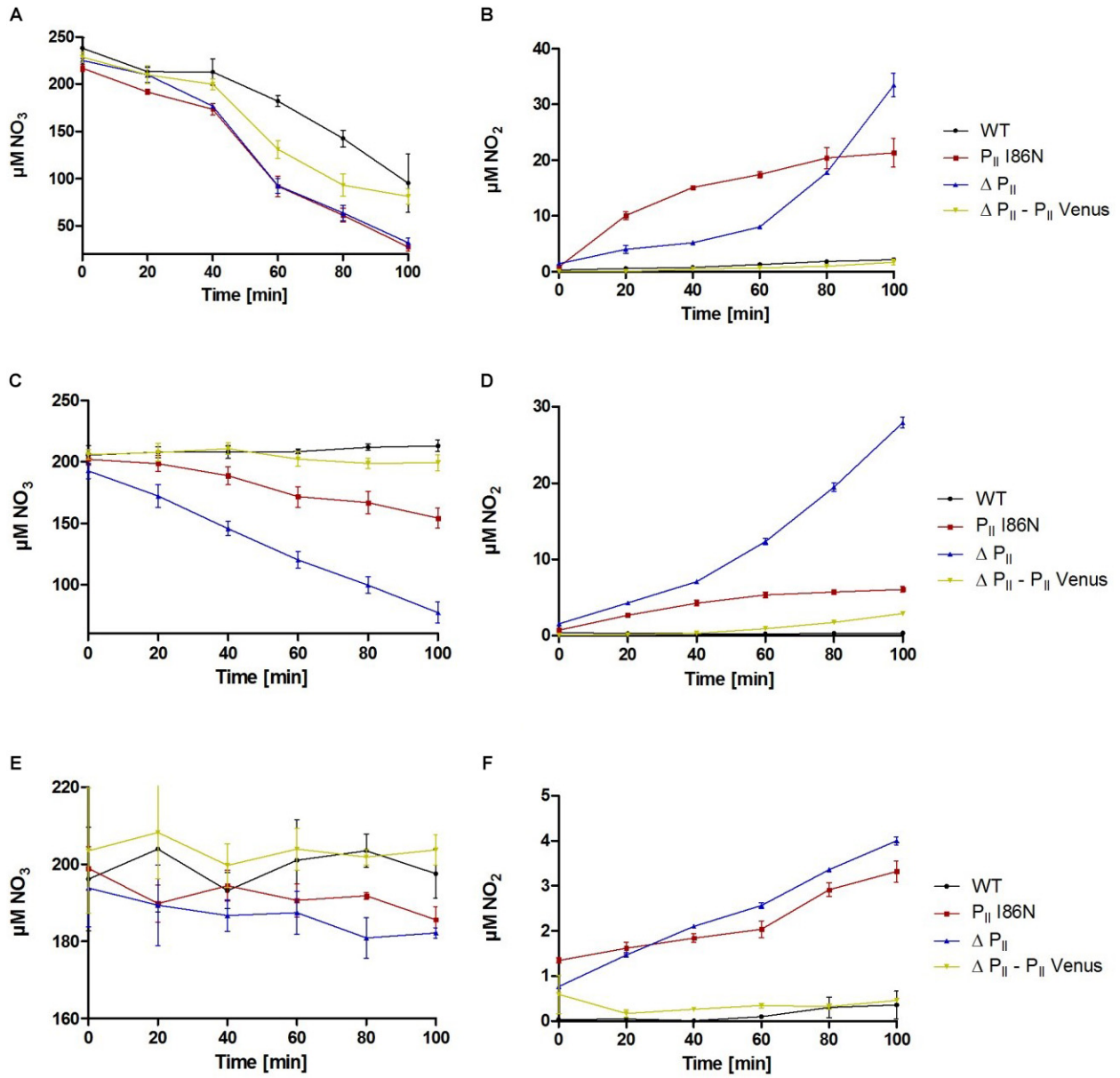

FIGURE 7 | Nitrate utilization and nitrite excretion of various *Synechocystis* strains as indicated. Exponentially growing and nitrate supplemented *Synechocystis* cells were washed and resuspended in a medium containing 200 µM nitrate. Shown are the means of three biological replicates. **(A)** Nitrate utilization and **(B)** nitrite excretion under constant illumination of 40 µmol photons m^{-2} s^{-1}. **(C)** Nitrate utilization and **(D)** nitrite excretion in presence of 2 mM ammonium and under constant illumination of 40 µmol photons m^{-2} s^{-1}. **(E)** Nitrate utilization and **(F)** nitrite excretion in the dark.

Addition of ammonium to nitrate grown cells leads to an immediate inhibition of nitrate uptake. This ammonium-dependent inhibition of nitrate uptake requires the presence of P_{II} protein or P_{II} phosphomimetic variants (Lee et al., 1998). Here, we tested if the P_{II}(I86N) mutant was able to perform the ammonium-dependent nitrate uptake inhibition. For this purpose, nitrate consumption rates were determined after the addition of 2 mM ammonium. Both, *Synechocystis* wild-type and the P_{II}-Venus comp. strains showed a complete inhibition of nitrate uptake in response to ammonium (**Figure 7C**). By contrast, the P_{II}(I86N) and ΔP_{II} mutant strains maintained nitrate uptake after ammonium addition. However, nitrate uptake in the P_{II}(I86N) mutant was clearly diminished as compared to the ΔP_{II} mutant (**Figure 7C**). The uncontrolled nitrate uptake of the P_{II}(I86N) and ΔP_{II} mutant caused excretion of nitrite. Due to the diminished uptake of nitrate by the P_{II}(I86N) mutant, its nitrite excretion was correspondingly lower as compared to the ΔP_{II} mutant (**Figure 7D**).

In addition to the absence of ammonium, active nitrate transport also requires photosynthetic CO_2 fixation

(Romero et al., 1985). Nitrogen assimilation is tightly regulated by light/dark transitions. A transition from light to dark causes an immediate inhibition of nitrate uptake and an inhibition of the ammonium assimilating GS (Romero et al., 1985; Marques et al., 1992). To reveal a role of P_{II} in this response, we tested the dark-switch-off of nitrate uptake in the various P_{II} mutant strains. Although the overall nitrate consumption was very low in darkness (**Figure 7E**) clear differences could be resolved. Notably, the P_{II}(I86N) and ΔP_{II} mutant strains showed slow but constant nitrate uptake as compared to the wild-type and the P_{II}-Venus comp. strain, which did not take up any nitrate. Corresponding to the uptake of nitrate, P_{II}(I86N) and ΔP_{II} mutant excreted small amounts of nitrite (**Figure 7F**), supporting the notion that the P_{II}(I86N) and ΔP_{II} mutants are unable to completely switch-off nitrate uptake in the dark.

P_{II} Signaling Mutants Show Impaired Urea Utilization

To validate the physiological relevance of the interaction of P_{II} with the UrtE subunit of the urea transporter UrtABCDE, we analyzed urea utilization in the different P_{II} mutants. For this purpose, exponentially growing cells were washed and incubated in BG-11^0 medium, containing 150 μM urea as sole nitrogen source with constant illumination of 40 μmol photons m^{-2} s^{-1}. Under these experimental conditions, *Synechocystis* wild-type and P_{II}(I86N) mutant strains utilized similar amounts of urea (**Figure 8A**), whereas both, the ΔP_{II} and P_{II}-Venus comp. strains consumed considerably higher amounts of urea (**Figure 8A**). The wild-type property of the P_{II}(I86N) variant is in agreement with the interaction of the P_{II}(I86N) protein with the UrtE subunit, which appeared to be T-loop independent according to BACTH assays. Urea is hydrolyzed to CO_2 and two molecules of ammonium by the enzyme urease (Mobley and Hausinger, 1989; Esteves-Ferreira et al., 2018). We wondered if an uncontrolled influx of urea could lead to an excretion of ammonium. Therefore, we measured ammonium concentrations in culture supernatant of those cells, which were incubated with 150 μM urea as the sole nitrogen source. Indeed, we detected ammonium excretion of the ΔP_{II} mutant proportional to its urea utilization (**Figure 8B**). In contrast, only minor amounts of ammonium could be detected in the culture supernatant of the *Synechocystis* wild-type, P_{II}(I86N) and P_{II}-Venus comp. strain (**Figure 8B**).

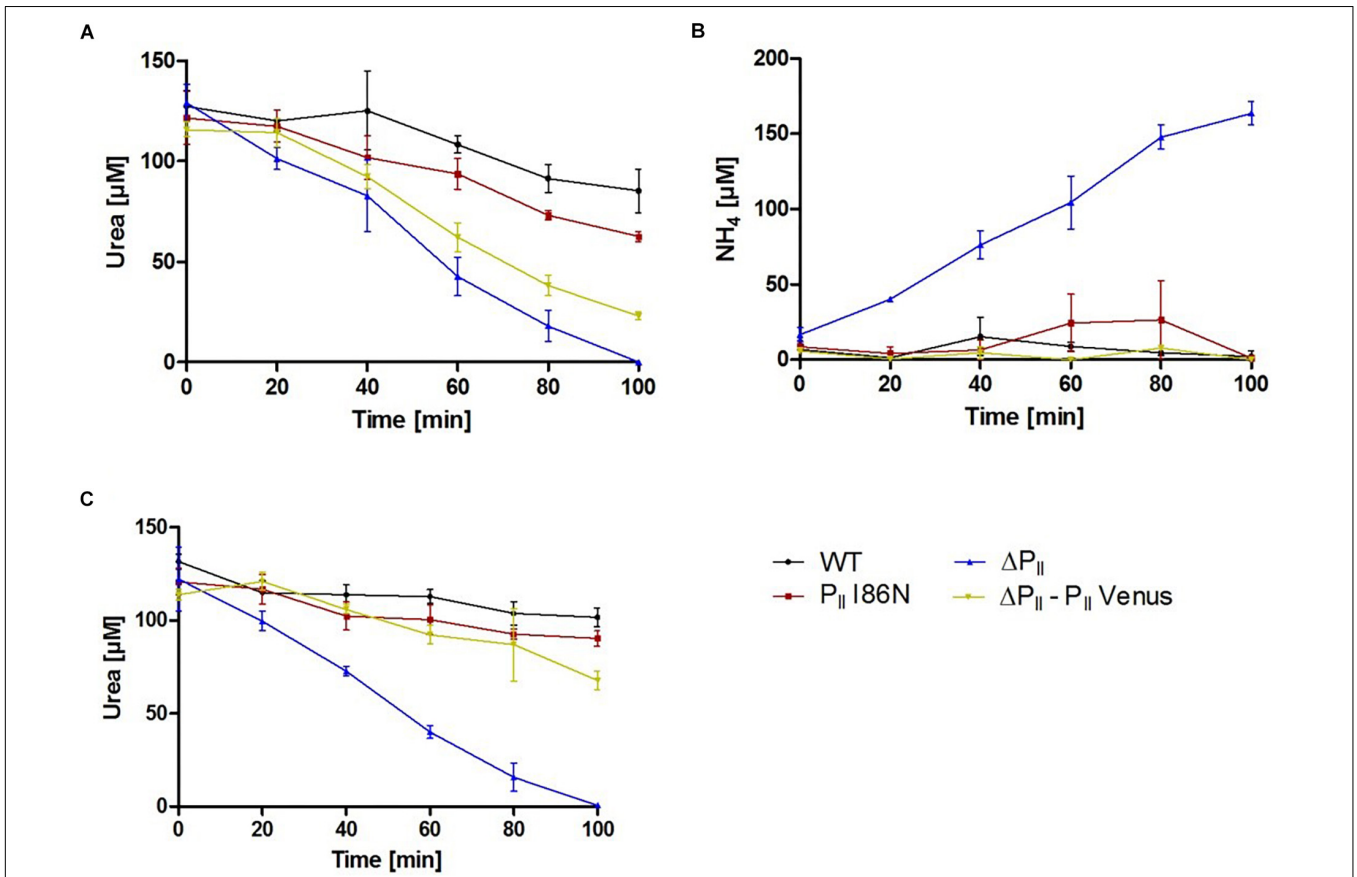

FIGURE 8 | Urea utilization and ammonium excretion of various *Synechocystis* strains as indicated. Exponentially growing and nitrate supplemented *Synechocystis* cells were washed and resuspended in a medium containing 150 μM urea. Shown are the means of three biological replicates. **(A)** Urea utilization and **(B)** ammonium excretion under constant illumination of 40 μmol photons m^{-2} s^{-1}. **(C)** Urea utilization in presence of 2 mM ammonium and under constant illumination of 40 μmol photons m^{-2} s^{-1}.

Synechocystis utilizes available nitrogen sources in a hierarchical order. In presence of ammonium, the uptake of external nitrogen sources is blocked (Muro-Pastor et al., 2005). To test ammonium-dependent inhibition of urea utilization, we determined urea consumption in presence of 2 mM ammonium. The *Synechocystis* wild-type, P_{II}(I86N) and P_{II}-Venus comp. strains showed a clear inhibition in urea utilization in response to the addition of ammonium. In contrast, urea uptake in the ΔP_{II} mutant was completely unaffected by ammonium addition (**Figures 8A,C**). This demonstrates that P_{II} also controls urea uptake, as suggested by the interaction assays.

P_{II} Localization Changes Upon Addition of Nitrate, Ammonium, and Urea

Our previous pull-down experiments and bacterial two-hybrid assays clearly showed interaction of *Synechocystis* P_{II} with Amt1 as well as with nitrate and urea transport components. All interactions appeared to be physiologically relevant. Since all these transporters are localized to the plasma membrane, we suspected that this interaction might affect the cellular localization of P_{II}. Therefore, we monitored P_{II} localization using the *Synechocystis* P_{II}-Venus comp. strain grown under different nitrogen regimes.

Nitrate-replete cells in the mid-exponential growth phase (OD_{750} ~ 0.5) showed heterogeneous distribution of P_{II}-Venus fluorescence in the cell. The majority of cells displayed a strong fluorescence signal in their center and peripheral cell boundary (**Figures 9A,B,D**). The intense signal in the center corresponds to the central cytoplasmic space, inside the multiple thylakoid layers. In this region, P_{II} might interact with different soluble proteins, like NAGK or PipX. The area with low Venus fluorescence is occupied by the thylakoid membranes. The P_{II}-Venus fluorescence at the cell boundary corresponds to the plasma membrane, where Amt1, NrtABCD and UrtABCDE are located (Hahn and Schleiff, 2014) (**Figure 9C**).

When cells are shifted to nitrogen-depleted conditions, they activate the NtcA regulon, including the *glnB* gene and various uptake systems for nitrogen compounds. During prolonged starvation, they undergo chlorosis, which includes a reduction of thylakoid membranes (Forchhammer and Schwarz, 2018). The chlorotic cells rapidly respond to the addition of combined nitrogen sources. Therefore, investigation of P_{II}-Venus fluorescence in chlorotic cells and following the addition of combined nitrogen sources was expected to reveal further insights in the *in vivo* dynamics of P_{II} interactions. To monitor the P_{II} localization in the chlorotic, nitrogen depleted state, cells were grown to an OD_{750} of 0.4–0.6, washed, and resuspended in BG-11^0. After 1 week of nitrogen starvation, the P_{II}-Venus signal was evenly distributed throughout the whole cell and its localization on the plasma membrane was not as distinct as during nitrate-supplemented exponential growth (**Figure 10A**). To test the localization following the addition of different nitrogen sources, 1 week nitrogen starved *Synechocystis* cultures were supplemented with 5 mM NO_3, 5 mM NH_4^+ or 5 mM urea, respectively. Immediately thereafter, a change in the P_{II} localization became visible. The majority of cells showed a clearly visible, distinct plasma membrane localized P_{II}-Venus fluorescence, while the remaining cytosol showed homogenously distributed fluorescence. The re-localization of P_{II} to the plasma

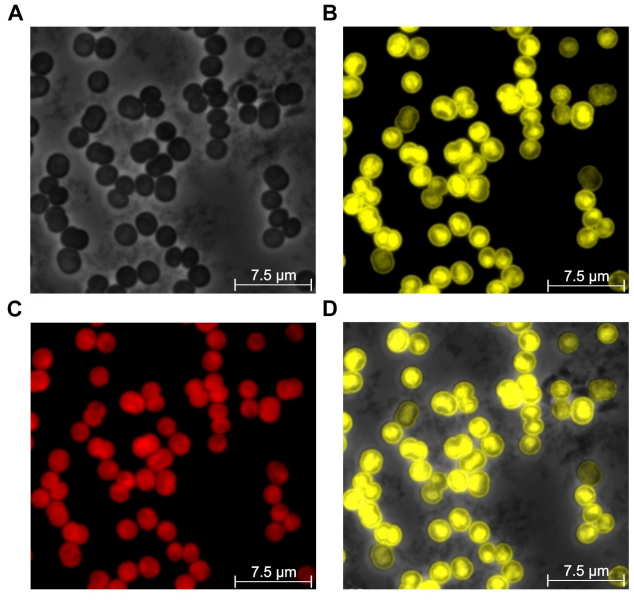

FIGURE 9 | Localization of P_{II}-Venus during exponential growth (OD_{750} of 0.5) of *Synechocystis* **(A)** Phase contrast image of cells. **(B)** Venus fluorescence. **(C)** Autofluorescence of thylakoid membranes. **(D)** Overlay of Venus fluorescence and phase contrast images.

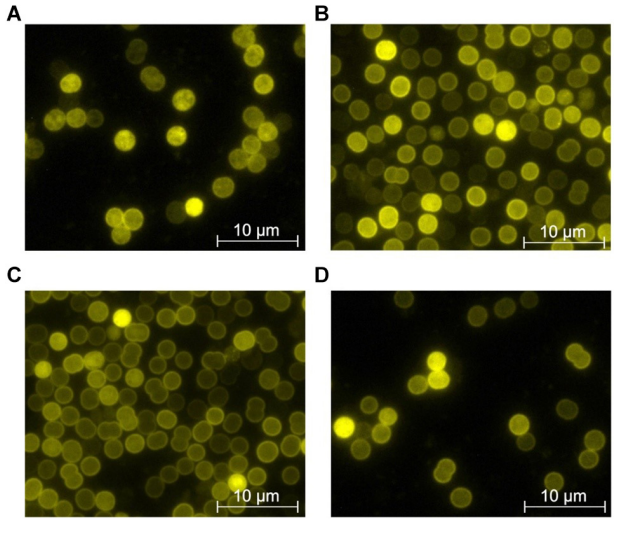

FIGURE 10 | P_{II}-Venus localization under different nitrogen supplemented conditions. **(A)** P_{II}-Venus fluorescence of 1 week nitrogen starved *Synechocystis* cells. **(B–D)** P_{II}-Venus fluorescence of *Synechocystis* during resuscitation from nitrogen starvation. One week nitrogen starved *Synechocystis* cultures were resuscitated by adding 5 mM nitrate **(B)**, 5 mM ammonium **(C)**, or 5 mM urea **(D)**. Fluorescence images were taken 1 h after addition of the nitrogen source.

membrane appeared most clearly in response to ammonium addition as compared to nitrate or urea (**Figures 10B–D**).

Since the fluorescence distribution is subject to a certain degree of heterogeneity with the bulk of single cells observed in the microscope, we attempted to quantitatively describe the average distribution of P_{II}-Venus in a representative set of cells. Therefore, a profile of the fluorescence intensities across median cell sections was determined from 54 individual cells per investigated time point. From these profiles, the relative fluorescence intensity distribution between plasma membrane localized signal to the average cytoplasmic signal was determined and displayed as box-plot (**Figure 11**). Under nitrogen depletion, the majority of the cells showed a higher cytoplasmic P_{II}-Venus localization than plasma membrane localization. Addition of a nitrogen source directly induced a re-localization of P_{II} toward the plasma membrane. In the first 2 h after addition of nitrate or urea, P_{II}-Venus showed a similar localization change (**Figures 11A,C,D**). Two hours after the addition of nitrate, the P_{II}-derived signal from the plasma membrane decreased again and re-appeared in the cytoplasmic space (**Figure 11A**), whereas in urea treated cells, P_{II} continued to accumulate at the plasma membrane (**Figure 11C**). Addition of ammonium induced the most prominent migration of P_{II}-Venus to the plasma membrane in the first hour as compared to nitrate or urea, but thereafter, P_{II}-Venus started to move back to the cytoplasm (**Figure 11B**).

DISCUSSION

The present investigation unraveled a so far unrecognized global function of the cyanobacterial P_{II} signaling protein in controlling the uptake of the major nitrogen sources ammonium, nitrate and urea. Previous studies already suggested occasionally involvement of P_{II} in the regulation of ammonium and nitrate transport (Kobayashi et al., 1997; Lee et al., 1998, 2000; Kloft and Forchhammer, 2005; Conroy et al., 2007), however, this issue was never addressed systematically using a combined biochemical, genetic and physiological approach. Starting from a series of pull-down experiments using FLAG-tagged P_{II} variants, we observed a putative interaction of P_{II} with various nitrogen transport systems. The interactions were verified by bacterial-two hybrid assays and the biological significance of the interaction was validated by physiological

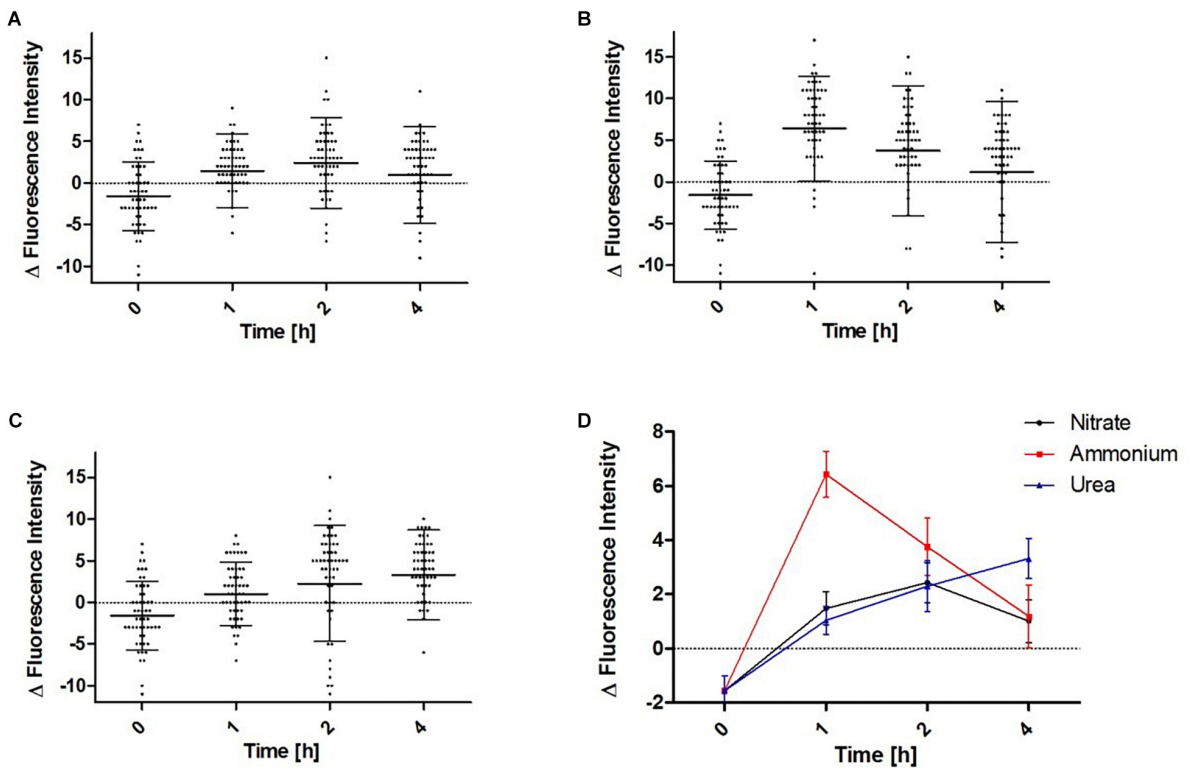

FIGURE 11 | Quantification of the P_{II}-Venus migration toward the plasma membrane in response to the addition of different nitrogen sources to nitrogen starved *Synechocystis* sp. cultures. A linear profile of the fluorescence intensities across midcell was recorded and evaluated as shown in **Supplementary Figure 1**. The maximum fluorescence intensity at the plasma membrane was normalized to the average intensity of the cytoplasm and then, the difference between plasma localized signal and average cytoplasmic signal was calculated (Δ fluorescence intensity). When Δ fluorescence intensity values are below 0, this indicates that the plasma membrane signal is weaker than the average cytoplasmic signal, while values above 0 indicate that the plasma membrane signal is higher than the average cytoplasmic signal. Resuscitation of 1 week nitrogen starved *Synechocystis* sp. cultures were induced by adding either 5 mM NO_3 **(A)**, 5 mM NH_4 **(B)**, or 5 mM urea **(C)**. 50–60 cells were measured per time point. Dots indicate single cell measurements; whiskers showing the standard-deviations; thick black lines show the arithmetic mean. **(D)** Direct comparison of the mean Δ fluorescence intensities from NO_3, NH_4, and urea induced resuscitation.

experiments. Finally, the proposed dynamic interaction of P_{II} with cytoplasmic membrane bound transporters was corroborated by fluorescence microscopy.

Significance Statement

P_{II} signaling proteins play versatile roles in the coordination of carbon- and nitrogen anabolism in prokaryotes and plant chloroplast. In different phylogenetic lineages, P_{II} controls a variety of different target proteins. In cyanobacteria, the P_{II} paralog GlnB has been shown to control global nitrogen-responsive gene expression by interacting with the transcriptional co-activator PipX. Furthermore, P_{II} controls nitrogen storage metabolism in cyanobacteria by regulating the key enzyme of arginine synthesis, *N*-acetylglutamate kinase. Finally, a key enzyme in fatty acid metabolism, the acetyl-CoA carboxylase, was shown to be a target of P_{II}. Several lines of evidences suggested that P_{II} might also be involved in the control of ammonium and nitrate uptake, however, direct involvement of P_{II} has not yet been shown. In this study, we revealed the interactome of P_{II} from the cyanobacterium *Synechocystis* by immunoprecipitating FLAG-tagged P_{II} protein. We found prominent enrichment of components of ammonium, nitrate and urea uptake systems. Direct protein–protein interaction was confirmed by bacterial-two hybrid analysis and the physiological relevance was verified by analyzing ammonium-, nitrate-, and urea-uptake in various P_{II} mutant strains of *Synechocystis*. This study, therefore, demonstrates that P_{II} is the master regulator of the most prominent nitrogen transport systems in cyanobacteria.

Synechocystis P_{II} Regulates Ammonium Uptake by Interacting With the Amt1 Ammonium Permease

In *E. coli*, the P_{II} homolog GlnK regulates AmtB by direct protein–protein interaction to control the influx of ammonium (Conroy et al., 2007). In the GlnK-AmtB complex, the nucleotide binding pockets of GlnK are occupied with ADP and the T-loop of GlnK adopts a vertically extended conformation that closes the ammonium gas channel (Conroy et al., 2007; Maier et al., 2011; Forcada-Nadal et al., 2018). Since the conformation of the T-loop changes upon binding of ATP-Mg^{2+}-2-oxoglutarate, the GlnK-AMT complex only forms under conditions of low 2-OG concentrations, which allows formation of the alternative GlnK-ADP complex (Radchenko et al., 2014).

The present results suggest that in *Synechocystis*, P_{II} regulates the major ammonium permease Amt1 in a similar manner than GlnK the AmtB channel. A weak interaction of Amt1 could still be detected with the phosphomimetic variant S49D. The reduced affinity indicates that the negative charge at position 49 reduces the affinity to Amt1. Therefore, S49 phosphorylated wild-type P_{II} is expected to have an even weaker affinity to Amt1 (two negative charges of phosphoserine as compared to one negative charge of aspartate). In this respect, phosphorylation of S49 would be analogous to uridylylation of Y51 in enterobacterial GlnK proteins, which prevents AmtB interaction (Conroy et al., 2007). Under conditions of strong P_{II} phosphorylation (nitrogen-poor conditions or high CO_2 to nitrate ratio), the Amt1 channel would remain open, allowing unrestricted uptake of ammonium ions. When cells are shifted to excess ammonium conditions, P_{II} becomes dephosphorylated (Ruppert et al., 2002) and diminished 2-OG levels allow formation of the P_{II}-ADP complex, which then can close the Amt1 pores.

In BACTH assays, the P_{II}(R9L) variant was completely impaired in Amt1 interaction. This variant is also unable to interact with NAGK, presumably due to a stabilizing function of the R9 residue at the interface to the binding partner (Fokina et al., 2010a). The failure of this variant to interact with Amt1 indicates that also for Amt1 interaction, the lower face of P_{II} with the protruding T-loops is involved in this protein–protein interaction, in agreement with the structure of the GlnK-AmtB complex.

The failure of the P_{II}(I86N) variant to interact with Amt1 corresponds to the loss of its affinity toward ADP (Fokina et al., 2010b). P_{II}(I86N) has one order of magnitude higher affinity toward ATP than toward ADP and thus, is expected to reside almost exclusively in the ATP-bound state, which would abrogate the interaction with Amt1.

Despite that ammonium uptake in the *Synechocystis* P_{II}(I86N) variant is no more under P_{II} control, this strain exhibits a higher ammonium tolerance than the ΔP_{II} mutant. This difference could be explained by different ammonium assimilation properties. In the P_{II} deletion mutant, the ammonium-scavenging arginine synthesis pathway is not active due to lacking activation of the key enzyme NAGK by P_{II} (Maheswaran et al., 2006). By contrast, *Synechocystis* P_{II}(I86N) highly enhances NAGK activity, resulting in high intracellular arginine concentrations that leads to accumulation of cyanophycin granules (Watzer et al., 2015). This pathway will foster the metabolic removal of excess ammonium and thus results in increased ammonium tolerance.

Analysis of the subcellular localization of P_{II} in response to ammonium stimuli agrees with the above-depicted concept. Only 1 h after the addition of ammonium to chlorotic cells, P_{II} shows a strong migration toward the plasma membrane. Providing ammonium to nitrogen-starved cells should cause a strong decrease of the cellular 2-OG levels. This leads to the observed accumulation of P_{II} to the cytoplasmic membrane, preventing an excess uptake of too much ammonium. After a while, a new equilibrium will be established leading to a partial re-localization of P_{II} to its cytoplasmic targets, such as NAGK. Indeed, *Synechocystis* cells recovering from nitrogen chlorosis start to produce cyanophycin already after a few hours (Watzer and Forchhammer, 2018).

P_{II} Regulates Nitrate Uptake by Interacting With NrtD and NrtC Subunits

Several previous studies documented an involvement of P_{II} in the regulation of nitrate/nitrite uptake. Our data provide novel insights regarding the mechanism of P_{II}-mediated regulation of the NrtABCD transporter. It appears that the NrtABCD complex is directly regulated by interaction of P_{II} with the cytoplasmic ATPase subunits NrtC and NrtD, as indicated by the co-isolation of wild-type P_{II} with both of these proteins. The inability of

the P_{II}(I86N) complemented strain to regulate nitrate utilization as well as the reduced interaction of P_{II}(I86N) with NrtC and NrtD subunits in BACTH assays could in principle be explained by the altered T-loop conformation or by the different ligand binding properties of this variant, discussed above. As shown by BACTH assays and by recent *in vitro* studies (Watzer and Forchhammer, unpublished), the P_{II}(I86N) variant is indeed able to interact with PipX. This interaction requires a vertically extended conformation of the T-loop (Llacer et al., 2010; Forcada-Nadal et al., 2018). Although P_{II}-PipX complexes are favored by the ADP-state of P_{II}, efficient PipX-P_{II} interaction also occurs with the P_{II}-ATP complex. As explained above, the P_{II}(I86N) variant is trapped in the ATP-bound state. The fact that this P_{II} variant binds PipX indicates, that the T-loop of P_{II}(I86N) is flexible enough to adopt various conformations. Therefore, it is likely that formation of the P_{II}-NrtC or NrtD complex requires the ADP-bound state of P_{II}, which is disabled in the P_{II}(I86N) variant. As for NAGK and Amt1, the P_{II}(R9L) variant is unable to interact with any of the NRT subunits, indicating that P_{II} interaction involves the lower part of the P_{II} body, where the T-loop emanates.

The phosphomimetic variant P_{II}(S49D) shows, albeit weaker, interaction with the NRT subunits. This positive interaction explains previous reports, that *Synechocystis* and *Synechococcus* strains expressing these phosphomimetic variants, display a wild-type like regulation of nitrate/nitrite utilization (Lee et al., 2000; Kobayashi et al., 2005). Why the diminished interaction measured by BACTH assays does not properly reflect the physiological behavior of the P_{II}(S49D) expressing strain (full complementation) could be due to different sensitivities of the assays. Kobayashi et al. (2005) used for the complementation of the *Synechocystis* deficient mutant plasmid-borne P_{II} constructs, which cause higher expression levels as in the wild-type genotype. Therefore, a weaker interaction of P_{II} with the NRT subunits could still be sufficient to inhibit NRT. The mechanism of NRT inhibition by P_{II} still awaits structure-functional explanation. Our BACTH assays indicate that P_{II} interacts with both ATPase subunits of NRT. Of these, the NrtC subunit seems to play a particular role: Truncation of the regulatory domain of NrtC results in an ammonium-insensitive NRT, despite the presence of a functional P_{II} system. The regulatory domain of NrtC possesses a putative binding site for nitrate (Koropatkin et al., 2006). Probably P_{II}, through binding to NrtC and NrtD, must act in concert with the regulatory NrtC domain, to stop nitrate uptake. If one of the two regulators is missing, ammonium inhibition would not work. It is tempting to speculate that the regulatory domain of NrtC directly senses the nitrate-state of the cells (Koropatkin et al., 2006) to prepare NRT for inhibition by the P_{II}-ADP complex, whereas P_{II} in the 2-OG-Mg-ATP complex (signaling high C/low N state) would not interact and, therefore, not inhibit NRT. This dual regulatory model combines information from the nitrate status with the global C/N and energy state sensing of P_{II} to tune NRT activity to the actual need. This model also explains the light-response of NRT: Low energy conditions favor the ADP-complex of P_{II}, explaining why in the dark, complete switch-off of NRT requires P_{II}.

P_{II} Regulates Urea Uptake by Interacting With the UrtE Subunit

In addition to Amt1 and NRT, our data also identified the ABC-type urea transporter (UrtABCDE) as a novel P_{II} target, with the UrtE subunit being the direct interaction partner of P_{II}. No BACTH interaction was observed for UrtD. This implies that the UrtD protein identified in the FLAG-tag pull-down resulted from pull-down of the entire URT complex. As deduced from the urea-utilization phenotype of the different P_{II} variant strains, as well as form the properties of BACTH interactions, the interaction of P_{II} with UrtE is distinct from the mode of Amt1 or NrtC and NrtD interaction. P_{II} interaction with UrtE seems to be T-loop independent, since the phosphomimetic S49D variant as well as the P_{II}(I86N) and P_{II}(R9L) variants interacted in BACTH assays like wild-type P_{II}. The ability of P_{II}(R9L) to interact with UrtE indicates that the interaction may involve a region of P_{II} distinct from the usual interaction face used by NAGK, PipX or Amt1.

In agreement with a different binding mode between P_{II} and UrtE, the P_{II}(I86N) variant could substitute wild-type P_{II} regarding the control of urea utilization. This suggests that the P_{II}-ATP complex is able to interact with UrtE in a non-conventional manner. The control of urea uptake prevents its futile hydrolysis and the consequent release of ammonium. Although the P_{II}-Venus variant displayed higher urea uptake rates than the P_{II} deficient mutant, it could prevent concomitant ammonium excretion, indicating that also the P_{II}-Venus variant successfully regulates urea utilization. Consistently, all the tested P_{II} variant strains (wild-type, I86N and P_{II}-Venus) were able to carry out ammonium inhibition of urea uptake. Careful examination of the data shows that the P_{II}-Venus strain displayed slightly higher urea uptake rates than the other two strains. It is possible that due to the bulky fluorescent proteins fused to P_{II} the interaction with P_{II} does not tune down urea uptake as efficient as in the case of the non-tagged P_{II} variants. Nevertheless, the P_{II}-Venus construct is functional, which also agrees with the re-localization of P_{II}-Venus to the plasma membrane upon addition of urea to nitrogen-starved cells. Under certain conditions, the entire multisubunit urease complex appeared in P_{II}-FLAG-tag pull-down experiments. This observation deserves further investigation. It suggests either a direct interaction of the urease complex with P_{II} or a possible metabolic channeling between the urea uptake system and the multisubunit urease complex, leading to a co-immunoprecipitation of the entire super-complex. Further studies are required to reveal the molecular mechanism of urea metabolism and the involvement of P_{II} in this process.

CONCLUSION

All together, the present study has expanded the insights in P_{II} regulatory interactions in *Synechocystis*. According to this study, the P_{II} regulatory network includes all relevant nitrogen uptake systems in *Synechocystis*. It is highly probable that the same holds true for other cyanobacteria. In *Synechococcus elongatus*, (Chang et al., 2013) genetic and physiological studies suggested that in addition to NRT, P_{II} is likely involved in the control of a cyanate ABC transporter (CynABC), which is not

present in *Synechocystis*. Localization of P_{II}-YFP fusions to the cytoplasmic membrane could also be seen in fluorescent images from *S. elongatus* (Espinosa et al., 2018). Control of transport proteins appears to be a highly conserved property of the P_{II} family members, as exemplified by the widely distributed GlnK-Amt interaction. Recently, a more distantly related member of the P_{II} superfamily, SbtB, an accessory component of the sodium-dependent bicarbonate transporter SbtA, was shown to be involved in regulation of bicarbonate metabolism in *Synechocystis* (Selim et al., 2018). Moreover, many putative non-characterized P_{II} family members are genetically linked to transport and channel proteins. However, except for GlnK-AmtB, no structures are known for P_{II}-protein complexes with membrane channel proteins. Whether the interactions of the P_{II} members with the channels follow a universal mode, or whether different types of interaction exist, remains to be demonstrated. However, the differences observed between the interactions of P_{II} variants with UrtE, NrtC/D and Amt1 suggest that the interactions could be as versatile as observed for the various soluble P_{II} interactors (Forcada-Nadal et al., 2018).

DATA AVAILABILITY

The datasets generated for this study can be found in the PRIDE ProteomeXchange consortium, PXD013411.

AUTHOR CONTRIBUTIONS

BW designed, conducted, and evaluated the cyanobacterial growth experiments, quantifications of nitrate, nitrite, ammonium, and urea utilization and carried out the microscopic experiments. RS constructed *Synechocystis* strains expressing tagged P_{II}. PS and OH carried out anti-FLAG pull-down experiments. PS and BM carried out and evaluated nanoLC-MS/MS analyses. MK designed and constructed bacterial two-hybrid vectors. NN carried out and evaluated bacterial two-hybrid assays. KF designed and supervised the study and wrote the manuscript with BW. All authors gave input and approved the manuscript.

FUNDING

This work was supported by grants from the DFG (Fo195/9-2) and the research training group GRK 1708. RS was supported by the project LO1416 of the Czech Ministry of Education.

SUPPLEMENTARY MATERIAL

The Supplementary Material for this article can be found online at: https://www.frontiersin.org/articles/10.3389/fmicb.2019.01428/full#supplementary-material

REFERENCES

Baker, K. M., Gobler, C. J., and Collier, J. L. (2009). Urease gene sequences from algae and heterotrophic bacteria in axenic and nonaxenic phytoplankton cultures. *J. Phycol.* 45, 625–634. doi: 10.1111/j.1529-8817.2009.00680.x

Battchikova, N., Vainonen, J. P., Vorontsova, N., Keranen, M., Carmel, D., and Aro, E. M. (2010). Dynamic changes in the proteome of *Synechocystis* 6803 in response to CO_2 limitation revealed by quantitative proteomics. *J. Proteome Res.* 9, 5896–5912. doi: 10.1021/pr100651w

Battesti, A., and Bouveret, E. (2012). The bacterial two-hybrid system based on adenylate cyclase reconstitution in *Escherichia coli*. *Methods* 58, 325–334. doi: 10.1016/j.ymeth.2012.07.018

Burillo, S., Luque, I., Fuentes, I., and Contreras, A. (2004). Interactions between the nitrogen signal transduction protein PII and *N*-acetyl glutamate kinase in organisms that perform oxygenic photosynthesis. *J. Bacteriol.* 186, 3346–3354. doi: 10.1128/jb.186.11.3346-3354.2004

Caldovic, L., and Tuchman, M. (2003). N-acetylglutamate and its changing role through evolution. *Biochem. J.* 372(Pt 2), 279–290. doi: 10.1042/BJ20030002

Chang, Y., Takatani, N., Aichi, M., Maeda, S.-I., and Omata, T. (2013). Evaluation of the effects of PII deficiency and the toxicity of PipX on growth characteristics of the PII-less mutant of the cyanobacterium *Synechococcus elongatus*. *Plant Cell Physiol.* 54, 1504–1514. doi: 10.1093/pcp/pct092

Cheah, E., Carr, P. D., Suffolk, P. M., Vasudevan, S. G., Dixon, N. E., and Ollis, D. L. (1994). Structure of the *Escherichia coli* signal transducing protein PII. *Structure* 2, 981–990.

Chellamuthu, V. R., Alva, V., and Forchhammer, K. (2013). From cyanobacteria to plants: conservation of PII functions during plastid evolution. *Planta* 237, 451–462. doi: 10.1007/s00425-012-1801-0

Chidgey, J. W., Linhartova, M., Komenda, J., Jackson, P. J., Dickman, M. J., Canniffe, D. P., et al. (2014). A cyanobacterial chlorophyll synthase-HliD complex associates with the Ycf39 protein and the YidC/Alb3 insertase. *Plant Cell* 26, 1267–1279. doi: 10.1105/tpc.114.124495

Conroy, M. J., Durand, A., Lupo, D., Li, X. D., Bullough, P. A., Winkler, F. K., et al. (2007). The crystal structure of the *Escherichia coli* AmtB-GlnK complex reveals how GlnK regulates the ammonia channel. *Proc. Natl. Acad. Sci. U.S.A.* 104, 1213–1218. doi: 10.1073/pnas.0610348104

Cox, J., Hein, M. Y., Luber, C. A., Paron, I., Nagaraj, N., and Mann, M. (2014). Accurate proteome-wide label-free quantification by delayed normalization and maximal peptide ratio extraction, termed MaxLFQ. *Mol. Cell. Proteomics* 13, 2513–2526. doi: 10.1074/mcp.M113.031591

Cox, J., and Mann, M. (2008). MaxQuant enables high peptide identification rates, individualized p.p.b.-range mass accuracies and proteome-wide protein quantification. *Nat. Biotechnol.* 26, 1367–1372. doi: 10.1038/nbt.1511

Dai, G. Z., Qiu, B. S., and Forchhammer, K. (2014). Ammonium tolerance in the cyanobacterium *Synechocystis* sp. strain PCC 6803 and the role of the psbA multigene family. *Plant Cell Environ.* 37, 840–851. doi: 10.1111/pce.12202

Drath, M., Kloft, N., Batschauer, A., Marin, K., Novak, J., and Forchhammer, K. (2008). Ammonia triggers photodamage of photosystem II in the cyanobacterium *Synechocystis* sp strain PCC 6803. *Plant Physiol.* 147, 206–215. doi: 10.1104/pp.108.117218

Espinosa, J., Forchhammer, K., Burillo, S., and Contreras, A. (2006). Interaction network in cyanobacterial nitrogen regulation: PipX, a protein that interacts in a 2-oxoglutarate dependent manner with PII and NtcA. *Mol. Microbiol.* 61, 457–469. doi: 10.1111/j.1365-2958.2006.05231.x

Espinosa, J., Forchhammer, K., and Contreras, A. (2007). Role of the *Synechococcus* PCC 7942 nitrogen regulator protein PipX in NtcA-controlled processes. *Microbiology* 153, 711–718.

Espinosa, J., Labella, J. I., Cantos, R., and Contreras, A. (2018). Energy drives the dynamic localization of cyanobacterial nitrogen regulators during diurnal cycles. *Environ. Microbiol.* 20, 1240–1252. doi: 10.1111/1462-2920.14071

Espinosa, J., Rodriguez-Mateos, F., Salinas, P., Lanza, V. F., Dixon, R., de la Cruz, F., et al. (2014). PipX, the coactivator of NtcA, is a global regulator in cyanobacteria. *Proc. Natl. Acad. Sci. U.S.A.* 111, E2423–E2430. doi: 10.1073/pnas.1404097111

Esteves-Ferreira, A. A., Inaba, M., Fort, A., Araujo, W. L., and Sulpice, R. (2018). Nitrogen metabolism in cyanobacteria: metabolic and molecular control,

growth consequences and biotechnological applications. *Crit. Rev. Microbiol.* 44, 541–560. doi: 10.1080/1040841X.2018.1446902

Fiddler, R. N. (1977). Collaborative study of modified AOAC method of analysis for nitrite in meat and meat products. *J. Assoc. Off. Anal. Chem.* 60, 594–599.

Flores, E., and Herrero, A. (1994). "Assimilatory nitrogen metabolism and its regulation," in *The Molecular Biology of Cyanobacteria*, ed. D. A. Bryant (Dordrecht: Springer), 487–517.

Fokina, O., Chellamuthu, V. R., Forchhammer, K., and Zeth, K. (2010a). Mechanism of 2-oxoglutarate signaling by the *Synechococcus elongatus* PII signal transduction protein. *Proc. Natl. Acad. Sci. U.S.A.* 107, 19760–19765. doi: 10.1073/pnas.1007653107

Fokina, O., Chellamuthu, V. R., Zeth, K., and Forchhammer, K. (2010b). A novel signal transduction protein PII variant from *Synechococcus elongatus* PCC 7942 indicates a two-step process for NAGK-PII complex formation. *J. Mol. Biol.* 399, 410–421. doi: 10.1016/j.jmb.2010.04.018

Forcada-Nadal, A., Forchhammer, K., and Rubio, V. (2014). SPR analysis of promoter binding of *Synechocystis* PCC6803 transcription factors NtcA and CRP suggests cross-talk and sheds light on regulation by effector molecules. *FEBS Lett.* 588, 2270–2276. doi: 10.1016/j.febslet.2014.05.010

Forcada-Nadal, A., Llacer, J. L., Contreras, A., Marco-Marin, C., and Rubio, V. (2018). The PII-NAGK-PipX-NtcA regulatory axis of cyanobacteria: a tale of changing partners, allosteric effectors and non-covalent interactions. *Front. Mol. Biosci.* 5:91. doi: 10.3389/fmolb.2018.00091

Forchhammer, K. (2004). Global carbon/nitrogen control by PII signal transduction in cyanobacteria: from signals to targets. *FEMS Microbiol. Rev.* 28, 319–333. doi: 10.1016/j.femsre.2003.11.001

Forchhammer, K. (2008). PII signal transducers: novel functional and structural insights. *Trends Microbiol.* 16, 65–72. doi: 10.1016/j.tim.2007.11.004

Forchhammer, K., and Hedler, A. (1997). Phosphoprotein PII from cyanobacteria-analysis of functional conservation with the PII signal-transduction protein from *Escherichia coli*. *Eur. J. Biochem.* 244, 869–875.

Forchhammer, K., IrmLer, A., Kloft, N., and Ruppert, U. (2004). PII signalling in unicellular cyanobacteria: analysis of redox-signals and energy charge. *Physiol. Plant.* 120, 51–56. doi: 10.1111/j.0031-9317.2004.0218.x

Forchhammer, K., and Luddecke, J. (2016). Sensory properties of the PII signalling protein family. *FEBS J.* 283, 425–437. doi: 10.1111/febs.13584

Forchhammer, K., and Schwarz, R. (2018). Nitrogen chlorosis in unicellular cyanobacteria - a developmental program for surviving nitrogen deprivation. *Environ. Microbiol.* 21, 1173–1184. doi: 10.1111/1462-2920.14447

Forchhammer, K., and Tandeau de Marsac, N. (1995). Phosphorylation of the PII protein (glnB gene product) in the cyanobacterium *Synechococcus* sp. strain PCC 7942: analysis of in vitro kinase activity. *J. Bacteriol.* 177, 5812–5817.

Gibson, D. G., Young, L., Chuang, R. Y., Venter, J. C., Hutchison, C. A. III, and Smith, H. O. (2009). Enzymatic assembly of DNA molecules up to several hundred kilobases. *Nat. Methods* 6, 343–345. doi: 10.1038/nmeth.1318

Giner-Lamia, J., Robles-Rengel, R., Hernández-Prieto, M. A., Muro-Pastor, M. I., Florencio, F. J., and Futschik, M. E. (2017). Identification of the direct regulon of NtcA during early acclimation to nitrogen starvation in the cyanobacterium *Synechocystis* sp. PCC 6803. *Nucleic Acids Res.* 45, 11800–11820. doi: 10.1093/nar/gkx860

Gruswitz, F., O'Connell, J., and Stroud, R. M. (2007). Inhibitory complex of the transmembrane ammonia channel, AmtB, and the cytosolic regulatory protein, GlnK, at 1.96 A. *Proc. Natl. Acad. Sci. U.S.A.* 104, 42–47. doi: 10.1073/pnas.0609796104

Hahn, A., and Schleiff, E. (2014). "The cell envelope," in *The Cell Biology of Cyanobacteria*, eds E. Flores and A. Herrero (Norfolk: Caister Academic Press), 29–87.

Hauf, W., Schmid, K., Gerhardt, E. C., Huergo, L. F., and Forchhammer, K. (2016). Interaction of the nitrogen regulatory protein GlnB PII with biotin carboxyl carrier protein (BCCP) controls acetyl-CoA levels in the cyanobacterium *Synechocystis* sp. PCC 6803. *Front. Microbiol.* 7:1700. doi: 10.3389/fmicb.2016.01700

Heinrich, A., Maheswaran, M., Ruppert, U., and Forchhammer, K. (2004). The *Synechococcus elongatus* PII signal transduction protein controls arginine synthesis by complex formation with N-acetyl-L-glutamate kinase. *Mol. Microbiol.* 52, 1303–1314. doi: 10.1111/j.1365-2958.2004.04058.x

Herrero, A., and Flores, E. (2008). *The Cyanobacteria: Molecular Biology, Genomics, and Evolution*. Norfolk: Caister Academic Press.

Hisbergues, M., Jeanjean, R., Joset, F., de Marsac, N. T., and Bedu, S. (1999). Protein PII regulates both inorganic carbon and nitrate uptake and is modified by a redox signal in *Synechocystis* sp PCC 6803. *FEBS Lett.* 463, 216–220.

Hollingshead, S., Kopečná, J., Jackson, P. J., Canniffe, D. P., Davison, P. A., Dickman, M. J., et al. (2012). Conserved chloroplast open-reading frame ycf54 is required for activity of the magnesium protoporphyrin monomethylester oxidative cyclase in *Synechocystis* PCC 6803. *J. Biol. Chem.* 287, 27823–27833. doi: 10.1074/jbc.M112.352526

Huergo, L. F., Pedrosa, F. O., Muller-Santos, M., Chubatsu, L. S., Monteiro, R. A., Merrick, M., et al. (2012). PII signal transduction proteins: pivotal players in post-translational control of nitrogenase activity. *Microbiology* 158(Pt 1), 176–190. doi: 10.1099/mic.0.049783-0

Jiang, P., Peliska, J. A., and Ninfa, A. J. (1998). Enzymological characterization of the signal-transducing uridylyltransferase/uridylyl-removing enzyme (EC 2.7.7.59) of *Escherichia coli* and its interaction with the PII protein. *Biochemistry* 37, 12782–12794. doi: 10.1021/bi980667m

Karimova, G., Ullmann, A., and Ladant, D. (2001). Protein-protein interaction between *Bacillus stearothermophilus* tyrosyl-tRNA synthetase subdomains revealed by a bacterial two-hybrid system. *J. Mol. Microbiol. Biotechnol.* 3, 73–82.

Kloft, N., and Forchhammer, K. (2005). Signal transduction protein PII phosphatase PphA is required for light-dependent control of nitrate utilization in *Synechocystis* sp. strain PCC 6803. *J. Bacteriol.* 187, 6683–6690. doi: 10.1128/JB.187.19.6683-6690.2005

Kobayashi, M., Rodriguez, R., Lara, C., and Omata, T. (1997). Involvement of the C-terminal domain of an ATP-binding subunit in the regulation of the ABC-type nitrate/nitrite transporter of the cyanobacterium *Synechococcus* sp. PCC 7942. *J. Biol. Chem.* 272, 27197–27201. doi: 10.1074/jbc.272.43.27197

Kobayashi, M., Takatani, N., Tanigawa, M., and Omata, T. (2005). Posttranslational regulation of nitrate assimilation in the cyanobacterium *Synechocystis* sp. strain PCC 6803. *J. Bacteriol.* 187, 498–506. doi: 10.1128/JB.187.2.498-506.2005

Koropatkin, N. M., Pakrasi, H. B., and Smith, T. J. (2006). Atomic structure of a nitrate-binding protein crucial for photosynthetic productivity. *Proc. Natl. Acad. Sci. U.S.A.* 103, 9820–9825. doi: 10.1073/pnas.0602517103

Lee, H. M., Flores, E., Forchhammer, K., Herrero, A., and de Marsac, N. T. (2000). Phosphorylation of the signal transducer PII protein and an additional effector are required for the PII mediated regulation of nitrate and nitrite uptake in the cyanobacterium *Synechococcus* sp PCC 7942. *Eur. J. Biochem.* 267, 591–600. doi: 10.1046/j.1432-1327.2000.01043.x

Lee, H. M., Flores, E., Herrero, A., Houmard, J., and de Marsac, N. T. (1998). A role for the signal transduction protein PII in the control of nitrate/nitrite uptake in a cyanobacterium. *FEBS Lett.* 427, 291–295.

Llacer, J. L., Contreras, A., Forchhammer, K., Marco-Marin, C., Gil-Ortiz, F., Maldonado, R., et al. (2007). The crystal structure of the complex of PII and acetylglutamate kinase reveals how PII controls the storage of nitrogen as arginine. *Proc. Natl. Acad. Sci. U.S.A.* 104, 17644–17649. doi: 10.1073/pnas.0705987104

Llacer, J. L., Espinosa, J., Castells, M. A., Contreras, A., Forchhammer, K., and Rubio, V. (2010). Structural basis for the regulation of NtcA-dependent transcription by proteins PipX and PII. *Proc. Natl. Acad. Sci. U.S.A.* 107, 15397–15402. doi: 10.1073/pnas.1007015107

Luque, I., Flores, E., and Herrero, A. (1994). Nitrate and nitrite transport in the cyanobacterium *Synechococcus* sp PCC 7942 are mediated by the same permease. *Biochim. Biophys. Acta Bioenerg.* 1184, 296–298.

Luque, I., and Forchhammer, K. (2008). "Nitrogen assimilation and C/N balance sensing," in *The Cyanobacteria. Molecular Biology, Genomics and Evolution*, eds A. Herrero and E. Flores (Norfolk: Caister Academic Press), 335–382.

Maeda, S. I., and Omata, T. (1997). Substrate-binding lipoprotein of the cyanobacterium *Synechococcus* sp strain PCC 7942 involved in the transport of nitrate and nitrite. *J. Biol. Chem.* 272, 3036–3041. doi: 10.1074/jbc.272.5.3036

Maheswaran, M., Urbanke, C., and Forchhammer, K. (2004). Complex formation and catalytic activation by the PII signaling protein of N-acetyl-L-glutamate kinase from *Synechococcus elongatus* strain PCC 7942. *J. Biol. Chem.* 279, 55202–55210. doi: 10.1074/jbc.M410971200

Maheswaran, M., Ziegler, K., Lockau, W., Hagemann, M., and Forchhammer, K. (2006). PII-regulated arginine synthesis controls accumulation of cyanophycin in *Synechocystis* sp strain PCC 6803. *J. Bacteriol.* 188, 2730–2734. doi: 10.1128/Jb.188.7.2730-2734.2006

Maier, S., Schleberger, P., Lu, W., Wacker, T., Pfluger, T., Litz, C., et al. (2011). Mechanism of disruption of the Amt-GlnK complex by PII-mediated sensing of 2-oxoglutarate. *PLoS One* 6:e26327. doi: 10.1371/journal.pone.0026327

Manzano, C., Candau, P., Gomez-Moreno, C., Relimpio, A. M., and Losada, M. (1976). Ferredoxin-dependent photosynthetic reduction of nitrate and nitrite by particles of *Anacystis nidulans*. *Mol. Cell. Biochem.* 10, 161–169.

Marques, S., Merida, A., Candau, P., and Florencio, F. J. (1992). Light-mediated regulation of glutamine-synthetase activity in the unicellular cyanobacterium *Synechococcus* sp PCC6301. *Planta* 187, 247–253.

Merrick, M. (2014). Post-translational modification of PII signal transduction proteins. *Front. Microbiol.* 5:763. doi: 10.3389/fmicb.2014.00763

Mobley, H. L. T., and Hausinger, R. P. (1989). Microbial ureases - significance, regulation and molecular characterization. *Microbiol. Rev.* 53, 85–108.

Montesinos, M. L., Muro-Pastor, A. M., Herrero, A., and Flores, E. (1998). Ammonium/methylammonium permeases of a cyanobacterium. Identification and analysis of three nitrogen-regulated amt genes in *Synechocystis* sp. PCC 6803. *J. Biol. Chem.* 273, 31463–31470.

Muro-Pastor, M. I., Reyes, J. C., and Florencio, F. J. (2001). Cyanobacteria perceive nitrogen status by sensing intracellular 2-oxoglutarate levels. *J. Biol. Chem.* 276, 38320–38328.

Muro-Pastor, M. I., Reyes, J. C., and Florencio, F. J. (2005). Ammonium assimilation in cyanobacteria. *Photosynth. Res.* 83, 135–150.

Nakao, M., Okamoto, S., Kohara, M., Fujishiro, T., Fujisawa, T., Sato, S., et al. (2010). CyanoBase: the cyanobacteria genome database update 2010. *Nucleic Acids Res.* 38, D379–D381. doi: 10.1093/nar/gkp915

Ohashi, Y., Shi, W., Takatani, N., Aichi, M., Maeda, S., Watanabe, S., et al. (2011). Regulation of nitrate assimilation in cyanobacteria. *J. Exp. Bot.* 62, 1411–1424. doi: 10.1093/jxb/erq427

Olsen, J. V., de Godoy, L. M. F., Li, G. Q., Macek, B., Mortensen, P., Pesch, R., et al. (2005). Parts per million mass accuracy on an orbitrap mass spectrometer via lock mass injection into a C-trap. *Mol. Cell. Proteomics* 4, 2010–2021. doi: 10.1074/mcp.T500030-MCP200

Omata, T., Andriesse, X., and Hirano, A. (1993). Identification and characterization of a gene-cluster involved in nitrate transport in the cyanobacterium *Synechococcus* sp PCC 7942. *Mol. Gen. Genet.* 236, 193–202. doi: 10.1007/Bf00277112

Radchenko, M., and Merrick, M. (2011). The role of effector molecules in signal transduction by PII proteins. *Biochem. Soc. Trans.* 39, 189–194. doi: 10.1042/BST0390189

Radchenko, M. V., Thornton, J., and Merrick, M. (2014). Association and dissociation of the GlnK-AmtB complex in response to cellular nitrogen status can occur in the absence of GlnK post-translational modification. *Front. Microbiol.* 5:731. doi: 10.3389/fmicb.2014.00731

Rappsilber, J., Mann, M., and Ishihama, Y. (2007). Protocol for micro-purification, enrichment, pre-fractionation and storage of peptides for proteomics using StageTips. *Nat. Protoc.* 2, 1896–1906. doi: 10.1038/nprot.2007.261

Rees, A. P., Woodward, E. M. S., and Joint, I. (2006). Concentrations and uptake of nitrate and ammonium in the Atlantic ocean between 60 degrees N and 50 degrees S. *Deep Sea Res. Part II Top. Stud. Oceanogr.* 53, 1649–1665. doi: 10.1016/j.dsr2.2006.05.008

Rippka, R., Deruelles, J., Waterbury, J. B., Herdman, M., and Stanier, R. Y. (1979). Generic assignments, strain histories and properties of pure cultures of cyanobacteria. *J. Gen. Microbiol.* 111, 1–61.

Romero, J. M., Lara, C., and Guerrero, M. G. (1985). Dependence of nitrate utilization upon active CO_2 fixation in *Anacystis nidulans* - a regulatory aspect of the interaction between photosynthetic carbon and nitrogen-metabolism. *Arch. Biochem. Biophys.* 237, 396–401.

Ruppert, U., IrmLer, A., Kloft, N., and Forchhammer, K. (2002). The novel protein phosphatase PphA from *Synechocystis* PCC 6803 controls dephosphorylation of the signalling protein PII. *Mol. Microbiol.* 44, 855–864.

Sakamoto, T., Inoue-Sakamoto, K., and Bryant, D. A. (1999). A novel nitrate/nitrite permease in the marine cyanobacterium *Synechococcus* sp. strain PCC 7002. *J. Bacteriol.* 181, 7363–7372.

Sato, S., Shimoda, Y., Muraki, A., Kohara, M., Nakamura, Y., and Tabata, S. (2007). A large-scale protein–protein interaction analysis in *Synechocystis* sp. PCC6803. *DNA Res.* 14, 207–216. doi: 10.1093/dnares/dsm021

Schindelin, J., Arganda-Carreras, I., Frise, E., Kaynig, V., Longair, M., Pietzsch, T., et al. (2012). Fiji: an open-source platform for biological-image analysis. *Nat. Methods* 9, 676–682. doi: 10.1038/Nmeth.2019

Schwanhausser, B., Busse, D., Li, N., Dittmar, G., Schuchhardt, J., Wolf, J., et al. (2011). Global quantification of mammalian gene expression control. *Nature* 473, 337–342. doi: 10.1038/nature10098

Selim, K. A., Haase, F., Hartmann, M. D., Hagemann, M., and Forchhammer, K. (2018). PII-like signaling protein SbtB links cAMP sensing with cyanobacterial inorganic carbon response. *Proc. Natl. Acad. Sci. U.S.A.* 115, E4861–E4869. doi: 10.1073/pnas.1803790115

Solomon, C. M., Collier, J. L., Berg, G. M., and Glibert, P. M. (2010). Role of urea in microbial metabolism in aquatic systems: a biochemical and molecular review. *Aquat. Microb. Ecol.* 59, 67–88. doi: 10.3354/ame01390

Soo, R. M., Hemp, J., Parks, D. H., Fischer, W. W., and Hugenholtz, P. (2017). On the origins of oxygenic photosynthesis and aerobic respiration in cyanobacteria. *Science* 355, 1436–1439. doi: 10.1126/science.aal3794

Spät, P., Macek, B., and Forchhammer, K. (2015). Phosphoproteome of the cyanobacterium *Synechocystis* sp PCC 6803 and its dynamics during nitrogen starvation. *Front. Microbiol.* 6:248. doi: 10.3389/fmicb.2015.00248

Sweetlove, L. J., and Fernie, A. R. (2018). The role of dynamic enzyme assemblies and substrate channelling in metabolic regulation. *Nat. Commun.* 9:2136. doi: 10.1038/s41467-018-04543-8

Valladares, A., Montesinos, M. L., Herrero, A., and Flores, E. (2002). An ABC-type, high-affinity urea permease identified in cyanobacteria. *Mol. Microbiol.* 43, 703–715. doi: 10.1046/j.1365-2958.2002.02778.x

Vegapalas, M. A., Flores, E., and Herrero, A. (1992). NtcA, a global nitrogen regulator from the cyanobacterium *Synechococcus* that belongs to the Crp family of bacterial regulators. *Mol. Microbiol.* 6, 1853–1859. doi: 10.1111/j.1365-2958.1992.tb01357.x

Vitousek, P. M., and Howarth, R. W. (1991). Nitrogen limitation on land and in the sea - how can it occur. *Biogeochemistry* 13, 87–115.

Vizcaino, J. A., Cote, R. G., Csordas, A., Dianes, J. A., Fabregat, A., Foster, J. M., et al. (2013). The proteomics identifications (PRIDE) database and associated tools: status in 2013. *Nucleic Acids Res.* 41, D1063–D1069. doi: 10.1093/nar/gks1262

Vogel, A. I., Furniss, B. S., and Vogel, A. I. (1989). *Vogel's Textbook of Practical Organic Chemistry*. New York, NY: Longman Scientific & Technical.

Watzer, B., Engelbrecht, A., Hauf, W., Stahl, M., Maldener, I., and Forchhammer, K. (2015). Metabolic pathway engineering using the central signal processor PII. *Microb. Cell Fact.* 14:192. doi: 10.1186/s12934-015-0384-4

Watzer, B., and Forchhammer, K. (2018). Cyanophycin synthesis optimizes nitrogen utilization in the unicellular cyanobacterium *Synechocystis* sp. PCC 6803. *Appl. Environ. Microbiol.* 84:e01298-18. doi: 10.1128/AEM.01298-18

Whitton, B. A. (2012). *Ecology of Cyanobacteria II: Their Diversity in Space and Time*. New York, NY: Springer.

Wirén, N. V., and Merrick, M. (2004). "Regulation and function of ammonium carriers in bacteria, fungi, and plants," in *Molecular Mechanisms Controlling Transmembrane Transport*, eds E. Boles and R. Krämer (Berlin: Springer), 95–120.

Xu, Y. B., Carr, P. D., Clancy, P., Garcia-Dominguez, M., Forchhammer, K., Florencio, F., et al. (2003). The structures of the PII proteins from the cyanobacteria *Synechococcus* sp PCC 7942 and *Synechocystis* sp. PCC 6803. *Acta Crystallogr. D Biol. Crystallogr.* 59(Pt 12), 2183–2190. doi: 10.1107/S0907444903019589

Zeth, K., Fokina, O., and Forchhammer, K. (2014). Structural basis and target-specific modulation of ADP sensing by the *Synechococcus elongatus* PII signaling protein. *J. Biol. Chem.* 289, 8960–8972. doi: 10.1074/jbc.M113.536557

Zhao, M. X., Jiang, Y. L., Xu, B. Y., Chen, Y., Zhang, C. C., and Zhou, C. Z. (2010). Crystal structure of the cyanobacterial signal transduction protein PII in complex with PipX. *J. Mol. Biol.* 402, 552–559. doi: 10.1016/j.jmb.2010.08.006

Conflict of Interest Statement: The authors declare that the research was conducted in the absence of any commercial or financial relationships that could be construed as a potential conflict of interest.

3. Accepted publication

M. Koch, K. Forchhammer (2020)

Storage polymers in cyanobacteria: friend or foe?

Cyanobacteria biotechnology, Wiley (book chapter)

Cyanobacterial biopolymers

Certain cyanobacteria, especially the model organism *Synechocystis* sp. PCC 6803, have the ability to produce a wide variety of different biopolymers. Among them are PHB (polyhydroxybutyrate), cyanophycin, polyphosphate and glycogen. Although all of them have a unique physiological function, only two of them, namely PHB and cyanophycin, are of current biotechnological relevance. In this chapter, we will focus mostly on these two biopolymers, their biosynthesis as well as their (potential) industrial applications.

PHB

Introduction

The fact that cyanobacteria produce poly-hydroxy-butyrate (PHB) is known for more than 50 years (Carr, 1966). PHB is a polyester, consisting of chains of 3-hydroxy-butyrate. Within the last century, PHB gained only little attention. This changed recently, due to two of humanities biggest ecological crises: the global pollution of our oceans with plastic waste (Li et al., 2016) as well as climate change, caused by the emission of greenhouse gases (Carleton and Hsiang, 2016). For both of these fundamental, life-threatening problems, PHB produced from cyanobacteria could contribute towards a sustainable solution (Koller, 2017). While cyanobacteria grow, they sequester CO_2 from the atmosphere, which they may convert into PHB (Dutt and Srivastava, 2018). The latter can then be used as a sustainable substitute for petroleum-based plastics, since it has comparable material properties and shows a good biodegradability (Narancic et al., 2018), hence not contributing to the pollution problem. These are also the main advantages compared to currently available bioplastics on the market, like poly-lactic-acid (PLA). Although PLA is also produced from biological resources, most of them are potential food sources (like corn), resulting in an ethical dilemma. Additionally, the biodegradability of PLA is limited, especially in marine environments (Narancic et al., 2018, Napper and Thompson, 2019). PHB has the potential to overcome all these shortcomings (Figure 1).

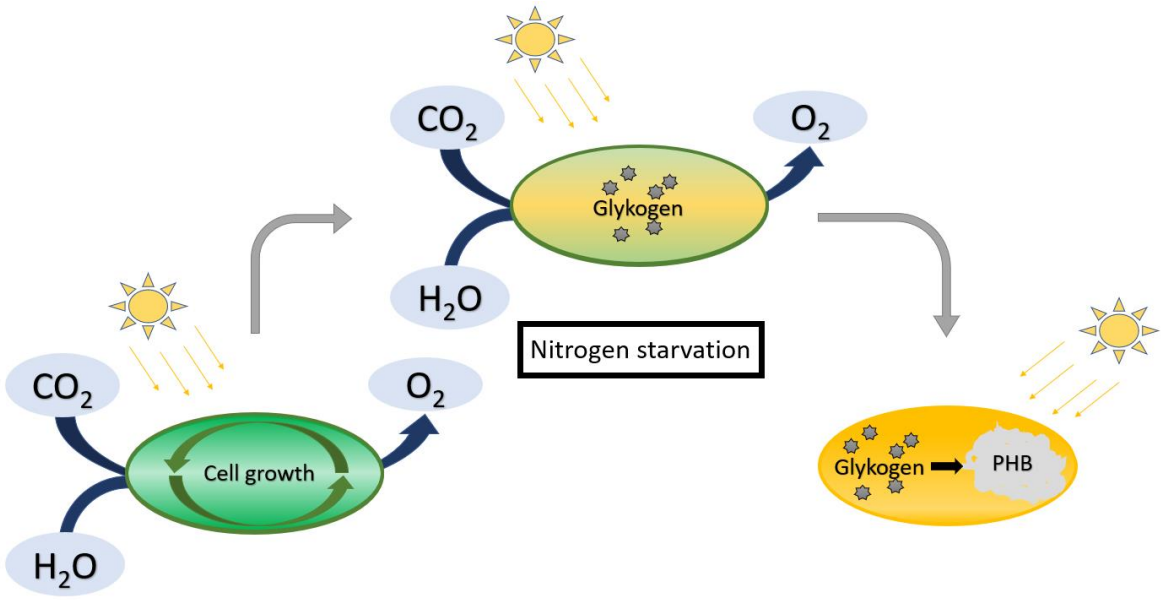

Figure 1. General idea of producing poly-hydroxy-butyrate (PHB) in cyanobacterial cells. Cyanobacteria take up CO_2 and H_2O during growth and convert it to biomass and O_2. As they are able to growth photosynthetically, sunlight is used as sole energy source. During nitrogen starvation, their metabolism changes. The cells start to build up glycogen, from where PHB is formed.

The increasing interest in cyanobacterial PHB resulted in numerous, recently published reviews (Vieira et al., 2018, Kamravamanesh et al., 2018, Katayama et al., 2018, Koller, 2017, Singh and Mallick, 2017). While PHB is naturally occurring in many different cyanobacterial species, this chapter will mainly focus on two strains, *Synechocystis* sp. PCC 6803 and *Synechococcus* sp. (hereafter "*Synechocystis*" and "*Synechococcus*", respectively). Both are well studied model organisms for the investigation of photosynthesis and cyanobacterial physiology. Hence, most studies regarding the production of PHB were conducted in their background. The aim of this chapter is to provide a comprehensive overview about the current knowledge on PHB production in cyanobacteria so far.

PHB metabolism in cyanobacteria

Many different cyanobacterial strains have been screened for their natural ability to produce PHB under different conditions (Ansari and Fatma, 2016). Several recent reviews summarized elaborately all strains which were investigated so far (Singh and Mallick, 2017, Kamravamanesh et al., 2018).

Although the formation of PHB in cyanobacteria is well known, many aspects of its metabolism, including its precise physiological function, remain unknown. Recent studies revealed that in cyanobacteria, PHB is not a primary storage polymer for carbon and energy (Klotz et al., 2016, Damrow et al., 2016). PHB is mainly produced during conditions of unbalanced nutrient availability, especially during an excess of carbon and a limitation of other macronutrients, like nitrogen, phosphate or potassium (Hauf et al., 2013). Especially the adaptation to nitrogen starvation, a process called chlorosis, is intensively studied during the past years (Gorl et al., 1998, Forchhammer and Schwarz, 2019). Herein, non-diazotrophic cyanobacteria undergo a transition into a resting state, which helps them to survive conditions

of nutrient limitation for long time periods (Klotz et al., 2016). Within the first day after onset of starvation, *Synechocystis* cells accumulate large quantities of glycogen (up to 60% per cell dry weight)(Klotz et al., 2016). Simultaneously, the cells start to degrade their photosynthetic machinery, including phycobilisome proteins and chlorophyll (Collier and Grossman, 1992). Over the next days, the colour of the cultures changes from intense blue-green to pale yellow (Allen and Smith, 1969). During this time, *Synechocystis* steadily builds up PHB, while glycogen is slowly getting degraded (Koch et al., 2019). The resulting chlorotic cells, which underwent a growth arrest, are able to survive prolonged time of nitrogen limitation (Doello et al., 2018). Interestingly, this process is completely reversible. Upon the addition of nitrogen, *Synechocystis* cells are able to fully recover and start exponential growth within the course of two days (Doello et al., 2018, Klotz et al., 2016). Until today, the induction of chlorosis by depleting nitrogen or phosphate, is the most commonly applied strategy to induce PHB production in cyanobacteria.

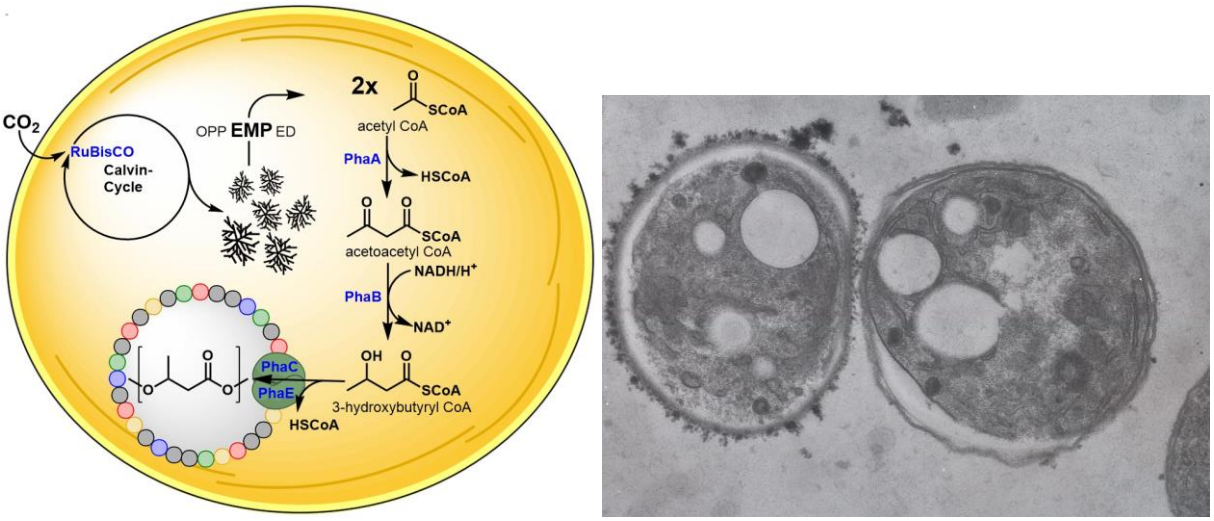

Figure 2. Left: PHB metabolism in Synechocystis. During chlorosis, CO_2 is taken up and stored in the form of glycogen. From there, glucose monomers are split off and further catabolized, mainly via the Embden-Meyerhof-Parnas (EMP) pathway, to acetyl-CoA. Two units of acetyl-CoA are then further processed by enzymatic reactions of PhaA, PhaB and PhaEC, resulting in the formation of PHB granules. Right: TEM picture of chlorotic Synechocystis cells after 3 weeks of nitrogen starvation. PHB granules are visible as white encapsulations within the cell.

Metabolically, the production of PHB starts with the uptake of CO_2, usually in the form of bicarbonate (Figure 2). During chlorosis, the carbon is first stored in the form of glycogen, from where it is gradually released and catabolized to PHB (Koch et al., 2019). This agrees with a study by Dutt et al., showing that PHB is produced by 74 % from intracellular carbon sources (Dutt and Srivastava, 2018). However, ongoing carbon fixation, even during chlorosis, still contributes to PHB (Dutt and Srivastava, 2018). The addition of organic carbon sources, such as acetate or fructose, can significantly spike the PHB production (Panda and Mallick, 2007).

Once the carbon has reached the acetyl-CoA pool, a β-ketothiolase (PhaA, encoded by *slr1993*) condenses two units of it into acetoacetyl-CoA. The latter is subsequently reduced by an acetoacetyl-CoA reductase (PhaB, *slr1994*) to form 3-hydroxy-butyrate, while oxidizing NADPH to $NADP^+$ (Taroncher-Oldenburg et al., 2000). Finally, a two-subunit PHA synthase, composed

of PhaC (*slr1830*) and PhaE (*slr1829*), polymerizes 3-hydroxybutyryl-CoA to a PHB polymer (Hein et al., 1998). It has been shown by Zhang et al., that FabG, which is the first NADPH-dependent reductase in the fatty acid biosynthesis pathway, can catalyse the same reaction as PhaB (Zhang et al., 2017). However, the physiological importance of this reaction seems to be rather small. Other organisms, like *Pseudomonas aeruginosa*, use other pathways, where 3-hydroxyacyl-ACP is converted to 3-hydroxyacl-CoA via the enzyme PhaG (Hoffmann et al., 2000). As a result, the latter enzyme connects PHB synthesis with fatty acid anabolism. In contrast to that, PhaJ, which catalyses the reaction from enoyl-CoA to 3-hydroxyacyl-CoA, links PHB metabolism with fatty acid catabolism (β -oxidation) (Reiser et al., 2000). Although these pathways have not been found in *Synechocystis,* they are potential routes to further increase the pool of PHB precursors (Philip et al., 2007). For an overview, Lu *et al*. have summarized PHA pathways present in different bacteria (Lu et al., 2009). A simplified overview is given in Figure 3.

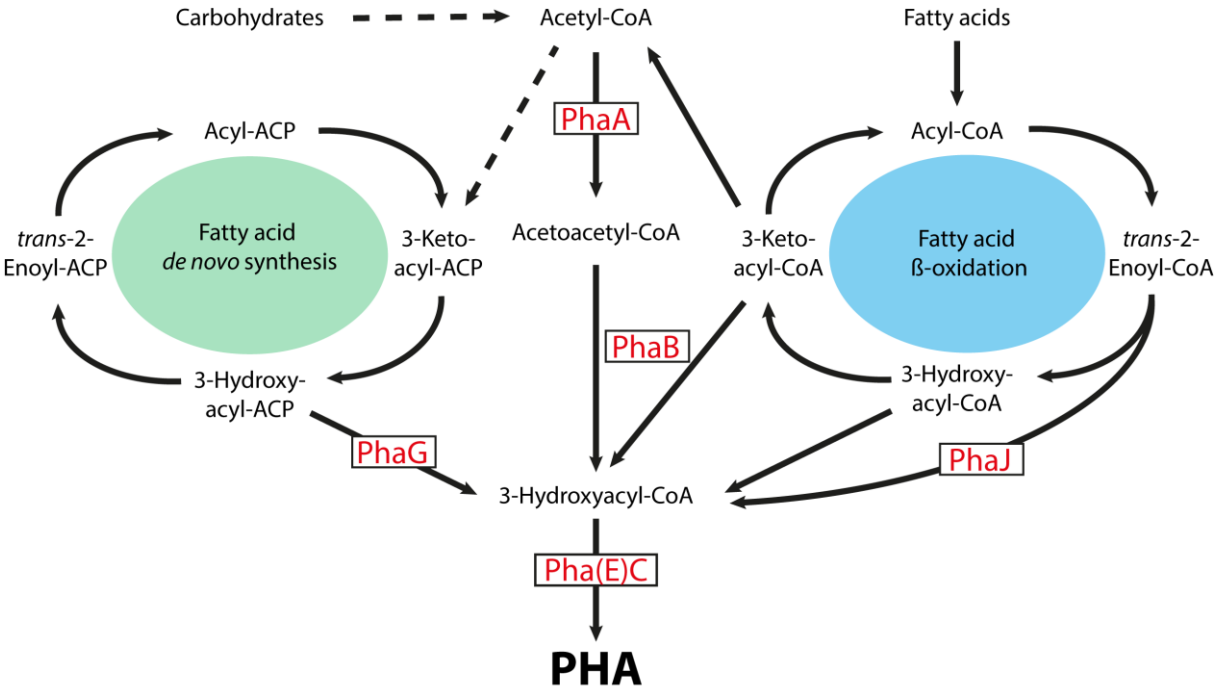

Figure 3. Potential PHA synthesis routes known from different organisms. The carbon can be derived from fatty acid synthesis (green) or degradation (blue) or carbohydrates. The most important enzymes are marked in red. Abbreviations: PhaA, 3-ketothiolase; PhaB - acetoacetyl-CoA reductase; PhaC - PHA polymerase (in Synechocystis the heterodimer PhaEC); PhaG, 3-hydroxyacyl ACP:CoA transacylase; PhaJ - enoyl-CoA hydratase (modified from (Aldor and Keasling, 2003).

Besides the mentioned enzymes PhaA, PhaB and PhaEC, other proteins, which are not directly involved in PHB metabolism, play important roles for the formation of PHB granules. One example is PhaP, a recently discovered protein, belonging to the group of phasins. It forms an outer layer, surrounding the PHB granules and thereby regulating their volume to size ratio (Hauf et al., 2015). Still, fundamental enzymes remain unknown. For example, any PHB degrading enzymes, like a PHB depolymerase (*phaZ*), have not been identified yet.

Besides this, the true physiological function of PHB in *Synechocystis* is still puzzling. Unlike in other organisms, where PHB serves mainly as a storage polymer for carbon and energy, no

growth disadvantage is visible when mutants deficient in PHB synthesis (such as Δ*phaEC* mutants) recover from nitrogen starvation (Damrow et al., 2016). It is known from literature, that PHB can serve various functions, besides being a storage polymer (Jendrossek and Pfeiffer, 2014, Slaninova et al., 2018, Batista et al., 2018, Nowroth et al., 2016). Further investigation is needed to better understand the physiological functions of PHB in cyanobacteria. This knowledge will help to further optimize cyanobacterial strains for industrial production of PHB.

Industrial application

Background

Nowadays, most industrially produced PHB comes from heterotrophic bacteria, like *Cupriavidus necator*. This organism comes with many advantages, as it is fast growing and shows high production rates of PHB (~90% / CDW) (Anderson and Dawes, 1990). However, one of its limitations is the large quantity of organic carbon source, which *C. necator* requires (Reis et al., 2003, Mudliar et al., 2007). Additionally, these organic carbon sources are usually produced from plants like maize, which requires valuable cropland. Especially in the future, when the degradation of arable farm land is progressing due to climate change, using food crops for the production of plastics would become more of an ethical problem (Harding et al., 2007, Issa et al., 2019, Posen et al., 2016). Hence, a more sustainable way of producing PHB, especially on a large scale, is urgently needed. As cyanobacteria could be helpful organisms to achieve this goal, their potential and obstacles for an industrial production of PHB are described in the following sub-chapters.

Physical properties of PHB and its derivates

PHB is a polymer consisting of 3-hydroxybutyryl-CoA monomers which are connected via an ester bondage (Rajan et al., 2017). It belongs to the group of polyhydroxy-alkanoates (PHA). PHB monomers are composed out of four carbon atoms, while other PHAs contain longer chain lengths (Anderson and Dawes, 1990). This drastically changes their physical properties. While PHB is rather brittle and not flexible, an elongation of the carbon chain from four to five (poly-hydroxy-valerate, PHV) or six (poly-hydroxy-hexanoate, PHH) carbon atoms creates much more flexible polymers with increased elongation properties (Steinbüchel, 1992). Depending on the length of the monomers, they are classified as short, medium or long-chain length PHAs. From an industrial point of view, a copolymer is desirable, as it combines the properties of the different monomers (Verhoogt et al., 1994). There have been various successful attempts to produce these co-polymers, like poly(3-hydroxybutyrate-co-3-hydroxyhexanoate), in heterotrophic bacteria (Park et al., 2005). Some of these co-polymers combine good tensile strength with sufficient elongation properties, while still having a good biodegradability (Noda et al., 2009). Their function can be further modified by the inclusion of aromatic PHAs (Ishii-Hyakutake et al., 2018). Since *Synechocystis* is harbouring a class III PHA polymerase, it is only able to produce short-chain-length PHAs though (Hein et al., 1998). *Synechococcus* sp*.,* on the other hand, is not a naturel producer of PHAs.

Biodegradability

Several studies have investigated the biodegradability of various kinds of bioplastics. It turned out that PHB and its variants in general harbour a better biodegradability than many other bioplastics, like PLA (Narancic et al., 2018). From an environmental point of view, the

ecological footprint of plastics can be further improved if the product is recyclable (Rujnić-Sokele and Pilipović, 2017). However, there are still many obstacles to overcome. One example is the similar weight and density of bioplastics and petroleum-based plastics, which hampers the sorting and separation process. In a marine and soil environment, PHB shows good biodegradability properties (Narancic et al., 2018). When kept under aerobic conditions, it decomposes to CO_2 and H_2O. However, under anaerobic conditions, CH_4 and CO_2 is formed instead (Vieira et al., 2018). Since CH_4 is a potent greenhouse gas, a controlled degradation is required to avoid the emission of undesirable products. Depending on the composition of the co-polymers, the degradation times also vary (Narancic et al., 2018). However, so far, the production in cyanobacteria focused mostly on PHB and neglected other PHAs or copolymers.

Application of PHB as plastic

There have been many potential applications proposed for PHB based plastics (Albuquerque and Malafaia, 2018). As the monomers D-3-hydroxybutyrate is part of the human blood, PHB shows good biocompatibility. This makes PHB an interesting raw material for the production of medical products, such as nanofibers or biocompatible implants (Luef et al., 2015). Another application of PHB includes the usage in agriculture, where it can be used for the production of agricultural foil. Due to its good biodegradability, the foil can be left behind on the field or ploughed into the soil.

The great advantage of PHB over other (bio-) plastics is its potential to be produced carbon neutral, as well as its good biodegradability. These advantages would be more relevant for the production of bulk chemicals, such as a possible substitute for conventional plastics for packaging. The total global production of plastics is estimated be more than 8300 million metric tons, from which the majority is used for packaging (Geyer et al., 2017). This shows the great potential of a carbon neutral bioplastic. However, so far bioplastics contribute only for about 2% to the global plastic market, from which 1.4% are PHAs in the European union (European-Bioplastics, 2018). The main obstacle to overcome are the high production costs of PHAs, which limits the potential to contribute a bigger part to the global plastic market.

Reactor types

To further increase the production yield of PHB and thereby decrease its price, effective reactor designs for cyanobacteria are required. So far, only very few attempts of medium size reactors have been constructed, while the feasibility of a large scale photobioreactor still needs to be demonstrated. To the best of our knowledge, the largest attempt so far has been constructed by the group around Troschl *et al.* (Troschl et al., 2017). With a total volume of 200 l, they have demonstrated the production of PHB in a larger photobioreactor. To further increase the production, the reactor was coupled to the chimney of a coal power plant, providing flue gas with increased CO_2 concentrations. Although production rates were with 9% / CDW rather low, other promising approaches have been introduced recently. One example is the “Christmas tree bioreactor”, which has been developed by the company GICON (GICON, 2019). This new reactor design allows for an overall usable volume of more than 1,000 l per reactor. However, its efficiency, especially regarding its production of PHB, needs to be demonstrated. Besides new reactor designs, alternative growth conditions promise high production rates. One example are mixed cultures, where a cyanobacterial strain is cultured together with another heterotrophic growing bacteria (Hoschek et al., 2019, Weiss et al.,

2017). In a similar approach, *Synechococcus* and *Pseudomonas putida* were cocultured, with the idea that the cyanobacterial strain fixes CO_2 and secretes it as sucrose. The latter can then be taken up by the heterotrophic strain, which converts the sugar into PHB. However, so far such approaches resulted in rather low yields (Löwe et al., 2017). Although there are many promising approaches how to culture cyanobacterial production of PHB, the production in a larger scale photobioreactors still has to be demonstrated.

The largest reactors used for microalgae cultivation so far have been open raceway ponds (Costa and de Morais, 2014). They are commonly used for the cultivation of *Spirulina* as a food supplement. The main disadvantages of open raceway ponds are difficulties to control growth parameters, such as pH, temperature and contaminations. On the other hand, they come with low construction costs and can easily be scaled up to larger volumes. In an economic comparison, Richardson *et al.* showed that open raceway ponds are more economical feasible than photobioreactors (Richardson et al., 2012).

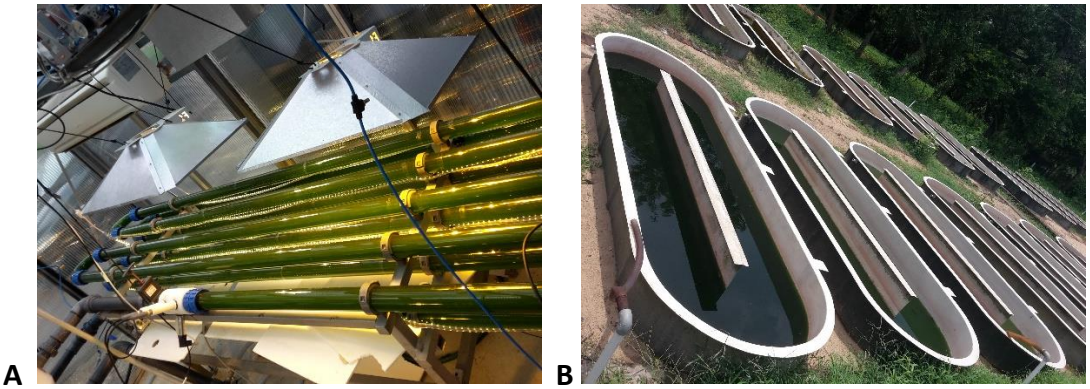

Figure 4. Examples for different reactor types. A) 200 l pilot plant for the production of PHB in cyanobacteria (Tulln, Austria). B) An open pond reactor for the production of cyanobacteria (Kharagpur, India).

Production process

Since PHB production is induced by depleting the cultivation medium (commonly BG_{11} is used) from one of the macronutrients nitrogen, phosphate or potassium (Panda and Mallick, 2007), cultures have to be shifted to nutrient –depleted medium This can either be done by centrifuging the bacterial culture and exchanging the medium. Alternatively, self-limitation occurs once cyanobacteria consumed all the available nitrogen in the medium (Kamravamanesh et al., 2017).

Besides the limitation of important nutrients, PHB production can be further increased by the addition of organic carbon sources, such as acetate (Panda et al., 2006). Although this yields in a significantly increase in PHB, acetate is a costly component, which increases the overall production costs. This could be overcome by using wastewater, such as sewage. The latter can have high contents of organic substances, which could be converted intracellularly into PHB. However, most studies about cyanobacterial cultivation in waste water showed only slow growth rates and limited PHB production (Samantaray et al., 2011, Panda et al., 2006).

Besides alterations of the media composition, there has been reports that the limitation of gas exchange further increased the overall yield of PHB (Panda and Mallick, 2007). In contrary to this study, Kamravamanesh *et al.* have detected a reduction of PHB production when they applied gas exchange limitation to Synechocystis sp. PCC 6714 (Kamravamanesh et al., 2017). To the best of our knowledge, this has not been tested on a larger scale reactor though. Other important factors are the adjustment of the pH, nutrients, temperature, CO_2 availability as well as light intensity (Panda et al., 2006, Esteves-Ferreira et al., 2017, van Alphen et al., 2018). While all these conditions can easily be adjusted in a controlled photobioreactor, they are challenging when open pond cultivation is considered. It is known, that an increased availability of light and CO_2 can boost cyanobacterial growth (Esteves-Ferreira et al., 2017). For example, the strain *Synechococcus elongatus* UTEX 2973 has a doubling time of only 1.9 hours when grown at 41°C under continuous 500 µmoles photons m^{-2} s^{-1} light with 3% CO_2 (Yu et al., 2015). At the same time, the supply of temperature, light and CO_2 is an additional cost factor. A potential solution could be the cultivation in countries, which have a higher overall temperature and light intensity. For example, the production of the cyanobacterium *Spirulina* sp. as a food supplement is produced in southern India (Figure 5 A). To increase the concentration of CO_2 while at the same time sequestering it from the atmosphere, flue gas from nearby powerplants can be used (Figure 5 B) (Troschl et al., 2017, Acién et al., 2012).

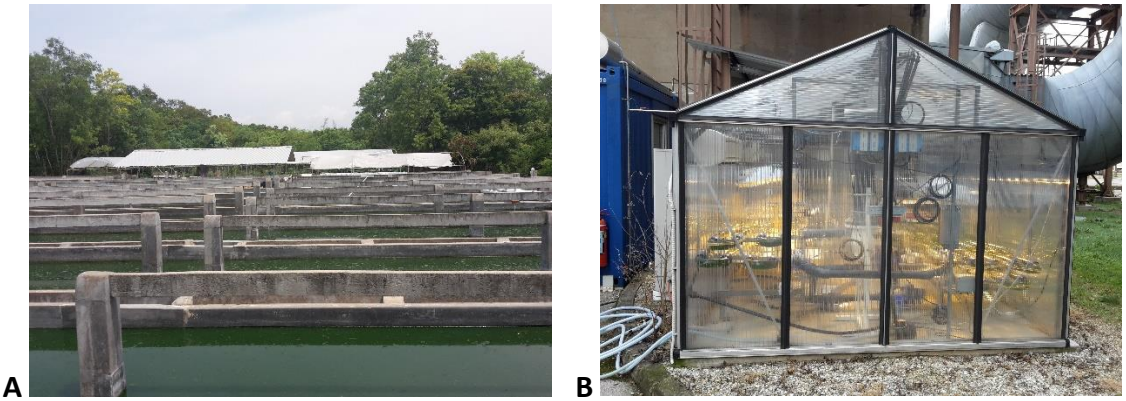

*Figure 5 (**A**) Open cultivation of Spirulina in Auroville, India. (**B**) Greenhouse in Tulln, Austria. It is located next to a coal power station, from where some of the exhaust is used to provide CO_2 to the cyanobacterial cultures.*

Overall, for many strain-optimization-approaches it remains challenging to either adapt the strain to optimal conditions, like they are present in a controlled bioreactor. In contrast to that, the requirements for strains and cultivation conditions for a large-scale incubation, such as an open racing pond, differ strongly. It is hence questionable, if the attempts to further optimize strains and conditions should focus on the highest efficiency possible in an artificial surrounding. Alternatively, adapting strains to simpler conditions, like they are present during outside cultivation, would be relevant.

Downstream processing

The purification of PHB from cyanobacteria remains a challenging task and is a relevant cost factor (Singh and Mallick, 2017). To purify PHB, cell disruption and pigment extraction are

required. There are different ways of cell disruption, including enzymatic or mechanical extraction, like milling. Solvent extraction can be performed in chloroform, ethanol, acetone or ethylene (Gangurde and Sayyed, 2012). Pigment extraction is necessary to achieve PHB in processable quality (Meixner et al., 2018). Detection of PHB is usually done with HPLC or GC (Kadiyala, 2014).

Metabolic engineering

While PHB represents an interesting biotechnological product, certain metabolic engineering strategies intend to reroute the metabolic fluxes away from PHB to other desired products (Grundel et al., 2012, Xie et al., 2011, Namakoshi et al., 2016). In this case it is a common approach to delete the PHB synthesis genes, *phaEC*, and thereby eliminate PHB production. Since a ΔPHB mutant shows no growth phenotype, this has no negative consequences, while at the same time production rates of other products can be increased (Damrow et al., 2016). However, many metabolic engineering strategies have been applied to further increase the PHB production. The most relevant ones are described in the following.

Alternative pathways

As already mentioned in the paragraph 'PHB metabolism in cyanobacteria' above, *Syenchocystis* operates just one pathway towards PHB, which is via acetyl-CoA. However, there are further metabolic routes known in other organisms. One strategy to boost PHB production is by increasing the amount of precursors, as in the form of acetyl-CoA. One approach was the introduction of a phosphoketolase pathway, as shown by Carpine *et al*. (Carpine et al., 2017). The phosphoketolase Xfpk from *Bifidobacterium breve* converts xylose 5-P or fructose 6-P into acetyl-P and glyceraldehyde 3-P, which can be further converted to acetyl-CoA. They reported a PHB content of 12% / CDW (Carpine et al., 2017). For the production of PHAs with longer chain length, the introduction of pathways, which produce longer precursors, could be helpful. One option represents the gene *phaG*, which connects the fatty acid biosynthesis with PHB production. To the best of our knowledge, this possibility has not been tested so far. It has recently been shown that the amount of reduction equivalents in the form of NADPH restricts the PHB production (Hauf et al., 2013). Hence, increasing the amount of NADPH could further boost the amount of intracellular PHB.

Furthermore, coupling the production of PHB with growth could be desirable. This would avoid the necessity to transfer the culture to nitrogen depleted medium. So far, there have only been very limited attempts to achieve this goal. One example is the overexpression of the native *phaAB* genes in *Synechocystis*, which resulted in a production of 9% / CDW, even under growth in BG_{11}(Khetkorn et al., 2016).

Genetical engineering

Besides introducing pathways to provide more PHB precursors, several other strategies have been applied to genetically alter *Synechocystis.* Detailed lists about created strains and their produced yield have been previously reviewed in several publications (Kamravamanesh et al., 2018, Singh and Mallick, 2017, Vieira et al., 2018).

The most common approach was to overexpress native or heterologous PHB synthesis genes (Khetkorn et al., 2016, Hondo et al., 2015, Takahashi et al., 1998, Sudesh et al., 2002). Often the genes *phaABC* of *Cupriavidus necator* were uses, since this strain can natively reach values of up to 80% PHB / CDW. These genes were then coupled to strong promotors, like psbA2, which originally sits in front of the D1 protein of the Photosystem II and shows very high expression levels (Khetkorn et al., 2016, Englund et al., 2016).

Another interesting approach has been suggested by Osanai *et al*., when they overexpressed the response regulator *rre37* (Osanai et al., 2014). This caused an acceleration of the glycogen catabolism. As shown recently (Hauf et al., 2013), the intracellular pools of PHB and glycogen are connected (Koch et al., 2019). Hence, a degradation of the latter causes an increase of the former. A similar effect was observed when the sigma factor *sigE* was overexpressed (Osanai et al., 2013). Again, an increase of glycogen degradation and PHB synthesis genes was observed, leading to higher overall values of PHB. However, the effects of upregulated glycogen/PHB metabolism genes appeared to be rather transient, since they are changing during the course of chlorosis (Nakaya et al., 2015).

With the emergence of new technologies, genetic alterations could be achieved even faster. The discovery of CRISPR Cas allows markerless genome editing (Wendt et al., 2016), while CRISPRi allows to specifically tune down the gene expression (Yao et al., 2016). However, the efficiency of this relatively new technique has to be further optimized (Behler et al., 2018, Ungerer and Pakrasi, 2016).

Some of the highest intracellular PHB values have been achieved in a random mutagenesis approach. By applying UV light, random mutations were introduced, which were then screened for strains with high PHB production rates (Kamrava et al., 2018). In one of these screenings, a mutant was discovered which produces 2.5 more PHB compared to the WT.

Conclusions and outlook

Limitations

PHB production in cyanobacteria has come a long way. However, there are still many obstacles, which have to be overcome to produce PHB for a compatible price. Still, the overall yield of PHB is too low, especially compared to heterotrophic bacteria (Kamravamanesh et al., 2018). Additionally, a slow growth rate further limits the final yield and production rate. While heterotrophic bacteria are able to produce PHB during exponential growth, cyanobacteria are

limited to a production during nutrient limited conditions. Uncoupling these two mechanisms could further boost the production rates. Finally, extraction of PHB from the cells remains challenging, due to their high pigment content (Ansari and Fatma, 2016).

Potential

To overcome these challenges, a combination of different strategies could be applied. For example, intracellular fluxes have to be further optimized to convert more carbon towards PHB. For this, systems biology provides helpful tools (Sarkar et al., 2019, Janasch et al., 2018). Controlling the flux from glycogen to the PHB pool represent promising opportunities (Dutt and Srivastava, 2018). Applying such strategies to filamentous cyanobacteria may help to generate strains, which facilitate downstream processing. In particular, cells, which are easy to separate from the medium are desirable, because harvesting of the cells requires large amounts of energy (Monshupanee et al., 2016, Singh and Mallick, 2017).

In order to make the cyanobacterial production of PHB more feasible, downstream processes, where also other side-products would be commercialized, like phycocyanin, have to be developed (Meixner et al., 2018). Furthermore, a combination of efficient production strains with state of the art photobioreactors have to be tested. As a next step, the upscaling of such a process will be necessary to demonstrate feasibility also on a large scale. Finally, more research in the field of life cycle assessment is required to completely understand the environmental impact of cyanobacterial bioplastics.

Liste

Uncategorized References

ACIÉN, F. G., FERNÁNDEZ, J. M., MAGÁN, J. J. & MOLINA, E. 2012. Production cost of a real microalgae production plant and strategies to reduce it. *Biotechnology Advances,* 30**,** 1344-1353.

ALBUQUERQUE, P. B. S. & MALAFAIA, C. B. 2018. Perspectives on the production, structural characteristics and potential applications of bioplastics derived from polyhydroxyalkanoates. *Int J Biol Macromol,* 107**,** 615-625.

ALDOR, I. S. & KEASLING, J. D. 2003. Process design for microbial plastic factories: metabolic engineering of polyhydroxyalkanoates. *Current Opinion in Biotechnology,* 14**,** 475-483.

ALLEN, M. M. & SMITH, A. J. 1969. Nitrogen chlorosis in blue-green algae. *Arch Mikrobiol,* 69**,** 114-20.

ANDERSON, A. J. & DAWES, E. A. 1990. Occurrence, Metabolism, Metabolic Role, and Industrial Uses of Bacterial Polyhydroxyalkanoates. *Microbiological Reviews,* 54**,** 450-472.

ANSARI, S. & FATMA, T. 2016. Cyanobacterial Polyhydroxybutyrate (PHB): Screening, Optimization and Characterization. *Plos One,* 11.

BATISTA, M. B., TEIXEIRA, C. S., SFEIR, M. Z. T., ALVES, L. P. S., VALDAMERI, G., PEDROSA, F. O., SASSAKI, G. L., STEFFENS, M. B. R., DE SOUZA, E. M., DIXON, R. & MULLER-SANTOS, M. 2018. PHB Biosynthesis Counteracts Redox Stress in Herbaspirillum seropedicae. *Front Microbiol,* 9**,** 472.

BEHLER, J., VIJAY, D., HESS, W. R. & AKHTAR, M. K. 2018. CRISPR-Based Technologies for Metabolic Engineering in Cyanobacteria. *Trends in Biotechnology,* 36**,** 996-1010.

CARLETON, T. A. & HSIANG, S. M. 2016. Social and economic impacts of climate. *Science,* 353**,** aad9837.

CARPINE, R., DU, W., OLIVIERI, G., POLLIO, A., HELLINGWERF, K. J., MARZOCCHELLA, A. & BRANCO DOS SANTOS, F. 2017. Genetic engineering of Synechocystis sp. PCC6803 for poly-β-hydroxybutyrate overproduction. *Algal Research,* 25**,** 117-127.

CARR, N. G. 1966. The occurrence of poly-beta-hydroxybutyrate in the blue-green alga, Chlorogloea fritschii. *Biochim Biophys Acta,* 120**,** 308-10.

COLLIER, J. L. & GROSSMAN, A. R. 1992. Chlorosis induced by nutrient deprivation in Synechococcus sp. strain PCC 7942: not all bleaching is the same. *J Bacteriol,* 174**,** 4718-26.

COSTA, J. A. V. & DE MORAIS, M. G. 2014. Chapter 1 - An Open Pond System for Microalgal Cultivation. *In:* PANDEY, A., LEE, D.-J., CHISTI, Y. & SOCCOL, C. R. (eds.) *Biofuels from Algae.* Amsterdam: Elsevier.

DAMROW, R., MALDENER, I. & ZILLIGES, Y. 2016. The Multiple Functions of Common Microbial Carbon Polymers, Glycogen and PHB, during Stress Responses in the Non-Diazotrophic Cyanobacterium Synechocystis sp. PCC 6803. *Front Microbiol,* 7**,** 966.

DOELLO, S., KLOTZ, A., MAKOWKA, A., GUTEKUNST, K. & FORCHHAMMER, K. 2018. A Specific Glycogen Mobilization Strategy Enables Rapid Awakening of Dormant Cyanobacteria from Chlorosis. *Plant Physiol,* 177**,** 594-603.

DUTT, V. & SRIVASTAVA, S. 2018. Novel quantitative insights into carbon sources for synthesis of poly hydroxybutyrate in Synechocystis PCC 6803. *Photosynth Res,* 136**,** 303-314.

ENGLUND, E., LIANG, F. & LINDBERG, P. 2016. Evaluation of promoters and ribosome binding sites for biotechnological applications in the unicellular cyanobacterium Synechocystis sp. PCC 6803. *Scientific Reports,* 6**,** 36640.

ESTEVES-FERREIRA, A. A., INABA, M., OBATA, T., FORT, A., FLEMING, G. T. A., ARAÚJO, W. L., FERNIE, A. R. & SULPICE, R. 2017. A Novel Mechanism, Linked to Cell Density, Largely Controls Cell Division in Synechocystis. *Plant Physiology,* 174**,** 2166-2182.

EUROPEAN-BIOPLASTICS 2018. Bioplastics market data.

FORCHHAMMER, K. & SCHWARZ, R. 2019. Nitrogen chlorosis in unicellular cyanobacteria – a developmental program for surviving nitrogen deprivation. *Environmental Microbiology,* 21**,** 1173-1184.

GANGURDE, D. N. & SAYYED, R. 2012. Poly-β-hydroxybutyrate (PhB): a Biodegradable Polymer of microbial origin.

GEYER, R., JAMBECK, J. R. & LAW, K. L. 2017. Production, use, and fate of all plastics ever made. *Science Advances,* 3**,** e1700782.

GICON 2019. Kultivierung von Mikroalgen.

GORL, M., SAUER, J., BAIER, T. & FORCHHAMMER, K. 1998. Nitrogen-starvation-induced chlorosis in Synechococcus PCC 7942: adaptation to long-term survival. *Microbiology,* 144 (Pt 9)**,** 2449-58.

GRUNDEL, M., SCHEUNEMANN, R., LOCKAU, W. & ZILLIGES, Y. 2012. Impaired glycogen synthesis causes metabolic overflow reactions and affects stress responses in the cyanobacterium Synechocystis sp. PCC 6803. *Microbiology,* 158**,** 3032-43.

HARDING, K. G., DENNIS, J. S., VON BLOTTNITZ, H. & HARRISON, S. T. L. 2007. Environmental analysis of plastic production processes: Comparing petroleum-based polypropylene and polyethylene with biologically-based poly-β-hydroxybutyric acid using life cycle analysis. *Journal of Biotechnology,* 130**,** 57-66.

HAUF, W., SCHLEBUSCH, M., HUGE, J., KOPKA, J., HAGEMANN, M. & FORCHHAMMER, K. 2013. Metabolic Changes in Synechocystis PCC6803 upon Nitrogen-Starvation: Excess NADPH Sustains Polyhydroxybutyrate Accumulation. *Metabolites,* 3**,** 101-18.

HAUF, W., WATZER, B., ROOS, N., KLOTZ, A. & FORCHHAMMER, K. 2015. Photoautotrophic Polyhydroxybutyrate Granule Formation Is Regulated by Cyanobacterial Phasin PhaP in Synechocystis sp. Strain PCC 6803. *Appl Environ Microbiol,* 81**,** 4411-22.

HEIN, S., TRAN, H. & STEINBÜCHEL, A. 1998. Synechocystis sp. PCC6803 possesses a two-component polyhydroxyalkanoic acid synthase similar to that of anoxygenic purple sulfur bacteria. *Archives of Microbiology,* 170**,** 162-170.

HOFFMANN, N., STEINBÜCHEL, A. & REHM, B. H. A. 2000. The Pseudomonas aeruginosa phaG gene product is involved in the synthesis of polyhydroxyalkanoic acid consisting of medium-chain-length constituents from non-related carbon sources. *FEMS Microbiology Letters,* 184**,** 253-259.

HONDO, S., TAKAHASHI, M., OSANAI, T., MATSUDA, M., HASUNUMA, T., TAZUKE, A., NAKAHIRA, Y., CHOHNAN, S., HASEGAWA, M. & ASAYAMA, M. 2015. Genetic engineering and metabolite profiling for overproduction of polyhydroxybutyrate in cyanobacteria. *J Biosci Bioeng,* 120**,** 510-7.

HOSCHEK, A., HEUSCHKEL, I., SCHMID, A., BUHLER, B., KARANDE, R. & BUHLER, K. 2019. Mixed-species biofilms for high-cell-density application of Synechocystis sp. PCC 6803 in capillary reactors for continuous cyclohexane oxidation to cyclohexanol. *Bioresource Technology,* 282**,** 171-178.

ISHII-HYAKUTAKE, M., MIZUNO, S. & TSUGE, T. 2018. Biosynthesis and Characteristics of Aromatic Polyhydroxyalkanoates. *Polymers (Basel),* 10.

ISSA, I., DELBRUCK, S. & HAMM, U. 2019. Bioeconomy from experts' perspectives - Results of a global expert survey. *PLoS One,* 14**,** e0215917.

JANASCH, M., ASPLUND-SAMUELSSON, J., STEUER, R. & HUDSON, E. P. 2018. Kinetic modeling of the Calvin cycle identifies flux control and stable metabolomes in Synechocystis carbon fixation. *Journal of Experimental Botany,* 70**,** 973-983.

JENDROSSEK, D. & PFEIFFER, D. 2014. New insights in the formation of polyhydroxyalkanoate granules (carbonosomes) and novel functions of poly(3-hydroxybutyrate). *Environmental Microbiology,* 16**,** 2357-2373.

KADIYALA, G. 2014. *Isolation Purification and Screening of Biodegradable Polymer PHB Producing Cyanobacteria from Marine and Fresh Water Resources*.

KAMRAVA, D., KOVÁCS, T., PFLÜGL, S., DRUZHININA, I., KROLL, P., LACKNER, M. & HERWIG, C. 2018. *Increased poly-B-hydroxybutyrate production from carbon dioxide in randomly mutated cells of cyanobacterial strain Synechocystis sp. PCC 6714: Mutant generation and Characterization*.

KAMRAVAMANESH, D., LACKNER, M. & HERWIG, C. 2018. Bioprocess Engineering Aspects of Sustainable Polyhydroxyalkanoate Production in Cyanobacteria. *Bioengineering (Basel, Switzerland),* 5**,** 111.

KAMRAVAMANESH, D., PFLÜGL, S., NISCHKAUER, W., LIMBECK, A., LACKNER, M. & HERWIG, C. 2017. Photosynthetic poly-β-hydroxybutyrate accumulation in unicellular cyanobacterium Synechocystis sp. PCC 6714. *AMB Express,* 7**,** 143-143.

KATAYAMA, N., IIJIMA, H. & OSANAI, T. 2018. Production of Bioplastic Compounds by Genetically Manipulated and Metabolic Engineered Cyanobacteria. *Adv Exp Med Biol,* 1080**,** 155-169.

KHETKORN, W., INCHAROENSAKDI, A., LINDBLAD, P. & JANTARO, S. 2016. Enhancement of poly-3-hydroxybutyrate production in Synechocystis sp. PCC 6803 by overexpression of its native biosynthetic genes. *Bioresour Technol,* 214**,** 761-8.

KLOTZ, A., GEORG, J., BUCINSKA, L., WATANABE, S., REIMANN, V., JANUSZEWSKI, W., SOBOTKA, R., JENDROSSEK, D., HESS, W. R. & FORCHHAMMER, K. 2016. Awakening of a Dormant Cyanobacterium from Nitrogen Chlorosis Reveals a Genetically Determined Program. *Curr Biol,* 26**,** 2862-2872.

KOCH, M., DOELLO, S., GUTEKUNST, K. & FORCHHAMMER, K. 2019. PHB is Produced from Glycogen Turn-over during Nitrogen Starvation in Synechocystis sp. PCC 6803. *Int J Mol Sci,* 20.

KOLLER, M. 2017. Advances in Polyhydroxyalkanoate (PHA) Production. *Bioengineering (Basel),* 4.

LI, W. C., TSE, H. F. & FOK, L. 2016. Plastic waste in the marine environment: A review of sources, occurrence and effects. *Science of The Total Environment,* 566-567**,** 333-349.

LÖWE, H., HOBMEIER, K., MOOS, M., KREMLING, A. & PFLÜGER-GRAU, K. 2017. Photoautotrophic production of polyhydroxyalkanoates in a synthetic mixed culture of Synechococcus elongatus cscB and Pseudomonas putida cscAB. *Biotechnology for biofuels,* 10**,** 190-190.

LU, J., TAPPEL, R. & NOMURA, C. 2009. *Mini-Review: Biosynthesis of Poly(hydroxyalkanoates)*.
LUEF, K. P., STELZER, F. & WIESBROCK, F. 2015. Poly(hydroxy alkanoate)s in Medical Applications. *Chem Biochem Eng Q,* 29**,** 287-297.
MEIXNER, K., KOVALCIK, A., SYKACEK, E., GRUBER-BRUNHUMER, M., ZEILINGER, W., MARKL, K., HAAS, C., FRITZ, I., MUNDIGLER, N., STELZER, F., NEUREITER, M., FUCHS, W. & DROSG, B. 2018. Cyanobacteria Biorefinery — Production of poly(3-hydroxybutyrate) with Synechocystis salina and utilisation of residual biomass. *Journal of Biotechnology,* 265**,** 46-53.
MONSHUPANEE, T., NIMDACH, P. & INCHAROENSAKDI, A. 2016. Two-stage (photoautotrophy and heterotrophy) cultivation enables efficient production of bioplastic poly-3-hydroxybutyrate in auto-sedimenting cyanobacterium. *Scientific Reports,* 6**,** 37121.
MUDLIAR, S. N., VAIDYA, A. N., SURESH KUMAR, M., DAHIKAR, S. & CHAKRABARTI, T. 2007. Techno-economic evaluation of PHB production from activated sludge. *Clean Technologies and Environmental Policy,* 10**,** 255.
NAKAYA, Y., IIJIMA, H., TAKANOBU, J., WATANABE, A., HIRAI, M. Y. & OSANAI, T. 2015. One day of nitrogen starvation reveals the effect of sigE and rre37 overexpression on the expression of genes related to carbon and nitrogen metabolism in Synechocystis sp. PCC 6803. *Journal of Bioscience and Bioengineering,* 120**,** 128-134.
NAMAKOSHI, K., NAKAJIMA, T., YOSHIKAWA, K., TOYA, Y. & SHIMIZU, H. 2016. Combinatorial deletions of glgC and phaCE enhance ethanol production in Synechocystis sp. PCC 6803. *Journal of Biotechnology,* 239**,** 13-19.
NAPPER, I. E. & THOMPSON, R. C. 2019. Environmental Deterioration of Biodegradable, Oxo-biodegradable, Compostable, and Conventional Plastic Carrier Bags in the Sea, Soil, and Open-Air Over a 3-Year Period. *Environmental Science & Technology,* 53**,** 4775-4783.
NARANCIC, T., VERSTICHEL, S., REDDY CHAGANTI, S., MORALES-GAMEZ, L., KENNY, S. T., DE WILDE, B., BABU PADAMATI, R. & O'CONNOR, K. E. 2018. Biodegradable Plastic Blends Create New Possibilities for End-of-Life Management of Plastics but They Are Not a Panacea for Plastic Pollution. *Environmental Science & Technology,* 52**,** 10441-10452.
NODA, I., BLAKE LINDSEY, S. & CARAWAY, D. 2009. Nodax™ Class PHA Copolymers: Their Properties and Applications.
NOWROTH, V., MARQUART, L. & JENDROSSEK, D. 2016. Low temperature-induced viable but not culturable state of Ralstonia eutropha and its relationship to accumulated polyhydroxybutyrate. *FEMS microbiology letters,* 363**,** fnw249.
OSANAI, T., NUMATA, K., OIKAWA, A., KUWAHARA, A., IIJIMA, H., DOI, Y., TANAKA, K., SAITO, K. & HIRAI, M. Y. 2013. Increased bioplastic production with an RNA polymerase sigma factor SigE during nitrogen starvation in Synechocystis sp. PCC 6803. *DNA Res,* 20**,** 525-35.
OSANAI, T., OIKAWA, A., NUMATA, K., KUWAHARA, A., IIJIMA, H., DOI, Y., SAITO, K. & HIRAI, M. Y. 2014. Pathway-level acceleration of glycogen catabolism by a response regulator in the cyanobacterium Synechocystis species PCC 6803. *Plant Physiol,* 164**,** 1831-41.
PANDA, B., JAIN, P., SHARMA, L. & MALLICK, N. 2006. Optimization of cultural and nutritional conditions for accumulation of poly-beta-hydroxybutyrate in Synechocystis sp. PCC 6803. *Bioresour Technol,* 97**,** 1296-301.
PANDA, B. & MALLICK, N. 2007. Enhanced poly-beta-hydroxybutyrate accumulation in a unicellular cyanobacterium, Synechocystis sp. PCC 6803. *Lett Appl Microbiol,* 44**,** 194-8.
PARK, S. J., CHOI, J.-I. & LEE, S. Y. 2005. Engineering of Escherichia coli fatty acid metabolism for the production of polyhydroxyalkanoates. *Enzyme and Microbial Technology,* 36**,** 579-588.
PHILIP, S., KESHAVARZ, T. & ROY, I. 2007. Polyhydroxyalkanoates: biodegradable polymers with a range of applications. *Journal of Chemical Technology and Biotechnology,* 82**,** 233-247.
POSEN, I. D., JARAMILLO, P. & GRIFFIN, W. M. 2016. Uncertainty in the Life Cycle Greenhouse Gas Emissions from U.S. Production of Three Biobased Polymer Families. *Environ Sci Technol,* 50**,** 2846-58.
RAJAN, K. P., THOMAS, S. P., GOPANNA, A. & CHAVALI, M. 2017. Polyhydroxybutyrate (PHB): A Standout Biopolymer for Environmental Sustainability. *In:* MARTÍNEZ, L. M. T., KHARISSOVA,

O. V. & KHARISOV, B. I. (eds.) *Handbook of Ecomaterials.* Cham: Springer International Publishing.

REIS, M. A. M., SERAFIM, L. S., LEMOS, P. C., RAMOS, A. M., AGUIAR, F. R. & VAN LOOSDRECHT, M. C. M. 2003. Production of polyhydroxyalkanoates by mixed microbial cultures. *Bioprocess and Biosystems Engineering,* 25**,** 377-385.

REISER, S. E., MITSKY, T. A. & GRUYS, K. J. 2000. Characterization and cloning of an (R)-specific trans-2,3-enoylacyl-CoA hydratase from Rhodospirillum rubrum and use of this enzyme for PHA production in Escherichia coli. *Appl Microbiol Biotechnol,* 53**,** 209-18.

RICHARDSON, J. W., JOHNSON, M. D. & OUTLAW, J. L. 2012. Economic comparison of open pond raceways to photo bio-reactors for profitable production of algae for transportation fuels in the Southwest. *Algal Research,* 1**,** 93-100.

RUJNIĆ-SOKELE, M. & PILIPOVIĆ, A. 2017. Challenges and opportunities of biodegradable plastics: A mini review. *Waste Management & Research,* 35**,** 132-140.

SAMANTARAY, S., NAYAK, J. K. & MALLICK, N. 2011. Wastewater Utilization for Poly-β-Hydroxybutyrate Production by the Cyanobacterium Aulosira fertilissima in a Recirculatory Aquaculture System. *Applied and Environmental Microbiology,* 77**,** 8735-8743.

SARKAR, D., MUELLER, T. J., LIU, D., PAKRASI, H. B. & MARANAS, C. D. 2019. A diurnal flux balance model of Synechocystis sp. PCC 6803 metabolism. *PLoS computational biology,* 15**,** e1006692-e1006692.

SINGH, A. K. & MALLICK, N. 2017. Advances in cyanobacterial polyhydroxyalkanoates production. *FEMS Microbiol Lett,* 364.

SLANINOVA, E., SEDLACEK, P., MRAVEC, F., MULLEROVA, L., SAMEK, O., KOLLER, M., HESKO, O., KUCERA, D., MAROVA, I. & OBRUCA, S. 2018. Light scattering on PHA granules protects bacterial cells against the harmful effects of UV radiation. *Appl Microbiol Biotechnol,* 102**,** 1923-1931.

STEINBÜCHEL, A. 1992. Biodegradable plastics. *Current Opinion in Biotechnology,* 3**,** 291-297.

SUDESH, K., TAGUCHI, K. & DOI, Y. 2002. Effect of increased PHA synthase activity on polyhydroxyalkanoates biosynthesis in Synechocystis sp. PCC6803. *International Journal of Biological Macromolecules,* 30**,** 97-104.

TAKAHASHI, H., MIYAKE, M., TOKIWA, Y. & ASADA, Y. 1998. Improved accumulation of poly-3-hydroxybutyrate by a recombinant cyanobacterium. *Biotechnology Letters,* 20**,** 183-186.

TARONCHER-OLDENBURG, G., NISHINA, K. & STEPHANOPOULOS, G. 2000. Identification and analysis of the polyhydroxyalkanoate-specific beta-ketothiolase and acetoacetyl coenzyme A reductase genes in the cyanobacterium Synechocystis sp. strain PCC6803. *Appl Environ Microbiol,* 66**,** 4440-8.

TROSCHL, C., MEIXNER, K. & DROSG, B. 2017. Cyanobacterial PHA Production-Review of Recent Advances and a Summary of Three Years' Working Experience Running a Pilot Plant. *Bioengineering (Basel),* 4.

UNGERER, J. & PAKRASI, H. B. 2016. Cpf1 Is A Versatile Tool for CRISPR Genome Editing Across Diverse Species of Cyanobacteria. *Scientific Reports,* 6**,** 39681.

VAN ALPHEN, P., ABEDINI NAJAFABADI, H., BRANCO DOS SANTOS, F. & HELLINGWERF, K. J. 2018. Increasing the Photoautotrophic Growth Rate of Synechocystis sp. PCC 6803 by Identifying the Limitations of Its Cultivation. *Biotechnol J,* 13**,** e1700764.

VERHOOGT, H., RAMSAY, B. A. & FAVIS, B. D. 1994. Polymer blends containing poly(3-hydroxyalkanoate)s. *Polymer,* 35**,** 5155-5169.

VIEIRA, C. J. A., BOTELHO, M. J., FRANCO, L. B., SILVA, B. V. D., AGUIAR, C. A. P. & DE, M. M. G. 2018. Recent Advances and Future Perspectives of PHB Production by Cyanobacteria. *Industrial Biotechnology,* 14**,** 249-256.

WEISS, T. L., YOUNG, E. J. & DUCAT, D. C. 2017. A synthetic, light-driven consortium of cyanobacteria and heterotrophic bacteria enables stable polyhydroxybutyrate production. *Metabolic Engineering,* 44**,** 236-245.

WENDT, K. E., UNGERER, J., COBB, R. E., ZHAO, H. & PAKRASI, H. B. 2016. CRISPR/Cas9 mediated targeted mutagenesis of the fast growing cyanobacterium Synechococcus elongatus UTEX 2973. *Microbial Cell Factories,* 15**,** 115.

XIE, J., ZHOU, J., ZHANG, H. & LI, Y. 2011. [Increasing reductant NADPH content via metabolic engineering of PHB synthesis pathway in Synechocystis sp. PCC 6803]. *Sheng Wu Gong Cheng Xue Bao,* 27**,** 998-1004.

YAO, L., CENGIC, I., ANFELT, J. & HUDSON, E. P. 2016. Multiple Gene Repression in Cyanobacteria Using CRISPRi. *ACS Synth Biol,* 5**,** 207-12.

YU, J., LIBERTON, M., CLIFTEN, P. F., HEAD, R. D., JACOBS, J. M., SMITH, R. D., KOPPENAAL, D. W., BRAND, J. J. & PAKRASI, H. B. 2015. Synechococcus elongatus UTEX 2973, a fast growing cyanobacterial chassis for biosynthesis using light and CO2. *Scientific Reports,* 5**,** 8132.

ZHANG, H. W., LIU, Y. H., YAO, C. H., CAO, X. P., TIAN, J. & XUE, S. 2017. FabG can function as PhaB for poly-3-hydroxybutyrate biosynthesis in photosynthetic cyanobacteria Synechocystis sp PCC 6803. *Bioengineered,* 8**,** 707-715.

Cyanophycin Granules

Introduction

Cyanophycin is a biopolymer from cyanobacteria consisting of equal parts of aspartate and arginine residues (multi-L-arginyl-poly-L-aspartic acid), which are polymerized by a non-ribosomal peptide synthetase reaction. Cyanophycin forms amorphous granular structures in the cytoplasm termed CGP (Cyanophycin Granule Peptide), which are visible by light microscopy. The potential application of cyanophycin has not been fully elaborated, however, it may be used in various medical or technical applications and is therefore of biotechnological interest (see below).

CGP was first described in 1887 by botanist Antonio Borzi during microscopic studies of filamentous cyanobacteria (Borzi, 1887). He observed light scattering inclusions by using light microscopy, which he termed *cianoficina*. With a C/N ratio of 2:1, CGP is extremely rich in nitrogen and consequently its synthesis is tightly linked to the state of nitrogen assimilation. Therefore, CGP was proposed to serve as a nitrogen reserve polymer in cyanobacteria. Recent research proposes that the metabolism of CGP is more complex and may serve various functions in cyanobacterial physiology.

CGP granules were isolated for the first time in 1971 from *Anabaena cylindrical* by differential centrifugation (Simon, 1971). CGP is insoluble under physiological conditions but soluble in either acidic, basic or highly ionic solutions. CGP can be solubilized by SDS but not by non-ionic detergents such as Triton X-100 (Lang et al., 1972). Routinely, CGP is extracted by alkali treatment and subsequent precipitation at neutral pH (Frey et al., 2002). The chemical structure of CGP was solved in 1976 by Simon and Weathers (Simon and Weathers, 1976). The polymer backbone of CGP consists of α-linked aspartic acid residues with the β-carboxylic group of every aspartyl moiety linked to the α-amino group of an arginine residue via isopeptide-bonds. CD spectroscopy data suggest that a substantial fraction of CGP has β-pleated sheet structure (Simon et al., 1980). The individual cyanophycin chains have no fixed length but show polydisperse size ranging from 25 to 100 kDa. This is in contrast to CGP producing heterotrophic bacteria such as *Acinetobacter* sp. ADP1, which synthesizes CGP with a lower molecular weight ranging from 21 to 28 kDa (Elbahloul et al., 2005). Cyanophycin, produced by genetic modified microorganisms harboring the CGP synthesizing enzymes also shows a lower molecular weight of 25–45 kDa (Steinle et al., 2008). The factors controlling the length of cyanophycin synthesis in cyanobacteria remain to be elucidated.

Biology of Cyanophycin

Cyanophycin is produced by many different cyanobacteria, both diazotrophic as well as non-diazotrophic strains of unicellular or filamentous nature (Figure 1). In diazotrophic strains, the formation of cyanophycin is directly linked to the nitrogen-fixation process, whereas in non-diazotrophic strains, the biological significance remained elusive until recently (see below).

In general, unicellular nitrogen-fixing cyanobacteria temporarily separate nitrogen fixation and photosynthesis on a diurnal basis, since these two processes are strictly incompatible due

to the oxygen sensitivity of nitrogenase. As shown in the cyanobacterium *Cyanothece* sp. ATCC 51142, the cells perform photosynthesis during the day where they accumulate fixed carbon in the form of glycogen. This storage material is catabolized during the night to support nitrogen fixation with energy and carbon skeletons (Sherman et al., 1998). The nitrogen fixation products are immediately converted to cyanophycin and stored as CGP, which accumulates during the night. In the subsequent day period, when photosynthesis is active again, CGP is degraded to mobilize the fixed nitrogen for anabolic reactions to support cell growth. A similar diurnal CPG accumulation during dark periods was also reported in the filamentous cyanobacterium *Trichodesmium* sp., which is the dominant diazotrophic cyanobacterium in tropical and subtropical seas and therefore of global importance in N and C cycling (Finzi-Hart et al., 2009).

Multicellular cyanobacteria of the order *Nostocales* are characterized by a spatial separation of photosynthesis and nitrogen fixation through a cell differentiation process. Nitrogenase is confined to specialized cells termed heterocysts, which differentiate along the filament in a semi-regular pattern from vegetative cells (Herrero et al., 2016). Heterocysts are terminally differentiated cells equipped with an oxygen diffusion barrier to provide the adjacent vegetative cells with products from nitrogen fixation. This type of metabolic differentiation requires an efficient metabolite transport system that connects all cells within a filament, a task that is performed by septal-localized channels resembling eukaryotic gap junctions (Weiss et al., 2019). In the heterocysts, CGP is particularly prominent. It appears in the form of “polar nodules” at the contact site to adjacent vegetative cells. The polar nodes are easily recognized by light microscopy and as such they are characteristic morphological signatures of heterocysts (Ziegler et al., 2001) (Figure 1). CGP in the polar nodules could serve as a sink for fixed nitrogen in the heterocyst to avoid feedback inhibition from soluble products of nitrogen fixation (Burnat et al., 2014). At the contact site to vegetative cells, CGP is cleaved by the action of cyanophycinase into Asp-Arg dipeptides, to provide fixed nitrogen to the vegetative cells. CGP catabolic enzymes are present at significantly higher levels in vegetative cells than in heterocysts, indicating a sophisticated spatial organization of nitrogen metabolism. Surprisingly, under standard laboratory conditions, this mode of metabolic organization appears to be dispensable, since mutants of *Anabaena* sp. PCC 7120 or *Anabaena variabilis,* lacking the CGP synthetic genes, were little affected in diazotrophic growth under usual cultivation conditions (Picossi et al., 2004). However, a growth defect was observed under stressful high light conditions (Ziegler et al., 2001, Burnat et al., 2014), indicating that cyanopyhcin plays a role in copin with metabolic stress. Moreover, diazotrophic growth is significantly decreased in strains, which are unable to degrade CGP (Picossi et al., 2004).

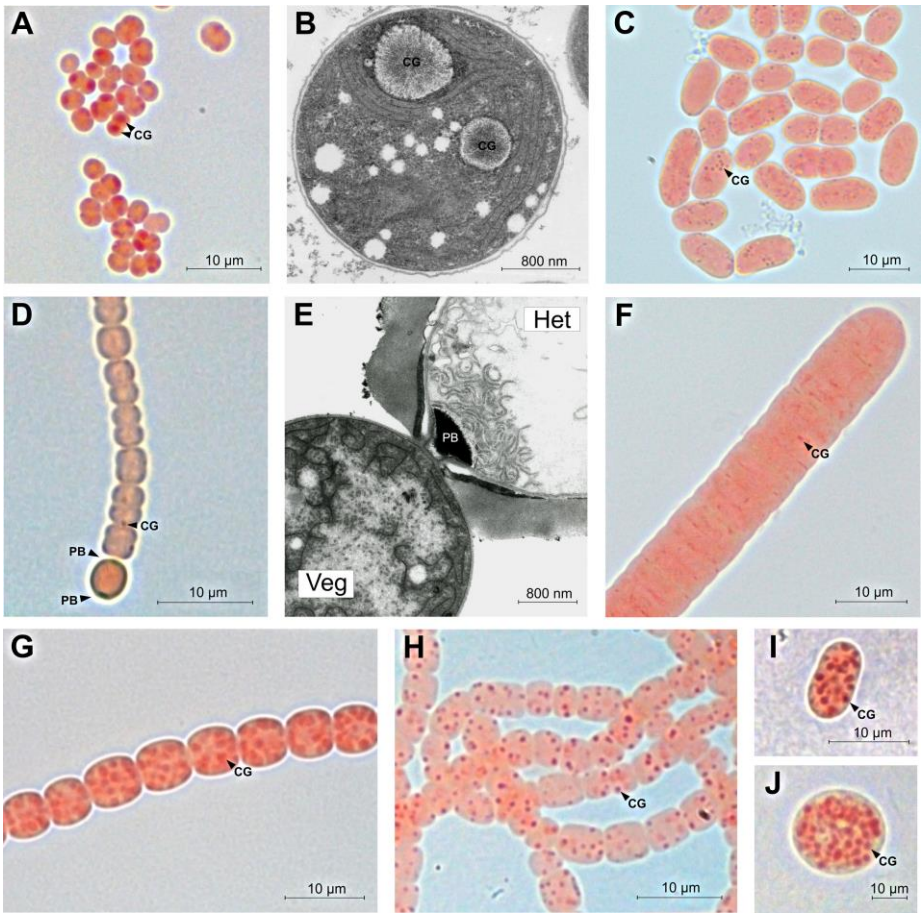

Figure 1 Light and electron microscopic pictures of CGP accumulating cyanobacteria. In light microscopic pictures, CGP were stained using the Sakaguchi reaction (Watzer et al., 2015). The intensity of the *red color* indicates the amount of arginine. Dark red to purple dots are CGP granules [CG]. A. and B. show phosphate starved *Synechocystis* sp. PCC 6803 in light and transmissionelectron microscopy, respectively. C. *Cyanothece* sp. PCC 7424 cultivated in presents of nitrate and continuous light. D. Filament of diazotrophic growing *Anabaena* sp. PCC 7120 with terminal heterocyst containing polar bodys [PB]. C. Transmission electron micrographs of a heterocyst and adjacent vegetative cell from *Anabaena* sp. PCC 7120, showing a GCP consisting polar body [PB]. D. filamentous cyanobacterium of genus *Oscillatoria* cultivated with nitrate supplementation, showing small CGP granules. G. phosphate starved *Anabaena variabilis ATCC 29413* under nitrate supplemented growth. H. *Nostoc punctiforme ATCC 29133* under phosphate starvation and nitrate supplementation. I and J. show mature akinetes of *Anabaena variabilis ATCC 29413* and *Nostoc punctiforme ATCC 29133*, respectively.

Several of the heterocyst-forming cyanobacteria are able to differentiate another type of specialized cells, the akinetes. These are resting cells able to survive long periods of unfavorable conditions. During akinete development, the cells transiently accumulate CGP in addition to other storage compounds such as glycogen or lipid droplets (Perez et al., 2016) (Figure 1). In mature akinetes, CGP disappears gradually and when the akinetes germinate, CGP reappears transiently (Perez et al., 2018). Apparently, synthesis of CGP seems inessential, since *Anabaena variabilis* akinetes lacking CGP granules are not impaired in germination. This

behavior agrees with early observations suggesting that CGP is not the direct nitrogen source for protein biosynthesis in germinating akinetes (Sutherland et al., 1985).

In non-diazotrophic cyanobacteria, CGP can only be detected under unbalanced growth conditions. In exponentially growing cells, its amount is usually less than 1 % of the cell dry mass. However, when growth is retarded or arrested due to unfavorable conditions, which impair growth but allow nitrogen assimilation (antibiotic treatment; sulfate, phosphate or potassium starvation), the cells may start to build up CGP, which can amount up to 18 % of the cell dry mass (Allen et al., 1980). When *Synechocystis* cells recover from prolonged nitrogen starvation, by adding nitrate to the starved cells, they transiently accumulate CGP. This raised the question regarding the biological significance of transient CGP accumulation. This issue was recently solved by Watzer and Forchhammer (Watzer and Forchhammer, 2018a). The transient accumulation of CGP becomes beneficial to the cells under conditions of fluctuating and limiting nitrogen supply. Whereas wildtype *Synechocystis* cells are able to fully recover from prolonged nitrogen chlorosis when they are provided with pulses of nitrate, recovery is severely delayed in a mutant deficient in cyanophycin synthesis (*cphA* mutant, see below). This phenotype becomes even more prominent when cells are cultivated in 12 h day/night cycles. From these findings, it can be concluded that under natural conditions, characterized by fluctuating nutrient and light supply, cyanophycin synthesis allows intracellular sequestration of nitrogen assimilation products, so that under periods of nitrogen shortage, cyanophycin degradation provides anabolic precursors to continue growth. Even under constant illumination and a constant but limited nitrogen supply, the wild-type has a growth advantage over the *cphA* mutant. This suggests that CGP synthesis optimizes the nitrogen assimilation process.

Genes and enzymes of CGP metabolism

The genes for cyanophycin synthesis (*cphA*) and degradation (*cphB*) are often clustered. In *Synechocystis* sp. PCC 6803, the *cphA* gene lies immediately downstream of *cphB,* but both genes area transcribed independently (Mitschke et al., 2011). In agreement with the more complex CGP metabolism in multicellular cyanobacteria two gene clusters encoding *cphA* and *cphB* paralogues were identified In *Anabaena* sp. PCC 7120, (Picossi et al., 2004). Generally, the expression from the *cph2* cluster is lower compared to *cph1* and expression is induced under diazotrophic growth conditions. Even a third set of ORFs containing putative *cphA* and *cphB* genes were found in *Nostoc punctiforme* PCC 73102 and *Anabaena variabilis* ATCC 29413 (Fuser and Steinbuchel, 2007),

Cyanophycin Synthetase

CGP is synthesized from aspartate and arginine monomers by the enzyme cyanophycin synthetase (CphA1), first described in 1976 (Simon, 1976, Berg et al., 2000) (Figure 2). In a two-step reaction, CphA first elongates the chain by the addition of aspartate and subsequently, attaches arginine via isopeptide bond formation to the free β-carboxyl group of the newly added aspartyl-residue. The in vitro elongation reaction requires ATP, KCl, $MgCl_2$ and a sulfhydryl reagent (-mercaptoethanol or DTT). To start the elongation reaction CphA1 needs a so far unknown CGP primer (Simon, 1976). The primer requires at least three Asp-Arg building blocks

(β-Asp-Arg)$_3$ (Berg et al., 2000). An exception is CphA1 of *Thermosynechococcus elongates* strain BP-1, which shows primer-independent CGP synthesis (Arai and Kino, 2008).

CphA1 enzymes range in size from 90 to 130 kDa (Watzer and Forchhammer, 2018b). In its active state, CphA1s from *Synechocystis* sp. PCC6308 and *Anabaena variabilis* PCC7937 are probably homodimeric (Ziegler et al., 1998), while the primer-independent CphA1 from *Thermosynechococcus elongates* strain BP-1 forms a homotetramer (Arai and Kino, 2008). In agreement with the reaction mechanism, the primary structure of CphA1 consists of two parts (Ziegler et al., 1998). The C-terminal part is similar to peptide ligases such as murein ligase and folylpolyglutamate ligase. The N-terminal part of CphA1 shows sequence similarities with another superfamily of ATP-dependent ligases like carboxylate-thiol and carboxylate-amine ligase. Accordingly, two different active sites, each one in the N- and C-terminal region, have been predicted (Berg et al., 2000).

The CGP elongation cycle starts at the free carboxy-group of the terminal aspartyl-residue of the growing cyanophycin chain. First, this group is activated by phosphorylation using ATP. Subsequently, a peptide bound is formed between the phosphorylated carboxyl-group and the amino-group of the newly attached aspartyl-residue. The reaction intermediate (β-Asp-Arg)$_n$-Asp is then translocated to the second active site of CphA1, where the β-carboxyl group of the newly attached aspartate becomes phosphorylated. Finally, the α-group of arginine is linked to the β-carboxyl group of aspartate, forming an isopeptide bond (Berg et al., 2000).

CphA1 of *Synechocystis* sp. PCC 6308 has been characterized in detail (Aboulmagd et al., 2001). Apparent K_m values were determined for aspartate (450 µM), for arginine (49 µM) for ATP (200µM) and for CGP as priming substance (35 µg/ml). The higher affinity for arginine compared to aspartate reflects the lower cellular level of arginine compared to the abundant amino acid aspartate. *In vitro*, CphA1 converts 1.3 ± 0.1 mol ATP to ADP per mol incorporated amino acid.

In general, CphA1 is the only cyanophycin synthesizing enzyme in non-diazotrophic cyanobacteria. However, in many nitrogen-fixing cyanobacteria, an additional version of cyanophycin synthetase is present, termed CphA2. Recently, the function of this isoenzyme has been resolved (Klemke et al., 2016). Compared to CphA1, CphA2 has a reduced size due to truncation of the C-terminal region with only the N-terminal active site being conserved. The substrate of CphA2 is the β-aspartyl-arginine dipeptide, which is back-converted to cyanophycin, consuming one molecule of ATP per reaction. Lack of CphA2 does not reduce the overall CGP content, but a CphA2-deficient mutant displays a similar phenotype as a CphA1 mutant under diazotrophic growth at high light intensities. The "futile cycle" of CGP hydrolysis and immediate repolymerization by CphA2 may be beneficial for the distribution of nitrogen fixation products in the filament (Forchhammer and Watzer, 2016).

Cyanophycin degrading enzymes

Degradation of CGP requires a special hydrolytic enzyme, since this polypeptide is resistant towards conventional proteases. In cyanobacteria, intracellular degradation of cyanophycin involves the cyanophycinase CphB, which catalyzes the hydrolytic cleavage of CGP to β-Asp-Arg dipeptides. CphB is a 29.4 kDa C-terminal exopeptidase, related to dipeptidase E (PepE) (Richter et al., 1999). CphB is highly specific to cyanophycin hydrolysis, probably to unique structural properties of the active site (Law et al., 2009). Distinct from CphB, several heterotrophic bacteria harbor an enzyme for the extracellular degradation of cyanophycin. For example, in the culture supernatant of *Pseudomonas anguilliseptica culture, a*n extracellular cyanophycinase was characterized, termed CphE (Obst et al., 2002).

Following the cleavage of CGP into β-Asp-Arg dipeptides, a dipeptidase activity releases the monomeric amino acids arginine and aspartate (Figure 2). The corresponding enzyme was identified as a "plant-type asparaginase" corresponding to ORF *sll0422* from *Synechocystis* sp. PCC 6803 or ORF *all3922* from *Anabaena* sp. PCC 7120 (Hejazi et al., 2002). These enzymes have quite broad substrate specificity. In addition to displaying asparaginase activity, they cleave various isoaspartyl peptides, which may arise from proteolytic degradation of modified proteins containing isoaspartyl residues or from the degradation of cyanophycin. The mature enzyme consists of two protein subunits, which are generated from a primary transcript by autoproteolytic cleavage forming an $\alpha_2\beta_2$ quaternary structure (α derived from the N-terminal part and β form the C-terminal part of the precursor).

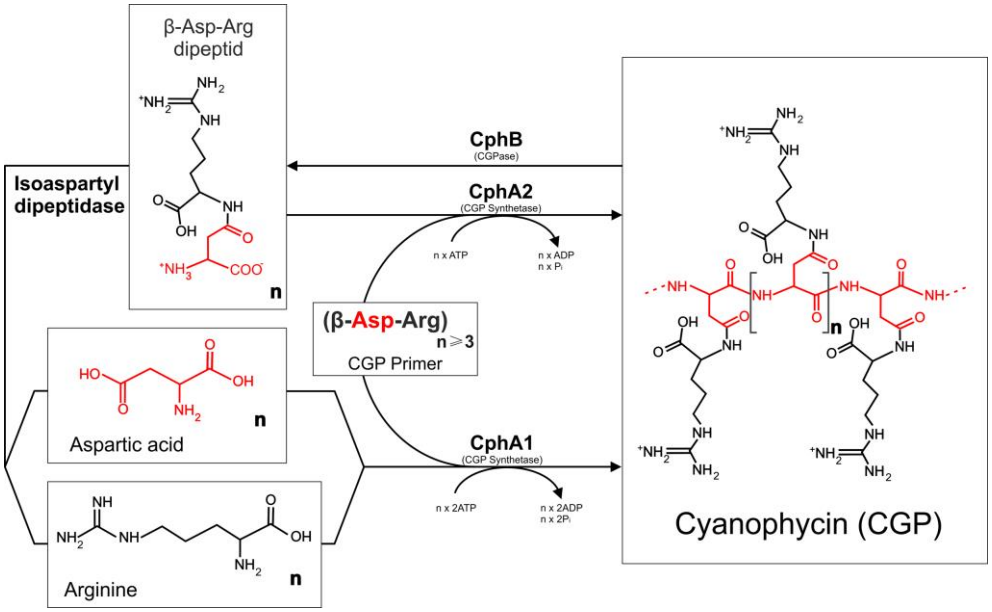

Figure 2 Schematic illustration of CGP metabolism in cyanobacteria. CGP is synthesized from aspartate and arginine by CGP Synthetase (CphA1) in an ATP-depending elongation reaction using CGP primers, containing of at least three Asp-Arg building blocks. Intracellular CGP degradation is catalyzed by the CGPase (CphB). The β-Asp-Arg dipeptides resulting from cleavage of CGP is further hydrolysed by isoaspartyl dipeptidase, releasing aspartate and arginine. In many nitrogen-fixing cyanobacteria, an second CGP synthetase, CphA2, is present. CphA2 requires β-aspartyl-arginine dipeptides to synthesize CGP.

Regulation of cyanophycin metabolism

In filamentous nitrogen fixing cyanobacteria, cyanophycin synthesis is of particular relevance during nitrogen-fixing conditions as outlined above. In *Anabaena* sp. PCC 7120, the genes for CGP synthetases and CGPases are much higher expressed in heterocysts than in vegetative cells, whereas asparaginase All3922 is present in significantly lower levels in heterocysts than in vegetative cells (Burnat et al., 2014). Deletion of All3922 causes elevated levels of CGP and β-Asp-Arg dipeptides and the mutant shows an impaired diazothrophic growth, similar to the phenotype from CphB deletion mutants. It is assumed that cleavage of the CGP in heterocyst polar nodules is catalyzed by CphB and the released β-Asp-Arg dipeptides are transported to

the adjacent vegetative cells. However, the detailed spatio-temporal regulation of cyanophycin metabolism in the multicellular cyanobacteria remains to be elucidated.

The situation is much clearer in unicellular non-diazotrophic cyanobacteria. Here, the accumulation of CGP is triggered exclusively by growth conditions that reduce or arrest growth and in presence of combined nitrogen sources. While during exponential growth the amino acids arginine and aspartate are used for protein biosynthesis, under growth-limiting conditions, protein biosynthesis is slowed down, making aspartate and arginine available for CGP synthesis (Watzer et al., 2015). In this regard, the availability of arginine is of particular relevance.

A link between regulation of arginine biosynthesis and CGP metabolism was suggested by the phenotype of a mutant deficient in arginine biosynthesis control (Maheswaran et al., 2006). Synthesis of arginine is controlled mainly by the first committed step of the ornithine pathway, catalyzed by N-acetylglutamate kinase (NAGK) (Llacer et al., 2008). NAGK activity is subjected to allosteric feedback-inhibition by arginine and is activated by the P_{II} signal transduction protein (see below) (Heinrich et al., 2004, Beez et al., 2009). The P_{II} signaling protein acts as a coordinator of central carbon/nitrogen assimilatory reactions by sensing the ATP/ADP ration of the cells and the level of 2-oxoglutarate (Forchhammer and Lüddecke, 2016). A P_{II} deficient mutant of *Synechocystis* PCC 6803 has low NAGK activities and is, therefore, unable to increase arginine levels in response to nitrogen-upshift. While in wild-type cells nitrogen-upshift increases the cellular arginine levels together with the accumulation of cyanophycin, the PII deficient mutant is unable to raise the arginine levels and fails to accumulate cyanophycin (Maheswaran et al., 2006).

The nitrogen-regulated response regulator NrrA has also influence on arginine and CGP biosynthesis. A NrrA-deficient mutant in *Synechocystis* sp. PCC 6803 shows reduced intracellular arginine levels and consequently, reduced CGP amount (Liu and Yang, 2014).

All these results and observations point towards arginine as main bottleneck of CGP biosynthesis, while aspartate plays a minor role. CGP accumulation occurs as a result of arginine enrichment in the cytoplasm.

Cyanophycin overproduction and potential industrial applications

Since arginine synthesis is a limiting factor for CGP accumulation, overproduction of CGP requires enhanced arginine synthesis. A single amino acid replacement in cyanobacterial P_{II} signaling protein (Ile86 to Asp86) generates a P_{II} variant (P_{II}-I86N) that constitutively binds to the controlling enzyme of arginine synthesis, NAGK, *in vitro* and enhances its activity (Fokina et al., 2010). Replacing the wild-type allele for P_{II} in *Synechocystis* by this variant results in a strain, which has constitutively high NAGK activity and 10-fold increased levels of arginine (BW86) (Watzer et al., 2015). Already under balanced growth conditions with nitrate as nitrogen source, strain BW86 accumulates up to 15.6 ± 5.4 % CGP relative to the cell dry mass (CDM), while CGP in the wild-type is barely detectable (Fig. 3). Phosphate or potassium starvation further increases the CGP content of strain BW86 up to 47.4 ± 2.3 % or 57.3 ± 11.1 % per CDM, respectively (Trautmann et al., 2016). The cyanophycin, which is produced by strain BW86, shows a high polydispersity ranging from 25 to 100 kDa, similar to the polydispersity of wild-type cyanobacterial CGP (Watzer et al., 2015). This contrasts CGP from recombinant producer strains using heterologous expression systems such as heterotrophic bacteria, yeasts or plants, whose recombinantly produced CGP shows polydispersity ranging from 25 to only 45 kDa (Frey et al., 2002, Watzer and Forchhammer, 2018b). The novel cyanobacterial producer stain for

cyanophycin may provide a valuable resource for the synthesis of large quantities of natural long-chain cyanophycin with so-far unexplored properties.

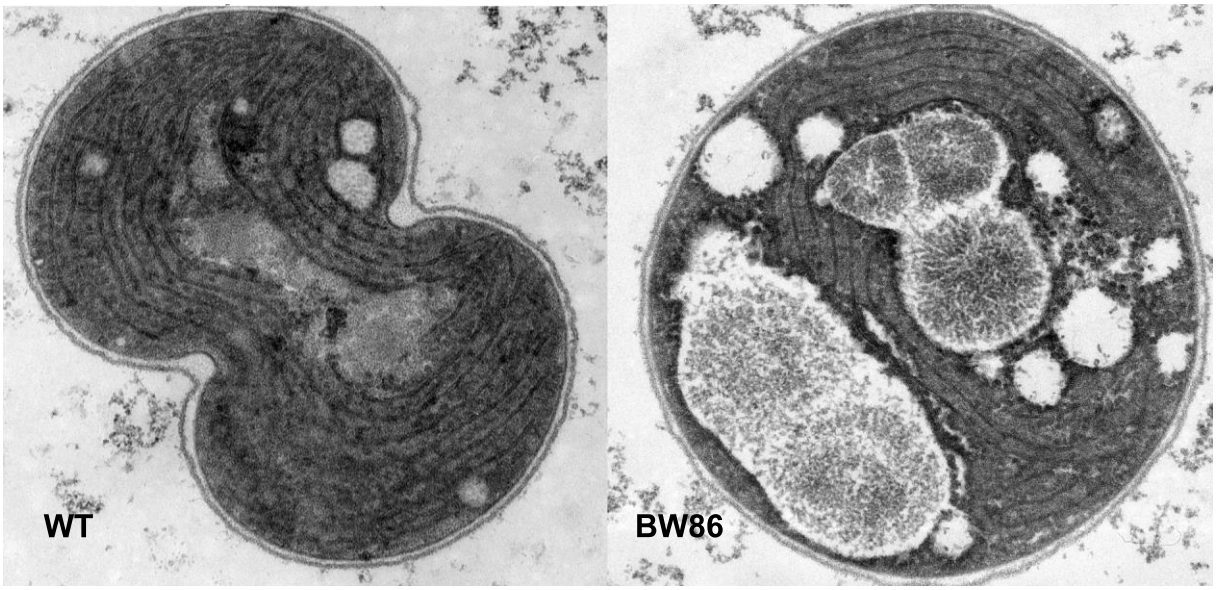

Fig. 3: Transmission electron micrographs of Synechocystis PCC6803 wild-type cell (left) in comparison to cyanophycin overproducing strain BW86 (right). The amorphous granular material with in the cell represents cyanophycin.

The natural compound cyanophycin has up to now no industrial application whereas chemical derivatives of CGP are of potential biotechnological interest. CGP can be converted via hydrolytic β-cleavage to poly(α-L-aspartic acid) (PAA) and free arginine. Arginine is a valuable product and PAA is biodegradable and has a high number of negatively charged carboxylic groups, making PAA to a possible substituent for polyacrylates (Khlystov et al., 2017). PAA can be employed as anti-sealant or dispersing ingredient in many fields of applications, including washing detergents or suntan lotions. Furthermore, PAA has potential application areas as an additive in paper, paint, building or oil industry (Obst and Steinbuchel, 2004).

In addition to its use as polymer, CGP can also serve as a source for constituent dipeptides and amino acids in food, feed and pharmaceutical industry. The amino acids arginine (semi-essential), aspartate (non-essential) and lysine (essential) derived from CGP have a broad spectrum of nutritional or therapeutic applications. Large scale production of these amino acids, as mixtures or dipeptides, is established in industry, with various commercial products already available on the market (Sallam and Steinbuchel, 2010).

Uncategorized References

ABOULMAGD, E., SANIO, F. B. O. & STEINBUCHEL, A. 2001. Purification of Synechocystis sp strain PCC6308 cyanophycin synthetase and its characterization with respect to substrate and primer specificity. *Applied and Environmental Microbiology,* 67**,** 2176-2182.

ACIÉN, F. G., FERNÁNDEZ, J. M., MAGÁN, J. J. & MOLINA, E. 2012. Production cost of a real microalgae production plant and strategies to reduce it. *Biotechnology Advances,* 30**,** 1344-1353.

ALBUQUERQUE, P. B. S. & MALAFAIA, C. B. 2018. Perspectives on the production, structural characteristics and potential applications of bioplastics derived from polyhydroxyalkanoates. *Int J Biol Macromol,* 107**,** 615-625.

ALDOR, I. S. & KEASLING, J. D. 2003. Process design for microbial plastic factories: metabolic engineering of polyhydroxyalkanoates. *Current Opinion in Biotechnology,* 14**,** 475-483.

ALLEN, M. M., HUTCHISON, F. & WEATHERS, P. J. 1980. Cyanophycin Granule Polypeptide Formation and Degradation *Journal of Bacteriology,* 141**,** 687-693.

ALLEN, M. M. & SMITH, A. J. 1969. Nitrogen chlorosis in blue-green algae. *Arch Mikrobiol,* 69**,** 114-20.

ANDERSON, A. J. & DAWES, E. A. 1990. Occurrence, Metabolism, Metabolic Role, and Industrial Uses of Bacterial Polyhydroxyalkanoates. *Microbiological Reviews,* 54**,** 450-472.

ANSARI, S. & FATMA, T. 2016. Cyanobacterial Polyhydroxybutyrate (PHB): Screening, Optimization and Characterization. *Plos One,* 11.

ARAI, T. & KINO, K. 2008. A cyanophycin synthetase from Thermosynechococcus elongatus BP-1 catalyzes primer-independent cyanophycin synthesis. *Applied Microbiology and Biotechnology,* 81**,** 69-78.

BATISTA, M. B., TEIXEIRA, C. S., SFEIR, M. Z. T., ALVES, L. P. S., VALDAMERI, G., PEDROSA, F. O., SASSAKI, G. L., STEFFENS, M. B. R., DE SOUZA, E. M., DIXON, R. & MULLER-SANTOS, M. 2018. PHB Biosynthesis Counteracts Redox Stress in Herbaspirillum seropedicae. *Front Microbiol,* 9**,** 472.

BEEZ, S., FOKINA, O., HERRMANN, C. & FORCHHAMMER, K. 2009. N-acetyl-L-glutamate kinase (NAGK) from oxygenic phototrophs: P(II) signal transduction across domains of life reveals novel insights in NAGK control. *J Mol Biol,* 389**,** 748-758.

BEHLER, J., VIJAY, D., HESS, W. R. & AKHTAR, M. K. 2018. CRISPR-Based Technologies for Metabolic Engineering in Cyanobacteria. *Trends in Biotechnology,* 36**,** 996-1010.

BERG, H., ZIEGLER, K., PIOTUKH, K., BAIER, K., LOCKAU, W. & VOLKMER-ENGERT, R. 2000. Biosynthesis of the cyanobacterial reserve polymer multi-L-arginyl-poly-L-aspartic acid (cyanophycin) - Mechanism of the cyanophycin synthetase reaction studied with synthetic primers. *European Journal of Biochemistry,* 267**,** 5561-5570.

BORZI, A. 1887. Le communicazioni intracellulari delle Nostochinee. *Malpighia,* 1**,** 28-74.

BURNAT, M., HERRERO, A. & FLORES, E. 2014. Compartmentalized cyanophycin metabolism in the diazotrophic filaments of a heterocystforming cyanobacterium. *Proceedings of the National Academy of Sciences of the United States of America,* 111**,** 3823-3828.

CARLETON, T. A. & HSIANG, S. M. 2016. Social and economic impacts of climate. *Science,* 353**,** aad9837.

CARPINE, R., DU, W., OLIVIERI, G., POLLIO, A., HELLINGWERF, K. J., MARZOCCHELLA, A. & BRANCO DOS SANTOS, F. 2017. Genetic engineering of Synechocystis sp. PCC6803 for poly-β-hydroxybutyrate overproduction. *Algal Research,* 25**,** 117-127.

CARR, N. G. 1966. The occurrence of poly-beta-hydroxybutyrate in the blue-green alga, Chlorogloea fritschii. *Biochim Biophys Acta,* 120**,** 308-10.

COLLIER, J. L. & GROSSMAN, A. R. 1992. Chlorosis induced by nutrient deprivation in Synechococcus sp. strain PCC 7942: not all bleaching is the same. *J Bacteriol,* 174**,** 4718-26.

COSTA, J. A. V. & DE MORAIS, M. G. 2014. Chapter 1 - An Open Pond System for Microalgal Cultivation. *In:* PANDEY, A., LEE, D.-J., CHISTI, Y. & SOCCOL, C. R. (eds.) *Biofuels from Algae.* Amsterdam: Elsevier.

DAMROW, R., MALDENER, I. & ZILLIGES, Y. 2016. The Multiple Functions of Common Microbial Carbon Polymers, Glycogen and PHB, during Stress Responses in the Non-Diazotrophic Cyanobacterium Synechocystis sp. PCC 6803. *Front Microbiol,* 7**,** 966.

DOELLO, S., KLOTZ, A., MAKOWKA, A., GUTEKUNST, K. & FORCHHAMMER, K. 2018. A Specific Glycogen Mobilization Strategy Enables Rapid Awakening of Dormant Cyanobacteria from Chlorosis. *Plant Physiol,* 177**,** 594-603.

DUTT, V. & SRIVASTAVA, S. 2018. Novel quantitative insights into carbon sources for synthesis of poly hydroxybutyrate in Synechocystis PCC 6803. *Photosynth Res,* 136**,** 303-314.

ELBAHLOUL, Y., KREHENBRINK, M., REICHELT, R. & STEINBUCHEL, A. 2005. Physiological conditions conducive to high cyanophycin content in biomass of Acinetobacter calcoaceticus strain ADP1. *Applied and Environmental Microbiology,* 71**,** 858-866.

ENGLUND, E., LIANG, F. & LINDBERG, P. 2016. Evaluation of promoters and ribosome binding sites for biotechnological applications in the unicellular cyanobacterium Synechocystis sp. PCC 6803. *Scientific Reports,* 6**,** 36640.

ESTEVES-FERREIRA, A. A., INABA, M., OBATA, T., FORT, A., FLEMING, G. T. A., ARAÚJO, W. L., FERNIE, A. R. & SULPICE, R. 2017. A Novel Mechanism, Linked to Cell Density, Largely Controls Cell Division in Synechocystis. *Plant Physiology,* 174**,** 2166-2182.

EUROPEAN-BIOPLASTICS 2018. Bioplastics market data.

FINZI-HART, J. A., PETT-RIDGE, J., WEBER, P. K., POPA, R., FALLON, S. J., GUNDERSON, T., HUTCHEON, I. D., NEALSON, K. H. & CAPONE, D. G. 2009. Fixation and fate of C and N in the cyanobacterium Trichodesmium using nanometer-scale secondary ion mass spectrometry (vol 106, pg 6345, 2009). *Proceedings of the National Academy of Sciences of the United States of America,* 106**,** 9931-9931.

FOKINA, O., CHELLAMUTHU, V. R., ZETH, K. & FORCHHAMMER, K. 2010. A Novel Signal Transduction Protein P-II Variant from Synechococcus elongatus PCC 7942 Indicates a Two-Step Process for NAGK-P-II Complex Formation. *J Mol Biol,* 399**,** 410-421.

FORCHHAMMER, K. & LÜDDECKE, J. 2016. Sensory properties of the PII signalling protein family. *FEBS Journal,* 283**,** 425-437.

FORCHHAMMER, K. & SCHWARZ, R. 2019. Nitrogen chlorosis in unicellular cyanobacteria – a developmental program for surviving nitrogen deprivation. *Environmental Microbiology,* 21**,** 1173-1184.

FORCHHAMMER, K. & WATZER, B. 2016. Closing a gap in cyanophycin metabolism. *Microbiology-Sgm,* 162**,** 727-729.

FREY, K. M., OPPERMANN-SANIO, F. B., SCHMIDT, H. & STEINBUCHEL, A. 2002. Technical-scale production of cyanophycin with recombinant strains of Escherichia coli. *Applied and Environmental Microbiology,* 68**,** 3377-3384.

FUSER, G. & STEINBUCHEL, A. 2007. Analysis of genome sequences for genes of cyanophycin metabolism: Identifying putative cyanophycin metabolizing prokaryotes. *Macromolecular Bioscience,* 7**,** 278-296.

GANGURDE, D. N. & SAYYED, R. 2012. Poly-β-hydroxybutyrate (PhB): a Biodegradable Polymer of microbial origin.

GEYER, R., JAMBECK, J. R. & LAW, K. L. 2017. Production, use, and fate of all plastics ever made. *Science Advances,* 3**,** e1700782.

GICON 2019. Kultivierung von Mikroalgen.

GORL, M., SAUER, J., BAIER, T. & FORCHHAMMER, K. 1998. Nitrogen-starvation-induced chlorosis in Synechococcus PCC 7942: adaptation to long-term survival. *Microbiology,* 144 (Pt 9)**,** 2449-58.

GRUNDEL, M., SCHEUNEMANN, R., LOCKAU, W. & ZILLIGES, Y. 2012. Impaired glycogen synthesis causes metabolic overflow reactions and affects stress responses in the cyanobacterium Synechocystis sp. PCC 6803. *Microbiology,* 158**,** 3032-43.

HARDING, K. G., DENNIS, J. S., VON BLOTTNITZ, H. & HARRISON, S. T. L. 2007. Environmental analysis of plastic production processes: Comparing petroleum-based polypropylene and

polyethylene with biologically-based poly-β-hydroxybutyric acid using life cycle analysis. *Journal of Biotechnology,* 130**,** 57-66.

HAUF, W., SCHLEBUSCH, M., HUGE, J., KOPKA, J., HAGEMANN, M. & FORCHHAMMER, K. 2013. Metabolic Changes in Synechocystis PCC6803 upon Nitrogen-Starvation: Excess NADPH Sustains Polyhydroxybutyrate Accumulation. *Metabolites,* 3**,** 101-18.

HAUF, W., WATZER, B., ROOS, N., KLOTZ, A. & FORCHHAMMER, K. 2015. Photoautotrophic Polyhydroxybutyrate Granule Formation Is Regulated by Cyanobacterial Phasin PhaP in Synechocystis sp. Strain PCC 6803. *Appl Environ Microbiol,* 81**,** 4411-22.

HEIN, S., TRAN, H. & STEINBÜCHEL, A. 1998. Synechocystis sp. PCC6803 possesses a two-component polyhydroxyalkanoic acid synthase similar to that of anoxygenic purple sulfur bacteria. *Archives of Microbiology,* 170**,** 162-170.

HEINRICH, A., MAHESWARAN, M., RUPPERT, U. & FORCHHAMMER, K. 2004. The Synechococcus elongatus P signal transduction protein controls arginine synthesis by complex formation with N-acetyl-L-glutamate kinase. *Mol Microbiol,* 52**,** 1303-14.

HEJAZI, M., PIOTUKH, K., MATTOW, J., DEUTZMANN, R., VOLKMER-ENGERT, R. & LOCKAU, W. 2002. Isoaspartyl dipeptidase activity of plant-type asparaginases. *Biochemical Journal,* 364**,** 129-136.

HERRERO, A., STAVANS, J. & FLORES, E. 2016. The multicellular nature of filamentous heterocyst-forming cyanobacteria. *Fems Microbiology Reviews,* 40**,** 831-854.

HOFFMANN, N., STEINBÜCHEL, A. & REHM, B. H. A. 2000. The Pseudomonas aeruginosa phaG gene product is involved in the synthesis of polyhydroxyalkanoic acid consisting of medium-chain-length constituents from non-related carbon sources. *FEMS Microbiology Letters,* 184**,** 253-259.

HONDO, S., TAKAHASHI, M., OSANAI, T., MATSUDA, M., HASUNUMA, T., TAZUKE, A., NAKAHIRA, Y., CHOHNAN, S., HASEGAWA, M. & ASAYAMA, M. 2015. Genetic engineering and metabolite profiling for overproduction of polyhydroxybutyrate in cyanobacteria. *J Biosci Bioeng,* 120**,** 510-7.

HOSCHEK, A., HEUSCHKEL, I., SCHMID, A., BUHLER, B., KARANDE, R. & BUHLER, K. 2019. Mixed-species biofilms for high-cell-density application of Synechocystis sp. PCC 6803 in capillary reactors for continuous cyclohexane oxidation to cyclohexanol. *Bioresource Technology,* 282**,** 171-178.

ISHII-HYAKUTAKE, M., MIZUNO, S. & TSUGE, T. 2018. Biosynthesis and Characteristics of Aromatic Polyhydroxyalkanoates. *Polymers (Basel),* 10.

ISSA, I., DELBRUCK, S. & HAMM, U. 2019. Bioeconomy from experts' perspectives - Results of a global expert survey. *PLoS One,* 14**,** e0215917.

JANASCH, M., ASPLUND-SAMUELSSON, J., STEUER, R. & HUDSON, E. P. 2018. Kinetic modeling of the Calvin cycle identifies flux control and stable metabolomes in Synechocystis carbon fixation. *Journal of Experimental Botany,* 70**,** 973-983.

JENDROSSEK, D. & PFEIFFER, D. 2014. New insights in the formation of polyhydroxyalkanoate granules (carbonosomes) and novel functions of poly(3-hydroxybutyrate). *Environmental Microbiology,* 16**,** 2357-2373.

KADIYALA, G. 2014. *Isolation Purification and Screening of Biodegradable Polymer PHB Producing Cyanobacteria from Marine and Fresh Water Resources*.

KAMRAVA, D., KOVÁCS, T., PFLÜGL, S., DRUZHININA, I., KROLL, P., LACKNER, M. & HERWIG, C. 2018. *Increased poly-B-hydroxybutyrate production from carbon dioxide in randomly mutated cells of cyanobacterial strain Synechocystis sp. PCC 6714: Mutant generation and Characterization*.

KAMRAVAMANESH, D., LACKNER, M. & HERWIG, C. 2018. Bioprocess Engineering Aspects of Sustainable Polyhydroxyalkanoate Production in Cyanobacteria. *Bioengineering (Basel, Switzerland),* 5**,** 111.

KAMRAVAMANESH, D., PFLÜGL, S., NISCHKAUER, W., LIMBECK, A., LACKNER, M. & HERWIG, C. 2017. Photosynthetic poly-β-hydroxybutyrate accumulation in unicellular cyanobacterium Synechocystis sp. PCC 6714. *AMB Express,* 7**,** 143-143.

KATAYAMA, N., IIJIMA, H. & OSANAI, T. 2018. Production of Bioplastic Compounds by Genetically Manipulated and Metabolic Engineered Cyanobacteria. *Adv Exp Med Biol,* 1080**,** 155-169.

KHETKORN, W., INCHAROENSAKDI, A., LINDBLAD, P. & JANTARO, S. 2016. Enhancement of poly-3-hydroxybutyrate production in Synechocystis sp. PCC 6803 by overexpression of its native biosynthetic genes. *Bioresour Technol,* 214**,** 761-8.

KHLYSTOV, N. A., CHAN, W. Y., KUNJAPUR, A. M., SHI, W. C., PRATHER, K. U. & OLSEN, B. D. 2017. Material properties of the cyanobacterial reserve polymer multi-L- arginyl-poly-L-aspartate (cyanophycin). *Polymer,* 109**,** 238-245.

KLEMKE, F., NURNBERG, D. J., ZIEGLER, K., BEYER, G., KAHMANN, U., LOCKAU, W. & VOLKMER, T. 2016. CphA2 is a novel type of cyanophycin synthetase in N-2-fixing cyanobacteria. *Microbiology-Sgm,* 162**,** 526-536.

KLOTZ, A., GEORG, J., BUCINSKA, L., WATANABE, S., REIMANN, V., JANUSZEWSKI, W., SOBOTKA, R., JENDROSSEK, D., HESS, W. R. & FORCHHAMMER, K. 2016. Awakening of a Dormant Cyanobacterium from Nitrogen Chlorosis Reveals a Genetically Determined Program. *Curr Biol,* 26**,** 2862-2872.

KOCH, M., DOELLO, S., GUTEKUNST, K. & FORCHHAMMER, K. 2019. PHB is Produced from Glycogen Turn-over during Nitrogen Starvation in Synechocystis sp. PCC 6803. *Int J Mol Sci,* 20.

KOLLER, M. 2017. Advances in Polyhydroxyalkanoate (PHA) Production. *Bioengineering (Basel),* 4.

LANG, N. J., SIMON, R. D. & WOLK, C. P. 1972. Correspondence of Cyanophycin Granules with Structured Granules in Anabaena-Cylindrica. *Archiv Fur Mikrobiologie,* 83**,** 313-&.

LAW, A. M., LAI, S. W. S., TAVARES, J. & KIMBER, M. S. 2009. The Structural Basis of beta-Peptide-Specific Cleavage by the Serine Protease Cyanophycinase. *Journal of Molecular Biology,* 392**,** 393-404.

LI, W. C., TSE, H. F. & FOK, L. 2016. Plastic waste in the marine environment: A review of sources, occurrence and effects. *Science of The Total Environment,* 566-567**,** 333-349.

LIU, D. & YANG, C. 2014. The Nitrogen-regulated Response Regulator NrrA Controls Cyanophycin Synthesis and Glycogen Catabolism in the Cyanobacterium Synechocystis sp PCC 6803. *Journal of Biological Chemistry,* 289**,** 2055-2071.

LLACER, J. L., FITA, I. & RUBIO, V. 2008. Arginine and nitrogen storage. *Curr Opin Struct Biol,* 18**,** 673-681.

LÖWE, H., HOBMEIER, K., MOOS, M., KREMLING, A. & PFLÜGER-GRAU, K. 2017. Photoautotrophic production of polyhydroxyalkanoates in a synthetic mixed culture of Synechococcus elongatus cscB and Pseudomonas putida cscAB. *Biotechnology for biofuels,* 10**,** 190-190.

LU, J., TAPPEL, R. & NOMURA, C. 2009. *Mini-Review: Biosynthesis of Poly(hydroxyalkanoates)*.

LUEF, K. P., STELZER, F. & WIESBROCK, F. 2015. Poly(hydroxy alkanoate)s in Medical Applications. *Chem Biochem Eng Q,* 29**,** 287-297.

MAHESWARAN, M., ZIEGLER, K., LOCKAU, W., HAGEMANN, M. & FORCHHAMMER, K. 2006. P(II)-Regulated Arginine Synthesis Controls Accumulation of Cyanophycin in Synechocystis sp. Strain PCC 6803. *Journal of Bacteriology,* 188**,** 2730-2734.

MEIXNER, K., KOVALCIK, A., SYKACEK, E., GRUBER-BRUNHUMER, M., ZEILINGER, W., MARKL, K., HAAS, C., FRITZ, I., MUNDIGLER, N., STELZER, F., NEUREITER, M., FUCHS, W. & DROSG, B. 2018. Cyanobacteria Biorefinery — Production of poly(3-hydroxybutyrate) with Synechocystis salina and utilisation of residual biomass. *Journal of Biotechnology,* 265**,** 46-53.

MITSCHKE, J., GEORG, J., SCHOLZ, I., SHARMA, C. M., DIENST, D., BANTSCHEFF, J., VOSS, B., STEGLICH, C., WILDE, A., VOGEL, J. & HESS, W. R. 2011. An experimentally anchored map of transcriptional start sites in the model cyanobacterium Synechocystis sp PCC6803. *Proceedings of the National Academy of Sciences of the United States of America,* 108**,** 2124-2129.

MONSHUPANEE, T., NIMDACH, P. & INCHAROENSAKDI, A. 2016. Two-stage (photoautotrophy and heterotrophy) cultivation enables efficient production of bioplastic poly-3-hydroxybutyrate in auto-sedimenting cyanobacterium. *Scientific Reports,* 6**,** 37121.

MUDLIAR, S. N., VAIDYA, A. N., SURESH KUMAR, M., DAHIKAR, S. & CHAKRABARTI, T. 2007. Techno-economic evaluation of PHB production from activated sludge. *Clean Technologies and Environmental Policy,* 10**,** 255.

NAKAYA, Y., IIJIMA, H., TAKANOBU, J., WATANABE, A., HIRAI, M. Y. & OSANAI, T. 2015. One day of nitrogen starvation reveals the effect of sigE and rre37 overexpression on the expression of genes related to carbon and nitrogen metabolism in Synechocystis sp. PCC 6803. *Journal of Bioscience and Bioengineering,* 120**,** 128-134.

NAMAKOSHI, K., NAKAJIMA, T., YOSHIKAWA, K., TOYA, Y. & SHIMIZU, H. 2016. Combinatorial deletions of glgC and phaCE enhance ethanol production in Synechocystis sp. PCC 6803. *Journal of Biotechnology,* 239**,** 13-19.

NAPPER, I. E. & THOMPSON, R. C. 2019. Environmental Deterioration of Biodegradable, Oxo-biodegradable, Compostable, and Conventional Plastic Carrier Bags in the Sea, Soil, and Open-Air Over a 3-Year Period. *Environmental Science & Technology,* 53**,** 4775-4783.

NARANCIC, T., VERSTICHEL, S., REDDY CHAGANTI, S., MORALES-GAMEZ, L., KENNY, S. T., DE WILDE, B., BABU PADAMATI, R. & O'CONNOR, K. E. 2018. Biodegradable Plastic Blends Create New Possibilities for End-of-Life Management of Plastics but They Are Not a Panacea for Plastic Pollution. *Environmental Science & Technology,* 52**,** 10441-10452.

NODA, I., BLAKE LINDSEY, S. & CARAWAY, D. 2009. Nodax™ Class PHA Copolymers: Their Properties and Applications.

NOWROTH, V., MARQUART, L. & JENDROSSEK, D. 2016. Low temperature-induced viable but not culturable state of Ralstonia eutropha and its relationship to accumulated polyhydroxybutyrate. *FEMS microbiology letters,* 363**,** fnw249.

OBST, M., OPPERMANN-SANIO, F. B., LUFTMANN, H. & STEINBUCHEL, A. 2002. Isolation of cyanophycin-degrading bacteria, cloning and characterization of an extracellular cyanophycinase gene (cphE) from Pseudomonas anguilliseptica strain BI - The cphE gene from P-anguilliseptica BI encodes a cyanophycin-hydrolyzing enzyme. *Journal of Biological Chemistry,* 277**,** 25096-25105.

OBST, M. & STEINBUCHEL, A. 2004. Microbial degradation of poly(amino acid)s. *Biomacromolecules,* 5**,** 1166-1176.

OSANAI, T., NUMATA, K., OIKAWA, A., KUWAHARA, A., IIJIMA, H., DOI, Y., TANAKA, K., SAITO, K. & HIRAI, M. Y. 2013. Increased bioplastic production with an RNA polymerase sigma factor SigE during nitrogen starvation in Synechocystis sp. PCC 6803. *DNA Res,* 20**,** 525-35.

OSANAI, T., OIKAWA, A., NUMATA, K., KUWAHARA, A., IIJIMA, H., DOI, Y., SAITO, K. & HIRAI, M. Y. 2014. Pathway-level acceleration of glycogen catabolism by a response regulator in the cyanobacterium Synechocystis species PCC 6803. *Plant Physiol,* 164**,** 1831-41.

PANDA, B., JAIN, P., SHARMA, L. & MALLICK, N. 2006. Optimization of cultural and nutritional conditions for accumulation of poly-beta-hydroxybutyrate in Synechocystis sp. PCC 6803. *Bioresour Technol,* 97**,** 1296-301.

PANDA, B. & MALLICK, N. 2007. Enhanced poly-beta-hydroxybutyrate accumulation in a unicellular cyanobacterium, Synechocystis sp. PCC 6803. *Lett Appl Microbiol,* 44**,** 194-8.

PARK, S. J., CHOI, J.-I. & LEE, S. Y. 2005. Engineering of Escherichia coli fatty acid metabolism for the production of polyhydroxyalkanoates. *Enzyme and Microbial Technology,* 36**,** 579-588.

PEREZ, R., FORCHHAMMER, K., SALERNO, G. & MALDENER, I. 2016. Clear differences in metabolic and morphological adaptations of akinetes of two Nostocales living in different habitats. *Microbiology-Sgm,* 162**,** 214-223.

PEREZ, R., WORMER, L., SASS, P. & MALDENER, I. 2018. A highly asynchronous developmental program triggered during germination of dormant akinetes of filamentous diazotrophic cyanobacteria. *Fems Microbiology Ecology,* 94.

PHILIP, S., KESHAVARZ, T. & ROY, I. 2007. Polyhydroxyalkanoates: biodegradable polymers with a range of applications. *Journal of Chemical Technology and Biotechnology,* 82**,** 233-247.

PICOSSI, S., VALLADARES, A., FLORES, E. & HERRERO, A. 2004. Nitrogen-regulated genes for the metabolism of cyanophycin, a bacterial nitrogen reserve polymer - Expression and mutational analysis of two cyanophycin synthetase and cyanophycinase gene clusters in the

heterocyst-forming cyanobacterium Anabaena sp PCC 7120. *Journal of Biological Chemistry,* 279**,** 11582-11592.

POSEN, I. D., JARAMILLO, P. & GRIFFIN, W. M. 2016. Uncertainty in the Life Cycle Greenhouse Gas Emissions from U.S. Production of Three Biobased Polymer Families. *Environ Sci Technol,* 50**,** 2846-58.

RAJAN, K. P., THOMAS, S. P., GOPANNA, A. & CHAVALI, M. 2017. Polyhydroxybutyrate (PHB): A Standout Biopolymer for Environmental Sustainability. *In:* MARTÍNEZ, L. M. T., KHARISSOVA, O. V. & KHARISOV, B. I. (eds.) *Handbook of Ecomaterials.* Cham: Springer International Publishing.

REIS, M. A. M., SERAFIM, L. S., LEMOS, P. C., RAMOS, A. M., AGUIAR, F. R. & VAN LOOSDRECHT, M. C. M. 2003. Production of polyhydroxyalkanoates by mixed microbial cultures. *Bioprocess and Biosystems Engineering,* 25**,** 377-385.

REISER, S. E., MITSKY, T. A. & GRUYS, K. J. 2000. Characterization and cloning of an (R)-specific trans-2,3-enoylacyl-CoA hydratase from Rhodospirillum rubrum and use of this enzyme for PHA production in Escherichia coli. *Appl Microbiol Biotechnol,* 53**,** 209-18.

RICHARDSON, J. W., JOHNSON, M. D. & OUTLAW, J. L. 2012. Economic comparison of open pond raceways to photo bio-reactors for profitable production of algae for transportation fuels in the Southwest. *Algal Research,* 1**,** 93-100.

RICHTER, R., HEJAZI, M., KRAFT, R., ZIEGLER, K. & LOCKAU, W. 1999. Cyanophycinase, a peptidase degrading the cyanobacterial reserve material multi-L-arginyl-poly-L-aspartic acid (cyanophycin) - Molecular cloning of the gene of Synechocystis sp PCC 6803, expression in Escherichia coli, and biochemical characterization of the purified enzyme. *European Journal of Biochemistry,* 263**,** 163-169.

RUJNIĆ-SOKELE, M. & PILIPOVIĆ, A. 2017. Challenges and opportunities of biodegradable plastics: A mini review. *Waste Management & Research,* 35**,** 132-140.

SALLAM, A. & STEINBUCHEL, A. 2010. Dipeptides in nutrition and therapy: cyanophycin-derived dipeptides as natural alternatives and their biotechnological production. *Applied Microbiology and Biotechnology,* 87**,** 815-828.

SAMANTARAY, S., NAYAK, J. K. & MALLICK, N. 2011. Wastewater Utilization for Poly-β-Hydroxybutyrate Production by the Cyanobacterium Aulosira fertilissima in a Recirculatory Aquaculture System. *Applied and Environmental Microbiology,* 77**,** 8735-8743.

SARKAR, D., MUELLER, T. J., LIU, D., PAKRASI, H. B. & MARANAS, C. D. 2019. A diurnal flux balance model of Synechocystis sp. PCC 6803 metabolism. *PLoS computational biology,* 15**,** e1006692-e1006692.

SHERMAN, L. A., MEUNIER, P. & COLON-LOPEZ, M. S. 1998. Diurnal rhythms in metabolism: A day in the life of a unicellular, diazotrophic cyanobacterium. *Photosynthesis Research,* 58**,** 25-42.

SIMON, R. D. 1971. Cyanophycin Granules from the Blue-Green Alga Anabaena cylindrica: A Reserve Material Consisting of Copolymers of Aspartic Acid and Arginine. *Proc Natl Acad Sci U S A,* 68**,** 265-7.

SIMON, R. D. 1976. Biosynthesis of Multi-L-Arginyl-Poly(L-Aspartic Acid) in Filamentous Cyanobacterium Anabaena-Cylindrica. *Biochimica Et Biophysica Acta,* 422**,** 407-418.

SIMON, R. D., LAWRY, N. H. & MCLENDON, G. L. 1980. Structural Characterization of the Cyanophycin Granule Polypeptide of Anabaena-Cylindrica by Circular-Dichroism and Raman-Spectroscopy. *Biochimica Et Biophysica Acta,* 626**,** 277-281.

SIMON, R. D. & WEATHERS, P. 1976. Determination of the structure of the novel polypeptide containing aspartic acid and arginine which is found in Cyanobacteria. *Biochim Biophys Acta,* 420**,** 165-76.

SINGH, A. K. & MALLICK, N. 2017. Advances in cyanobacterial polyhydroxyalkanoates production. *FEMS Microbiol Lett,* 364.

SLANINOVA, E., SEDLACEK, P., MRAVEC, F., MULLEROVA, L., SAMEK, O., KOLLER, M., HESKO, O., KUCERA, D., MAROVA, I. & OBRUCA, S. 2018. Light scattering on PHA granules protects

bacterial cells against the harmful effects of UV radiation. *Appl Microbiol Biotechnol,* 102**,** 1923-1931.
STEINBÜCHEL, A. 1992. Biodegradable plastics. *Current Opinion in Biotechnology,* 3**,** 291-297.
STEINLE, A., OPPERMANN-SANIO, F. B., REICHELT, R. & STEINBUCHEL, A. 2008. Synthesis and accumulation of cyanophycin in transgenic strains of Saccharomyces cerevisiae. *Applied and Environmental Microbiology,* 74**,** 3410-3418.
SUDESH, K., TAGUCHI, K. & DOI, Y. 2002. Effect of increased PHA synthase activity on polyhydroxyalkanoates biosynthesis in Synechocystis sp. PCC6803. *International Journal of Biological Macromolecules,* 30**,** 97-104.
SUTHERLAND, J. M., REASTON, J., STEWART, W. D. P. & HERDMAN, M. 1985. Akinetes of the Cyanobacterium Nostoc Pcc 7524 - Macromolecular and Biochemical-Changes during Syndronous Germination. *Journal of General Microbiology,* 131**,** 2855-2863.
TAKAHASHI, H., MIYAKE, M., TOKIWA, Y. & ASADA, Y. 1998. Improved accumulation of poly-3-hydroxybutyrate by a recombinant cyanobacterium. *Biotechnology Letters,* 20**,** 183-186.
TARONCHER-OLDENBURG, G., NISHINA, K. & STEPHANOPOULOS, G. 2000. Identification and analysis of the polyhydroxyalkanoate-specific beta-ketothiolase and acetoacetyl coenzyme A reductase genes in the cyanobacterium Synechocystis sp. strain PCC6803. *Appl Environ Microbiol,* 66**,** 4440-8.
TRAUTMANN, A., WATZER, B., WILDE, A., FORCHHAMMER, K. & POSTEN, C. 2016. Effect of phosphate availability on cyanophycin accumulation in Synechocystis sp PCC 6803 and the production strain BW86. *Algal Research-Biomass Biofuels and Bioproducts,* 20**,** 189-196.
TROSCHL, C., MEIXNER, K. & DROSG, B. 2017. Cyanobacterial PHA Production-Review of Recent Advances and a Summary of Three Years' Working Experience Running a Pilot Plant. *Bioengineering (Basel),* 4.
UNGERER, J. & PAKRASI, H. B. 2016. Cpf1 Is A Versatile Tool for CRISPR Genome Editing Across Diverse Species of Cyanobacteria. *Scientific Reports,* 6**,** 39681.
VAN ALPHEN, P., ABEDINI NAJAFABADI, H., BRANCO DOS SANTOS, F. & HELLINGWERF, K. J. 2018. Increasing the Photoautotrophic Growth Rate of Synechocystis sp. PCC 6803 by Identifying the Limitations of Its Cultivation. *Biotechnol J,* 13**,** e1700764.
VERHOOGT, H., RAMSAY, B. A. & FAVIS, B. D. 1994. Polymer blends containing poly(3-hydroxyalkanoate)s. *Polymer,* 35**,** 5155-5169.
VIEIRA, C. J. A., BOTELHO, M. J., FRANCO, L. B., SILVA, B. V. D., AGUIAR, C. A. P. & DE, M. M. G. 2018. Recent Advances and Future Perspectives of PHB Production by Cyanobacteria. *Industrial Biotechnology,* 14**,** 249-256.
WATZER, B., ENGELBRECHT, A., HAUF, W., STAHL, M., MALDENER, I. & FORCHHAMMER, K. 2015. Metabolic pathway engineering using the central signal processor P-II. *Microbial Cell Factories,* 14.
WATZER, B. & FORCHHAMMER, K. 2018a. Cyanophycin Synthesis Optimizes Nitrogen Utilization in the Unicellular Cyanobacterium Synechocystis sp. Strain PCC 6803. *Applied and Environmental Microbiology,* 84.
WATZER, B. & FORCHHAMMER, K. 2018b. Cyanophycin: A Nitrogen-Rich Reserve Polymer. *Intech open,* DOI: 10.5772/intechopen.77049.
WEISS, G. L., KIENINGER, A. K., MALDENER, I., FORCHHAMMER, K. & PILHOFER, M. 2019. Structure and Function of a Bacterial Gap Junction Analog. *Cell,* 178**,** 374-384 e15.
WEISS, T. L., YOUNG, E. J. & DUCAT, D. C. 2017. A synthetic, light-driven consortium of cyanobacteria and heterotrophic bacteria enables stable polyhydroxybutyrate production. *Metabolic Engineering,* 44**,** 236-245.
WENDT, K. E., UNGERER, J., COBB, R. E., ZHAO, H. & PAKRASI, H. B. 2016. CRISPR/Cas9 mediated targeted mutagenesis of the fast growing cyanobacterium Synechococcus elongatus UTEX 2973. *Microbial Cell Factories,* 15**,** 115.

XIE, J., ZHOU, J., ZHANG, H. & LI, Y. 2011. [Increasing reductant NADPH content via metabolic engineering of PHB synthesis pathway in Synechocystis sp. PCC 6803]. *Sheng Wu Gong Cheng Xue Bao,* 27**,** 998-1004.

YAO, L., CENGIC, I., ANFELT, J. & HUDSON, E. P. 2016. Multiple Gene Repression in Cyanobacteria Using CRISPRi. *ACS Synth Biol,* 5**,** 207-12.

YU, J., LIBERTON, M., CLIFTEN, P. F., HEAD, R. D., JACOBS, J. M., SMITH, R. D., KOPPENAAL, D. W., BRAND, J. J. & PAKRASI, H. B. 2015. Synechococcus elongatus UTEX 2973, a fast growing cyanobacterial chassis for biosynthesis using light and CO2. *Scientific Reports,* 5**,** 8132.

ZHANG, H. W., LIU, Y. H., YAO, C. H., CAO, X. P., TIAN, J. & XUE, S. 2017. FabG can function as PhaB for poly-3-hydroxybutyrate biosynthesis in photosynthetic cyanobacteria Synechocystis sp PCC 6803. *Bioengineered,* 8**,** 707-715.

ZIEGLER, K., DIENER, A., HERPIN, C., RICHTER, R., DEUTZMANN, R. & LOCKAU, W. 1998. Molecular characterization of cyanophycin synthetase, the enzyme catalyzing the biosynthesis of the cyanobacterial reserve material multi-L-arginyl-poly-L-aspartate (cyanophycin). *European Journal of Biochemistry,* 254**,** 154-159.

ZIEGLER, K., STEPHAN, D. P., PISTORIUS, E. K., RUPPEL, H. G. & LOCKAU, W. 2001. A mutant of the cyanobacterium Anabaena variabilis ATCC 29413 lacking cyanophycin synthetase: growth properties and ultrastructural aspects. *FEMS Microbiol Lett,* 196**,** 13-8.

Outlook

Much research has been done on investigating cyanobacterial biopolymers. Nevertheless, so far there are only very few examples of products which have been introduced to the market. Especially for the biopolymers glycogen and polyphosphate, more

Still, technical innovations always occur within the constraints of a political system. The societal awareness for environmental problems, for example caused by single-use plastics, is on the rise. Hence, a regulation of fossil-based-plastic production within the next years seems likely. The introduction of the political framework supporting sustainable products would make the latter more feasible. This could be the case in form of higher taxation of petroleum-based products, by a ban of conventional single-use plastics or by financial support of research regarding sustainable products. All of this will further foster the usage of a carbon neutral production in cyanobacteria.

4. Accepted publication

M. Koch, T. Orthwein, J. T. Alforth, K. Forchhammer (2020).

Investigation of PHB related proteins in Synechocystis sp. PCC 6803 revealed novel phasin Slr0058.

Frontiers in Microbiology, 2020, 11:809

frontiers in Microbiology

ORIGINAL RESEARCH
published: 30 April 2020
doi: 10.3389/fmicb.2020.00809

The Slr0058 Protein From *Synechocystis* sp. PCC 6803 Is a Novel Regulatory Protein Involved in PHB Granule Formation

*Moritz Koch, Tim Orthwein, Janette T. Alford and Karl Forchhammer**

Interfaculty Institute of Microbiology and Infection Medicine, Eberhard Karls Universität Tübingen, Tübingen, Germany

During phases of nitrogen starvation, the photosynthetic cyanobacterium *Synechocystis* sp. PCC 6803 produces polyhydroxybutyrate (PHB). This polymer is of high biotechnological relevance because of its potential as biodegradable plastic. Analysis of the *Synechocystis* genome revealed an operon (*slr0058-slr0061*) containing several genes, which are putatively related to the PHB metabolism. While Slr0058 show similarities with the regulatory phasin PhaF, the protein Slr0060 could serve as an intracellular PHB depolymerase. Investigation of respective knock-out mutants showed no distinct phenotype for the strain lacking Slr0060, whereas the Δ*slr0058* mutant displayed a growth impairment as well as a change in pigmentation. During nitrogen starvation, the Δ*slr0058* mutant produced in average more than twice the amount of PHB granules per cell, while the overall amount of PHB remained the same. This indicates that Slr0058 plays a role in PHB granule formation and controls it surface-to-volume ratio. GFP-tagged Slr0058 did not co-localize with PHB granules during nitrogen starvation but aggregated in distinct foci during vegetative growth. This work helps to better understand the PHB metabolism of *Synechocystis* sp. PCC 6803, coming closer to a sustainable, industrial production of PHB.

Keywords: PHB (poly-(3-hydroxybutyrate)), Cyanobacteria, bioplastic, Sustainability, *Synechocystis* 6803, phasin, PHB-depolymerase, biodegradability

OPEN ACCESS

Edited by:
Thomas E. Hanson, University of Delaware, United States

Reviewed by:
Francisco J. Florencio, University of Seville, Spain
Takashi Osanai, Meiji University, Japan
Cheng-Cai Zhang, Chinese Academy of Sciences (CAS), China

***Correspondence:**
Karl Forchhammer
karl.forchhammer@uni-tuebingen.de

Specialty section:
This article was submitted to Microbial Physiology and Metabolism, a section of the journal Frontiers in Microbiology

Received: *26 February 2020*
Accepted: *06 April 2020*
Published: *30 April 2020*

Citation:
Koch M, Orthwein T, Alford JT and Forchhammer K (2020) The Slr0058 Protein From Synechocystis sp. PCC 6803 Is a Novel Regulatory Protein Involved in PHB Granule Formation. Front. Microbiol. 11:809. doi: 10.3389/fmicb.2020.00809

INTRODUCTION

Cyanobacteria are a diverse group of bacteria, which are able to perform oxygenic photosynthesis. Due to their phototrophic lifestyle they are considered as potential hosts for the sustainable production of industrially relevant compounds. The cyanobacterium *Synechocystis* sp. PCC 6803 (hereafter *Synechocystis*) is one of the best-studied cyanobacterial model strains (Yu et al., 2013). Its fully sequenced genome and the availability of various genetical tools make *Synechocystis* to a versatile microbial chassis (Kaneko et al., 1995; Liu and Pakrasi, 2018). Besides that, *Synechocystis* is also an important strain for basic research, due to its diverse lifestyles, as it supports phototrophic, heterotrophic or mixotrophic growth (Zavřel et al., 2017). Depending on the growth conditions, *Synechocystis* evolved to produce numerous biopolymers, such as polyphosphate, cyanophycin glycogen or polyhydroxybutyrate (PHB) (Damrow et al., 2016). The last two are particularly relevant under the conditions of nitrogen starvation. For this condition, *Synechocystis* has evolved a unique adaptation strategy, namely chlorosis (Collier and Grossman, 1992; Krasikov et al., 2012).

During this highly orchestrated process, the cells undergo a transformation into a resting state, allowing the cells to survive prolonged periods of nitrogen starvation (Schwarz and Forchhammer, 2005). As defined for *Synechococcus elongatus*, chlorosis can be divided into several successive steps (Görl et al., 1998). Immediately upon nitrogen depletion, the cells start to accumulate large quantities of glycogen and they rapidly degrade the major antenna proteins, the phycobiliproteins. Subsequently, in a second phase, the photosynthetic apparatus with chlorophyll *a* is degraded until only traces of photosynthetic activity remain. Finally, the cells enter a state of metabolic quiescence in which they remain viably for prolonged periods of time. In principle, the same process occurs in *Synechocystis*, with the main difference that *Synechocystis* gradually accumulates PHB by glycogen turnover in the second phase of chlorosis (Koch et al., 2019). Upon the addition of nitrogen, the chlorotic process is reversed: in a two-phase event, cells mobilize glycogen to restore their photosynthetic machinery and then switch to phototrophy (Klotz et al., 2016; Doello et al., 2018).

Although *Synechocystis* is a well-studied model strain, many aspects of PHB granule formation and metabolism remain unknown. Until today, the physiological function remains puzzling (Damrow et al., 2016) and only few studies have characterized the physical properties of PHB (Osanai et al., 2013; Troschl et al., 2017). Additionally, many essential components yet have to be discovered, like a PHB degrading depolymerase. So far, only one PHB granule associated protein has been identified, the phasin PhaP, which appears to be involved in controlling the upper size of PHB granules (Hauf et al., 2015). It is known from other PHB producing bacteria that the PHB metabolism is a complex process, where many different proteins are involved. Due to its complexity, the term "carbonosom" was suggested for PHB granules (Jendrossek, 2009). The model strains *Cupriavidus necator* and *Pseudomonas putida* harbor a set of different proteins which are involved in the PHB metabolism, often referred to as phasins. Among them are PHB polymerases (PhaC) and depolymerases (PhaZ and PhaY), transcriptional regulators (PhaI), or other regulatory phasins such as PhaF and PhaM (Pfeiffer and Jendrossek, 2011). Preliminary work in our lab indicated that in an operon of so far uncharacterized proteins, novel PHB associated proteins may be present. This work aims to characterize the two putative phasins Slr0058 and Slr0060 and their role for the PHB metabolism. The knowledge could help to further improve the synthesis of PHB in cyanobacteria for a sustainable production of bioplastics.

MATERIALS AND METHODS

All experiments shown in this work are based on three biological replicates unless stated otherwise. The arithmetic mean was calculated including the standard deviation, as indicated by the error bars at each measurement point.

Cyanobacterial Cultivation Conditions

For preculturing and growth experiments, *Synechocystis* was cultivated in BG_{11} medium (Rippka et al., 1979). All cultivations with *Synechocystis* were performed in baffle free Erlenmeyer shaking flasks. Standard cultivation was performed at 28°C with 125 rpm shaking and continuous illumination of ∼50 μE m^{-2} s^{-1} unless stated otherwise. Aeration was ensured by continuous shaking and ambient air. No additional gassing with CO_2 was applied. Either 50 or 200 ml of cell suspension were cultivated in 100 or 500 ml Erlenmayer flasks, respectively. Whenever necessary, appropriate antibiotics were added to the different strains to ensure the continuity of the mutation.

Chlorosis was induced by changing the medium to nitrogen-depleted BG_0, which contains the same components as BG_{11}, except sodium nitrate. For the medium change, *Synechocystis* cultures were precultivated in BG_{11} medium up to an OD_{750} of ∼0.8. The cells were washed with BG_0. For this, the cells were centrifuged, resuspended in BG_0 medium and adjusted to OD_{750} of 0.4. Cells were resuscitated from nitrogen starvation by exchanging the growth medium to standard BG_{11}.

For viability assays, BG_{11} plates containing 1.5% agar were used. Cultures of OD_{750} = 0.4 (10^0) were diluted to 10^{-1}, 10^{-2}, 10^{-3}, and 10^{-4}. Of each dilution, 5 μl were dropped on a BG_{11} agar plate. The plates were cultivated seven days at either continuous light or day-night conditions (12 h light and 12 h darkness).

A list of all used strains for this study is provided in **Supplementary Table S1**.

Molecular Cloning and Transformation Into Synechocystis

For the assembly of DNA, Gibson cloning was used (Gibson et al., 2009). Lists of all used primers and plasmids of this study are provided in **Supplementary Tables S2, S3**. Cultivation of *Escherichia coli* was done as previously described (Sambrook, 2001). Successful cloning was verified via sequencing. Transformation into *Synechocystis* cells were done via natural transformation in the case of insertions in the genome. Successful segregation was checked via colony PCR. Whenever transient plasmids were introduced, triparental mating was used.

Microscopy and Staining Procedures

The visualization of PHB granules was achieved via Nile red staining and subsequent analysis using fluorescent microscopy. For this purpose, the Leica DM5500 B with the Leica CTR 5500 illuminator was used. The integrated Leica DFC 360 FX camera was used for image acquisition. Settings were adjusted by the Leica Application Suite Advanced Fluorescence (4.0). For staining of PHB granules, 100 μl *Synechocystis* culture was centrifuged at 16.000 × *g* for 1 min. The supernatant (80 μl) was discarded and the pellet was resuspended 10 μl Nile red solution (1 μg/ml). From this mixture, 10 μl were dropped on an agarose coated microscope slide and were observed with 1000-fold magnification using the Leica HCX PL FLUATAR (100x/1,30 PH3) with immersion oil. The fluorescence of Nile red was induced with light of 558 nm wavelength (Cy3 channel). For electron microscopy pictures, *Synechocystis* cells were stained using glutaraldehyde and potassium permanganate. Subsequently, ultrathin sections were stained with citrate and

uranyl acetate, as described before (Fiedler et al., 1998). The samples were then examined, using a Philips Tecnai 10 electron microscope at 80 kHz.

PHB Quantification

Polyhydroxybutyrate was quantified by high-performance liquid chromatography (HPLC) of crotonic acid. For this, a volume of 11 ml chlorotic culture (or ∼25 ml of vegetative culture) was centrifuged at 4,000 × *g* for 10 min at room temperature. The supernatant was discarded, and the pellet transferred into a pre-balanced 2 ml reaction tube. Subsequently the pellet was dried with a vacuum dryer. The reaction tube was cradled again and the cell dry weight (CDW) of the culture was calculated. The cells were boiled for 1 h in concentrated H_2SO_4 (18 M). During this treatment, the cells were lysed and PHB converted to crotonic acid. Next, 110 µl of this solution was diluted 1:10 with 14 mM sulfuric acid solution and centrifuged 5 min at 25,000 × *g*. Subsequently, 500 µl of the clear supernatant was mixed with 500 µl 14 mM H_2SO_4, pelleted again and 300 µl of the supernatant was used for analytical HPLC. For this, a HP1090 M chromatography system was used, equipped with a thermostated autosampler und diode-array-detector, HP Kayak XM 600 workstation. The crotonic acid was detected by measuring the absorbance at 210 nm.

Glycogen Quantification

The glycogen content of *Synechocystis* cultures was detected as described previously (Grundel et al., 2012) with modifications described (Klotz et al., 2016). In short, 2 ml of cell culture were centrifuged for 1 min at 16,000 × *g*. The supernatant was discarded, and the pelleted cells were used for the measurement. Degradation of glycogen was performed with 4,4 U/µl amyloglucosidase from *Aspergillus* (Sigma Aldrich) for 2 h at 60°C. The concentration of resulting glucose units was measured with an o-toluidine assay at a wavelength at 635 nm. The glycogen concentration was determined by comparison with a glucose standard calibration curve.

Spectra and Pigment Determination

The absorption spectra between 350 and 750 nm of *Synechocystis* strains were detected with a Specord50 and the software WinAspect (Jena Analytik). The content of chlorophyll *a* (Chl *a*) in cells was detected with a methanol extraction method. For this, 1.5 ml of an exponential culture was transferred into a 1.5 ml reaction tube and centrifuged at 10,000 × *g* for 10 min. The supernatant was discarded, and the pellet was resuspended in 90% Methanol. The suspension was mixed and subsequently incubated for 30 min in the dark. The suspension was centrifuged again and the supernatant was transferred into a 1.5 ml reaction tube. Another 500 µl 90% methanol were added to the cell pellet and treated as described above. Both supernatants were combined and transferred into a cuvette. The absorbance was measured at wavelengths of 665 and 650 nm, and the Chl *a* concentration was calculated according to the equation previously described (Richmond and Hu, 2013).

Pulse-Amplitude-Modulation Fluorometry

The pulse-amplitude-modulation fluorometry (PAM) was used to detect the photosynthetic activity by measuring the relative quantum yield of photosystem (PS) II of the photosynthetic apparatus. For this, the WATER-PAM Chlorophyll Fluorometer with WinControl Software of Heinz Walz GmbH (Effeltrich) was used. In the measuring cuvette, cell suspensions between OD_{750} = 0.4 – 1 were diluted 1:20. The cuvette was placed in the measuring device and the yield was measured three times with a time constant of 30 s.

Overexpression and Purification of Slr0058

Escherichia coli Lemo21 (DE3) (NEB) containing the plasmid pET15b-slr0058-His was grown overnight at 37°C in 5 ml LB-medium containing 50 µg/ml ampicillin and 30 µg/ml chloramphenicol. The Cells were transferred into 1 l of fresh LB-medium, containing the same antibiotics and growth was continued at 37°C to an OD_{600} of 0.6. Slr0058 overexpression was induced by the addition of 0.5 mM IPTG to the culture, which was subsequently grown overnight at 20°C. Cells were harvested by centrifugation at 6500 rpm for 10 min at 4°C. The resulting pellet was resuspended in buffer containing 300 mM NaCl, 50 mM NaH_2PO_4, 10 mM imidazole, 1 mM DTT, 0.2 mM PMSF, DNase I and was adjusted to pH 8. The cells were lysed by four cycles of ultrasonication (Branson Ultrasonics™), with a sonication time of 3 min per cycle. Remaining cells and cell debris were removed by centrifugation at 10000 rpm for 60 min at 4°C and subsequently filtering the resulting supernatant through a 0.45 µm syringe filter. The supernatant was loaded on a 1 mL HisTrap FF Ni-NTA column (GE Healthcare), using a flowrate of 1 ml/min. The column was washed with buffer (pH 8) containing 300 mM NaCl, 50 mM NaH_2PO_4, and 20 mM imidazole followed by a washing step with an imidazole concentration of 40 mM to remove unspecifically bound protein. Finally, the His-tagged protein was eluted by increasing the imidazole concentration to 250 mM. The eluted protein was transferred to a buffer containing 100 mM KCl, 50 mM Tris–HCl, pH 7.8, 5 mM $MgCl_2$, 1 mM DTT, 0.5 mM EDTA and 50% (v/v) glycerol via dialysis overnight at 4°C and then stored at −20°C. The eluted protein, as well as samples from each purification step were analyzed by SDS-PAGE.

Size Exclusion Chromatography

To investigate the size and oligomerization states of Slr0058, size exclusion chromatography was performed on a ÄKTAmicro (GE Healthcare) using a Superose™ 6 Increase 10/300 GL column (GE Healthcare). The column was equilibrated with a buffer containing 100 mM KCl, 50 mM Tris–HCl, pH 7.8 and 5 mM $MgCl_2$. The Slr0058 protein was transferred into the same buffer and a volume of 100 µl with a concentration of 0.313 mg/ml was used for the size exclusion chromatography. Data were analyzed with UNICORN 5.20.

RESULTS

By analyzing the *Synechocystis* genome for putative homologies of phasins, we identified an operon of genes of unknown function, containing members that show similarities to phasins from other organisms. The transcriptional unit TU2718 consists of four genes, namely *slr0058 – slr0061*. Transcriptome analysis revealed that the entire operon is upregulated during chlorosis (Mitschke et al., 2011; Klotz et al., 2016). For one of these proteins, a BLAST analysis revealed that the protein Slr0058 has similarity with the protein PhaF of *Pseudomonas putida*. This protein ensures an equal distribution of the PHB granules among the daughter cells during cell division by attaching the granules to the chromosome (Maestro et al., 2013). Unlike PhaF from *P. putida* Slr0058 showed no DNA binding domain though (**Figure 1**).

Another gene in this operon, *slr0060*, encodes a protein, which was previously isolated during the purification of PHB granules. Subsequent bioinformatic analysis showed that Slr0060 was only found in cyanobacteria known to produce PHB (Schlebusch, 2012). A recent proteome study revealed distinct compartment organization of the *Synechocystis* proteins. Here Slr0060 was found in a distinct group together with other PHB related proteins, PhaP, PhaE and PhaC, further supporting its relevance for PHB metabolism (Baers et al., 2019). BLAST search of Slr0060 predicts a patatin domain, which was also found in phospholipases/acylesterases. This indicates that Slr0060 might serve as an intracellular PHB depolymerase (1 B).

To characterize the function of *slr0058* and *slr0060*, knock-out strains were constructed (pMK17 and pMK16, respectively). For this, the genes were replaced by an antibiotic-cassette using double homologous recombination. Plasmids containing DNA fragments, which are flanked by homologous sequences of *slr0058* or *slr0060*, were transferred into *Synechocystis* by natural transformation. To prevent any unintended effects on genes located downstream of the deleted gene, the native promoter was introduced downstream of the antibiotic cassettes. The structure of the plasmids is shown in **Supplementary Figure S1**.

The construction of pMK16 and pMK17 was performed using Gibson Assembly. The vector backbone pUC19 was linearized using the restriction enzymes *Xba*I and *Pst*I. Successful cloning was verified by colony PCR and subsequent sequencing. From now on, *Synechocystis* mutants transformed with pMK16 are referred to as Δ*slr0060* and mutants edited with pMK17 as Δ*slr0058*.

Growth Behavior of Δ*slr0058* and Δ*slr0060* Strains

To characterize the created mutant strains Δ*slr0058* and Δ*slr0060*, their growth in liquid medium under various culturing

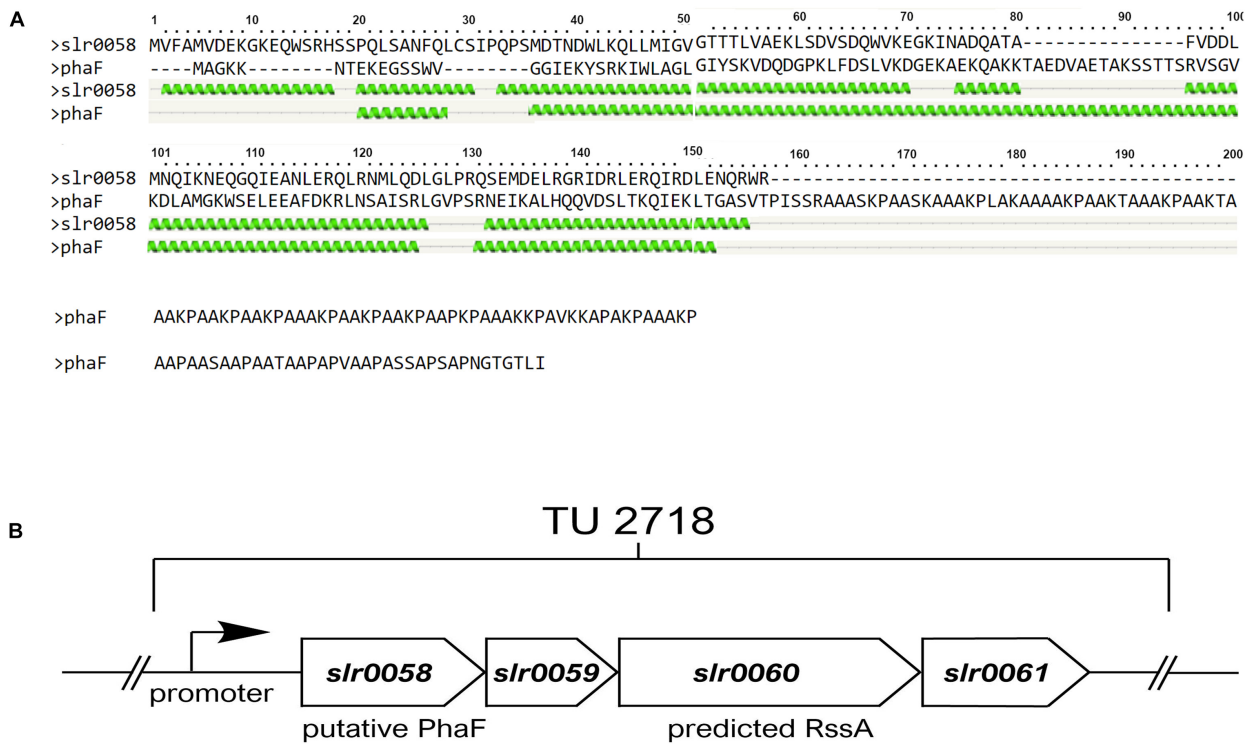

FIGURE 1 | *In silico* analysis of a PHB related gene cluster. **(A)** Sequence allignment and the predicted structure of PhaF from *Pseudomonas putida* and Slr0058 from *Synechocystis*. Both proteins show regular pattern of helix structures at the N-terminus (indicated as green helices). Unlike PhaF, Slr0058 shows no prolonged C-terminal coil structure though, which is important for the interaction with the DNA in *Pseudomonas putida*. **(B)** Schema of the transcriptional unit 2718 in *Synechocystis.* The operon contains four genes, *slr0058–slr0061*. Two of them, namely *slr0058* and *slr0060*, have sequence similarities with either PhaF, or a PHB depolymerase, respectively.

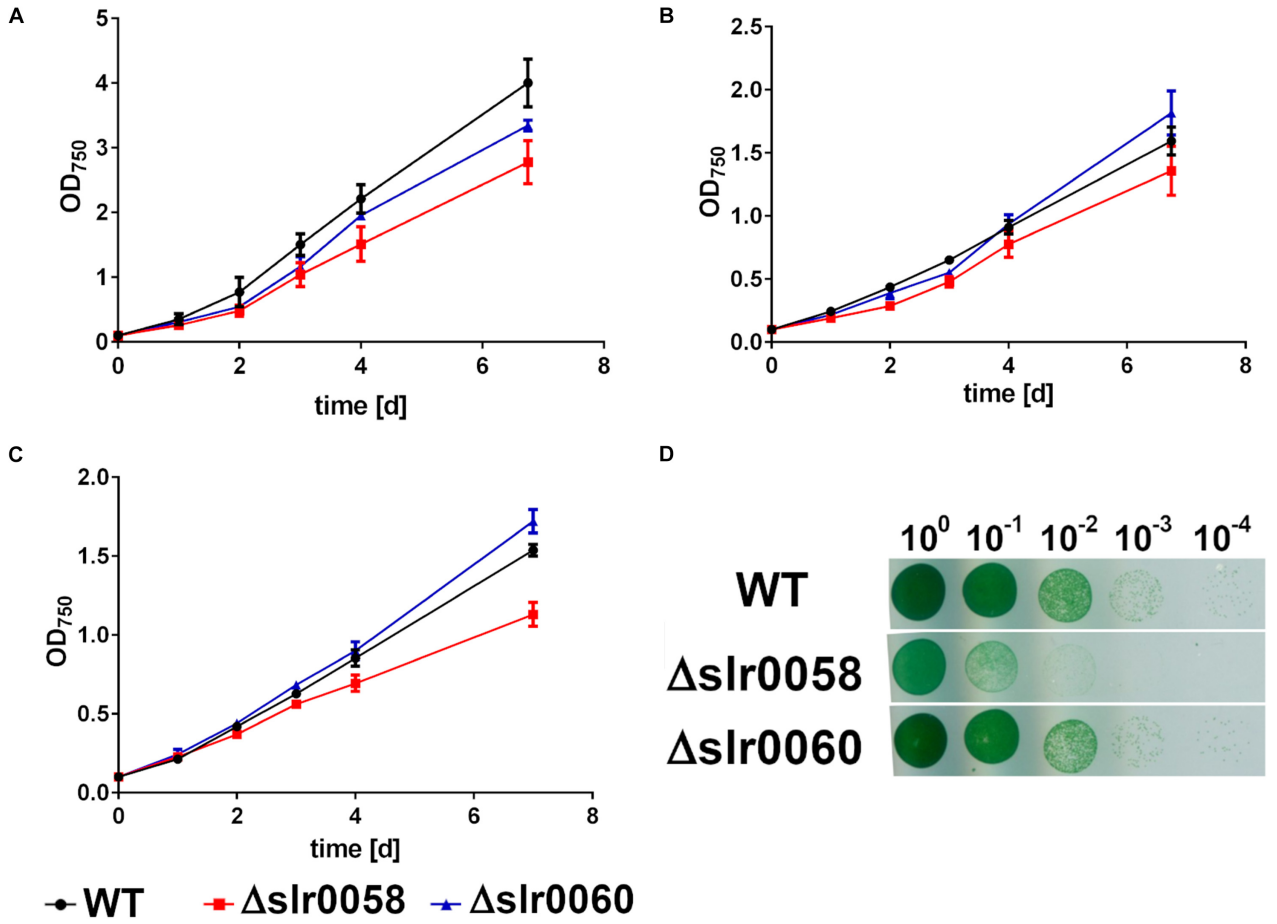

FIGURE 2 | Growth behavior of WT, Δ*slr0058*, and Δ*slr0060* at different cultivation conditions. **(A)** Cultivation under continuous illumination and with shaking. **(B)** Cultivation with 12 h day/night cycle and shaking. **(C)** Cultivation with 12 h day/night cycle and without shaking. Each point represents a mean of three independent biological replicates. **(D)** Growth determination using the drop plate method of 10-fold dilutions at continuous light cultivation. The plate shown in the figure is representative for three individually grown biological replicates.

conditions and on solid agar plates was compared to a wildtype strain (WT) (**Figure 2**).

To characterize the growth in liquid medium, several combinations of illumination and shaking were tested. Besides standard laboratory conditions, where the cells were shaken under continuous illumination, they were also grown under naturally occurring day-night rhythm. Here they were either shaken or grown under standing conditions resulting in reduced aeration (**Figures 2A–C**, respectively). Cell growth was observed by measuring OD_{750} every 24 h of three independent biological replicates. Under all conditions, the strains WT and Δ*slr0060* showed similar growth. In contrast, the strain Δ*slr0058* showed a slight growth deficiency under all tested conditions. The strongest effect was visible during day-night rhythm with standing cultures (**Figure 2C**). The growth deficiency was even more clearly visible during growth on solid agar plates (**Figure 2D**).

Besides the different growth characteristics, the strains showed also a difference in their pigmentation. While only little differences were visible between the color of WT and Δ*slr0060* strains, the Δ*slr0058* culture appeared more bluish (**Figure 3A**).

Spectral analysis revealed that a slightly reduced absorption at ∼430 nm for the strain Δ*slr0058,* indicating a lower abundancy of Chl *a* content (**Figure 3B**). This correlates well with the measured chlorophyll content, which was reduced in the strain Δ*slr0058* compared to the WT (2.33 to 2.83 $\mu g/10^8$ cells, respectively). While the strain Δ*slr0060* showed higher values of chlorophyll content (3.53 $\mu g/10^8$ cells), no strong difference was visible in the appearance of the culture. During vegetative growth, the amount of PHB produced in the WT and Δ*slr0060* were below the detection limit (**Figure 3C**). In contrast, the mutant strain Δ*slr0058* produced detectable amounts of PHB during exponential and stationary growth (∼2 and ∼1%/CDW, respectively) under diurnal light/dark regime. Despite the presence of considerable amounts of PHB, no fluorescent granules could be observed by microscopy after staining the cells with BODIPY. This indicates that PHB produced during vegetative growth is not aggregated into stainable PHB granules. When grown under continuous light, there was no PHB detected in any of the strains.

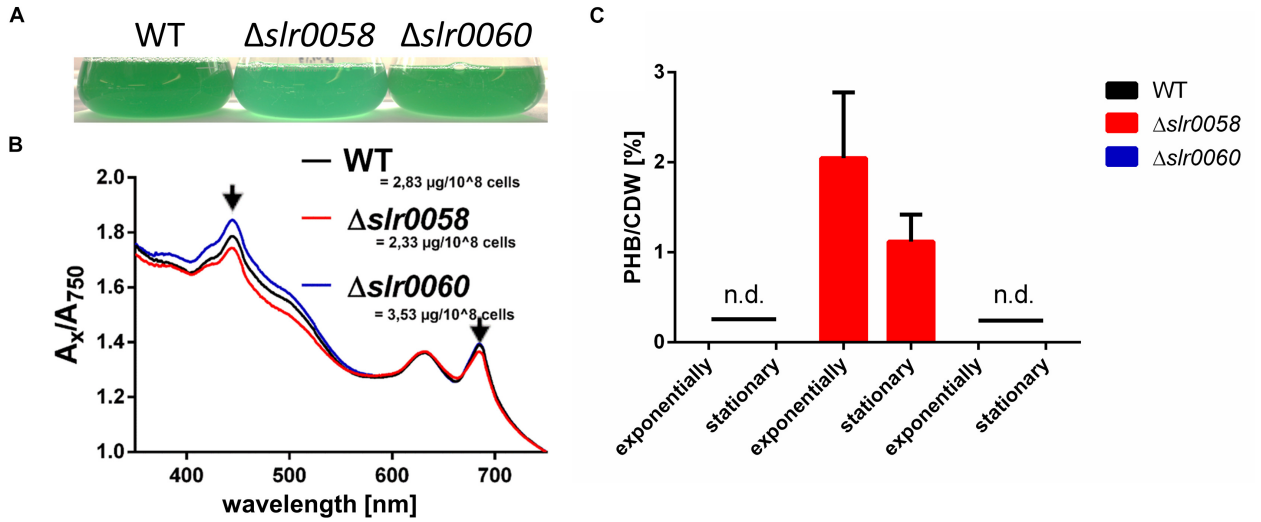

FIGURE 3 | Phenotypical analysis of WT, Δ*slr0058*, and Δ*slr0060* during vegetative growth. **(A)** Picture of representative WT, Δ*slr0058* and Δ*slr0060* cultures, at OD_{750} = 0.8. **(B)** Spectra and chlorophyll *a* concentrations of the same cultures as in panel **(A)**. **(C)** PHB produced during vegetative growth. Samples were taken during exponential or stationary growth phases (OD_{750} ∼1 or ∼4, respectively). The values measured for the WT and Δ*slr0060* were below to the detection limit. n.d. = not detectable.

Mutant Phenotype During Chlorosis

To determine the effect of the absence of Slr0058 and Slr0060 during conditions where PHB is formed, chlorosis was induced by shifting the cultures to nitrogen-depleted medium. As previously reported from our laboratory, PHB is mainly formed from glycogen. Hence, PHB and glycogen were measured during the course of 28 days (**Figures 4A,B**).

In all three strains the intracellular PHB increased over time. As compared to the WT, both mutant strains showed reduced amounts of PHB during the course of the experiment. Like in previous studies, the cells rapidly accumulated glycogen during the initial phase of the chlorosis, to a maximum level which then slowly declined. Although the overall pattern was similar. the two mutant strains showed slightly elevated glycogen values compared to the WT. The OD_{750} of the WT and Δ*slr0060* were comparable and remained constant during the course of chlorosis. In contrast, the OD_{750} of Δ*slr0058* constantly decreased during the 4 weeks of the experiment (**Supplementary Figure S2A**). This decrease indicates a decrease in cell number, suggesting that the Δ*slr0058* mutant is impaired in maintaining long-term viability.

To estimate size and number of PHB granules, cells in chlorosis for 21 days were stained with Nile red and analyzed using fluorescence microscopy (**Figures 4C,D**).

The strain Δ*slr0058* showed a strong increase in the amount of PHB granules compared to the WT and the Δ*slr0060* strain (**Figure 4C**). To quantify this, the visible granules from 70 cells in three biological replicates were counted and plotted in a box blot (**Figure 4D**). The granule number was determined within 28 days of nitrogen depletion. The analysis confirmed the visible effect of the microscopic pictures of an altered granule number within the strains. The WT and Δ*slr0060* showed very similar amounts of PHB granules. Compared to this, Δ*slr0058* showed a more than 2-fold increase in the number of granules. This observation was also confirmed by electron microscopic pictures (**Figures 4E–G**).

As already indicated by fluorescence microscopy (**Figure 4C**), the Δ*slr0058* mutant cells (**Figure 4F**) contained a strongly increased number of PHB granules compared to the WT and Δ*slr0060* cells (**Figures 4E,G**, respectively).

Similar than during exponential growth, the cultures showed a difference in their pigmentation (**Figure 5A**). Compared to the WT, the culture was less pigmented, indicating a reduction in the carotenoid content. This assumption was confirmed by a spectral analysis of the cultures, where a lower absorption between 450 and 550 nm is visible (**Figure 5B**).

To check if the phenotypes observed for the Δ*slr0058* strain, in particular the growth impairment and altered pigmentation are related to the synthesis of PHB, a mutant lacking the PHB synthase was created by deleting the *phaEC* operon (Δ*phaEC* strain). To validate how the absence of PHB synthesis affects the phenotype of the Δ*slr0058* strain, both deletions were combined in one strain (Δ*slr0058* and Δ*phaEC*). As shown in **Figure 5**, the deletion of *phaEC* complemented the phenotype of the Δ*slr0058* strain by restoring the original color (**Figures 5A,B**). The double mutant Δ*slr0058*Δ*phaEC* showed also no difference in its growth behavior compared to the WT (**Figure 5C**). This suggests that the phenotype of the Δ*slr0058* strain is caused by the formation of PHB in the absence of Slr0058 protein.

Resuscitation From Nitrogen Chlorosis

A putative PHB depolymerase is expected to be most active during conditions of PHB degradation. Since such conditions should prevail during resuscitation from nitrogen chlorosis, recovery experiments of long-term nitrogen-starved cells were performed. A mutant lacking PHB depolymerase should be unable to degrade PHB during the recovery from chlorosis.

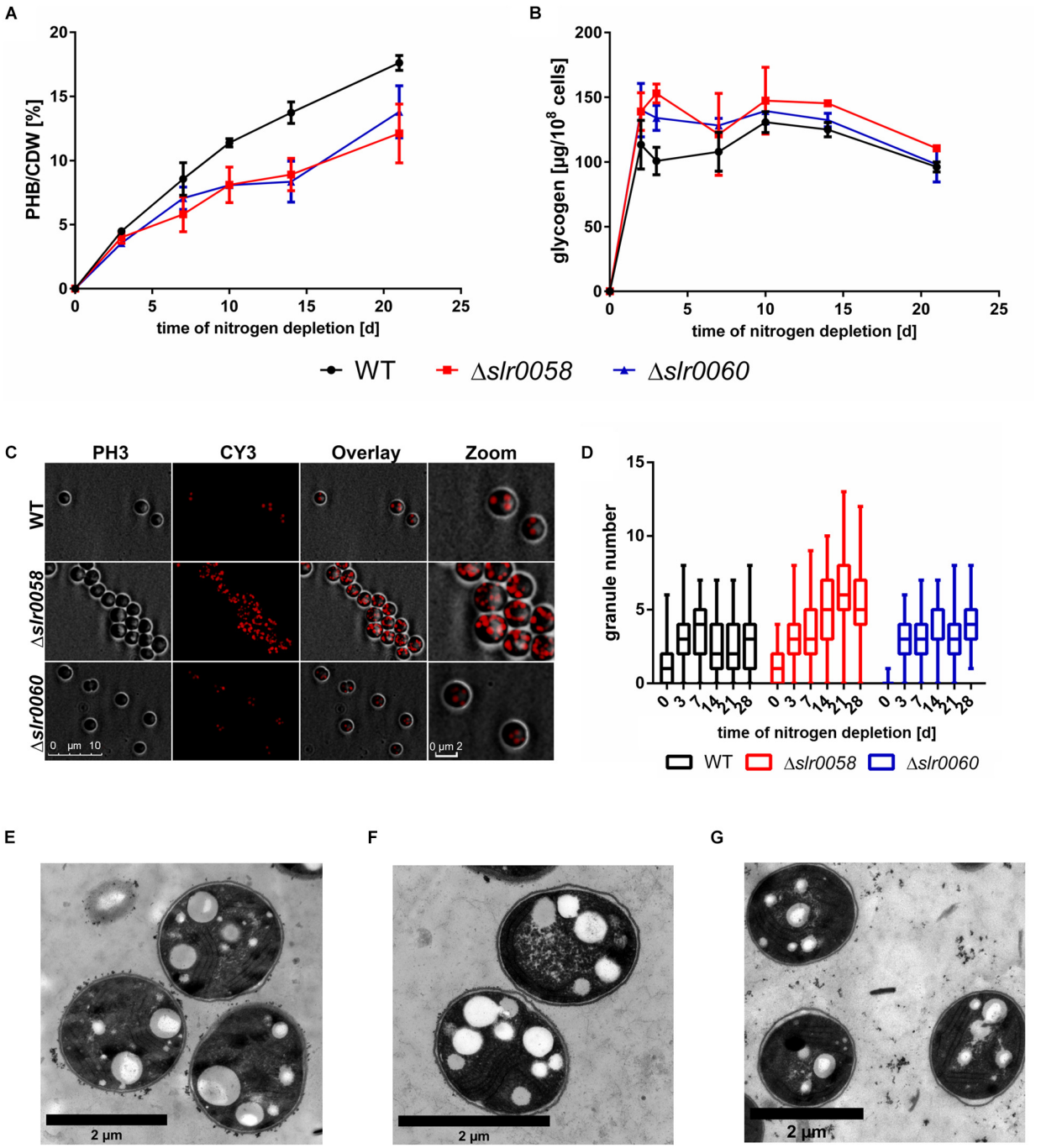

FIGURE 4 | Phenotypical analysis of WT, Δ*slr0058*, and Δ*slr0060* during chlorosis. **(A)** Accumulation of PHB per cell dry weight (CDW) during 21 days of chlorosis. **(B)** Accumulation of glycogen normalized to OD_{750} during 21 days of chlorosis. Each point represents a mean of three independent biological replicates. **(C)** 3-D deconvoluted microscopic images of 21-day nitrogen depleted cultures of all three strains. The cells were stained with Nile red to visualize PHB granules. From left to right: image of the phase contrast channel; image of the Cy3 channel with Nile-red stained PHB granules; overlay of both channels. **(D)** Box plot of the granule number at different time points of chlorosis. Each time point represents the count of 70 cells in three independent cultures. The line within the boxes represents the median. **(E–G)** Electron microscopic pictures of WT **(E)**, Δ*slr0058* **(F)**, and Δ*slr0060* **(G)** cells after 17 days of nitrogen starvation. PHB granules are visible as white inclusions inside the cell.

Furthermore, such experiments could reveal differences between different strains in their efficiency to recover from nitrogen starvation. The experiments were performed with 14-day chlorotic cultures. The levels of PHB were determined every 24 h for four consecutive days and a final measurement after 1 week. The amount of PHB was normalized against the cell-dry-weight

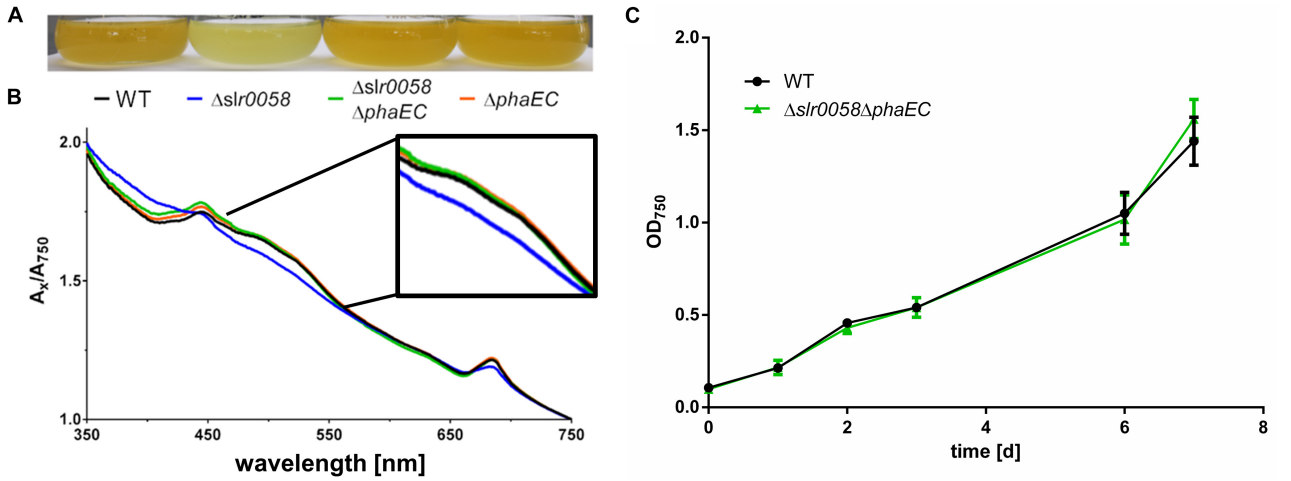

FIGURE 5 | Photograph **(A)** and spectra **(B)** of WT, Δ*slr0058* and Δ*slr0060* cultures during chlorosis compared with a PHB free mutants (Δ*phaEC*). The spectra of the different strains were normalized to OD_{750} = 1. **(C)** Growth behavior of WT and Δ*slr0058*Δ*phaEC* with 12 h day/night cycle and without shaking.

(CDW) as well as against the culture volume (to consider the increase of CDW due to cell growth). Before and after each sampling, the cultures were weighted, and the evaporated volume was restored with sterile ultrapure water. The results of PHB during recovery are shown in **Figure 6**.

When normalized to the CDW, the amount of PHB per CDW in all three strains decreased steadily during the course of 5 days, as already shown previously (**Figure 6A**). In contrast, when the absolute quantity of PHB per culture volume was determined, a surprising different pattern appeared. The total amount of PHB remained constant in all three strains during the entire resuscitation process (**Figure 6B**). Since PHB is usually normalized to the CDW, this observation has not been made before. While the overall amount of PHB remained constant, the abundance of granules declined in all three strains ($\bar{X}_{\mathrm{WT,0d}} = 2.8 \pm 1.6$, $\bar{X}_{\mathrm{WT,3d}} = 1.7 \pm 1.4$; $\bar{X}_{\Delta slr0058,0d} = 5.5 \pm 2.0$, $\bar{X}_{\Delta slr0058,3d} = 2.4 \pm 2.7$; $\bar{X}_{\Delta slr0060,0d} = 3.7 \pm 1.7$, $\bar{X}_{\Delta slr0060,3d} = 1.4 \pm 1.1$) (**Figure 6C**).

To test whether the mutants were affected in their pigmentation during the recovery from nitrogen starvation, spectra measurements were performed. Additionally, the same cultures were used to test their viability after chlorosis via a drop-plate assay, shown in **Figure 7**.

The whole cell spectrum of WT cells at the beginning of the resuscitation shows the typical wavelength-dependent light scattering of low-pigmented cells (**Figure 7A**). After 2 days of recovery, distinctive absorption peaks for Chl *a* and phycobiliproteins appear at 430, 625, and 680 nm. The same appearance of absorption peaks was observed in the mutant strains Δ*slr0058* and Δ*slr0060* (**Figures 7B,C**). However both strains showed a visible delay. Particularly Δ*slr0060* required 2 days more to reach the same absorption in the range from 350 to 400 nm as the WT.

The recovery assays via the drop-plate method performed under continuous light or day-night rhythm (**Figures 7D,E**, respectively) revealed an impairment of the Δ*slr0058* strain. This impairment of growth for Δ*slr0058* was also visible when chlorotic cells resuscitated in liquid culture (**Supplementary Figure S2B**). However, the impairment of growth is in the same order of magnitude as during normal growth, indicating that this effect can be explained by a growth delay and not a deficiency during the recovery process. During the resuscitation, no difference in the recovery rate of the photosynthetic activity was visible (**Supplementary Figure S3**).

Complementation of Δ*slr0058* and Intracellular Localization of Slr0058

The results of the Δ*slr0058* characterization showed that the Δ*slr0058* phenotypes are connected to the formation of PHB. To validate that the phenotype can be traced back to the deleted gene, a complementation strain of the gene *slr0058* was created (*slr0058*-pMK23). The latter is expected to restore the WT-phenotype. Additionally, the expression of a green fluorescence protein (GFP) tagged to Slr0058 (pMK25) should reveal its localization via fluorescence microscopy. The design of both constructs is shown in **Supplementary Figure S4**.

The assembly of the plasmids was done via Gibson Assembly. After transformation into *Synechocystis* cells, positive clones were screened via colony PCR. To ensure a successful complementation, the PHB granules were counted after one and 2 weeks in the WT, the *slr0058* and the complemented *slr0058*-pMK23 strain (**Figure 8**).

As expected, the insertion of pMK23 into the background of Δ*slr0058* restored the WT-phenotype, with respect to the average PHB granule number per cell. The WT and the Δ*slr0058*pMK23 complemented strain contained around three granules per cell on average ($\bar{X}_{\mathrm{WT,7d}} = 3.2 \pm 0.1$, $\bar{X}_{\mathrm{WT,14d}} = 3.1 \pm 0.1$; $\bar{X}_{\Delta slr0058\mathrm{pMK23},7d} = 3.4 \pm 0.1$, $\bar{X}_{\Delta slr0058\mathrm{pMK23},14d} = 3.2 \pm 0.1$). Compared to this, the average amount of granules in the strain Δ*slr0058* were almost 2-fold higher compared to the WT and the complemented strain ($\bar{X}_{\Delta slr0058,7d} = 5.5 \pm 0.2$, $\bar{X}_{\Delta slr0058,14d} = 5.7 \pm 0.2$). The results show that the effect

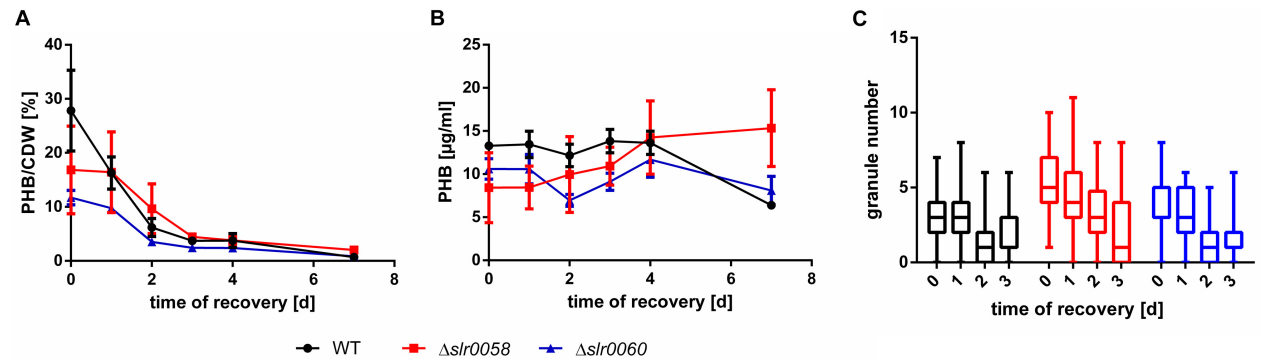

FIGURE 6 | PHB amount and granule number in WT, Δ*slr0058* and Δ*slr0060* during resuscitation from 14-day chlorosis. **(A)** PHB amount normalized to the cell dry weight and **(B)** absolute amounts per volume. Each point represents a mean of three independent samples. CDW = cell-dry-weight. **(C)** Box plot of the granule number within the first 3 days of resuscitation. Each time point represents the count of >100 cells in three independent cultures. The line within the boxes represents the median.

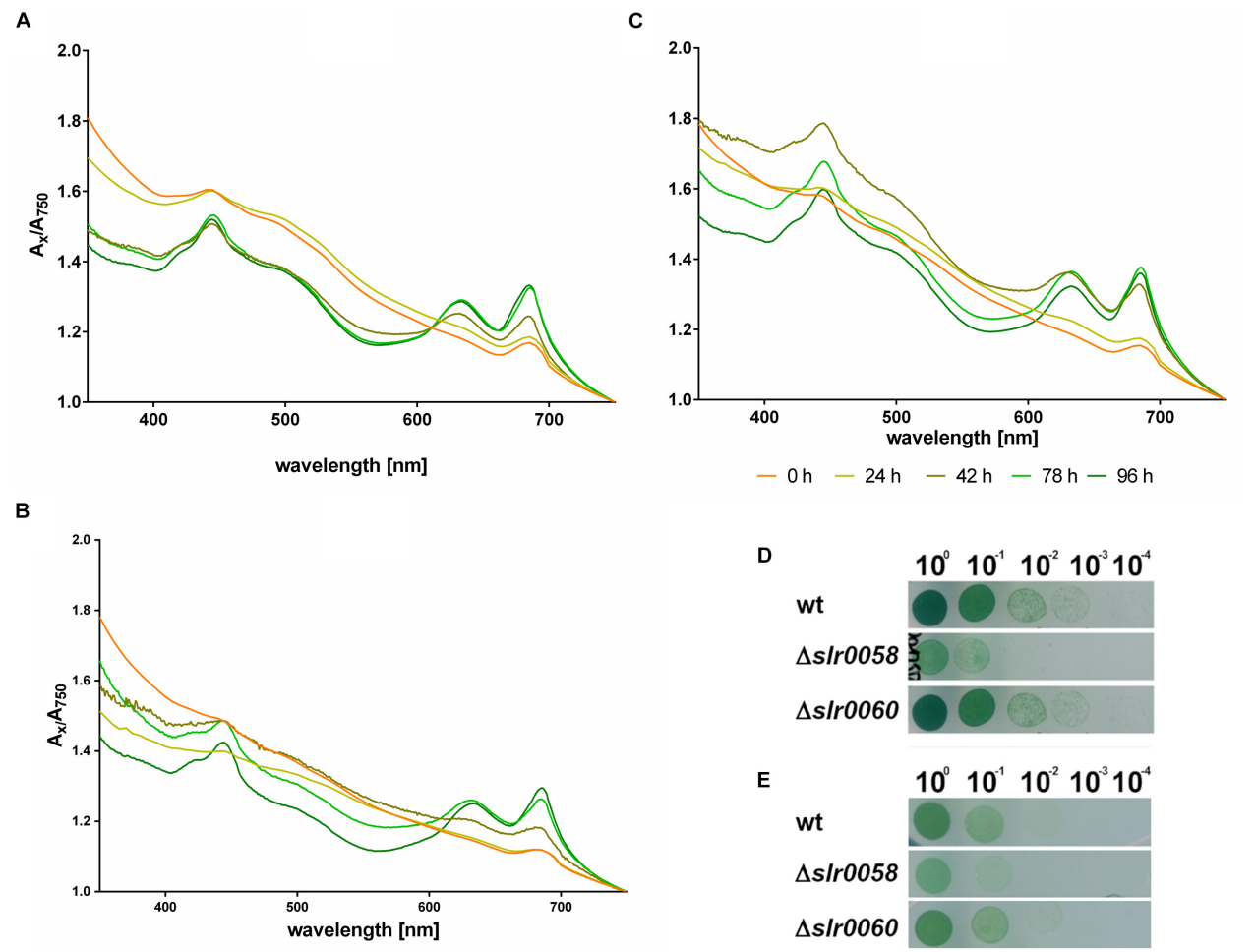

FIGURE 7 | Pigment synthesis during resuscitation and viability after 14 days of chlorosis. Whole cell spectra from 350 to 750 nm of WT **(A)**, Δ*slr0058* **(B)** and Δ*slr0060* **(C)** after 0–4 days of resuscitation from nitrogen starvation. Each line represents the mean of the spectra from three independent biological triplicates. The spectra were normalized to their corresponding value at 750 nm. **(D)** Viability assays via drop-plate method as visible after 7 days of incubation under continuous illumination **(E)** and day-night illumination after 14 days of chlorosis. The images show a representative assay of triplicates.

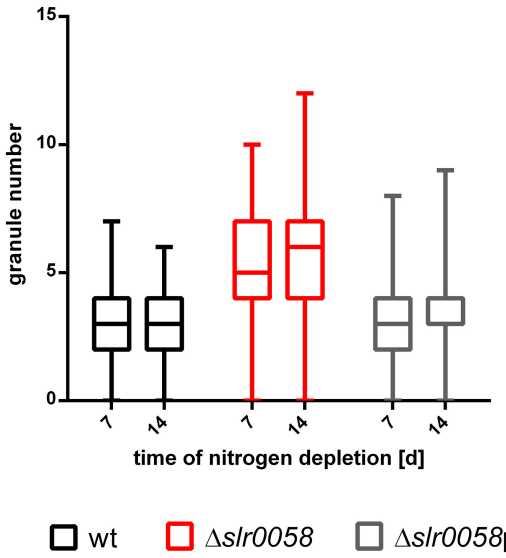

FIGURE 8 | Box plot of the granule number at different time points of chlorosis of WT, Δ*slr0058* and complemented Δ*slr0058*pMK23. Each time point represents the result of a count of 150 cells in three independent cultures.

of the elevated number of PHB granules is caused by the absence of Slr0058.

To reveal the subcellular localization of Slr0058, an eGFP-tagged Slr0058 variant (pMK25) was inserted into the Δ*slr0058* background. The localization of Slr0058 was observed under different growth conditions using fluorescence microscopy with a GFP channel for the eGFP excitation. WT and pMK25 cells were observed during vegetative growth and after a shift to nitrogen depletion. Microscopic pictures of these conditions are shown in **Figure 9**.

During vegetative growth, a low fluorescence signal in the GFP channel was visible in the WT cells, which could be caused by bleed-through effects of autofluorescence of Chl *a*. In comparison, a much higher fluorescence signal was detected in the strain pMK25, often in specific foci. These spots of strong fluorescence indicate focal aggregation of Slr0058 in the cytoplasm. After the induction of chlorosis, these spots started to disappear. No colocalization of the GFP-Slr0058 foci with Nile red stained PHB granules could be seen (white arrows, **Figure 9**). During the course of chlorosis, the GFP aggregates further disappeared. In agreement with the *in vivo* formation of foci, recombinant purified His-tagged Sll0058 protein, analyzed by size-exclusion chromatography, displayed different aggregation states (**Supplementary Figure S5**).

DISCUSSION

Characterization of *slr0060* and Its Role for PHB Degradation

The gene product of *slr0060* was recently located in the same subcellular region as other PHB-related proteins, indicating a relevance of Slr0060 for the PHB metabolism (Baers et al., 2019). Furthermore, its sequence-homology to esterases suggests a role as a putative intracellular PHB depolymerase. However, a knock-out strain showed only minor difference to the WT in its growth during vegetative growth, chlorosis or resuscitation (**Figure 2** and **Supplementary Figure S2**). The biggest difference compared to the WT was an increased chlorophyll content (**Figure 3**), as well as a reduced amount of produced PHB (**Figure 4A**). Furthermore, a slightly different whole cell light scattering was detected during resuscitation from chlorosis. However, the deletion of a putative PHB depolymerase is expected to cause enhanced levels of PHB or larger granules than the WT, particularly during the recovery process, which was not the case (**Figure 6**). Hence, the true function of *slr0060* remains unknown. One explanation for the missing phenotype could be a second, so far undiscovered PHB depolymerase homolog, which compensates the loss of Slr0060. *Synechocystis* is known for possessing two homologs sets of enzymes for central reactions in carbohydrate metabolism, such as paralog pairs of GlgA1/2, GlgP1/2, or GlgX1/2 (Doello et al., 2018; Koch et al., 2019). Accordingly, this could also be the case for another, yet undiscovered PHB depolymerase.

Interestingly, our analysis revealed that the total amount of PHB polymers is not diminished during resuscitation. This phenomenon was not detected before, since earlier studies normalized the amount of PHB to the CDW (as shown in **Figure 6A**; Klotz et al., 2016). However, this normalization is biased by the fact that during resuscitation, the CDW increases strongly. This raises the hypothesis that the disappearance of PHB granules, that is observed during recovery from nitrogen chlorosis, is primarily not the result of PHB depolymerization, but rather results from disaggregation and distribution of PHB fragments among dividing daughter cells (**Figure 6C**). The lack of complete PHB consumption provides a new perspective on the physiological function of PHB. One hypothesis is that PHB may serve as an intracellular pool of reduction equivalents. Accordingly, the degradation of PHB would only be necessary under conditions of insufficient generation of reduction equivalents. However, growth at laboratory conditions usually provides a surplus of reduction equivalents, making the degradation of PHB potentially less relevant. Further studies are necessary to reveal the physiological function of PHB and the role of a putative depolymerase.

Absence of Slr0058 Causes Growth Deficiency and More PHB Granules

Bioinformatic analysis predicts structural similarities between Slr0058 and the regulator PhaF, suggesting its involvement in the PHB metabolism (**Figure 1A**). Like other phasins, it is expected to be located at the granule surface and thereby influence the formation or degradation of PHB.

A knock-out mutant Δ*slr0058* shows impaired growth compared to the WT during various conditions of vegetative growth (**Figure 2**), as well as during chlorosis (**Supplementary Figure S2A**). This phenotype is merely caused by the absence of Slr0058, since a complementation restores the WT phenotype

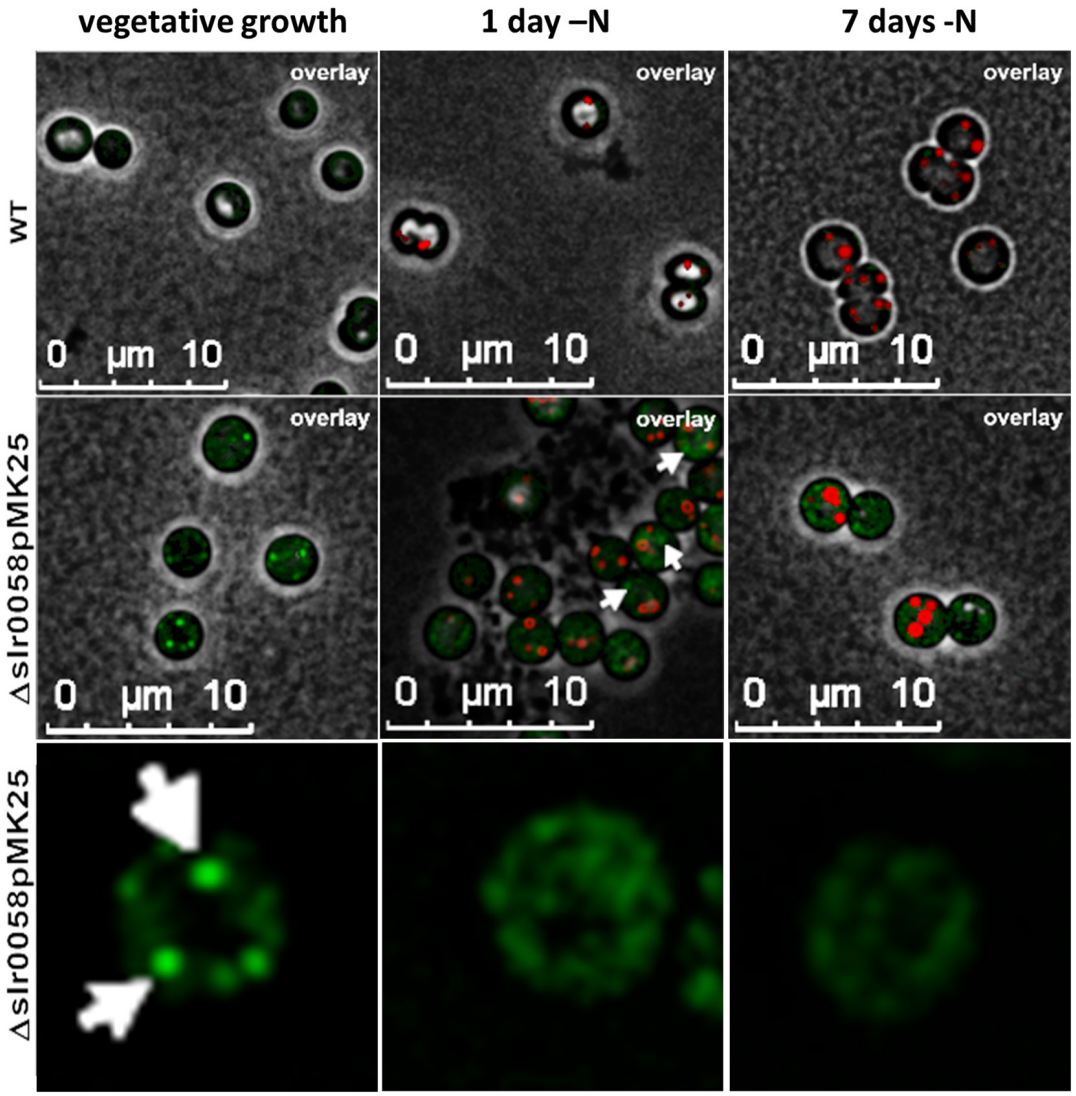

FIGURE 9 | 3-D deconvoluted microscopic images of WT and GFP-tagged-Slr0058 in the background of Δ*slr0058* (Δ*slr0058*pMK25) during vegetative growth and after 1 and 7 days of nitrogen starvation. PHB granules were stained with Nile red. White arrows indicate foci of aggregated GFP signal. The last row shows a zoom to individual, representative Δ*slr0058*pMK25 cells, in the GFP channel.

(**Figure 8**). This impaired growth is accompanied with a change in the absorption spectrum to a more bluish or yellowish color during vegetative growth or chlorosis, respectively (**Figures 3**, **5**). This effect can clearly be linked to the synthesis of PHB, since a PHB synthase lacking double mutant Δ*slr0058*-Δ*PhaEC* is rescued from the phenotypes and behaves like the WT (**Figure 5**). Although chemical analytics clearly detected PHB in vegetatively growing Δ*slr0058* cell, no visible PHB granules could be detected. However, under appropriate conditions resulting in 2% PHB/CDW of the WT a substantial portion of the cells would contain visible granules. Since this is not the case here, PHB might be present in a non-aggregated or mis-aggregated form, which is not stained by Nile red and therefore not visible by fluorescence microscopy. The not correctly aggregated form of PHB is putatively harmful for the cells, resulting in the observed growth disadvantage of strain Δ*slr0058*, which can be rescued by preventing PHB synthesis. The synthesis of a higher residual amount of PHB in vegetatively growing Δ*slr0058* cells further implies that this protein is involved in the control of PHB synthesis.

One of the most striking features of the Δ*slr0058* strain is the greatly increased number of PHB granules during chlorosis (**Figures 4C,D**). This hints toward an involvement of Slr0058 in the regulation of PHB granule formation. Surprisingly, in chlorotic cells, Slr0058 seems not to be located directly at the surface of the granules (**Figure 9**). Instead, it aggregates in foci during vegetative growth, which slowly disappear during the course of chlorosis. The formation of GFP-Slr0058 aggregates corresponds to *in vitro* properties of purified Slr0058 protein, where the protein was mostly present in the form of dimers

and trimers (**Supplementary Figure S5**). Possibly, the Slr0058 structures are involved in the initiation of PHB granule formation. In their absence, PHB is not properly aggregated and upon initiation of excess PHB synthesis, for example during nitrogen depletion, PHB starts to aggregate in an uncontrolled manner in numerous granules.

Polyhydroxybutyrate granules are hydrophobic structures. The surface-volume ratio of the PHB granules, and thereby the surface exposed to the cytoplasm, increases with decreasing granule size. This could lead to unintended interactions with intracellular structures, like the thylakoid membranes, resulting in a growth delay as well as a change in the pigmentation composition (**Figure 3A**). This requires a strict control of the surface-volume ratio. We have previously characterized the first cyanobacterial phasin, PhaP, which is essential for controlling the surface-volume ratio of PHB granules (Hauf et al., 2015). There, we have demonstrated that a lack of the phasin PhaP led to a lower average number of PHB granules per cell. Apparently, in the absence of PhaP, the cells reduce the PHB surface to volume ratio by producing less, but bigger granules. As it is known from other bacteria, PHB granules are complex and highly regulated organelles, and hence sometimes referred to as carbonosomes (Jendrossek, 2009). In other organisms, like for example *Cupriavidus necator*, many different proteins are involved in the exact formation and regulation of these organelles. It seems likely that also cyanobacteria have a strict regulation of PHB granules, where Slr0058 could play an important role for the initiation and size of such granules.

Although the physiological importance of PHB remains unclear (Damrow et al., 2016), the findings of this study increase our knowledge about PHB synthesis in cyanobacteria. A better understanding of the complex process of PHB granule formation is a step forward toward a sustainable production of biodegradable plastics from phototrophic organisms.

DATA AVAILABILITY STATEMENT

All datasets generated for this study are included in the article/**Supplementary Material**.

AUTHOR CONTRIBUTIONS

MK and KF conceptualized the study, reviewed and edited the manuscript and were responsible for the project administration. TO, JA, MK, and KF contributed to methodology. TO, JA, and MK carried out the investigation. MK, TO, and KF prepared the original draft. KF supervised the study.

FUNDING

This research was funded by the Studienstiftung des Deutschen Volkes and the RTG 1708 "Molecular principles of bacterial survival strategies". We acknowledge support by Deutsche Forschungsgemeinschaft and Open Access Publishing Fund of University of Tübingen.

ACKNOWLEDGMENTS

We thank Eva Nussbaum for the maintenance of the cyanobacterial strain collection, Claudia Menzel for technical assistance of the TEM pictures as well as Andreas Kulik for the operation of the HPLC.

SUPPLEMENTARY MATERIAL

The Supplementary Material for this article can be found online at: https://www.frontiersin.org/articles/10.3389/fmicb.2020.00809/full#supplementary-material

REFERENCES

Baers, L. L., Breckels, L. M., Mills, L. A., Gatto, L., Deery, M. J., Stevens, T. J., et al. (2019). Proteome mapping of a Cyanobacterium reveals distinct compartment organization and cell-dispersed metabolism. *Plant Physiol.* 181:1721. doi: 10.1104/pp.19.00897

Collier, J. L., and Grossman, A. R. (1992). Chlorosis induced by nutrient deprivation in *Synechococcus* sp. strain PCC 7942: not all bleaching is the same. *J. Bacteriol.* 174, 4718–4726. doi: 10.1128/jb.174.14.4718-4726.1992

Damrow, R., Maldener, I., and Zilliges, Y. (2016). The multiple functions of common microbial carbon polymers, glycogen and phb, during stress responses in the non-diazotrophic Cyanobacterium *Synechocystis* sp. PCC 6803. *Front. Microbiol.* 7:966–966. doi: 10.3389/fmicb.2016.00966

Doello, S., Klotz, A., Makowka, A., Gutekunst, K., and Forchhammer, K. (2018). A specific glycogen mobilization strategy enables rapid awakening of dormant *Cyanobacteria* from Chlorosis. *Plant Physiol.* 177, 594–603. doi: 10.1104/pp.18.00297

Fiedler, G., Arnold, M., Hannus, S., and Maldener, I. (1998). The Devbca exporter is essential for envelope formation in heterocysts of the cyanobacterium *Anabaena* sp. strain PCC 7120. *Mol. Microbiol.* 27, 1193–1202. doi: 10.1046/j.1365-2958.1998.00762.x

Gibson, D. G., Young, L., Chuang, R.-Y., Venter, J. C., Hutchison, C. A., and Smith, H. O. (2009). Enzymatic assembly of DNA molecules up to several hundred kilobases. *Nat. Methods* 6, 343–345. doi: 10.1038/nmeth.1318

Görl, M., Sauer, J., Baier, T., and Forchhammer, K. (1998). Nitrogen-starvation-induced chlorosis in *Synechococcus* PCC 7942: adaptation to long-term survival. *Microbiology* 144, 2449–2458. doi: 10.1099/00221287-144-9-2449

Grundel, M., Scheunemann, R., Lockau, W., and Zilliges, Y. (2012). Impaired glycogen synthesis causes metabolic overflow reactions and affects stress responses in the cyanobacterium *Synechocystis* sp. PCC 6803. *Microbiology* 158, 3032–3043. doi: 10.1099/mic.0.062950-0

Hauf, W., Watzer, B., Roos, N., Klotz, A., and Forchhammer, K. (2015). Photoautotrophic Polyhydroxybutyrate Granule Formation Is Regulated by Cyanobacterial Phasin PhaP in *Synechocystis* sp. Strain PCC 6803. *Appl. Environ. Microbiol.* 81, 4411–4422. doi: 10.1128/AEM.00604-15

Jendrossek, D. (2009). Polyhydroxyalkanoate granules are complex subcellular organelles (Carbonosomes). *J. Bacteriol.* 191, 3195–3202. doi: 10.1128/jb.01723-08

Kaneko, T., Tanaka, A., Sato, S., Kotani, H., Sazuka, T., Miyajima, N., et al. (1995). Sequence analysis of the genome of the unicellular cyanobacterium *Synechocystis* sp. strain PCC6803. I. Sequence features in the 1 Mb region

from map positions 64% to 92% of the genome. *DNA Res.* 2, 191–198. doi: 10.1093/dnares/2.4.191

Klotz, A., Georg, J., Bučinská, L., Watanabe, S., Reimann, V., Januszewski, W., et al. (2016). Awakening of a dormant Cyanobacterium from Nitrogen Chlorosis reveals a genetically determined program. *Curr. Biol.* 26, 2862–2872. doi: 10.1016/j.cub.2016.08.054

Koch, M., Doello, S., Gutekunst, K., and Forchhammer, K. (2019). Phb is produced from glycogen turn-over during nitrogen starvation in *Synechocystis* sp. PCC 6803. *Int. J. Mol. Sci.* 20:1942. doi: 10.3390/ijms20081942

Krasikov, V., Aguirre Von Wobeser, E., Dekker, H. L., Huisman, J., and Matthijs, H. C. P. (2012). Time-series resolution of gradual nitrogen starvation and its impact on photosynthesis in the cyanobacterium *Synechocystis* PCC 6803. *Physiol. Plant* 145, 426–439. doi: 10.1111/j.1399-3054.2012.01585.x

Liu, D., and Pakrasi, H. B. (2018). Exploring native genetic elements as plug-in tools for synthetic biology in the cyanobacterium *Synechocystis* sp. PCC 6803. *Microb. Cell Fact.* 17:48. doi: 10.1186/s12934-018-0897-8

Maestro, B., Galán, B., Alfonso, C., Rivas, G., Prieto, M. A., and Sanz, J. M. (2013). A new family of intrinsically disordered proteins: structural characterization of the major phasin PhaF from *Pseudomonas putida* Kt2440. *PLoS One* 8:e56904. doi: 10.1371/journal.pone.0056904

Mitschke, J., Georg, J., Scholz, I., Sharma, C. M., Dienst, D., Bantscheff, J., et al. (2011). An experimentally anchored map of transcriptional start sites in the model cyanobacterium *Synechocystis* sp. PCC6803. *Proc. Natl. Acad. Sci. U.S.A.* 108, 2124–2129. doi: 10.1073/pnas.1015154108

Osanai, T., Numata, K., Oikawa, A., Kuwahara, A., Iijima, H., Doi, Y., et al. (2013). Increased bioplastic production with an rna polymerase sigma factor SigE during nitrogen starvation in *Synechocystis* sp. PCC 6803. *DNA Res.* 20, 525–535. doi: 10.1093/dnares/dst028

Pfeiffer, D., and Jendrossek, D. (2011). Interaction between poly(3-hydroxybutyrate) granule-associated proteins as revealed by two-hybrid analysis and identification of a new phasin in Ralstonia eutropha H16. *Microbiology* 157, 2795–2807. doi: 10.1099/mic.0.051508-0

Richmond, A., and Hu, Q. (2013). *Handbook of Microalgal Culture: Applied Phycology and Biotechnology*, 2nd Edn. Hoboken, NJ: John Wiley & Sons.

Rippka, R., Deruelles, J., Waterbury, J. B., Herdman, M., and Stanier, R. Y. (1979). Generic assignments, strain histories and properties of pure cultures of cyanobacteria. *Microbiology* 111, 1–61. doi: 10.1099/00221287-111-1-1

Sambrook, J. (2001). *Molecular Cloning : A Laboratory Manual*, 3rd Edn. Cold Spring Harbor, N.Y: Cold Spring Harbor Laboratory Press.

Schlebusch, M. (2012). *Analysis of the Sll0783 Function in Phb Synthesis in Synechocystis PCC 6803: a Crucial Role of Nadph in N-Starvation*, Ph.D. dissertation, Tübingen University, Tübingen, Germany.

Schwarz, R., and Forchhammer, K. (2005). Acclimation of unicellular cyanobacteria to macronutrient deficiency: emergence of a complex network of cellular responses. *Microbiology* 151, 2503–2514. doi: 10.1099/mic.0.27883-0

Troschl, C., Meixner, K., and Drosg, B. (2017). Cyanobacterial Pha production-review of recent advances and a summary of three years' working experience running a pilot plant. *Bioengineering* 4:26. doi: 10.3390/bioengineering4020026

Yu, Y., You, L., Liu, D., Hollinshead, W., Tang, Y. J., and Zhang, F. (2013). Development of *Synechocystis* sp. PCC 6803 as a phototrophic cell factory. *Mar. Drugs* 11, 2894–2916. doi: 10.3390/md11082894

Zavřel, T., Očenášová, P., and Červený, J. (2017). Phenotypic characterization of *Synechocystis* sp. PCC 6803 substrains reveals differences in sensitivity to abiotic stress. *PLoS One* 12:e0189130. doi: 10.1371/journal.pone.0189130

Conflict of Interest: The authors declare that the research was conducted in the absence of any commercial or financial relationships that could be construed as a potential conflict of interest.

5. Accepted publication

M. Koch, K. Berendzen, K. Forchhammer (2020).

On the role and production of PHB in the cyanobacterium *Synechocystis* sp. PCC 6803.

Life, 2020, 10, 47

life

MDPI

Article

On the Role and Production of Polyhydroxybutyrate (PHB) in the Cyanobacterium *Synechocystis* sp. PCC 6803

Moritz Koch [1], Kenneth W. Berendzen [2], and Karl Forchhammer [1,*]

[1] Interfaculty Institute of Microbiology and Infection Medicine Tübingen, Eberhard-Karls-Universität Tübingen, 72076 Tübingen, Germany; moritz.koch@uni-tuebingen.de

[2] Center for Plant Molecular Biology, Eberhard-Karls-Universität Tübingen, 72076 Tübingen, Germany; kenneth.berendzen@zmbp.uni-tuebingen.de

* Correspondence: karl.forchhammer@uni-tuebingen.de; Tel.: +49-7071-29-72096

Received: 17 March 2020; Accepted: 21 April 2020; Published: 22 April 2020

Abstract: The cyanobacterium *Synechocystis* sp. PCC 6803 is known for producing polyhydroxybutyrate (PHB) under unbalanced nutrient conditions. Although many cyanobacteria produce PHB, its physiological relevance remains unknown, since previous studies concluded that PHB is redundant. In this work, we try to better understand the physiological conditions that are important for PHB synthesis. The accumulation of intracellular PHB was higher when the cyanobacterial cells were grown under an alternating day–night rhythm as compared to continuous light. In contrast to previous reports, a reduction of PHB was observed when the cells were grown under conditions of limited gas exchange. Since previous data showed that PHB is not required for the resuscitation from nitrogen starvation, a series of different abiotic stresses were applied to test if PHB is beneficial for its fitness. However, under none of the tested conditions did cells containing PHB show a fitness advantage compared to a PHB-free-mutant (Δ*phaEC*). Additionally, the distribution of PHB in single cells of a population *Synechocystis* cells was analyzed via fluorescence-activated cell sorting (FACS). The results showed a considerable degree of phenotypic heterogeneity at the single cell level concerning the content of PHB, which was consistent over several generations. These results improve our understanding about how and why *Synechocystis* synthesizes PHB and gives suggestions how to further increase its production for a biotechnological process.

Keywords: cyanobacteria; bioplastic; PHB; sustainable; resuscitation; chlorosis; bacterial survival; *Synechocystis*; biopolymers

1. Introduction

Cyanobacteria have colonized our planet for more than two billion years and are widespread within the light-exposed biosphere [1]. Their ability to conduct oxygenic photosynthesis enables them to survive under extreme environmental conditions, even in the absence of organic carbon sources. In adaption to these diverse environments, many cyanobacteria have evolved the ability to produce a variety of biopolymers [2]. Most of the mentioned polymers serve to store macro-nutrients, like carbon (in the form of glycogen), phosphate (polyphosphate), or nitrogen (cyanophycin). Although it has been known since 1966 that cyanobacteria also possess polyhydroxybutyrate (PHB), its function remains puzzling [3–5].

Around 30 years later, Hein et al. found that the required biosynthetic genes for the PHB synthesis are also present in the model organism *Synechocystis* sp. PCC 6803 (hereafter

"*Synechocystis*" or "WT" for wild-type) [6]. Soon after, it has been shown that this strain is indeed capable of producing PHB under nutrient limited conditions [7]. It has been hypothesized that the polymer serves as an additional carbon and energy storage, similarly to glycogen, which could help to survive environmental stress conditions. However, until today, the true physiological function remains unknown [5].

In other organisms, PHB can fulfill manifold functions. The polymer often accumulates under nutrient limitation or unbalanced conditions (e.g., an excess of carbon) [8]. In certain organisms like *Ralstonia eutropha*, it is also accumulated during normal growth phase [9]. In the strain *Azospirillum brasilense*, for example, heat, UV irradiation, desiccation, osmotic shock, and osmotic pressure affect the growth of a PHB deficient strain [10]. In the strain *Herbaspirillum seropedicae*, PHB is able to reduce redoxstress. Hence, PHB could serve as an electron sink to eliminate a surplus of reducing equivalents [11]. A similar behavior has been shown in the anoxygenic phototrophic bacterium *Chromatium vinosum*: it converts glycogen to PHB (under anerobic, dark metabolism) [12]. Thereby, the strain does not lose carbon, compared to other bacteria, which secrete their fermentation products. In agreement, it has been shown that excess NADPH sustains PHB accumulation [13].

A better understanding about the production of PHB in cyanobacteria would be beneficial for the biotechnological production of the biopolymer. PHB from cyanobacteria is suggested as a sustainable source for biodegradable plastics [14]. However, the current production rates are rather low, making it difficult to commercially compete with the PHB production in heterotrophic organisms [15]. So far, most attempts to increase the PHB yield focused on either medium optimization or metabolic engineering approaches. At the same time, fundamental questions about the PHB metabolism and PHB-forming conditions have been neglected. For instance, it has just recently been discovered that PHB is mostly formed from intracellular glycogen [16,17]. This work therefore aims to better understand the conditions, under which PHB is produced in *Synechocystis*, as well as gaining further insights in the physiological function of PHB within the cyanobacterial metabolism.

This knowledge will be helpful for both basic and applied research, since *Synechocystis* is considered a promising host for the industrial production of bioplastic from PHB [18].

2. Materials and Methods

2.1. Cyanobacterial Cultivation Conditions

Synechocystis sp. PCC 6803 cells were grown in standard BG_{11} medium as described before [19]. Additionally, 5 mM $NaHCO_3$ were added. All used strains are listed in Table A1. To ensure the preservation of the genetic modifications, appropriate antibiotics were added to the different mutant strains. All cells were pre-adapted to their growth conditions by growing a pre-culture for 3 days at the same condition. For normal growth, cells were grown under constant illumination of ~50 μE m^{-2} s^{-1} and at 28 °C. Aeration was provided by continuous shaking at 120 rpm. Either 50 or 200 mL bacterial culture were grown in baffle free Erlenmayer flasks. Whenever nitrogen starvation was required, cells were shifted to nitrogen depleted medium as previously described [20]. In short, 200 mL exponentially growing cells at an OD_{750} of ~0.8 were centrifuged at 4000 g for 10 min. The pellet was resuspended in 100 mL BG_0 (BG11 without any sodium-nitrate) and centrifuged again. The pellet was then resuspended in BG_0 once more and the OD_{750} was adjusted to 0.4. For resuscitation experiments, a chlorotic culture was spun down and resuspended in BG_{11} medium.

2.2. Physical Stress Conditions

To test whether the formation of PHB is advantageous under conditions of physical stress, chlorotic WT and Δ*phaEC* cells, which were starved from nitrogen for ~2 weeks, were used. The cells were treated with the conditions described in category 1 of Table 1 and subsequently recovered on BG_{11} plates. Afterwards, a serial dilution of cell suspension, from OD_{750} ~1 (= 100) until 10-4, was prepared. From each dilution, 5 μL were dropped on an BG11 agar plates containing 1.5 % agar and incubated for 1–2 weeks under continuous light, until visible colonies formed. Alternatively,

chlorotic cells were recovered on BG_{11} plates with additional ingredients (category 2 of Table 1) which can cause stress, e.g., high salt concentrations. The number of formed colonies was compared between the WT and ΔphaEC cells.

Table 1. List of abiotic stresses applied to WT and Δ*phaEC* cells, which were starved for two weeks of combined nitrogen sources. A detailed description is listed under "Treatment". For the first category of experiments, cells either treated for a specific time with the conditions listed under (1). After the treatment, cells were grown on BG_{11} agar plates according to the drop plate method as depicted in Figure 4. Alternatively, chlorotic cells were transferred to BG_{11} plates containing the ingredients listed under category (2) to apply the abiotic stress during the recovery process. Observed differences are listed under "Effect". When "no difference" was observed, both strains (WT and Δ*phaEC*) showed similar amounts of colonies. "All cells were dead" indicates experiments, where no colonies appeared. All treatments were tested in three different biological replicates.

Abiotic Stress	Treatment	Effect
	(1)	
Cold	4 °C over night	No difference
	1 h at −20°C; 14 h at −20 °C	
Heat	45 min at 40 °C;	No difference
	45 min at 40°C and 20 min at 50°C	All cells were dead
Physical Force	Centrifugation for 30 min at 20,000 g; 1 h at 25,000 g	No difference
	3 × 5 min at 4 m/s glass-bead milling in Ribolyser;	No difference
	3 × 5 min at 7 m/s Ribolyser	All cells were dead
Darkness	1 day; 2 days, 5 days; 8 days; 10 days; 15 days	No difference
Low Light	14 days at 5 µE	No difference
Alternating Light	12/12 light/dark	No difference
Drought	30 min at 30 °C SpeedVac	All cells were dead
Nitrogen Starvation	3 weeks	No difference
	10 weeks	Δ*phaEC* showed weak growth advantage
High Light	1 day incubation at 500 µE	No difference
	(2)	
Buffered Medium	BG_{11} agar plates containing 300 µL, 1 mL, 3 mL TES buffer	No difference
Salt	Recovery at BG_{11} agar plates with:	
	- 100, 150, 300 mM NaCl	No difference
	- 2 × BG_{11} salts	No difference
Carbon Availability	0, 10, 50, 150 mM bicarbonate (added to BG_{11} agar plates)	No difference

2.3. Oxygen Measurements

To measure oxygen levels in a liquid culture, an oxygen detecting sensor was placed at the bottom of a standing culture. The readout was performed using an OXY-1 SMA device (PreSens, Regensburg, Germany). At the beginning of the measurements, *Synechocystis* cells were shifted to nitrogen free BG0 medium and the oxygen levels were monitored for three constitutive days. The equilibrium of dissolved oxygen within the cultures was measured at 360 µM/L.

2.4. Microscopy and Staining Procedures

To visualize cell morphology and PHB granules within the cells, 100 µL of cyanobacterial culture were centrifuged. The resulting pellet was resuspended in a mixture of 10 µL Nile red and 20 µL water. From the resuspended mixture, 10 µL were used and dropped on an agarose-coated microscopy slide. A Leica DM5500B microscope (Leica, Wetzlar, Germany) with a 100 × /1.3 oil objective was used for fluorescence microscopy. For the detection of Nile red stained PHB granules,

a suppression filter BP 610/75 was used, together with an excitation filter BP 535/50. The pictures were taken by a Leica DFC360FX.

2.5. Electron Microscopy

For detailed pictures of the intracellular PHB granules, electron microscopy was used. For this, glutaraldehyde and potassium permanganate were used to fix and postfix *Synechocystis* cells. Citrate and uranyl acetate were used to stain ultrathin sections, as described before [21]. Finally, a Philips Tecnai 10 electron microscope (Philips, Amsterdam, Netherlands) was used to examine the samples at 80 kHz.

2.6. Spectral Analysis

To measure the whole-cell absorption spectrum, a Specord 50 with the software WinAspect (Analytik Jena, Jena, Germany) was used. The absorption was measured between 350 and 750 nm. The spectra were normalized to the OD_{750}. To determine the recovery of the photopigments, the change in absorption between the induction of the recovery (t0) and after three days (t72) was determined (normalized to OD_{750}). For this, the specific wavelengths for phycobilisomes and chlorophyll (absorption at 630 nm and 680, respectively) were compared.

2.7. PAM

To detect the photosynthetic activity, pulse–amplitude–modulation fluorometry (PAM) was used. This measures the relative quantum yield of the photosystem II, Y(II). A Heinz Walz GmbH (Effeltrich, Germany) WATER-PAM Chlorophyll Fluorometer with WinControl Software was used. For the measurements, a cell suspension with an OD_{750} between 0.4 and 1 was used and diluted 20-fold. After 5 min incubation in the dark, the maximum PSII quantum yield (Fv/Fm) was determined applying the saturation pulse method [22]. For each time point, three measurements with a time constant of 30 s were taken.

2.8. PHB Quantification

To determine the intracellular PHB content, ~15 mL of cells were centrifuged at 4000 g for 10 min. The pellet was dried for at least 2 h at 60 °C in a speed vac until all pellets were dry. Next, 1 mL of concentrated sulfuric acid (18 M H_2SO_4) were added and the mixture was boiled for 1 h at 100 °C. This process releases PHB from the cells and converts it to crotonic acid. From this, 100 µL were taken and diluted with 900 µL of 14 mM H_2SO_4. The sample was centrifuged for 5 min at 20,000 g. From the supernatant, 500 µL were transferred into a new tube and combined with 500 µL H_2SO_4. The samples were centrifuged once more for 5 min at max speed and 400 µL of the resulting supernatant was used for further HPLC analysis. For this, a Nucleosil 100 C 18 column was used (125 by 3 mm). For a liquid phase, 20 mM phosphate buffer with pH 2.5 was used. Crotonic acid was detected at 250 nm. As a standard, commercially available crotonic acid was used, with a conversion rate to PHB of 0.893.

2.9. FACS and Flow Cytometry

Synechocystis cells that were starved from nitrogen for ~2 weeks before FACS experiments. Cells were sorted with a MoFlo XDP (Beckman Coulter, Munich, Germany) into 500 µL PBS buffer using a 70 uM CytoNozzle at 30 p.s.i. and PBS [pH 7.0] as sheath. Before FACS or analysis, 1 µL of BODIPY (5 mg/mL) was added to 500 µL of cells and incubated for 10 min. Cells were identified based on their scatter (SSC-LA vs. FSC-LA), chlorophyll-fluorescence (670/30) captured from a 488 nm (70 mW) laser. Cells were divided into low and high producers based on their emission profile and at 534/30 (BODIPY) when compared to unstained and PHB deficient cells. For analysis, the software Summit FACS and FCS Express was used. BODIPY staining was also scored using a Cytoflex analyzer (Beckmann Coulter, Munich, Germany) equipped with a single 488 nm laser. Principle BODIPY emission was captured with a 525/40 bandpass and plotted against scatter to remove

clumplets and distinguish BODIPY. PHB content was inferred when compared to unstained and PHB deficient cells. For analysis and illustration of the date, the software programs CytoExpert (Beckman Coulter, Munich, Germany) and FlowJo (FlowJo LLC, Oregon, USA) were used.

3. Results

3.1. The Influence of Environmental Conditions and Central Pathways on PHB Production

In PHB producing cyanobacteria, PHB synthesis is efficiently induced by depleting the nitrogen source from the medium. This is also the case for the model cyanobacterium *Synechocystis* sp. PCC 6803 used in this study. To further understand the conditions, under which PHB is produced, cells, which were transferred to nitrogen-depleted medium, were grown under different conditions of aeration and illumination (Figure 1).

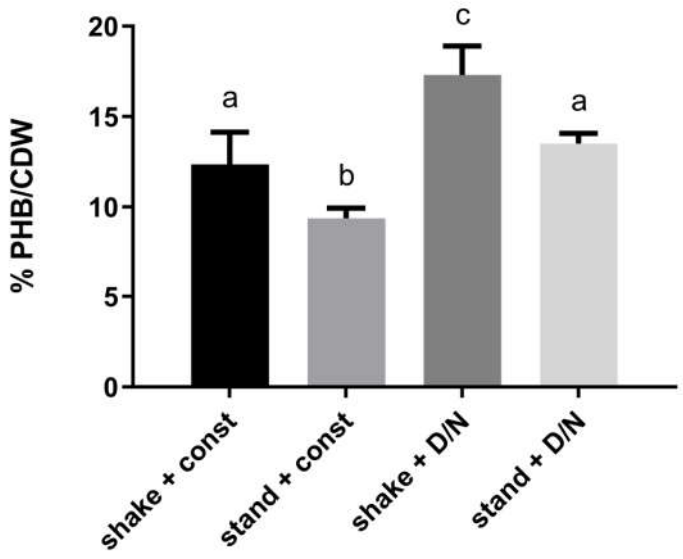

Figure 1. Quantification of polyhydroxybutyrate (PHB) content after 13 days of nitrogen starvation. WT cells were grown under different conditions of aeration and illumination. All cells were pre-adapted to these conditions three days before the shift to nitrogen starvation. Shake = continuous shaking at 120 rpm. Stand = cultures were standing without any shaking. Const = constant illumination with ~50 μE. D/N = altering illumination with 12 h of light (50 μE) and 12 h dark. Data shown as mean ± SD of three biological experiments; levels not connected by the same letter are significantly different ($p \leq 0.05$). CDW = cell dry weight.

It was shown in a previous study that the limitation of gas exchange can boost the PHB production [23]. To verify this observation, cells were grown without any shaking to create a situation of reduced aeration. Under these standing conditions, the cells produced oxygen and were oxygen-oversaturated during the day, whereas they consumed it during the night, resulting in transient periods of limited oxygen availability (Figure A2). Furthermore, cyanobacteria are naturally adapted to day-night rhythms, while they are commonly grown under continuous light in the laboratory. To test whether this affects the PHB production, PHB was quantified from cells grown under both light regimes. It turned out that, compared to standard laboratory conditions of continuous light and shaking, a limitation in gas exchange always led to a reduced PHB content. In contrast, the growth under day-night rhythm resulted, both in standing and shaken cultures, and in an increased content of PHB per cell-dry-weight (CDW). Therefore, the maximal PHB production was achieved in shaken cultures in a 12 h light/dark regime.

To test whether these effects are linked to a specific carbon pathway, knockout mutants of two central pathways were used: The mutant Δ*pfk* is unable to metabolize carbon via the the EMP (Embden–Meyerhof–Parnas) pathway and the mutant Δ*zwf* cannot use the OPP (oxidative pentose phosphate) and ED (Entner–Doudoroff) pathway. Both strains and a WT control were grown under the same conditions as in the previous experiment and their PHB content was then compared (Figure 2).

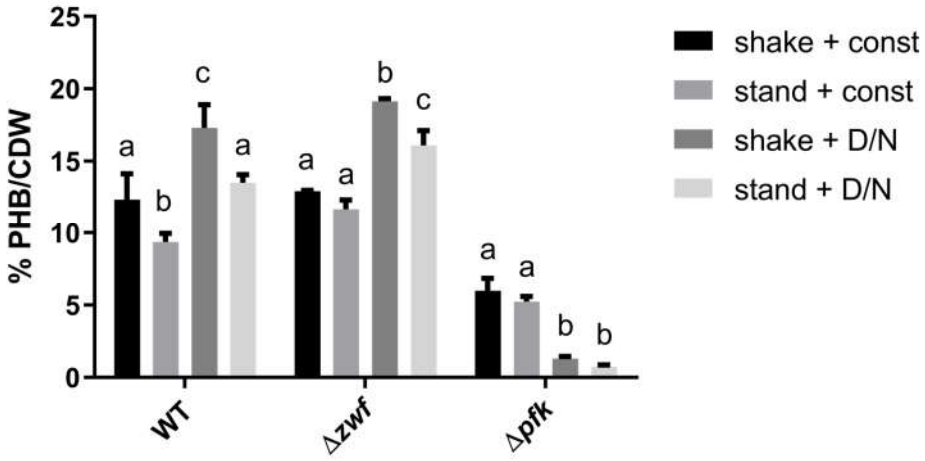

Figure 2. Quantification of PHB content after 13 days of nitrogen starvation. Mutant strains lacking either the EMP (Δ*pfk*) or the OPP and ED pathway (Δ*zwf*) were compared to the WT strain to test the influence of these carbon pathways on the PHB production. The cells were grown under different conditions of aeration and illumination. Shake = continuous shaking at 120 rpm. Stand = cultures were standing without any shaking. Const = constant illumination with ~50 μE. D/N = altering illumination with 12 h of light (50 μE) and 12 h dark. Data shown as mean ± SD of three biological experiments; levels not connected by the same letter are significantly different ($p \leq 0.05$; only within the same genetic background).

The Δ*zwf* mutant lacks glucose-6P dehydrogenase, which feeds sugar catabolites into the two central pathways ED and OPP, which are crucial for vegetative growth. These pathways are neglectable for the production of PHB under nitrogen starvation, since the Δ*zwf* mutant showed the same production pattern as the WT under all tested conditions (see Figure 2). In contrast, the Δ*pfk* mutant, which is unable to use the EMP pathway, showed a strongly impaired PHB production under all conditions. Interestingly, growth with a 12 h light/dark regime caused increased PHB production in the WT and the Δ*zwf* mutant, whereas it resulted in a severe reduction of PHB in the Δ*pfk* strain.

3.2. Recovery from Nitrogen Starvation

To test whether the formation of PHB plays a role for the recovery from nitrogen chlorosis under specific conditions, WT and a PHB-free mutant (Δp*haEC*) were nitrogen-starved for 18 days and were transferred to standard BG_{11} medium to induce resuscitation. Thereafter, parameters, which indicate the process of the resuscitation, such as the yield of the photosynthetic activtity (Y(II)) and reconstruction of light absorbing pigments, were analyzed over three days (Figure 3).

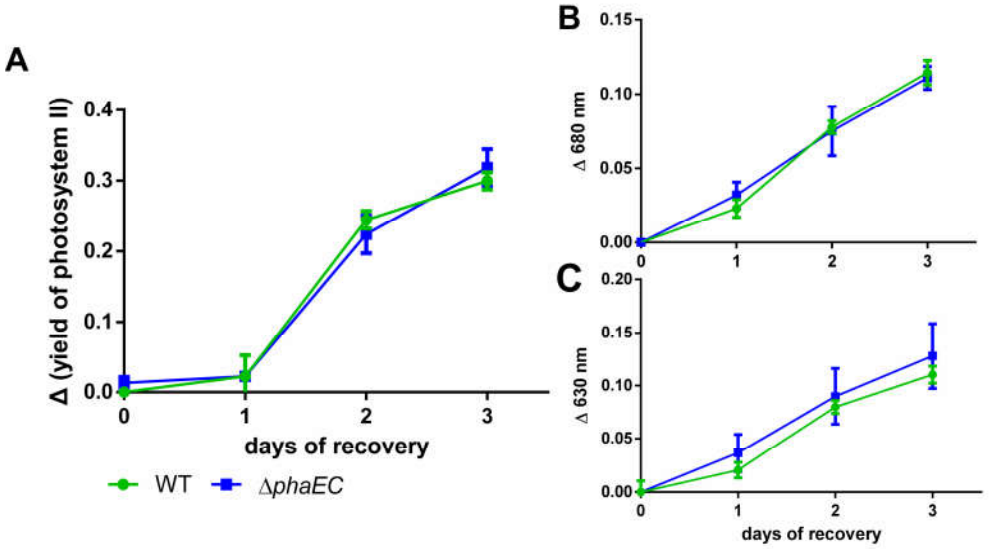

Figure 3. Physiological parameters during the resuscitation after 18 days of nitrogen starvation. Cells were grown under alternating day-night rhythm and continuous shaking; (**A**) PAM measurements to determine the maximum PSII quantum yield (Fv/Fm). The measurements were normalized to the yield at timepoint 0; (**B**) and (**C**): difference in absorption of normalized spectra during resuscitation. Spectra, which were normalized to OD_{750} (Figure A1), were used to calculate the difference between the initial absorption values (at wavelength of 630 and 680 nm) at time point 0 (day 0) and the various time points during resuscitation. All samples represent three individual biological replicates.

During the course of resuscitation, the photosynthetic activity of the WT recovered at the same pace as the Δ*phaEC* mutant (Figure 3A). Likewise, there was no difference in the re-appearance of photosynthetic pigments, indicated by the absorption at 630 nm and 680 nm (Figure 3B and C, respectively). The full spectra between 600 and 750 nm are shown in Figure A1.

To test if the formation of PHB is beneficial for chlorotic cells under conditions of certain abiotic stresses, WT and Δ*phaEC* cells were nitrogen starved for two weeks to induce PHB production. Subsequently, one of the following experimental setups was performed: (1) One specific abiotic stress was applied to the chlorotic culture for a specific time, before the culture was plated on BG_{11} agar plates and the formation of CFU was determined. (2) Chlorotic cells were plated on BG_{11} plates, which contained additional components causing stress (for example, higher salt concentrations). The results are summarized in Table 1.

Under all tested conditions, no growth advantage was observed for the WT compared to the Δp*haEC* mutant strain. Some conditions were too harsh for any cells to survive—for example, the simulation of heat at 50 °C. To illustrate what a typical result looked like, a representative drop plate assay is depicted in Figure 4. In this example, no viability difference between WT and Δ*phaEC* cells was observed after resuscitation from prolonged chlorosis and growth on 100 mM NaCl. In summary, there was no condition found where the possession of PHB was advantageous for the WT.

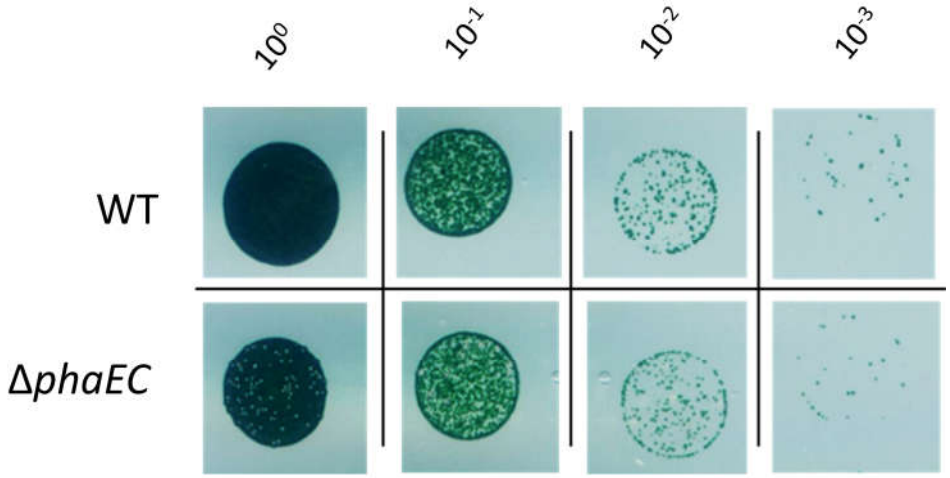

Figure 4. Viability assay of *Synechocystis* WT and Δp*haEC* mutant cells using the drop plate method after two weeks of nitrogen starvation and subsequent growth in BG_{11} plates with 100 mM NaCl. Several dilution steps were dropped on BG_{11} agar plates, ranging from OD_{750} = 1 (represents dilution 10^0) to OD_{750} = 0,001 (represents dilution 10^{-3}).

3.3. Heterogeneity of PHB Production

In microscopic studies, we noticed that the number of PHB granules varied strongly between individual WT cells during nitrogen starvation. While most cells did contain PHB, the amount varied greatly, both in the size as well as in the number of PHB granules (Figure 5).

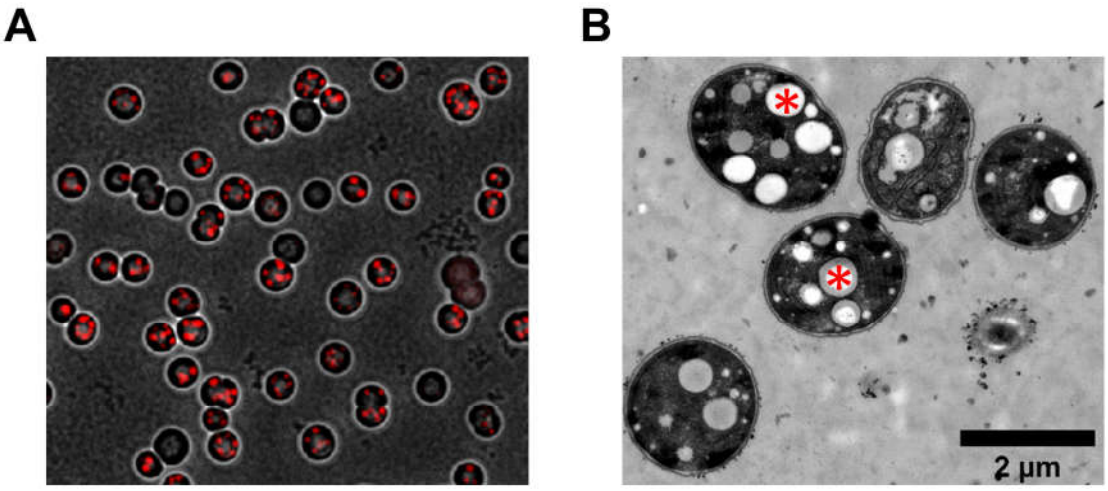

Figure 5. Microscopic analysis of varying PHB contents in WT cells; (**A**) fluorescence microscopy of WT cells after 14 days of nitrogen starvation. PHB granules are visualized by staining with Nile red; (**B**) TEM picture of WT cells after 17 days of nitrogen starvation. Representative PHB granules are indicated in two different cells by red asterisks.

Since this observation has not been systematically addressed before, we further investigated this phenomenon via flow cytometry (FC). Therefore, *Synechocystis* cells were starved for two weeks from nitrogen and stained with Bodipy. To distinguish the fluorescence signal of Bodipy stained PHB from background signals, two controls were performed: (1) determination of the unspecific background fluorescence from unstained WT cells as well as (2) the fluorescence of Bodipy stained PHB free Δ*phaEC* cells (Figure 6).

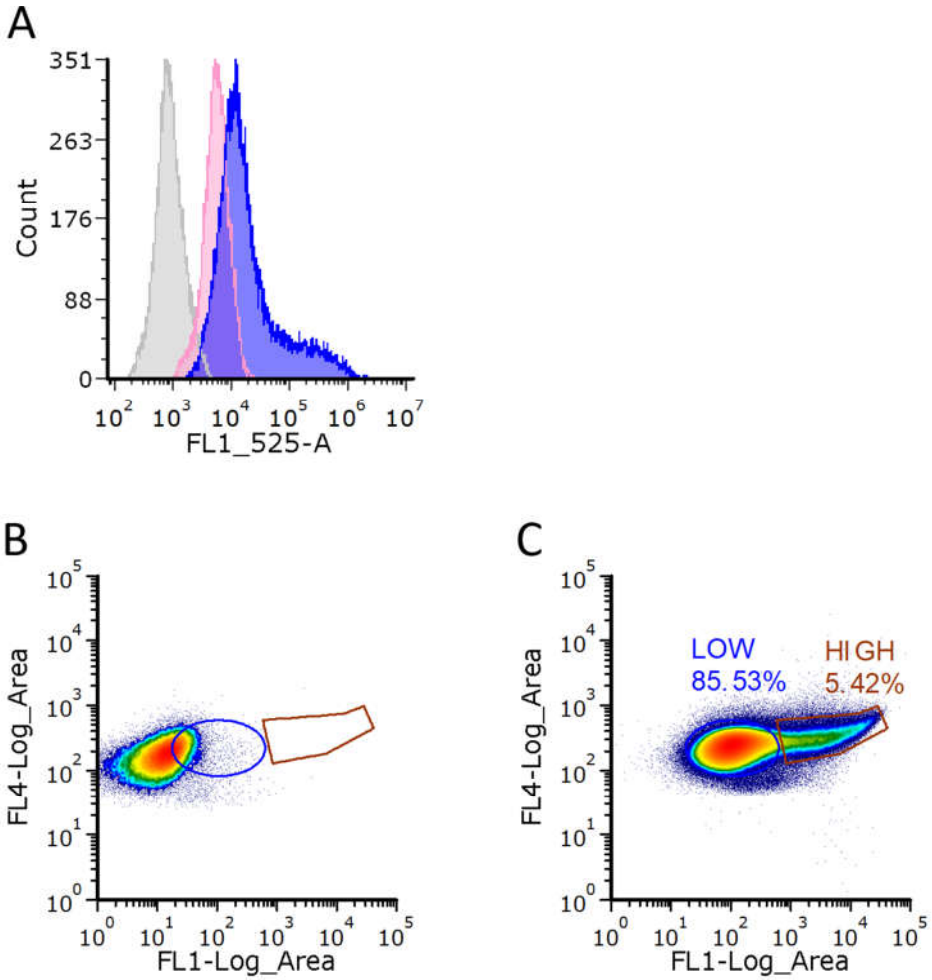

Figure 6. Analysis of intracellular PHB content using FC to detect *Synechocystis* cells stained with Bodipy. (**A**) overlay of the measurements for unstained WT (grey), Δp*haEC* mutant strain stained with Bodipy (red) and WT stained with Bodipy (blue). To illustrate how the cells were separated with FACS, the sort regions for Δp*haEC* mutant strain and WT are shown in (**B**) and (**C**), respectively. The red peak of Δp*haEC* cells in (A) corresponds to the cell population in (B), while the blue peak of WT cells in (A) corresponds to the cell population in (C). Sort regions in WT for low- and high producers are indicated as a blue or brown circle, respectively, in (B) and (C). FL4 = Chlorophyll emission and FL1 = Bodipy emission.

Compared to the unstained WT cells, the Δ*phaEC* cells showed a higher fluorescence signal, which is caused by unspecific staining of hydrophobic structures within the cells by Bodipy. Compared to the Bodipy stained Δ*phaEC* cells, a large portion of the Bodipy stained WT cell showed a fluorescence signal that was partially overlapping with that of Δ*phaEC* cells, but, on average, shifted to higher intensities (Figure 6, blue circle). This corresponds to a major population of cells that contained only low to medium amounts of PHB. From these, a second part of the WT population could clearly be distinguished, which showed much higher fluorescence signals (Figure 6, brown circle). This corresponds to a subpopulation of high PHB producing cells. Since the cells used for PHB production are derived from a single clone, they are assumed to be genetically identical. To definitively clarify that the different PHB synthesis phenotypes are not caused by (epi)genetic differences but are more likely, and are based on stochastic regulation of PHB synthesis, we isolated low and high PHB producing cells by FACS sorting. Single cells were recovered and grown on BG_{11} agar plates until colonies appeared. Several colonies derived from high- or low-producing cells were separately pooled and used to inoculate a fresh BG_{11} culture. Afterwards,

the cultures were shifted again to nitrogen free BG_0 medium to trigger PHB synthesis and the cells were again investigated using FC as described above. The results are shown in Figure 7.

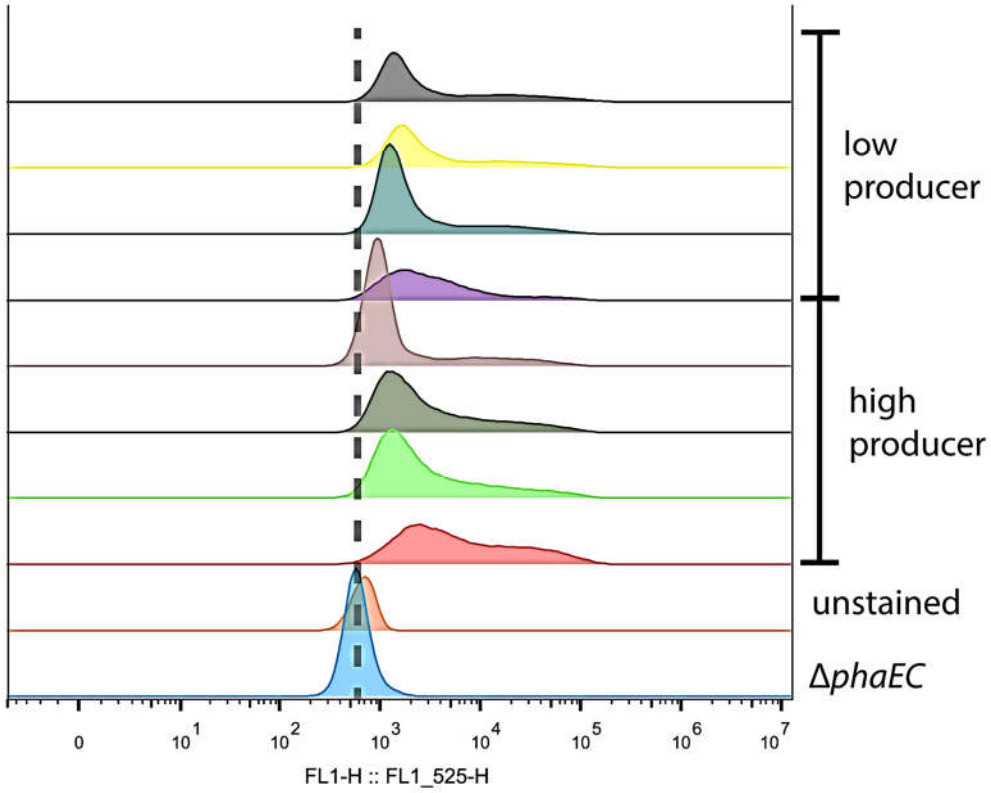

Figure 7. FC analysis of intracellular PHB content. "Low" and "high" represent four individual biological replicates from FACS, which were based on cells that contained low or high amounts of PHB, respectively. Cells were starved from nitrogen for two weeks and stained with Bodipy (except for the unstained control).

Undoubtedly, the cells in these new cultures established again the same PHB heterogeneity as in the previous experiment, regardless if they were derived from previously low- or high-producing cells. As previously described, all Bodipy stained WT cells showed a higher overall fluorescence compared to the unstrained control and the Bodipy stained ΔphaEC mutant strain, indicating that most cells did contain PHB. Furthermore, all replicates showed the characteristic shoulder in the FC analysis, representing cells with high PHB contents. This result demonstrates that the regulation of PHB synthesis in nitrogen-starved cells follows a stochastic program, resulting in a mixed population with a majority of low- to medium PHB producers and a minority of high PHB producing cells.

4. Discussion

4.1. Heterogeneity of PHB Content

When living in a changing environment, being prepared for different potential outcomes can be beneficial. In order to be prepared for unpredictable future scenarios, many bacteria have evolved a strategy of phenotypical heterogeneity for bed hedging [24]. This allows them to have a certain part of their population being well prepared for either outcome. In this work, we could show that the formation of PHB in *Synechocystis* also represents this form of phenotypical heterogeneity. We observed this via fluorescence and electron microscopy (Figure 5) and further confirmed it by flow-cytometry (Figure 6). As already hypothesized, this heterogeneity has no inheritable reason,

since cells that were separated into low- and high producers produced progeny with the same heterogeneity in PHB content as the ancestral generation (Figure 7). It is likely that the heterogeneity results from a probabilistic genetic program (bet-hedging) that results in the observed distribution of PHB production. The expression of key enzymes (such as PhaEC) might be quite variable, resulting in some cells that do produce more PHB than others. It was shown before that transcriptional infidelity promotes heritable phenotypic changes, which could also explain the PHB heterogeneity [25]. The phenomenon of a bet-hedging strategy in PHB contents has also been described in a different manner for some heterotrophic bacteria, such as *Sinorhizobium meliloti.* Here, when dividing *S. meliloti* cells face starvation, they form two daughter cells with different phenotypes, one with low and one with high PHB content. These daughter cells are adapted to either short- or long-term starvation, respectively [26].

4.2. Physiological Function of PHB

Since the majority of cells contained only minor or medium amounts of PHB, it has to be assumed that the conditions, under which it is beneficial to contain large PHB quantities, are rather seldom. To better understand PHB metabolism, this work aimed at providing additional information about when and why PHB is formed. We show clear evidence that the PHB content within the cells is increased when the bacteria are grown under alternating day–night rhythm (Figure 1, Figure 2). This is in coherence with a recently published transcriptomic data set [27]. Here, the authors have analyzed the transcription of genes under two consecutive dark- and light phases. We extracted all known PHB related genes from this data set and found a clear correlation between the genes of PHB metabolism and the diurnal rhythm (Figure A3). The assumption that PHB might play a role during dark, anaerobic conditions was already hypothesized before [28].

Since PHB is formed from intracellular glycogen pools [17] and cyanobacteria catabolize glycogen during the night [29], this phenotype might be explained by an increased carbon availability from glycogen during the night. Furthermore, *Synechocystis* accumulated less PHB when grown under standing conditions (Figure 1). These findings are in line with previous reports, which showed a generally decreased metabolic activity under conditions of limited gas-exchange and CO_2 availability [30]. In addition, photosynthetically active *Synechocystis* cells produce oxygen, which accumulates in the medium when grown under standing conditions (Figure A2). Excess of oxygen is known to impair the efficiency of the RuBisCO enzyme by causing the oxygenase reaction, which likely resulted in a reduced PHB reduction due to the carbon loss caused by photorespiration.

The results fit to the observation that the EMP pathway proved to be the most important carbon pathway for PHB production (Figure 2). Studies have shown that cyanobacteria employ the EMP pathway for degradation of glucose residues to pyruvate [30]. This is also the case for growth in dark phases [31]. Furthermore, the EMP produces less NADPH and more ATP, compared to other glycolytic routes, such as the OPP (oxidative-pentose-phosphate pathway) or the ED (Entner-Doudoroff) pathway. Although the cultivation under standing conditions is not a strictly anaerobic condition (Figure A2), the O_2 limitation during the dark phase could be sufficient to induce fermentation-like processes. It is known that cyanobacteria carry out fermentation under dark/anoxic conditions and produce a variety of different fermentation products [32]. Although PHB is so far not considered a cyanobacterial fermentation product, these conditions of limited oxygen availability and absence of light could explain the observed increase of intracellular PHB (Figure 1).

In contrast to the common belief, the ability to produce PHB under conditions of nitrogen starvation was not shown to be beneficial since we could not detect any physiological differences between WT and Δ*phaEC* cells during the resuscitation process (Figure 3). Even when additional abiotic stresses were added, no growth advantage was observed (Table 1). It might be that growth under the controlled environment of laboratory conditions is not limiting the cells, neither in carbon nor energy, and hence no phenotypes were visible.

It was previously shown that excess NADPH under nitrogen-starved conditions sustains PHB accumulation [13]. Hence, PHB might serve as an intracellular pool for electrons under conditions of

excess reduction equivalents. The fact that we did not observe any phenotypical difference under conditions of electron excess (for example under high amounts of light).

Table 1 might be explained by other regulatory mechanisms compensating for the lack of PHB. Since the correct regulation of intracellular redox-state is crucial for the cell physiology, *Synechocystis* has evolved various strategies to cope with high levels of reduction equivalents. One example for such a mechanism is the flavodiiron protein Flv3, which serves as a sink for excess electrons from the photosynthetic light reaction, by converting O_2 to H_2O. A recent publication showed indeed increased PHB synthesis in a Flv3 deficient strain [33]. If PHB is indeed serving as an intracellular electron sink, its absence might be compensated by a higher activity of Flv3. Alternative ways of getting rid of reduction equivalents could be the secretion of reduced organic molecules, such as acetate. It can be assumed that the correct regulation of the ATP/NADPH ratio is crucial for cyanobacterial cells. Since the production of PHB from glycogen provides ATP but consumes NADPH, the biopolymer could help the cells to regulate this ratio under conditions of electron excess [33].

5. Conclusions

This work describes different factors that influence the formation of PHB. However, the conditions where PHB is advantageous during nitrogen starvation have yet to be discovered. The results of this work can help to create strains with enhanced PHB contents. Besides applying dark phases, finding regulators of the EMP pathway to unlock the carbon flow from glycogen to PHB could further boost the production [17]. One alternative strategy could be the deletion of other NAPDH consuming pathways, as already shown in a Δflv3 strain. Finally, a deeper understanding of the PHB-heterogeneity might result in a more homogenous culture of high-producing cells, which is beneficial for the overall yield.

Author Contributions: Conceptualization, M.K. and K.F.; Methodology, M.K., K.W.B., and K.F.; Investigation, M.K. and K.W.B.; Writing—Original Draft Preparation, M.K., K.W.B. and K.F.; Writing—Review and Editing, M.K. and K.F.; Supervision, K.F.; Project Administration, M.K. and K.F. All authors have read and agreed to the published version of the manuscript.

Funding: This research was funded by the Studienstiftung des Deutschen Volkes and the RTG 1708 "Molecular principles of bacterial survival strategies". We acknowledge support by the Open Access Publishing Fund of University of Tübingen.

Acknowledgments: We would like to thank Eva Nussbaum for maintaining the strain collection and Andreas Kulick for assistance with HPLC analysis. We also thank Markus Maisch and Andreas Kappler for instructions for the oxygen measurement device. Furthermore, we thank Claudia Menzel for technical assistance with the electron microscope.

Conflicts of Interest: The authors declare no conflict of interest.

Appendix A

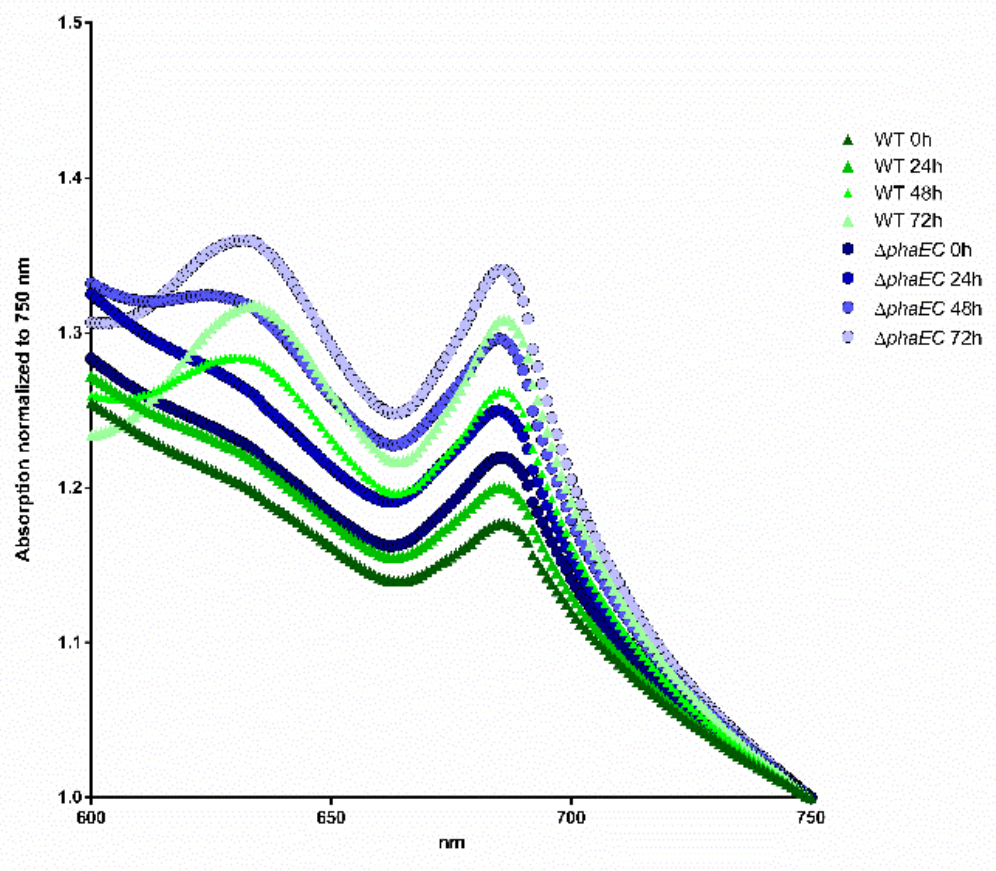

Figure A1. Cell spectra from 600 nm to 750 nm of WT and Δ*phaEC* after 0–4 days of resuscitation from nitrogen starvation. Each line represents the mean of the spectra from three independent biological triplicates. The spectra were normalized to their corresponding value at 750 nm.

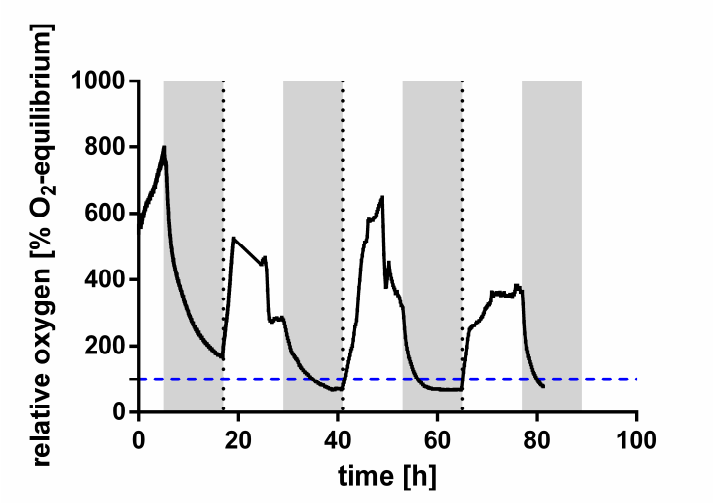

Figure A2. Oxygen measurements of a standing WT culture at light/dark regime. At timepoint 0, nitrogen starvation was induced. The amount of oxygen (green) within the culture was measured during three adjacent days. Grey bars in the back represent the dark phases. The equilibrated oxygen levels are shown in a blue dashed line.

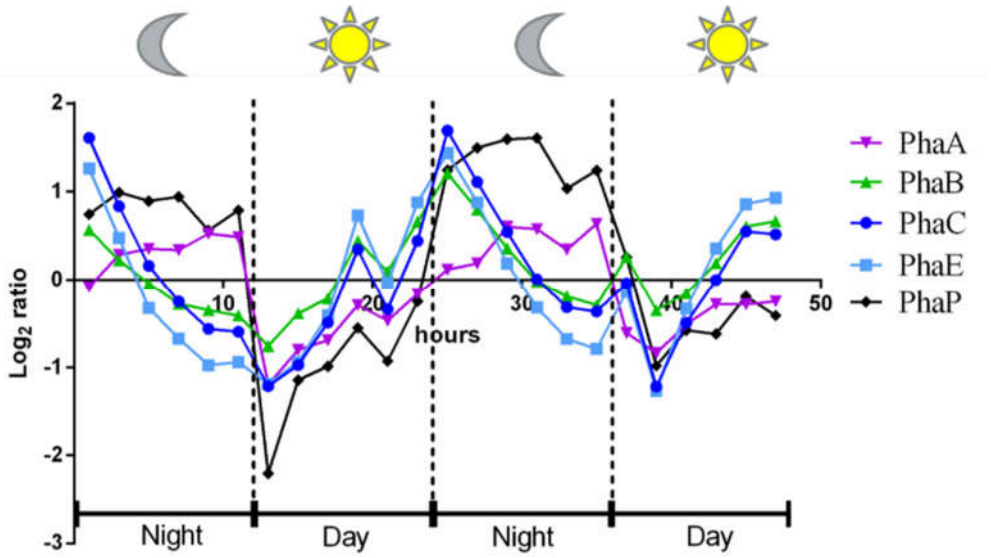

Figure A3. Transcriptomic data of PHB related genes [28]. The data are based on two consecutive days, including two 12 h phases with and without light.

Table A1. List of used strains.

Strain	Relevant Marker of Genotype	Reference
Synechocystis sp. PCC 6803	-	Pasteur culture collection
Δ*zwf*	*Slr1843::cmR*	Chen et al. 2016
Δ*pfkB1/2*	*sll1196::kmR , sll0745::spR*	Chen et al. 2016
Δ*phaEC*	*slr1829,slr1830::kmR*	Klotz et al. 2016

References

1. Herrero, A.; Flores, E. *The Cyanobacteria: Molecular Biology, Genomics and Evolution*; Caister Academic Press: Norfolk, UK, 2008.
2. Allen, M.M. Cyanobacterial cell inclusions. *Annu. Rev. Microbiol.* **1984**, *38*, doi:10.1146/annurev.mi.38.100184.000245.
3. Carr, N.G. The occurrence of poly-beta-hydroxybutyrate in the blue-green alga, Chlorogloea fritschii. *Biochim. Biophys. Acta* **1966**, *120*, 308–310.
4. Damrow, R.; Maldener, I.; Zilliges, Y. The Multiple Functions of Common Microbial Carbon Polymers, Glycogen and PHB, during Stress Responses in the Non-Diazotrophic Cyanobacterium *Synechocystis* sp. PCC 6803. *Front. Microbiol.* **2016**, *7*, 966.
5. Klotz, A.; Georg, J.; Bučinská, L.; Watanabe, S.; Reimann, V.; Januszewski, W.; Sobotka, R.; Jendrossek, D.; Hess, W.R.; Forchhammer, K. Awakening of a Dormant Cyanobacterium from Nitrogen Chlorosis Reveals a Genetically Determined Program. *Curr. Biol.* **2016**, *26*, 2862–2872.
6. Hein, S.; Tran, H.; Steinbuchel, A. *Synechocystis* sp. PCC6803 possesses a two-component polyhydroxyalkanoic acid synthase similar to that of anoxygenic purple sulfur bacteria. *Arch. Microbiol.* **1998**, *170*, 162–170.
7. Wu, G.F.; Wu, Q.Y.; Shen, Z.Y. Accumulation of poly-beta-hydroxybutyrate in cyanobacterium *Synechocystis* sp. PCC6803. *Bioresour. Technol.* **2001**, *76*, 85–90.
8. Anderson, A.J.; Dawes, E.A. Occurrence, Metabolism, Metabolic Role, and Industrial Uses of Bacterial Polyhydroxyalkanoates. *Microbiol. Rev.* **1990**, *54*, 450–472.
9. Jendrossek, D.; Pfeiffer, D. New insights in the formation of polyhydroxyalkanoate granules (carbonosomes) and novel functions of poly(3-hydroxybutyrate). *Environ. Microbiol.* **2014**, *16*, 2357–2373.
10. Kadouri, D.; Jurkevitch, E.; Okon, Y. Involvement of the reserve material poly-beta-hydroxybutyrate in *Azospirillum brasilense* stress endurance and root colonization. *Appl. Environ. Microbiol.* **2003**, *69*, 3244–3250.

11. Batista, M.B.; Teixeira, C.S.; Sfeir, M.Z.T.; Alves, L.P.S.; Valdameri, G.; de Oliveira Pedrosa, F.; Sassaki, G.L.; Steffens, M.B.R.; de Souza, E.M.; Dixon, R.; et al. PHB Biosynthesis Counteracts Redox Stress in *Herbaspirillum seropedicae*. *Front. Microbiol.* **2018**, *9*, 472.
12. van Gemerden, H. On the ATP generation by Chromatium in darkness. *Arch. Mikrobiol*. **1968**, *64*, 118–124.
13. Hauf, W.; Schlebusch, M.; Hüge, J.; Kopka, J.; Hagemann, M.; Forchhammer, K. Metabolic Changes in *Synechocystis* PCC6803 upon Nitrogen-Starvation: Excess NADPH Sustains Polyhydroxybutyrate Accumulation. *Metabolites* **2013**, *3*, 101–118.
14. Balaji, S.; Gopi, K.; Muthuvelan, B. A review on production of poly β hydroxybutyrates from cyanobacteria for the production of bio plastics. *Algal Res.* **2013**, *2*, 278–285.
15. Knöttner, S.; Drosg, B.; Ellersdorfer, M.; Meixner, K.; Fritz, I. Photoautotrophic production of poly-hydroxybutyrate—First detailed cost estimations. *Algal Res.* **2019**, *41*, 101558.
16. Dutt, V.; Srivastava, S. Novel quantitative insights into carbon sources for synthesis of poly hydroxybutyrate in *Synechocystis* PCC 6803. *Photosynth. Res.* **2018**, *136*, 303–314.
17. Koch, M.; Doello, S.; Gutekunst, K.; Forchhammer, K. PHB is Produced from Glycogen Turn-over during Nitrogen Starvation in *Synechocystis* sp. PCC 6803. *Int. J. Mol. Sci.* **2019**, *20*, 1942.
18. Martin, K.; Lukas, M. Cyanobacterial Polyhydroxyalkanoate Production: Status Quo and Quo Vadis? *Curr. Biotechnol.* **2015**, *4*, 464–480.
19. Rippka, R.; Deruelles, J.; aterbury, J.B.; Herdman, M.; Stanier, R.Y. Generic Assignments, Strain Histories and Properties of Pure Cultures of Cyanobacteria. *Microbiol. Soc.* **1979**, *111*, doi:10.1099/00221287-111-1-1.
20. Schlebusch, M.; Forchhammer, K. Requirement of the nitrogen starvation-induced protein Sll0783 for polyhydroxybutyrate accumulation in *Synechocystis* sp. strain PCC 6803. *Appl. Environ. Microbiol*. **2010**, *76*, 6101–6107.
21. Fiedler, G.; Arnold, M.; Hannus, S.; Maldener, I. The DevBCA exporter is essential for envelope formation in heterocysts of the cyanobacterium *Anabaena* sp. strain PCC 7120. *Mol. Microbiol*. **1998**, *27*, 1193–1202.
22. Schreiber, U.; Endo, T.; Mi, H.; Asada, K. Quenching Analysis of Chlorophyll Fluorescence by the Saturation Pulse Method: Particular Aspects Relating to the Study of Eukaryotic Algae and Cyanobacteria. *Plant Cell Physiol.* **1995**, *36*, 873–882.
23. Panda, B.; Mallick, N. Enhanced poly-beta-hydroxybutyrate accumulation in a unicellular cyanobacterium, *Synechocystis* sp. PCC 6803. *Lett. Appl. Microbiol*. **2007**, *44*, 194–198.
24. Veening, J.W.; Smits, W.K.; Kuipers, O.P. Bistability, epigenetics, and bet-hedging in bacteria. *Annu. Rev. Microbiol.* **2008**, *62*, 193–210.
25. Gordon, A.J.E.; Halliday, J.A.; Blankschien, M.D.; Burns, P.A.; Yatagai, F.; Herman, C. Transcriptional Infidelity Promotes Heritable Phenotypic Change in a Bistable Gene Network. *PLoS Biol.* **2009**, *7*, e1000044.
26. Ratcliff, W.C.; Denison, R.F. Individual-level bet hedging in the bacterium *Sinorhizobium meliloti*. *Curr. Biol*. **2010**, *20*, 1740–1744.
27. Saha, R.; Liu, D.; Hoynes-O'Connor, A.; Liberton, M.; Yu, J.; Bhattacharyya-Pakrasi, M.; Balassy, A.; Zhang, F.; Moon, T.S.; Maranas, C.D.; et al. Diurnal Regulation of Cellular Processes in the Cyanobacterium *Synechocystis* sp. Strain PCC 6803: Insights from Transcriptomic, Fluxomic, and Physiological Analyses. *mBio* **2016**, *7*, e00464-16.
28. Ueda, S.; Kawamura, Y.; Iijima, H.; Nakajima, M.; Shirai, T.; Okamoto, M.; Kondo, A.; Hirai, M.Y.; Osanai, T. Anionic metabolite biosynthesis enhanced by potassium under dark, anaerobic conditions in cyanobacteria. *Sci. Rep.* **2016**, *6*, 32354.
29. Smith, A.J. Modes of cyanobacterial carbon metabolism. *Ann. Inst. Pasteur/Microbiol.* **1983**, *134B*, 93–113.
30. Stal, L.J.; Moezelaar, R. Fermentation in cyanobacteria1. *FEMS Microbiol. Rev.* **1997**, *21*, 179–211.
31. Makowka, A.; Nichelmann, L.; Schulze, D.; Spengler, K.; Wittmann, C.; Forchhammer, K.; Gutekunst, K. Glycolytic Shunts Replenish the Calvin-Benson-Bassham Cycle as Anaplerotic Reactions in Cyanobacteria. *Mol. Plant* **2020**, *13*, 471–482.

32. Heyer, H.; Krumbein, W.E. Excretion of Fermentation Products in Dark and Anaerobically Incubated Cyanobacteria. *Arch. Microbiol.* **1991**, *155*, 284–287.
33. Thiel, K.; Patrikainen, P.; Nagy, C.; Fitzpatrick, D.; Pope, N.; Aro, E.-M.; Kallio, P. Redirecting photosynthetic electron flux in the cyanobacterium *Synechocystis* sp. PCC 6803 by the deletion of flavodiiron protein Flv3. *Microb. Cell Fact.* **2019**, *18*, 189.

6. Manuscript in preparation

M. Koch, Jonas Bruckmoser, Jörg Scholl, Waldemar Hauf, Bernhard Rieger, K. Forchhammer.

Maximizing PHB content in *Synechocystis* sp. PCC 6803: development of a new photosynthetic overproduction strain.

Microbial Cell Factories

Article

Maximizing PHB content in *Synechocystis sp.* PCC 6803: development of a new photosynthetic overproduction strain.

Moritz Koch [1], Jonas Bruckmoser [2], Jörg Scholl [1], Waldemar Hauf [1], Bernhard Rieger [2] and Karl Forchhammer [1,*]

[1] Interfaculty Institute of Microbiology and Infection Medicine Tübingen, Eberhard-Karls-Universität Tübingen, Tübingen, Germany; karl.forchhammer@uni-tuebingen.de
[2] Wacker-Chair of Macromolecular Chemistry, TUM Department of Chemistry, Technical University of Munich, Munich, Germany
* Correspondence: karl.forchhammer@uni-tuebingen.de; Tel.: + 49 7071 29 72096

Abstract: PHB (poly-hydroxy-butyrate) represents a promising bioplastic variety with good biodegradation properties. Furthermore, PHB can be produced completely carbon-neutral when synthesized in the natural producer cyanobacterium *Synechocystis sp.* PCC 6803. This model strain has a long history of various attempts to further boost its low amounts of produced intracellular PHB of ~15 % per cell-dry-weight (CDW).

We have created a new strain that lacks the regulatory protein PirC (gene product of *sll0944*), which causes a rapid conversion of the intracellular glycogen pools to PHB under nutrient limiting conditions. To further improve the intracellular PHB content, two genes from the PHB metabolism, phaA and phaB from the known production strain *Cupriavidus necator*, were introduced under the regime of the strong promotor P*psbA2*. The created strain, termed PPT1 (Δ*sll0944*-RE*phaAB*), produced high amounts of PHB under continuous light as well under day-night rhythm. When grown in nitrogen and phosphor depleted medium, the cells produced up to 63 % / CDW. Upon the addition of acetate, the content was further increased to 81 % / CDW. The produced polymer consists of pure PHB, which is highly isotactic.

The achieved amounts were the highest ever reported in any known cyanobacterium and demonstrate the potential of cyanobacteria for a sustainable, industrial production of PHB.

Keywords: cyanobacteria, physiology, PHB, metabolic engineering, *Synechocystis*, 6803, biopolymers, bioplastic, sustainable.

1. Introduction

The global contamination with non-degradable plastic is a huge environmental burden of our time (Jambeck et al., 2015, Li et al., 2016). While bioplastics have been suggested as a potential solution, they still represents only a very small fraction of the overall used plastics (Geyer et al., 2017). Furthermore, many of these bioplastics have unsatisfying biodegradation properties. The most common bioplastic, PLA (poly-lactic-acid), is almost undegradable in marine environments (Narancic et al., 2018). This led to the emerging interest in another class of bioplastics with improved degradation properties: PHAs (poly-hydroxy-alkanoates). The most common variant in this chemical class is PHB (poly-hydroxy-butyrate) which is produced by various microorganisms. Currently, PHB is produced by fermentation using heterotrophic bacteria, such as *Cupriavidus necator* or *Escherichia coli (Chen, 2009)*. However, since these production processes require crop-derived organic carbon sources for growth and production, it conflicts with human food-supply. An alternative way of producing PHB, which is independent of cropland use, is the usage of phototrophic organisms, such as cyanobacteria (Balaji et al., 2013, Akiyama et al., 2011).

Synechocystis sp. PCC 6803 (hereafter *Synechocystis*) is a well-studied model organism for phototrophic growth and a natural producer of PHB (Hein et al., 1998, Wu et al., 2001). Under conditions of nutrient limitation, for example nitrogen starvation, the cells transform into a resting state during a process that is called chlorosis (Allen and Smith, 1969). During chlorosis, they do not only degrade their photosynthetic apparatus, but also accumulate large quantities of glycogen as a carbon- and energy-storage (Klotz et al., 2016, Doello et al., 2018). During the later stages of chlorosis, the cells start to degrade glycogen and convert it to PHB (Koch et al., 2019). However, the produced amounts of intracellular PHB are rather low and only range between 10 - 20 % / CDW (cell dry weight). A recent economic analysis suggests that one of the limiting factors to compete with PHB derived from fermentative processes is the low ratio of PHB / CDW in cyanobacteria (Knöttner et al., 2019). One major goal is therefore, to optimize cyanobacteria so that they achieve higher intracellular PHB contents. This would not only increase the yield but would also simplify the downstream-process of extracting the PHB from the cells.

There have been various attempts to further boost the amount of PHB in cyanobacterial cells. A selection of important approaches has been listed in **Table 1**.

Table 1. Previous attempts to optimized the medium or genetic background of *Synechocystis sp.* PCC 6803 with for the production of PHB. Further approaches (also in other cyanobacteria) have been reviewed recently (Kamravamanesh et al., 2018b).

Genotype	PHB content (% CW)	Substrate	Production condition	Polymer composition	Reference
WT	29	0.4 % acetate	-P	PHB	(Panda et al., 2006)
overexpression *phaAB* (native)	35	0.4 % acetate	-N	PHB	(Khetkorn et al., 2016a)
overexpression *phaABC* (*Cupriavidus necator*)	11	10 mM acetate	-N	PHB	(Sudesh et al., 2002)
overexpression nphT7, phaB, phaC	41	0.4 % acetate	Limited air exchange, -N	-	(Lau et al., 2014)
overexpression Xfpk	12	CO_2	-N, -P	PHB	(Carpine et al., 2017)
overexpression *sigE*	1.4	CO_2	-N	PHB	(Osanai et al., 2013)
overexpression *rre37*	1.2	CO_2	-N	PHB	(Osanai et al., 2014)

Most of the attempts in the past have focused on genetical engineering approaches to reroute the intracellular flux towards PHB (Carpine et al., 2017, Lau et al., 2014, Osanai et al., 2013, Osanai et al., 2014). *Synechocystis* is naturally producing PHB from acetyl-CoA via the enzymes acetyl-CoA acetyltransferase (PhaA), acetoacetyl-CoA reductase (PhaB) and the heterodimeric PHB synthase (PhaEC). The overproduction of the genes encoding for those enzymes is known for increasing the PHB content within the cells (Khetkorn et al., 2016a, Sudesh et al., 2002).

The highest reported rate of photosynthetically produced PHB in a wildtype (WT) cyanobacterium was achieved in a strain isolated from a wet volcanic rock in Japan. This strain,

Synechococcus sp. MA19, achieved 27 % / CDW (Miyake et al., 1996). It has to be mentioned though that other groups, who tried to work with this strain, reported that they were unable to obtain it from any known strain collection or laboratory (Markl et al., 2018). Hence, it has to be assumed that this strain disappeared. Another mentionable approach was achieved by applying UV radiation for random mutagenesis (Kamravamanesh et al., 2018a). The created *Synechocystis sp*. PCC 6714 strain produced up to 37 % PHB / CDW under phototrophic growth with CO_2 as the sole carbon source.

Besides genetical engineering, applying optimized growth conditions and medium was demonstrated to also increase PHB production (Panda et al., 2006). A study investigating 137 different cyanobacterial species found that 88 of them produced PHB, depending on the nutrient, which was lacking in the growth medium (Kaewbai-Ngam et al., 2016). The highest yields were often achieved when cells were starved for nitrogen. Furthermore, the addition of organic carbon sources, like acetate or fructose, resulted in increased PHB production (Panda et al., 2006). A comprehensive overview about different approaches can be found in recent reviews (Kamravamanesh et al., 2018b, Singh and Mallick, 2017). Conflicting results concerning PHB synthesis were reported from attempts, where cells were grown under conditions of limited gas exchange. Whereas some groups reported increased yields (Panda et al., 2006, Lau et al., 2014), other groups reported that they were unable to reproduce this effect (Kamravamanesh et al., 2017). Furthermore, a recent study demonstrated that cells, which were grown under standing-conditions and were thereby also exposed to limited gas-exchange, exhibited a decreased PHB accumulation (Koch et al., 2020). Despite these various approaches to further increase the PHB content in *Synechocystis,* the highest PHB contents reached so far are still far beyond what was accomplished in heterotrophic bacteria, where more than 80 % of biomass is converted into the desired product.

We have recently identified a gene, sll0944, whose deletion resulted in significantly increased PHB synthesis. The Sll0944 ("PirC") deficient mutant converted its intracellular glycogen pool under nitrogen starvation rapidly to PHB (Orthwein et al., 2020). Therefore, the aim of this study was to create a strain with maximized PHB content by combining the sll0944 mutation with other factors that improve PHB synthesis. This resulted in a strain that can accumulate more than 80% PHB, which is by far the most efficient PHB producing oxygenic photosynthetic organism reported to date.

2. Results

In this study, we wanted to test if the PHB content of a mutant strain based on a Δ*sll0944* background can be further increased. Recently it was shown, that overexpression of the PHB synthase PhaEC in *Synechocystis* PCC 6803 can cause a reduction of the PHB production, while overexpression of its *phaAB* genes caused an increase in intracellular PHB accumulation (Khetkorn et al., 2016a). Here, we cloned and overexpressed *phaA* and *phaB* from the known PHB production strain *Cupriavidus necator* (formerly known as *Ralstonia eutropha*) into a Δ*sll0944* strain. We used these genes, since they are derived from an highly efficient PHB synthesizing organism. Furthermore, the expression of heterologous enzymes ensures that these enzymes are not inhibited by intracellular regulatory mechanisms. Both genes were cloned into a pVZ322 vector under the regime of a strong promotor P*psbA2*. The plasmid was then transformed into the strain Δ*sll0944*, thereby creating the strain Δ*sll0944*-RE*phaAB* (Figure S1). For simplifications, the strain was termed PPT1 (for PHB Producer Tübingen 1).

Strain characterization

To compare the growth of the newly generated strain with the WT, both strains were grown under continuous illumination as well as under a 12/12 hours light/dark regime (**Figure 1**).

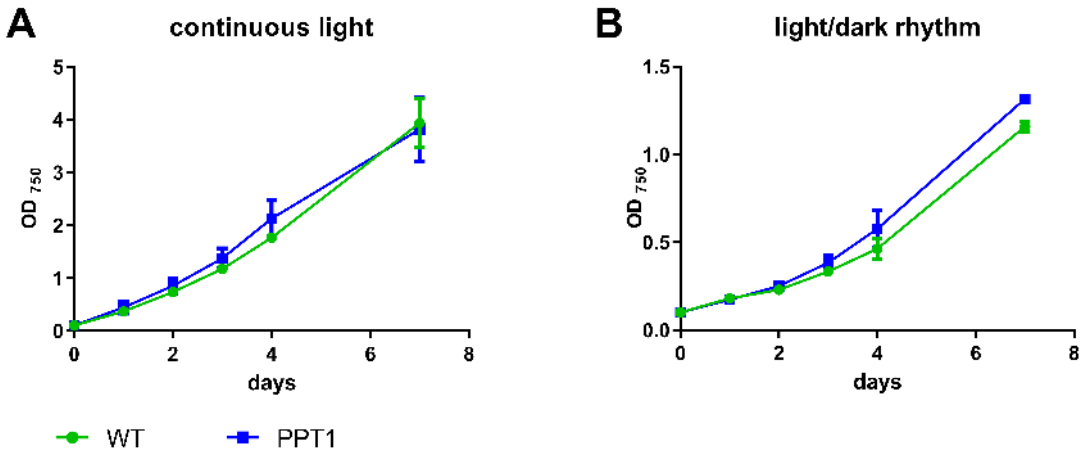

Figure 1. Growth behavior of WT and PPT1 strains grown under continuous illumination (A) or under a 12/12 hour light/dark regime (B). The growth was determined over 7 days by recording the OD_{750}. Each point represents a mean of three independent biological replicates.

Under both light regimes, WT and PPT1 strain exhibited similar growth rates. This was also the case when the strains were grown on solid agar plates (Figure S2). To test whether the mutant strain was able to produce PHB under vegetative growth, the PHB production of both strains was tested in BG_{11} medium during exponential and stationary growth stages (OD_{750} ~1 and ~3, respectively) (Figure S3). While the WT did not produce any detectable amounts of PHB under exponential growth, the mutant accumulated ~ 0.5 % / CDW. Under stationary conditions, none of both strains produced any detectable amount of PHB.

To test, whether the newly generated mutant is able to accumulate higher amounts of PHB under production conditions, different cultivation conditions were systematically tested. The conditions of the highest production rates were then used for further experiments. First, the impact of continuous illumination compared to day-night cycles was tested. Therefore, WT and PPT1 cells were shifted to nitrogen-free BG_0 medium to induce chlorosis and were subsequently grown under 12/12 hours light /dark cycle or under continuous illumination; the amount of intracellular PHB was quantified and normalized to the CDW (Figure 2). For an easier comparison, all following graphs about PHB accumulation have the same y-axis scalation.

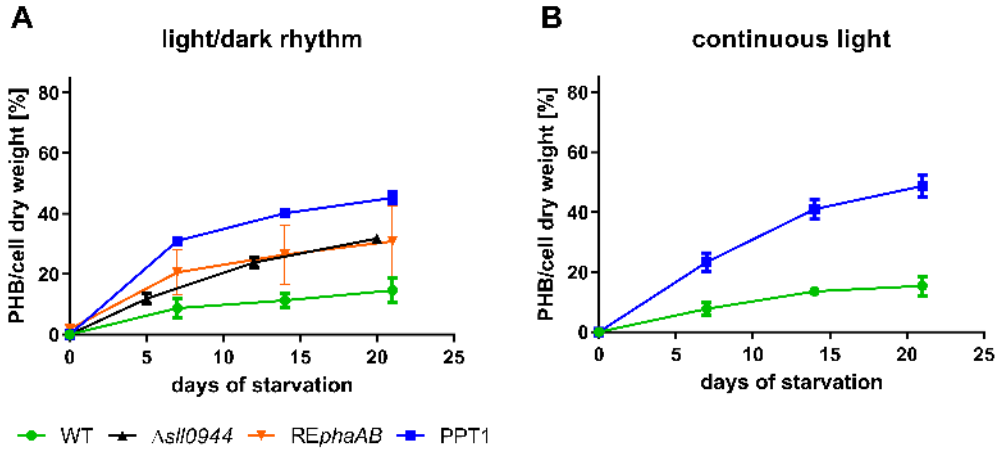

Figure 2. PHB content of WT (blue), Δ*sll0944* (black), RE*phaAB* (orange) and PPT1 (green) cells with different light regimes. Exponentially grown cells were shifted to nitrogen free BG_0 and cultivated

under either diurnal (12 hours light/12 hours darkness) (A) or continuous light (B). Each point represents a mean of three independent biological replicates.

To test the influence of the individual genetic modifications, the PHB content of two strains harbouring only one of the two genetic alterations (Δ*sll0944* or RE*phaAB*, respectively) were measured. Compared to the WT, the Δ*sll0944* and the RE*phaAB* strains produced higher amounts of PHB (32 and 31 % / CDW, respectively) after three weeks of chlorosis. When both mutations were combined (PPT1), the accumulation of PHB was further increased to 48 and 45 % PHB / CDW at dark/light or continuous light, respectively. With 31 % of PHB per CDW after 7 days in diurnal cultivation, the initial rate of PHB synthesis in the PPT1 cells was higher as compared to continuous illumination, where PHB amounted to 23 %. Therefore, these conditions were further investigated.

Medium optimization

Other studies have reported that, besides nitrogen, the lack of other elements can also induce the biosynthesis of PHB in *Synechocystis* (Kaewbai-Ngam et al., 2016). To test this effect on the newly generated strain, WT and PPT1 cells were shifted to either sulphur, phosphor or nitrogen/phosphor-free medium and the content of intracellular PHB was quantified (Figure 3).

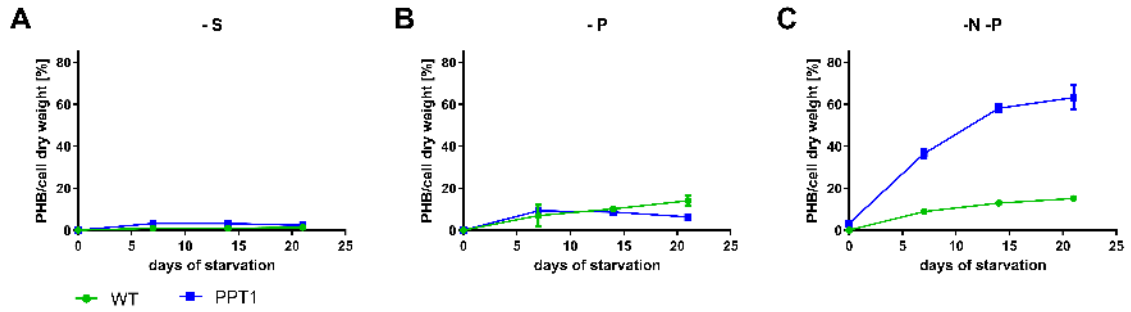

Figure 3. PHB content of WT (green) and PPT1 (blue) cells grown in different media under dark/light rhythm. To induce PHB production, exponentially grown cells were shifted to either sulphur, phosphor or nitrogen/phosphor free medium (A, B and C, respectively). Each point represents a mean of three independent biological replicates.

Whenever phosphate free production conditions were used, the precultures were already grown in phosphate-free BG_{11}, in order to deplete the intracellular polyphosphate storage pools of *Synechocystis*. In sulphur- as well as in phosphor-free medium, both strains produced only minor amounts of PHB. However, when the cells were shifted to nitrogen/phosphor-free medium, the mutant strain accumulated after three weeks high amounts of up to 63 % / CDW. Under the same conditions, the WT accumulated only 15 % / CDW. All further experiments will be based on cultures grown in nitrogen- and phosphor depleted BG_{11} medium.

To test, if the produced PHB amounts can be further increased by the addition of an additional carbon sources, either 100 mM $NaHCO_3$ or 10 mM acetate were added after the shift to nitrogen/phosphor-free medium (Figure 4).

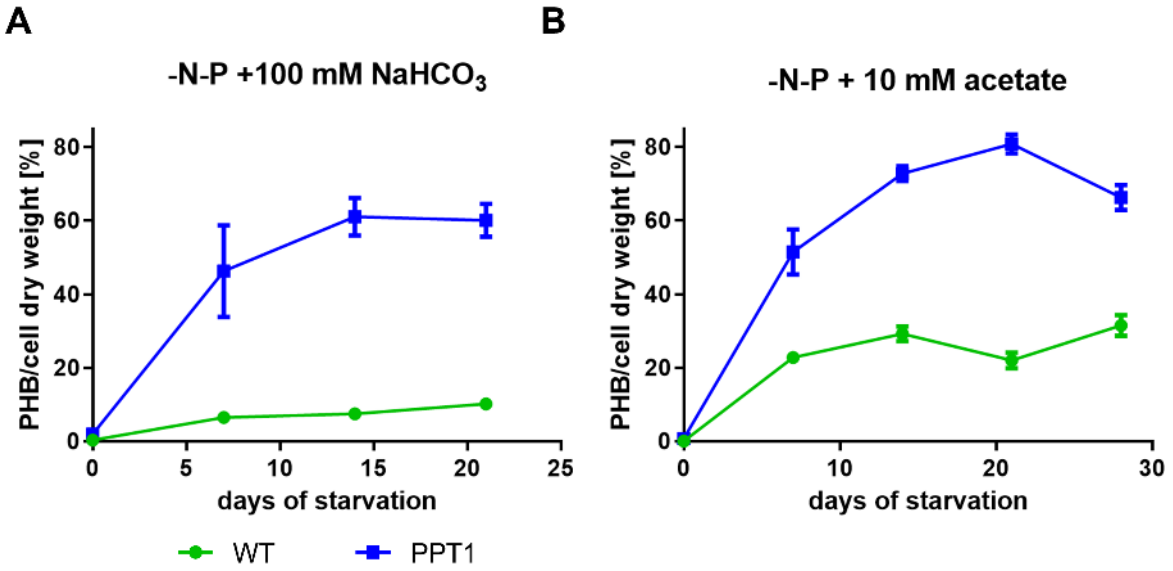

Figure 4. PHB production of WT (green) and PPT1 (blue) cells grown under alternating light/dark regime. (A) Cells shifted to nitrogen/phosphor free medium with the addition of 100 mM $NaHCO_3$. (B) Cells shifted to nitrogen/phosphor free medium with the addition of 10 mM acetate. Each point represents a mean of three independent biological replicates.

As in the previous experiments, cells were again cultivated in diurnal light/dark regime. When $NaHCO_3$ was added, the PPT1 cells reached intracellular PHB contents of up to 61 % / CDW after two weeks, while the WT accumulated only 10 % / CDW. Notably, the initial production rate was further increased, leading to an average of 46 % / CDW in the PPT1 after one week. When instead of $NaHCO_3$ 10 mM acetate were added, the WT reached intracellular PHB contents of up to 32 % / CDW after four weeks, while the PPT1 mutant accumulated up to 81 % / CDW after three weeks of starvation (Figure 4 A). A further starvation of another week did not further increase the yields, but instead slightly reduced the intracellular amount of PHB. When cells were grown under the same conditions but with continuous illumination, the produced amounts of PHB were much lower (Figure S4).

To test if the limitation of gas-exchange could lead to a further increase of PHB production, nitrogen-phosphorus starved cells were grown in sealed vessels. However, after an initial increase of intracellular PHB, the amount dropped strongly (Figure S5).

Visualization of PHB granules

To find out how the high PHB values that were quantified by HPLC analysis affect the morphology of the cells, and how these masses of PHB are organized within the cells, fluorescence microscopy as well as transmission-electron-microscopy (TEM) pictures were taken (Figure 5).

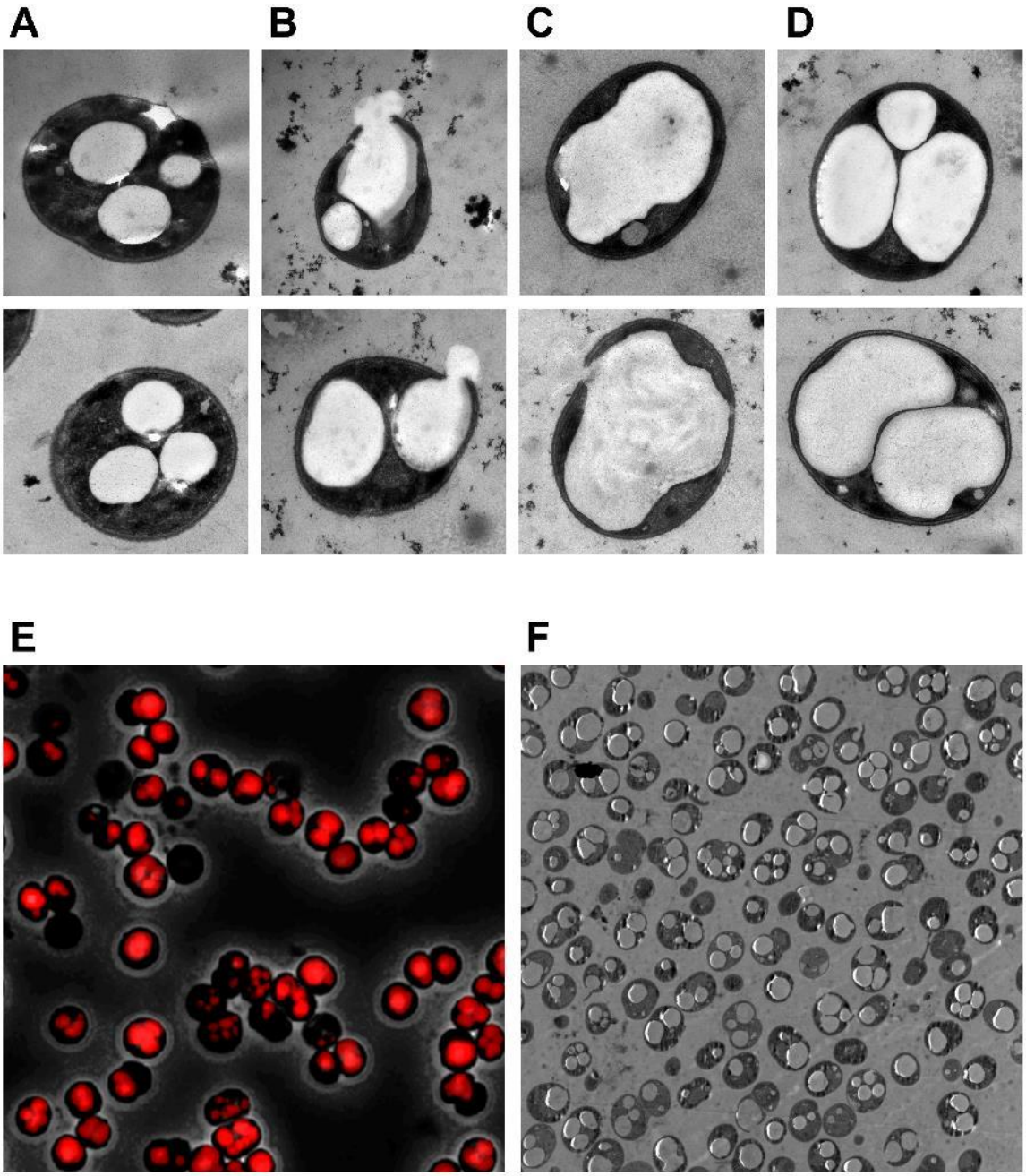

Figure 5. WT (A) and PPT1 cells (B-F) after 21 days of nitrogen-phosphorus-starvation with 10 mM acetate grown under alternating light/dark regime. (A) WT cells for comparison. (B) PTT1 cells showing a ruptured cell wall. (C) PPT1 cells with a single PHB granule. (D) PPT1 cells with multiple granules. (E) Fluorescence microscopic picture of PPT1 cells; PHB granules are visualized as red inclusions after staining with Nile red. (F) Overview of multiple PPT1 cells.

The samples for the images in Figure 5 were taken from the same cells, which were used for the experiment shown in Figure 4 B after 21 days (PPT1 cells, nitrogen-phosphorus starvation with 10 mM acetate). Electron-microscopic images show that the cells are fully packed with PHB granules (Figure 5 C, D). Although some heterogeneity among the cells is visible, most of the cells contained large quantities of PHB. The TEM pictures revealed that the interior of many cells was vastly filled up by PHB (Figure 5 C, D). Interestingly, most cells contained not multiple, but only one large PHB granule, indicating a potential fusion from smaller granules. In several cases, the observed cells were

already ruptured, releasing PHB into their environment (Figure 5 B). In overview TEM pictures, it became apparent that most cells contained large quantities of PHB (Figure 5 F).

Qualitative analysis of PHB

To further characterize the material properties of the produced PHB, PPT1 cells were cultivated for four weeks under nitrogen and phosphorus starvation. The cells were broken by sodium hypochlorite treatment and the purified PHB was analysed via gel permeation chromatography (GPC), 1H-NMR and 13C-NMR, to determine the molecular weight, the dispersity, the purity and the tacticity of the polymer, respectively. GPC analysis showed that PPT1 produces a high-molecular-weight polymer with relatively narrow dispersity (Figure 6). The number-average molecular weight was determined at Mn = 503 kg/mol ($Đ$ = 1.74), which was more than twice as high than the control (Mn = 246 kg/mol, $Đ$ = 2.33).

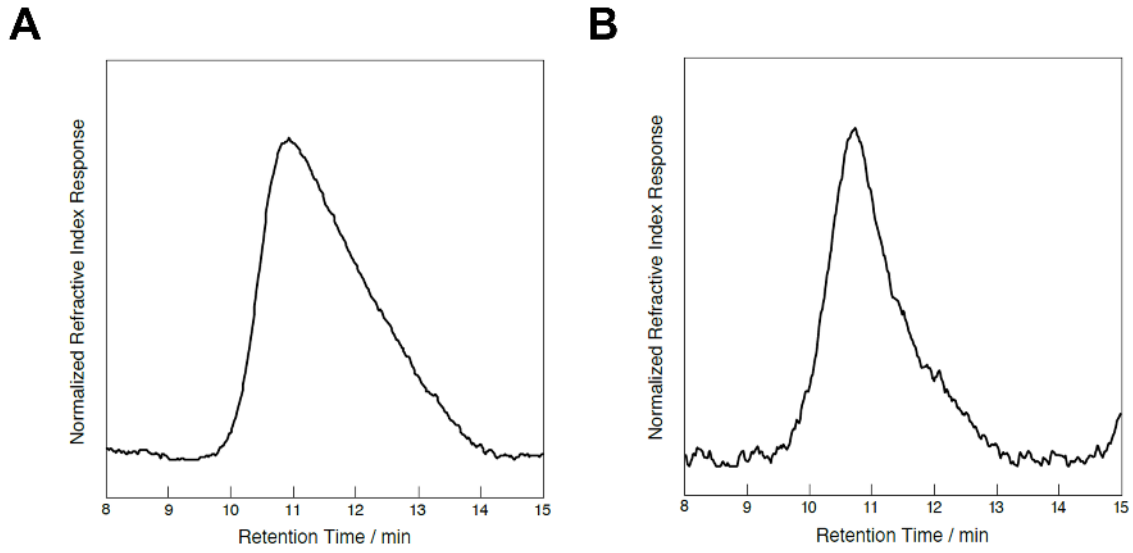

Figure 6. GPC analysis of PHB from an industrial standard (A) and PPT1 (B).

The chemical structure of the polymer was confirmed by 1H and 13C NMR spectroscopy to be completely pure PHB (Figure S6, S7). Furthermore, the observed singlet resonances in the 13C NMR spectrum indicated that the PHB derived from PPT1 is highly isotactic (Figure S8).

3. Discussion

Δsll0944-REphaAB produces maximum amounts of PHB

As previous studies have shown, PHB is derived from the intracellular glycogen pools (Koch et al., 2019). Furthermore, this carbon flux is regulated by the protein Sll0944, which controls a central enzyme of the glycogen catabolism (phosphoglyceratemutase) (Orthwein et al., 2020). Deletion of Sll0944 results in strongly increased glycogen catabolism during prolonged nitrogen starvation. By the additional expression of the genes *phaA* and *phaB*, most of the carbon is redirected from the acetyl-CoA to the PHB pool. Since the reaction catalyzed by PhaB is converting one NADPH to NADP, the reaction yielding hydroxybutyryl-CoA is strongly favored during nitrogen starvation, where NADPH pools are increased (Hauf et al., 2013), driving PHB forward (Figure S1).

When grown in nutrient-replete balanced medium, the growth behavior of the PPT1 strain was comparable to the WT, in liquid medium as well as on solid agar plates (Figure 1, Figure S2). It is

expected that both strains behave similar under these conditions, since there was hardly any PHB produced under vegetative grow (Figure S3) and since *sll0944* is mostly expressed during nitrogen starvation (Klotz et al., 2016b). The newly generated strain PPT1 shows a combinatory phenotype of both individual strains Δ*sll0944* and RE*phaAB*: while both individual strains have increased PHB production under nitrogen starvation by ~10 % / CDW, the strain PPT1 showed an additive phenotype of both effects and thereby reached values of up to 45 % / CDW (Figure 2 A). Similar PHB contents were reached regardless of the applied light regime, indicating that the production of PHB is not limited by the availability of light (Figure 2). The accumulation of PHB was further boosted by combined nitrogen-phosphorus starvation (Figure 3 C). This is in accordance with previous studies, where the combined nitrogen-phosphorus starvation caused the highest PHB production (Carpine et al., 2017). In contrast, the individual limitation of either sulfur or phosphorus resulted in only small intracellular PHB accumulations (Figure 3 A and B). It was shown before, that nitrogen limitation is most efficient for the induction of PHB synthesis in cyanobacteria (Kaewbai-Ngam et al., 2016). In a recently created strain though, it was shown that a random mutation in a phosphate specific membrane protein PstA caused a strong increase in PHB accumulation, hinting towards the importance of phosphorus for PHB production (Kamrava et al., 2018).

When 100 mM $NaHCO_3$ were added to PPT1 cells cultivated in nitrogen-phosphorus depleted medium, a further increase of intracellular PHB levels was reached in the initial phase. This indicates that a limitation of carbon was impairing the PHB production in previous experiments. Since PHB is mostly formed from intracellular carbon (Dutt and Srivastava, 2018), carbon availability could be exhausted at such high PHB contents and thereby limit further accumulation of PHB. Notably, one of the three biological replicates exhibited a PHB content of 61 % / CDW after one week, indicating the potential to accelerate the pace of PHB formation by process engineering. The overall content was further increased by the addition of 10 mM acetate, hinting towards a limitation of the precursor acetyl-CoA. Since acetate can be converted to acetyl-CoA in a single enzymatic reaction, it is more efficiently metabolized to PHB compared to $NaHCO_3$.

Interestingly, the highest PHB content was reached under light/dark regime, while its accumulation was strongly diminished under continuous light, even upon the addition of acetate (Figure 4 and Figure S4). This fits to previous observations, where cultivation under diurnal light/dark cycles was shown to increase the PHB production (Koch et al., 2020). Cells which were cultivated under conditions of gas-exchange limitation showed reduced PHB accumulation. This was also reported by other groups (Kamravamanesh et al., 2017) and might be explained by the lack of oxygen during the night, which is necessary for maintaining cell metabolism. Alternatively, excess of oxygen during the day could cause an increased oxygenase reaction which wastes energy and thereby slows down cell metabolism.

Morphology of PHB granules

TEM pictures showed *Synechocystis* cells fully packed with PHB granules (Figure 5). Additionally, a certain number of cells displayed fractured cell envelops, leading to PHB granules leaking out of the cells. The rupture of cells could be due to intracellular mechanical pressure from the expanding PHB granules or it could be caused from mechanical stress during the preparation process. Whatever the cause of the ruptures was, it indicates an increased cell fragility due to the massive accumulation of PHB, since the effect was not detected in WT cells, which contained less PHB but were treated with the same procedure. This indicates that some PPT1 cells have reached an upper limit of how much PHB a cell can accumulate, above which cell viability is severely challenged. It was previously hypothesized that *Synechocystis* cells cannot accumulate larger quantities of PHB due to sterical hindrance of the thylakoid membranes. This study demonstrates that it is possible to manipulate *Synechocystis* in such a way that it accumulates vast amounts of PHB. Interestingly, most cells which contained large PHB-quantities possessed only very few granules, often just one single granule. This indicates that PHB granules merge together once they exceed a certain size.

Qualitative analysis of PHB

Analysis of the extracted PHB derived from PPT1 revealed that it consists of PHB only. While other bacteria are able to produce PHAs with different side chains, such as 3-hydroxyvalaerate, the PhaEC enzyme, which is present in *Synechocystis*, is producing selectively PHB. For future experiments, a mutant strain harbouring a heterologous PHA polymerase could be created for the production of heteropolymers with improved material properties, such as poly(3-hydroxybutyrate-co-3-hydroxyvalerate) (PHBV). Other cyanobacteria, like *Nostoc microscopicum*, have already shown to possess PHA-polymerases which are able to produce PHBV (Tarawat et al., 2020). In previous analysis the average molecular weight of PHB from *Synechocystis* and *Synechocystis* sp. PCC 6714 was determined at Mn ~ 130 and 316 kg mol^{-1}, respectively (Osanai et al., 2014, Lackner et al., 2019). Compared to this, the PHB derived from PPT1 is high-molecular, showing an average weight of 503 kg/mol. The PHB derived from PPT1 turned out to be highly isotactic, which is beneficial for good biodegradation properties.

Conclusiosn and outlook

To further accelerate PHB production, overexpressing a strong PHB-polymerase could be beneficial. Although it was shown that higher levels of PhaEC can lower the PHB content (Khetkorn et al., 2016b), its activity could be rate limiting once such high values as in this present study are reached. The insertion of another short-chain-length PHA-polymerase could furthermore lead to the production of PHAs with improved material properties (PHBV). In order to improve the overall production yields, increased growth rates would be necessary, for example by the cultivation in high-density cultivators. In similar approaches, *Synechocystis* cultures reached OD_{750} of above 50 when higher light and CO_2 concentrations were applied (Dienst et al., 2019, Lippi et al., 2018). Under those ideal conditions, up to 8 g of dry biomass l^{-1} d^{-1} were reached. If the time for chlorosis is assumed to be similar to the time required for cultivation and an intracellular PHB content of 60 % is reached, 2,4 g PHB l^{-1} d^{-1} could be produced under completely phototrophic conditions. Since the PHB production in the strain PPT1 is optimal under light/dark regime, the strain is also well suited for outdoor cultivation. Scaling up the cultivation to larger reactors would further reduce the production costs of PHB (Panuschka et al., 2019). Additionally, the ability of autotrophic cyanobacteria to sequester CO_2 from the atmosphere could be beneficial for CO_2 emission trading. Alternatively, a growth-coupled PHB production could be beneficial for certain kinds of cultivation.

In summary, this study shows for the first time that cyanobacteria have the potential to accumulate large quantities of PHB. Furthermore, we demonstrate that also under cultivation with CO_2 as the only carbon source, *Synechocystis* is able to produce quantities of PHB, which is of high relevance for the sustainable production of PHB as a bioplastic. This study helps to come closer to an industrial production of carbon neutral plastic alternatives.

5. Materials and Methods

Cyanobacterial cultivation conditions

If not stated differently, *Synechocystis sp.* PCC 6803 cultures were grown in standard BG_{11} medium with the addition of 5 mM $NaHCO_3$ (Rippka et al., 1979). The cultures were constantly shaken at 125 rpm, 28°C and at a illumination of ~50 µE. A 100 ml Erlenmeyer flask was used to grow 50 ml of bacterial culture. When cells were grown under alternating light/dark rhythm (12 hours each), the precultures were already adapted to these conditions by cultivating them under light/dark rhythm for two days. Whenever required, appropriate antibiotics were added to the mutant strains. When cultivation in depletion-medium was required, the following were used: for nitrogen starvation BG_0 (BG_{11} without $NaNO_3$); for sulfur starvation BG_{11} with MgCl instead of $MgSO_4$; for phosphor starvation KCl instead of K_2HPO_4. Since *Synechocystis* has intracellular polyphosphate storage polymers, a preculture in phosphorus free medium was inoculated two days before the actual shift

to phosphor free medium. For all starvations, exponentially grown cells (OD_{750} 0.4-0.8) were washed twice in the appropriate medium. For this, the cells were harvested at 4,000 g for 10 min, the supernatant discarded and the pellet resuspended in the appropriate medium. Afterwards the culture was adjusted to an OD_{750} of 0.4. For growth on solid surfaces, cells of an OD_{750} = 1 were dropped on BG_{11} plates containing 1.5 % agar. A serial dilution of the initial culture was prepared in order to count individual colony-forming-units. A list of used strains in this study is provided in Table 2.

Table 2. List of strains used in this study.

Name	Genotype	Reference
WT	*Synechcoystis sp.* PCC 6803	Pasteur culture collection
Δ*sll0944*	KanR	(Orthwein et al., 2020)
RE*phaAB*	pVZ322 with psbA2 regulated *phaAB* genes from *Cupriavidus necator*; GenR	This study
PPT1 (Δ*sll0944*-RE*phaAB*)	KanR, GenR	This study

Construction of RE*phaAB* and Δ*sll0944*-RE*phaAB* mutants

The promotor psbA2 and *phaAB* were amplified from genomic DNA of *Synechocystis* and C*upriavidus necator*, respectively. For this, the primer psbaA2fw2/psbA2rv2 or RephaABA2fw/RephaABA2rv were used (Table 3). A Q5 high-fidelity polymerase (NEB) was used to amplify the DNA fragments. The latter were subsequently assembled in pVZ322 vector (Gibson et al., 2009), which was beforehand opened at the XbaI site. The resulting vector was propagated in *E. coli* Top10 and isolated using a NEB miniprep kit. The plasmid was subsequently sequenced to verify sequence integrity. The correct plasmid was then transformed into *Synechocystis* using triparental mating (Wolk et al., 1984), resulting in the strain RE*phaAB*. The same RE*phaAB* plasmid was also transformed in the strain Δ*sll0944*, resulting in the strain PPT1 (Δ*sll0944*-RE*phaAB*).

Table 3. List of oligonucleotides used in this study.

Primer name	Sequence
psbA2fw2	gcttccagatgtatgctcttctgctcctgcaggtcgactcatttttccccattgccccaaaatac
psbA2rv2	gatacgatgacaacgtcagtcattttggttataattccttatgtatttg
RePhaABA2fw	caaatacataaggaattataaccaaaatgactgacgttgtcatcgtatc
RePhaABA2rv	atgaatgttccgttgcgctgcccggattacagatcctctatcagcccatgtgcaggccgccgttg

Gas exchange limitation

When gas exchange limitation was applied, 10 ml of culture were transferred to a 15 ml reaction tube. The tube was closed and additionally sealed with several layers of parafilm. During the incubation, the reaction tubes were constantly shaken.

Microscopy and staining procedures

To analyze the intracellular PHB granules, 100 µl of *Synechocystis* culture were centrifuged (10,000 g, 2 min) and 80 µl of the supernatant discarded. Nile red (10 µl) was added and the pellet resuspended. From this mixture, 10 µl were dropped on an agarose-coated microscopy slide. For the detection, a Leica DM5500 B with an 100x /1.3 oil objective was used. An excitation filter BP 535/50 was used to detect Nile red stained granules.

PHB quantification

To determine the intracellular PHB content, ~10 ml of cells were harvested by centrifugation (10 min at 4,000 g). The supernatant was discarded, and the remaining cell-pellet dried in a Speed-Vac for at least 2 h at 60°C. The weight of the dried pellet was measured to determine the CDW. Next, 1 ml of concentrated sulfuric acid (18 M H_2SO_4) was added and the sample was boiled for 1 h at 100°C. This process converts PHB to crotonic acid at a ratio of 1 to 0.893. The samples were diluted by transferring 100 µl to 900 µl of 14 mM H_2SO_4. Subsequently, the tubes were centrifuged for 10 min at 10,000 g. Next, 500 µl of the supernatant were transferred to a new tube and 500 µl of 14 mM H_2SO_4 were added. The samples were centrifuged again and 400 µl of the clear supernatant was transferred into a glass vile for HPLC analysis. For this, a 100 C 18 column (125 by 3 mm) was used with 20 mM phosphate buffer at pH 2.5 for the liquid phase. As a standard, a dilution series of commercially available crotonic acid was used. The final amount of crotonic acid was detected at 250 nm.

Electron microscopy

For electron microscopic pictures, *Synechocystis* cells were fixed and post-fixed with glutaraldehyde and potassium permanganate, respectively. Subsequently, ultrathin sections were stained with lead citrate and uranyl acetate (Fiedler et al., 1998). The samples were then examined using a Philips Tecnai 10 electron microscope at 80 kHz.

Purification of PHB

For the analysis of PHB, PPT1 cells were cultivated for four weeks in BG_{11} medium (without phosphorus and nitrogen) at light/dark regime. The cells were harvested by centrifugation for 10 min at 4,000 g. The cell pellet was resuspended in 15 ml freshly bought sodium hypochlorite solution (6 %) and shaken over night at room temperature. The next day, the cell debris were centrifuged and washed with water (10 times), until the chlorine smell disappeared. Subsequently, the pellet was washed once with 80 % ethanol and once with acetone.

NMR and GPC

To characterize the chemical properties of PHB derived from PPT1, NMR spectra were recorded on a Bruker AVIII-400 spectrometer at ambient temperatures. As a control, an industrial standard PHB was used (BASF, Ludwigshafen, Germany). ^{1}H and ^{13}C NMR spectroscopic chemical shifts δ were referenced to internal residual solvent resonances and are reported as parts per million relative to tetramethylsilane. The tacticity of the polymer was analysed by ^{13}C NMR spectroscopy according to literature (Bloembergen et al., 1989). As NMR solvent, $CDCl_3$ was used (Sigma-Aldrich, Taufkirchen, Germany).

Measurements of polymer weight-average molecular weight (M_w), number-average molecular weight (M_n) and molecular weight distributions or dispersity indices ($Đ = M_w / M_n$) were performed via gel permeation chromatography (GPC) relative to polystyrene standards on an PL-SEC 50 Plus instrument from Polymer Laboratories using a refractive index detector. The analysis was performed at ambient temperatures using chloroform as the eluent at a flow rate of 1.0 mL min^{-1}.

Supplementary Materials

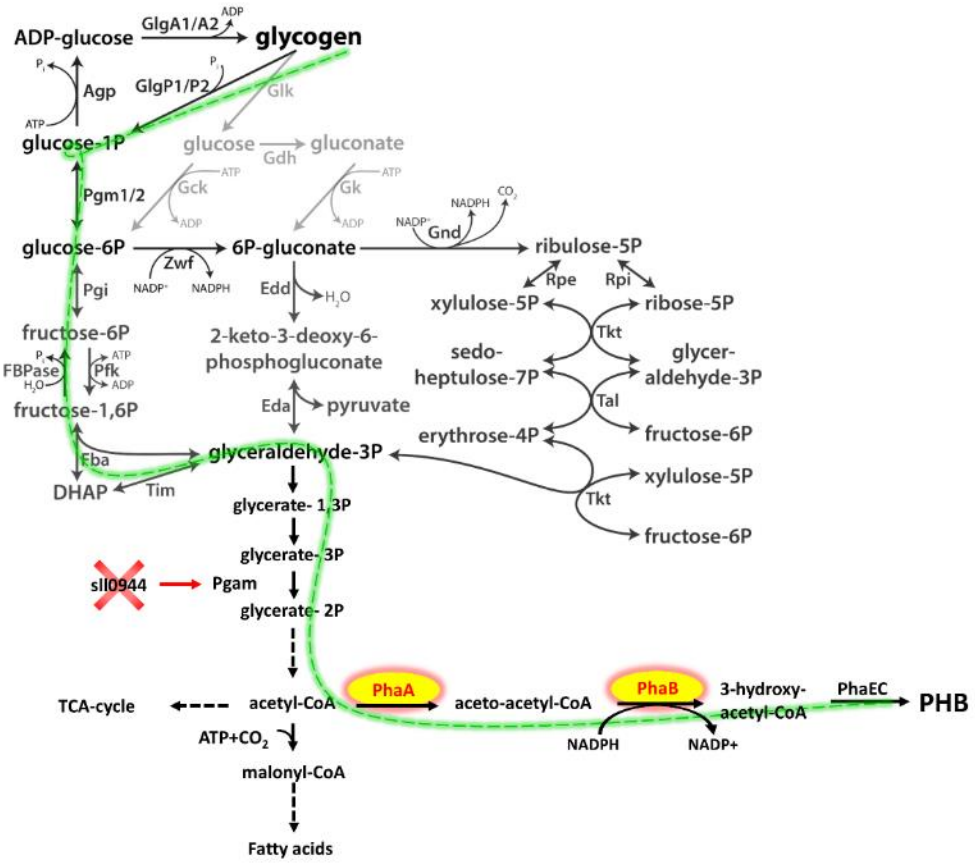

Figure S1. Overview about the central carbon-pathways in *Synechocystis*. It was previously shown, that the glycogen and PHB pool are interconnected via the EMP pathway (green) (Koch et al., 2019). Highlighted are the deleted protein Sll0944 and its target, the phosphoglyceratmutase, as well as the two overexpressed enzymes, PhaA and PhaB.

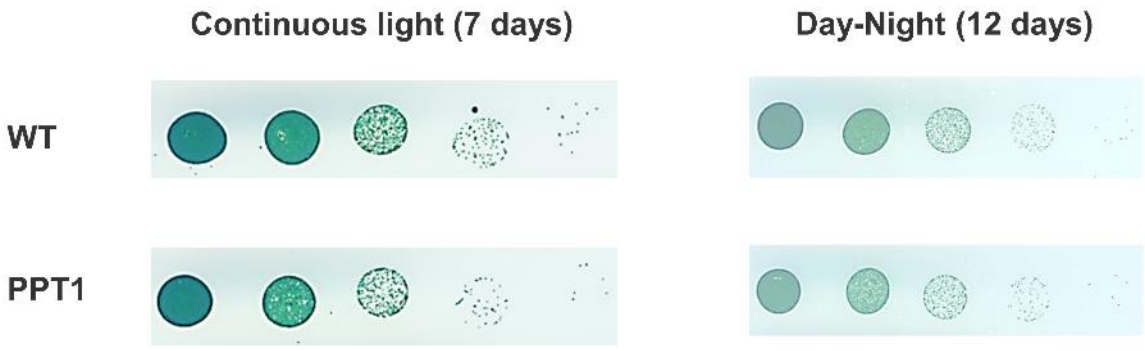

Figure S2. Drop plate assay of the WT and PPT1. Vegetative cells at an OD_{750} of 1 were diluted 10-fold for five times (10^0 to 10^4, respectively). The dilutions were then dropped on a BG_{11} agar plate

and grown at continuous light or light/dark rhythm for 7 or 12 days, respectively. The plate shown in the figure is representative for 3 individually grown biological replicates.

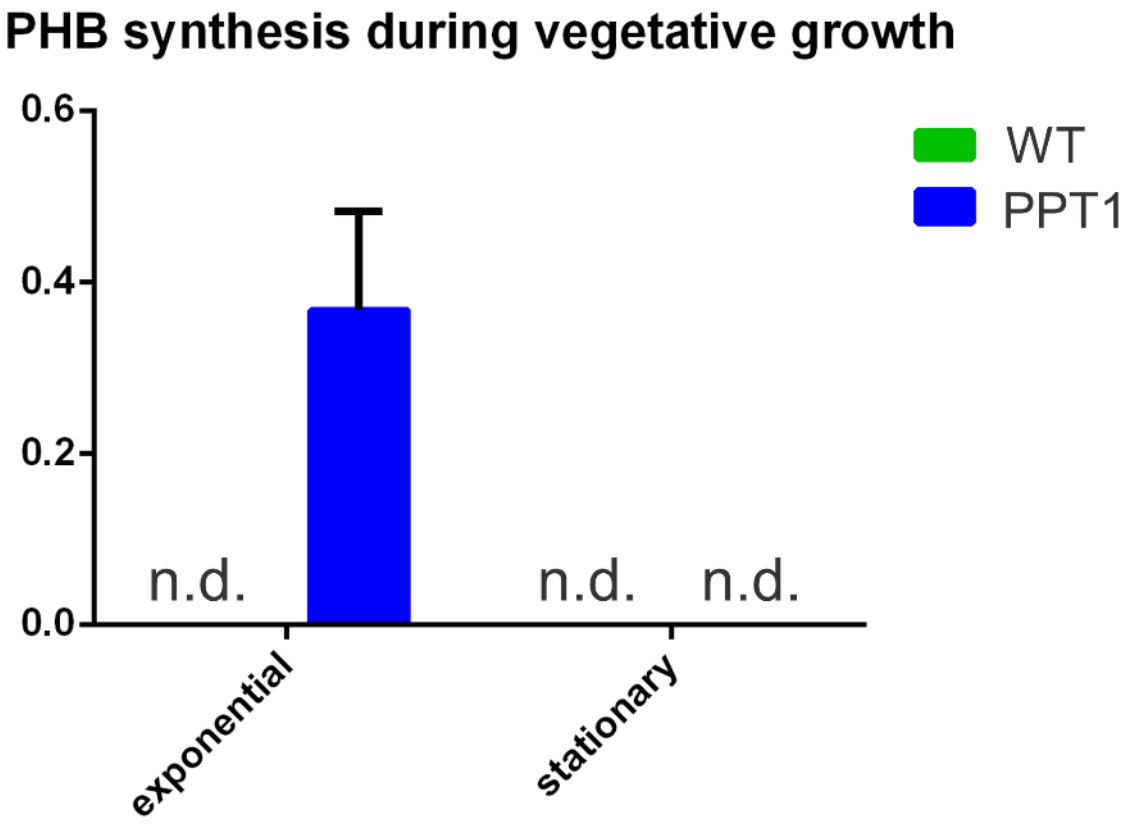

Figure S3. PHB accumulation under vegetative growth. WT and PPT1 cells were sampled during exponential or stationary phase (OD ~1 and ~3, respectively) at continuous lighting. n.d. = not detectable. Each point represents a mean of three independent biological replicates.

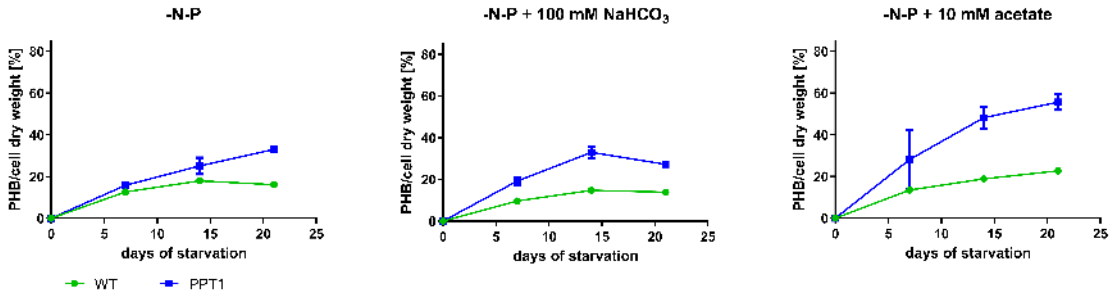

Figure S4. PHB production of WT (green) and PPT1 (blue) cells grown under continuous lighting. Cells shifted to nitrogen/phosphor free medium (A) and with additional 100 mM $NaHCO_3$ (B) or 10 mM acetate (C). Each point represents a mean of three independent biological replicates.

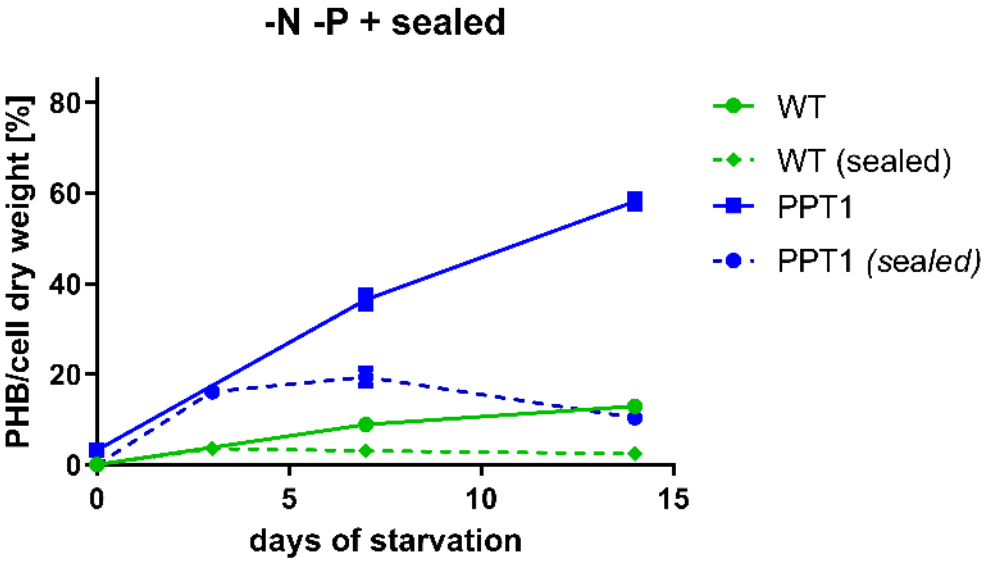

446

447 **Figure S5.** PHB content of WT (green) and PPT1 (blue) cells grown in nitrogen/phosphor free
448 medium under light/dark regime. Dashed lines indicate growth in sealed vessels. Each point
449 represents a mean of three independent biological replicates.

450

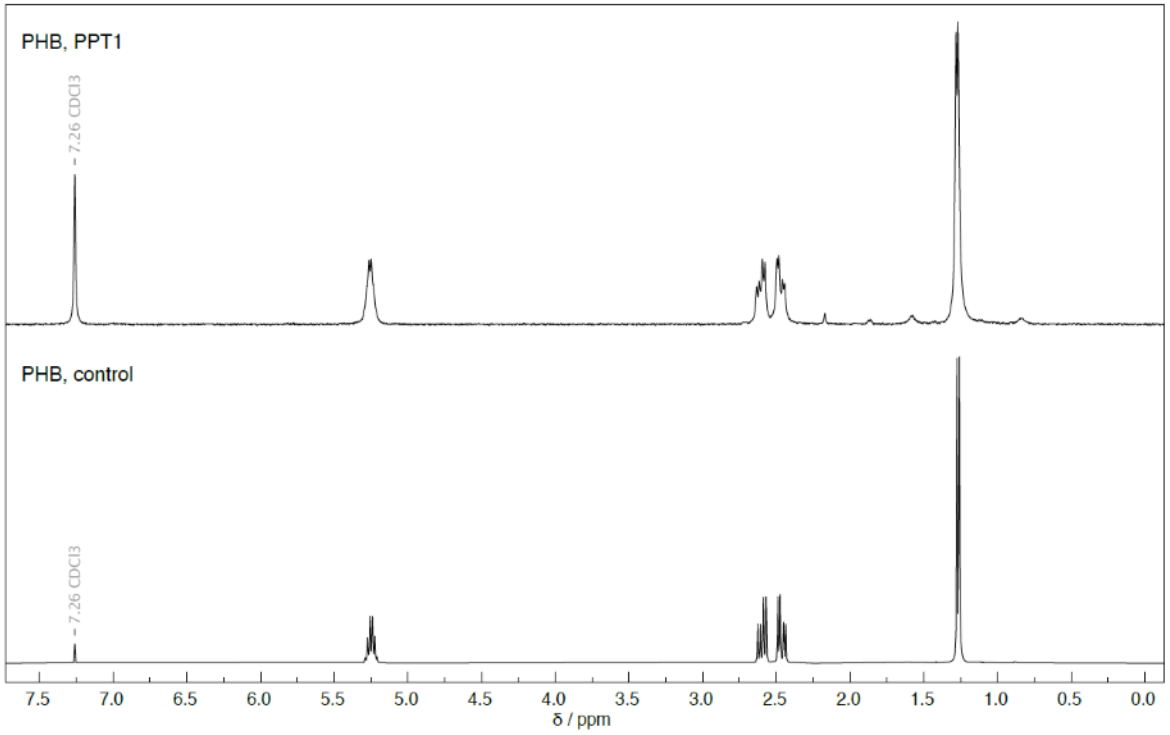

451

452 **Figure S6.** ^{1}H NMR ($CDCl_3$, 400 MHz) spectrum of PHB derived from PPT1 compared to an
453 industrial standard sample.

454

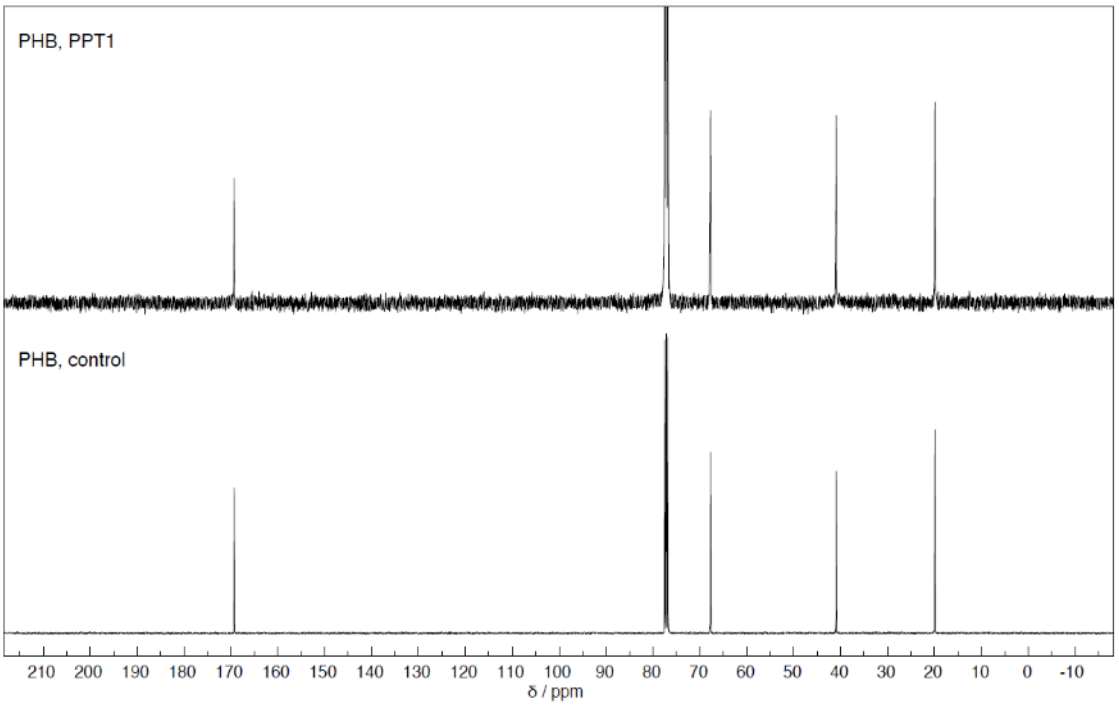

455

456 **Figure S7.** ^{13}C NMR spectrum ($CDCl_3$, 101 MHz) of PHB derived from PPT1 compared to an
457 industrial standard sample.

458

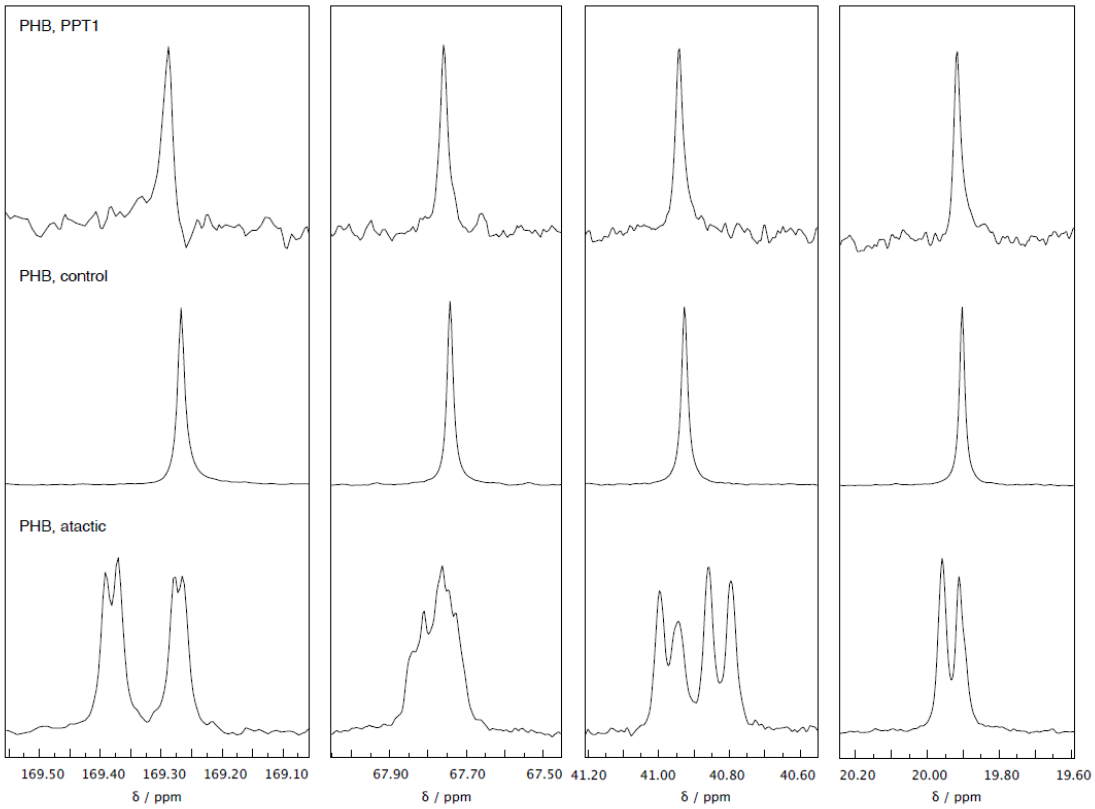

459

460 **Figure S8.** ^{13}C NMR spectrum to analyse the tacticity of PHB derived from PPT1. For comparison,
461 industrial standard PHB (isotactic) and atactic PHB (produced from ß-butyrolactone via
462 ring-opening polymerization) are shown.

Author Contributions: Conceptualization, M.K. and K.F.; Methodology, M.K. and K.F.; Investigation, M.K.; Writing-Original Draft Preparation, M.K. and K.F.; Writing-Review & Editing, M.K and K.F.; Supervision, K.F.; Project Administration, M.K. and K.F.

Funding: This research was funded by the Studienstiftung des Deutschen Volkes and the RTG 1708 "Molecular principles of bacterial survival strategies". We acknowledge support by Deutsche Forschungsgemeinschaft and Open Access Publishing Fund of University of Tübingen.

Acknowledgments: We thank Claudia Menzel for the preparation of the TEM pictures, Eva Nußbaum for the maintenance of cyanobacterial strains and technical assistance as well as Andreas Kulik for the operation of the HPLC.

Conflicts of Interest: The authors declare no conflict of interest

Abbreviations

AKIYAMA, H., OKUHATA, H., ONIZUKA, T., KANAI, S., HIRANO, M., TANAKA, S., SASAKI, K. & MIYASAKA, H. 2011. Polyhydroxyalkanoate (PHA) Production from Carbon Dioxide by Recombinant Cyanobacteria. *Bioresource technology,* 102**,** 11039-42.

ALLEN, M. M. & SMITH, A. J. 1969. Nitrogen chlorosis in blue-green algae. *Archiv für Mikrobiologie,* 69**,** 114-120.

BALAJI, S., GOPI, K. & MUTHUVELAN, B. 2013. A review on production of poly β hydroxybutyrates from cyanobacteria for the production of bio plastics. *Algal Research,* 2**,** 278-285.

BLOEMBERGEN, S., HOLDEN, D. A., BLUHM, T. L., HAMER, G. K. & MARCHESSAULT, R. H. 1989. Stereoregularity in synthetic β-hydroxybutyrate and β-hydroxyvalerate homopolyesters. *Macromolecules,* 22**,** 1656-1663.

CARPINE, R., DU, W., OLIVIERI, G., POLLIO, A., HELLINGWERF, K. J., MARZOCCHELLA, A. & BRANCO DOS SANTOS, F. 2017. Genetic engineering of Synechocystis sp. PCC6803 for poly-β-hydroxybutyrate overproduction. *Algal Research,* 25**,** 117-127.

CHEN, G.-Q. 2009. ChemInform Abstract: A Microbial Polyhydroxyalkanoates (PHA) Based Bio- and Materials Industry. *Chemical Society reviews,* 38**,** 2434-46.

DIENST, D., WICHMANN, J., MANTOVANI, O., RODRIGUES, J. & LINDBERG, P. 2019. *High density cultivation for efficient sesquiterpenoid biosynthesis in Synechocystis sp. PCC 6803*.

DOELLO, S., KLOTZ, A., MAKOWKA, A., GUTEKUNST, K. & FORCHHAMMER, K. 2018. A Specific Glycogen Mobilization Strategy Enables Rapid Awakening of Dormant Cyanobacteria from Chlorosis. *Plant Physiology,* 177**,** 594-603.

DUTT, V. & SRIVASTAVA, S. 2018. Novel quantitative insights into carbon sources for synthesis of poly hydroxybutyrate in Synechocystis PCC 6803. *Photosynth Res,* 136**,** 303-314.

FIEDLER, G., ARNOLD, M., HANNUS, S. & MALDENER, I. 1998. The DevBCA exporter is essential for envelope formation in heterocysts of the cyanobacterium Anabaena sp. strain PCC 7120. *Mol Microbiol,* 27**,** 1193-202.

GEYER, R., JAMBECK, J. R. & LAW, K. L. 2017. Production, use, and fate of all plastics ever made. 3**,** e1700782.

GIBSON, D. G., YOUNG, L., CHUANG, R.-Y., VENTER, J. C., HUTCHISON, C. A. & SMITH, H. O. 2009. Enzymatic assembly of DNA molecules up to several hundred kilobases. *Nature Methods,* 6**,** 343-345.

HAUF, W., SCHLEBUSCH, M., HUGE, J., KOPKA, J., HAGEMANN, M. & FORCHHAMMER, K. 2013. Metabolic Changes in Synechocystis PCC6803 upon Nitrogen-Starvation: Excess NADPH Sustains Polyhydroxybutyrate Accumulation. *Metabolites,* 3**,** 101-18.

HEIN, S., TRAN, H. & STEINBUCHEL, A. 1998. Synechocystis sp. PCC6803 possesses a two-component polyhydroxyalkanoic acid synthase similar to that of anoxygenic purple sulfur bacteria. *Archives of Microbiology,* 170**,** 162-170.

JAMBECK, J. R., GEYER, R., WILCOX, C., SIEGLER, T. R., PERRYMAN, M., ANDRADY, A., NARAYAN, R. & LAW, K. L. 2015. Plastic waste inputs from land into the ocean. 347**,** 768-771.

KAEWBAI-NGAM, A., INCHAROENSAKDI, A. & MONSHUPANEE, T. 2016. Increased accumulation of polyhydroxybutyrate in divergent cyanobacteria under nutrient-deprived photoautotrophy: An efficient conversion of solar energy and carbon dioxide to polyhydroxybutyrate by Calothrix scytonemicola TISTR 8095. *Bioresour Technol,* 212**,** 342-347.

KAMRAVA, D., KOVÁCS, T., PFLÜGL, S., DRUZHININA, I., KROLL, P., LACKNER, M. & HERWIG, C. 2018. *Increased poly-B-hydroxybutyrate production from carbon dioxide in randomly mutated cells of cyanobacterial strain Synechocystis sp. PCC 6714: Mutant generation and Characterization*.

KAMRAVAMANESH, D., KOVACS, T., PFLUGL, S., DRUZHININA, I., KROLL, P., LACKNER, M. & HERWIG, C. 2018a. Increased poly-beta-hydroxybutyrate production from carbon dioxide in randomly mutated cells of cyanobacterial strain Synechocystis sp. PCC 6714: Mutant generation and characterization. *Bioresour Technol,* 266**,** 34-44.

KAMRAVAMANESH, D., LACKNER, M. & HERWIG, C. 2018b. Bioprocess Engineering Aspects of Sustainable Polyhydroxyalkanoate Production in Cyanobacteria. *Bioengineering (Basel, Switzerland),* 5**,** 111.

KAMRAVAMANESH, D., PFLÜGL, S., NISCHKAUER, W., LIMBECK, A., LACKNER, M. & HERWIG, C. 2017. Photosynthetic poly-β-hydroxybutyrate accumulation in unicellular cyanobacterium Synechocystis sp. PCC 6714. *AMB Express,* 7**,** 143-143.

KHETKORN, W., INCHAROENSAKDI, A., LINDBLAD, P. & JANTARO, S. 2016a. Enhancement of poly-3-hydroxybutyrate production in Synechocystis sp. PCC 6803 by overexpression of its native biosynthetic genes. *Bioresource Technology,* 214**,** 761-768.

544 KHETKORN, W., INCHAROENSAKDI, A., LINDBLAD, P. & JANTARO, S. 2016b.
545 Enhancement of poly-3-hydroxybutyrate production in Synechocystis sp. PCC 6803
546 by overexpression of its native biosynthetic genes. *Bioresour Technol,* 214**,** 761-8.
547 KLOTZ, A., GEORG, J., BUČINSKÁ, L., WATANABE, S., REIMANN, V.,
548 JANUSZEWSKI, W., SOBOTKA, R., JENDROSSEK, D., HESS, WOLFGANG R.
549 & FORCHHAMMER, K. 2016. Awakening of a Dormant Cyanobacterium from
550 Nitrogen Chlorosis Reveals a Genetically Determined Program. *Current Biology,* 26**,**
551 2862-2872.
552 KNÖTTNER, S., DROSG, B., ELLERSDORFER, M., MEIXNER, K. & FRITZ, I. 2019.
553 Photoautotrophic production of poly-hydroxybutyrate – First detailed cost
554 estimations. *Algal Research,* 41**,** 101558.
555 KOCH, M., BERENDZEN, K. W. & FORCHHAMMER, A. K. 2020. On the Role and
556 Production of Polyhydroxybutyrate (PHB) in the Cyanobacterium Synechocystis sp.
557 PCC 6803. *Life (Basel),* 10.
558 KOCH, M., DOELLO, S., GUTEKUNST, K. & FORCHHAMMER, K. 2019. PHB is
559 Produced from Glycogen Turn-over during Nitrogen Starvation in Synechocystis sp.
560 PCC 6803. *International journal of molecular sciences,* 20**,** 1942.
561 LACKNER, M., KAMRAVAMANESH, D., KRAMPL, M., ITZINGER, R., PAULIK, C.,
562 CHODAK, I. & HERWIG, C. 2019. Characterization of photosynthetically
563 synthesized poly(3-hydroxybutyrate) using a randomly mutated strain of
564 Synechocystis sp. PCC 6714. *International Journal of Biobased Plastics,* 1**,** 48-59.
565 LAU, N.-S., FOONG, C. P., KURIHARA, Y., SUDESH, K. & MATSUI, M. 2014.
566 RNA-Seq Analysis Provides Insights for Understanding Photoautotrophic
567 Polyhydroxyalkanoate Production in Recombinant Synechocystis Sp. *PLOS ONE,* 9**,**
568 e86368.
569 LI, W. C., TSE, H. F. & FOK, L. 2016. Plastic waste in the marine environment: A review of
570 sources, occurrence and effects. *Science of The Total Environment,* 566-567**,**
571 333-349.
572 LIPPI, L., BÄHR, L., WÜSTENBERG, A., WILDE, A. & STEUER, R. 2018. Exploring the
573 potential of high-density cultivation of cyanobacteria for the production of
574 cyanophycin. *Algal Research,* 31**,** 363-366.
575 MARKL, E., GRÜNBICHLER, H. & LACKNER, M. 2018. Cyanobacteria for PHB
576 Bioplastics Production: A Review.
577 MIYAKE, M., ERATA, M. & ASADA, Y. 1996. A thermophilic cyanobacterium,
578 Synechococcus sp. MA19, capable of accumulating poly-β-hydroxybutyrate. *Journal*
579 *of Fermentation and Bioengineering,* 82**,** 512-514.
580 NARANCIC, T., VERSTICHEL, S., REDDY CHAGANTI, S., MORALES-GAMEZ, L.,
581 KENNY, S. T., DE WILDE, B., BABU PADAMATI, R. & O'CONNOR, K. E.
582 2018. Biodegradable Plastic Blends Create New Possibilities for End-of-Life
583 Management of Plastics but They Are Not a Panacea for Plastic Pollution.
584 *Environmental Science & Technology,* 52**,** 10441-10452.
585 ORTHWEIN, T., SCHOLL, J., SPÄT, P., LUCIUS, S., KOCH, M., MACEK, B.,
586 HAGEMANN, M. & FORCHHAMMER, K. 2020. The Novel PII-Interacting

587 Regulator PirC (Sll0944) Identifies 3-Phosphoglycerate Mutase (PGAM) as Central
588 Control Point of Carbon Storage Metabolism in Cyanobacteria. *bioRxiv*, **,**
589 2020.09.11.292599.
590 OSANAI, T., NUMATA, K., OIKAWA, A., KUWAHARA, A., IIJIMA, H., DOI, Y.,
591 TANAKA, K., SAITO, K. & HIRAI, M. Y. 2013. Increased bioplastic production
592 with an RNA polymerase sigma factor SigE during nitrogen starvation in
593 Synechocystis sp. PCC 6803. *DNA research : an international journal for rapid*
594 *publication of reports on genes and genomes,* 20**,** 525-535.
595 OSANAI, T., OIKAWA, A., NUMATA, K., KUWAHARA, A., IIJIMA, H., DOI, Y.,
596 SAITO, K. & HIRAI, M. Y. 2014. Pathway-Level Acceleration of Glycogen
597 Catabolism by a Response Regulator in the Cyanobacterium
598 Synechocystis Species PCC 6803. *Plant Physiology,* 164**,**
599 1831.
600 PANDA, B., JAIN, P., SHARMA, L. & MALLICK, N. 2006. Optimization of cultural and
601 nutritional conditions for accumulation of poly-beta-hydroxybutyrate in
602 Synechocystis sp. PCC 6803. *Bioresour Technol,* 97**,** 1296-301.
603 PANUSCHKA, S., DROSG, B., ELLERSDORFER, M., MEIXNER, K. & FRITZ, I. 2019.
604 Photoautotrophic production of poly-hydroxybutyrate – First detailed cost
605 estimations. *Algal Research,* 41**,** 101558.
606 RIPPKA, R., DERUELLES, J., WATERBURY, J. B., HERDMAN, M. & STANIER, R. Y.
607 1979. Generic Assignments, Strain Histories and Properties of Pure Cultures of
608 Cyanobacteria. 111**,** 1-61.
609 SINGH, A. K. & MALLICK, N. 2017. Advances in cyanobacterial polyhydroxyalkanoates
610 production. *FEMS Microbiol Lett,* 364.
611 SUDESH, K., TAGUCHI, K. & DOI, Y. 2002. Effect of increased PHA synthase activity on
612 polyhydroxyalkanoates biosynthesis in Synechocystis sp. PCC6803. *International*
613 *Journal of Biological Macromolecules,* 30**,** 97-104.
614 TARAWAT, S., INCHAROENSAKDI, A. & MONSHUPANEE, T. 2020. Cyanobacterial
615 production of poly(3-hydroxybutyrate-co-3-hydroxyvalerate) from carbon dioxide or
616 a single organic substrate: improved polymer elongation with an extremely high
617 3-hydroxyvalerate mole proportion. *Journal of Applied Phycology*.
618 WOLK, C. P., VONSHAK, A., KEHOE, P. & ELHAI, J. 1984. Construction of shuttle
619 vectors capable of conjugative transfer from Escherichia coli to nitrogen-fixing
620 filamentous cyanobacteria. 81**,** 1561-1565.
621 WU, G. F., WU, Q. Y. & SHEN, Z. Y. 2001. Accumulation of poly-beta-hydroxybutyrate in
622 cyanobacterium Synechocystis sp. PCC6803. *Bioresour Technol,* 76**,** 85-90.

623

7. Manuscript in preparation

M. Koch and K. Forchhammer.

Polyhydroxybutyrate – a versatile biopolymer with more functions to be discovered.

Microbial Physiology

Review Article

Polyhydroxybutyrate – a versatile biopolymer with more functions to be discovered

Moritz Koch[a], Karl Forchhammer[a]

[a] Interfaculty Institute of Microbiology and Infection Medicine Tübingen, Eberhard-Karls-University Tübingen, Tübingen, Germany

Short Title: PHB – a versatile biopolymer

Corresponding Author: Prof. Karl Forchhammer

Full name: Prof. Karl Forchhammer

Department: Interfaculty Institute of Microbiology and Infection Medicine Tübingen

Institute/University/Hospital: Eberhard-Karls-University Tübingen

Street Name & Number: Auf der Morgenstelle 28

City, State, Postal code, Country: 72076 Tübingen

Tel: + 49 7071 29 72096

E-mail: karl.forchhammer@uni-tuebingen.de

Number of Tables: 0

Number of Figures: 5

Word count: 5398

Keywords: PHB, bacteria, physiology, cyanobacteria, survival strategies

Abstract

Polyhydroxybutyrate (PHB) is a carbon polymer with diverse functions, varying strongly on the organism producing it. This microreview describes the current knowledge about PHB metabolism, structure and different physiological roles known today. Although PHB is also present in numerous cyanobacterial strains, no condition, where PHB is advantageous for such cells, was yet discovered. Hence, the potential functions of PHB in the phylum cyanobacteria are discussed.

The characteristics and classification of polyhydroxybutyrate

Polyhydroxybutyrate (PHB) was already discovered in *Bacillus megaterium* in 1926 (Lemoigne, 1926). PHB is composed of 3-hydroxy-butyrate monomers. This subunit has a simple structure, as it consists of the four carbon fatty acid butyrate with an hydroxy group at the third carbon atom. When several 3-hydroxybutyrate monomers are connected via an ester bond they form PHB (Jendrossek, 2009). The latter accumulates in the form of water insoluble inclusions within the cell. The general structure of PHB is shown in Fig. ***1***.

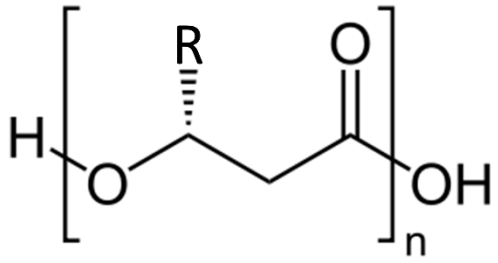

R-group	Carbon	Polymer
hydrogen	C_3	Poly(3-hydroxypropionate)
methyl	**C_4**	**Poly(3-hydroxybutyrate)**
ethyl	C_5	Poly(3-hydroxyvalerate)
propyl	C_6	Poly(3-hydroxyhexanoate)
pentyl	C_8	Poly(3-hydroxyoctanoate)
nonyl	C_{12}	Poly(3-hydroxydodecanoate)

Fig. 1. General structure of PHA. Depending on the side chain R, several different types of PHA are formed. In the case of PHB, the side chain corresponds to a methyl group.The monomeric units (n) of PHAs are linked via an ester bond between the hydroxy- and the carboxyl groups, forming the respective PHA.

Six decades after PHB was first discovered, in 1983 researchers showed that when grown on long chain fatty acids, *Pseudomonas oleovorans* produces poly-beta-hydroxyoctanoate granules (de Smet et al., 1983). This was the first time, that the microbial production of other polyhydroxyalkanoates (PHA) was discovered. PHAs are classified in three different groups, depending on the length of their side chain: short- (C_3-C_5), medium- (C_6-C_{16}) and long-chain-length PHA (scl, mcl and lcl, respectively) (Jendrossek, 2009). A selection of different PHA types is given in Fig. ***2***.

Production of PHA is described from representatives from all three kingdoms of life: archaea, bacteria and eukaryotes. Just recently it has been reported, that also eukaryotic algae can naturally produce PHB, namely *Chlorella* (Cassuriaga et al., 2018) and *Botryococcus* (Kavitha et al., 2016). However, PHA production is best characterized in bacteria, such as *Pseudomonas putida* (Timm and Steinbüchel, 1990), *Cupriavidus necator* (formerly known as *Ralstonia eutropha*) (Wilde, 1962), *Bacillus megaterium* (Griebel et al., 1968), *Rhodococcus ruber* (Haywood et al., 1991), *Acinetobatcer sp.* (Schembri et al., 1995). Besides a few exceptions, mcl PHAs are mainly produced by fluorescent *Pseudomonads* strains such as *P. putida* (Prieto et al., 2007). Since PHB is by far the most widely distributed type of PHA in bacteria, this review focuses mostly on PHB. For the sake of completeness, however, some aspects related to other PHAs are also mentioned.

Due to its physical and chemical properties, PHB is often considered as a potential substitute for thermoplastic polymers, such as polypropylene. However, there are strong differences compared to commonly used plastics. For example, its structure exhibits low elasticity but high rigidness, which are undesirable material properties for many applications (van der Walle et al., 2001). However, these physical properties vary strongly among the different PHAs. Depending on the length of the side chain, the material becomes more elastic and less brittle with longer side chains. Additionally, alternative side chains, such as aromatic groups, can further alter the properties of the PHA (Ishii-Hyakutake et al., 2018, Ward and O'Connor, 2005). Finally, heteropolymers, such as poly(3-hydroxybutyrate-co-3-hydroxyvalerate) (PHBV) further increase the range of physical properties of PHA-based polymers (Rivera-Briso and Serrano-Aroca, 2018).

PHB metabolism

PHB synthesis starts with acetyl-CoA monomers. In the first step, an acetyl-CoA acetyltransferase, termed PhaA, catalyses the condensation of two units of acetyl-CoA to acetoacetyl-CoA. In the next step, an acetoacetyl-CoA reducatase (PhaB), reduces acetoacetyl-CoA to 3-hydroxyacetly-CoA, while oxidizing one molecule of NADPH to $NADP^+$. Finally, a PhaC polymerase connects a 3-hydroxyacetly-CoA to an elongated PHB polymer (Fig. 2).

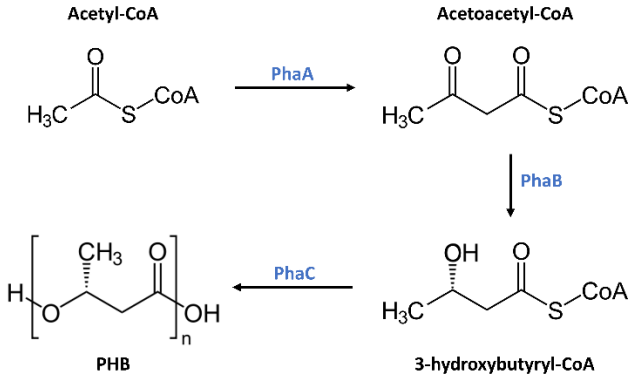

Fig. 2. PHB synthesis pathway. Two units of acetyl-CoA are condensated to acetoacetyl-CoA via PhaA. Next, PhaB reduces it to 3-hydroxybutyryl-CoA. The latter serves as a monomer which gets polymerized to PHB by PhaC.

On the basis of primary sequence, substrate specificity and subunit composition, different classes of PHB polymerases can be distinguished (Amara and Moawad, 2011). The first class of PhaC comprises polymerases, which are PhaC homodimers and are present for example in *C. necator*. Similarly, class II, which contains PhaC1 and PhaC2 synthases and is present in *P. putida*, form also homodimers. In contrast to that, class III comprises heterodimers, such as PhaC-PhaE in *Synechcoystis sp.* PCC 6803. Also class IV synthases, which are for example present in *Bacillus sp.*,

are composed of two subunits. However, in the case of class IV, heterodimeric polymerases are composed of PhaC and PhaR. A main difference between these four classes is that only class II is able to produce mcl PHA, while all other classes produce predominantly scl PHA, such as PHB (Jendrossek, 2009). It is known that the presence of certain metabolites, such as acetyl-phosphate, can alter the activity of PHB polymerase (Miyake et al., 1997).

The elongated polymer can subsequently be catabolized by PHA depolymerases, termed PhaZ. The latter can be either intra- or extracellular, depending on their purpose. In *C. necator*, there are seven different depolymerases annotated, indicating the importance of a regulated mobilization of PHB (Pohlmann et al., 2006).

Besides the enzymes mentioned above, some bacteria (like *P. putida*) possess further enzymes, which enable them to convert additional substrates into PHA . One enzyme is PhaJ, which converts enoyl-CoA into R-3-hydroxyacly-CoA and thereby connects the fatty acid ß-oxidation with the PHA synthesis. PhaG, another enzyme found in *P. putida*, converts acyl-ACP to (R)-3-acyl-CoA and thereby links the fatty acid *de novo* synthesis to the PHA metabolism. The fatty acid and PHA pathways are further interconnected by enzymes, which catalyse reactions in both pathways. For example, the enzyme FabG, which is actually part of the fatty acid biosynthesis, can also catalyse the same function as PhaB, but with a lower catalytic efficiency (Zhang et al., 2017). A complete model of the different pathways involved in the PHA metabolism is shown in Fig. ***3*** (except the PHA depolymerization).

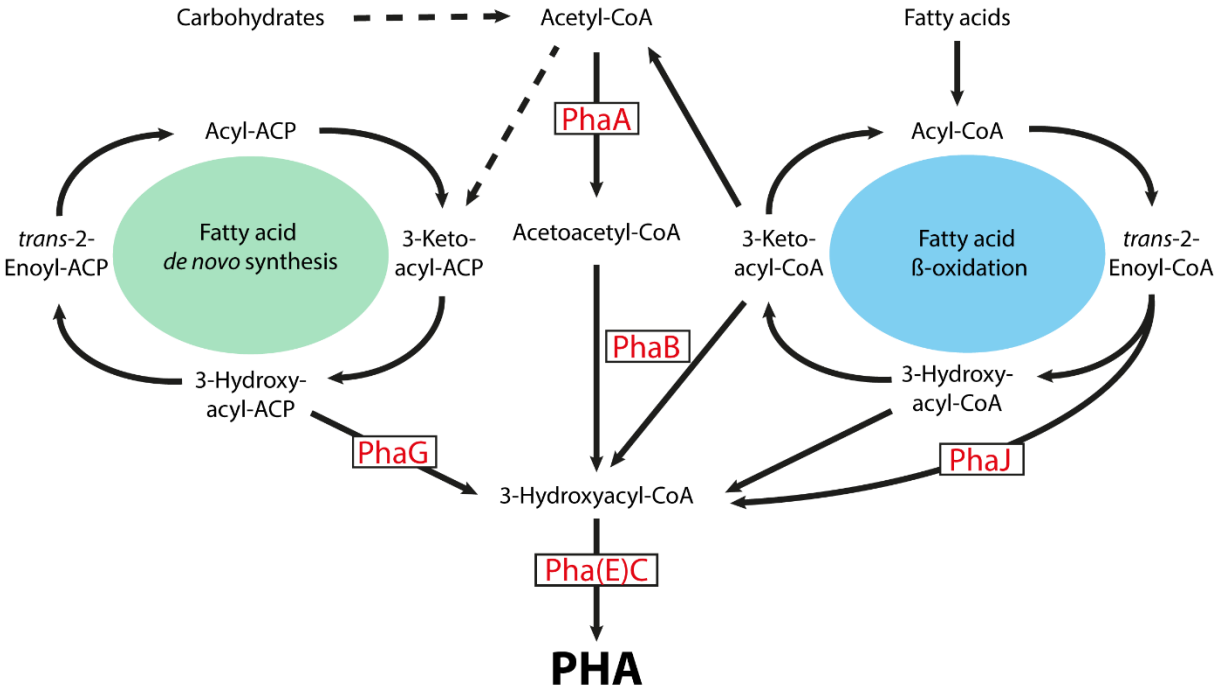

Fig. 3. PHA metabolism and different metabolic pathways (Koch and Forchhammer, 2020). Important enzymes are highlighted in red. Not shown is the PHA depolymerization, which is utilized by PhaZ.

With all those enzymes in place, the entire PHA cycle is complete and acetyl-CoA can be completely metabolized to PHA and back again. Interestingly, some studies suggest that there could be a constant carbon flow of PHA synthesis and degradation. This way the cells could ensure that the right metabolic intermediates are available and could adapt the cell to environmental conditions. It was shown that PHA synthase and depolymerase are active at the same time, further supporting the initial hypothesis (Arias et al., 2013).

Proteins associated to PHB granules

Despite the simple structure of PHB, its granules are much more complex. Several proteins are located on the granule-surface or are involved in its metabolism and regulation. Due to this complexity, the name carbonosomes has been suggested to highlight that PHB granules are rather subcellular organelles and not just a prolonged chain of molecules (Jendrossek, 2009). In the following, the most important proteins, which are involved in PHB granule formation, maintenance and degradation, are described.

Phasins are low-molecular-weight proteins, which are directly attached to the surface of PHB granules (Mezzina and Pettinari, 2016). They are very abundant and serve various different purposes, such as structural, biosynthetic, catabolic and regulatory functions. Often these phasins

are the predominant protein covering large parts of the granule-surface, whereby they also shield the cytoplasm from the hydrophobic PHB surface. A representative of such phasins is PhaP from *C. necator*. Here, several different kinds of PhaP are present, which cover the surface of the PHB granules. The amount of PhaP is tightly regulated and corresponds with the amount of intracellular PHB (York et al., 2001). A PhaP homologue was recently discovered in *Synechocystis sp*. (Hauf et al., 2015). In *P. putida*, PhaF and PhaI are the main granule associated proteins (Prieto et al 1999).

Besides just covering the granules surface, phasins exhibit further functions. For example, PhaF from *P. putid*a organizes PHA granules along the long-axis of the cell and ensures equal granule sharing upon cell division (Galán et al., 2011).When PhaF is not present, cells still produce PHA, but the entire cell population divides into cells with and other without PHA. PhaF is present as a homomeric tetramer, where the monomers possess an N-terminal helix and a short leucine zipper, potentially used for protein-protein interaction (Maestro et al 2013). With its DNA binding domain, PhaF furthermore serves as a regulator of the *pha* genes (Galán et al., 2011). The protein PhaI shares large similarities with the N-terminal region of PhaF, but without the leucine zipper. Although PhaI can be partially substituted by PhaF, both enzymes together are essential for a proper PHA metabolism.

Similarly to PhaF, in *C. necator* PhaM has the function to bind to the PHB granulum as well as the DNA and thereby ensures equal distribution among the daughter cells. Additionally, PhaM activates the PHB synthase PhaC1 and thereby directly influences the PHB metabolism (Pfeiffer and Jendrossek, 2014). While PhaM regulates the PHB synthesis on the protein level, the regulators PhaR and PhaD regulate *pha* genes on a transcriptional level. In *C. necator*, PhaR binds upstream of *phaP* and thereby represses its transcription. Additionally, PhaR is also associated to PHB granules (York et al., 2002). PhaD, on the other hand, serves as an activator in *P. putida*. Contrary to a long-time belief, it was recently demonstrated that PHB granules do not contain phospholipids on their surface (Bresan et al., 2016).

Physiological role of PHB in bacteria

The ability to produce PHB is widespread among different organisms. A phylogenetic analysis found the presence of the *phaC* gene in organisms from 40 different genera and within a wide range of taxonomical groups, highlighting how abundant the ability to produce PHB is (Kalia et al.,

2007). This also demonstrates, how different the organisms are, which produce PHB, indicating different physiological functions of PHB based on the environment of the individual organism.

PHBs are in general considered as carbon and energy storage, which are built up in time periods of carbon excess and which provide advantages in times of carbon shortage (Anderson and Dawes, 1990). This long-time belief still holds true for many bacteria, although more and more other physiological functions are recently discovered. Also, for some bacteria like cyanobacteria, no physiological relevance of PHB was yet discovered. The most important roles of PHB are described in the following.

In many organisms, PHB accumulates under conditions of nutrient limitation or unbalanced conditions, such as nitrogen limitation (Anderson and Dawes, 1990). However, there are also bacteria, like *C. necator*, which do accumulate PHB even during normal growth and under balanced conditions (Jendrossek and Pfeiffer, 2014). Nevertheless, the amount of accumulated PHB is usually higher when grown under nutrient limitation.

Another important aspect of PHB, besides serving as a storage polymer, is the ability to increase resistance against various kinds of stress. In *Azospirillum brasilense* for example, PHB deficient strains are more susceptible against abiotic stresses, such as UV irradiation, heat, desiccation, osmotic pressure and osmotic shock (Kadouri et al., 2003a). In *Sinorhizobium* strains, an induced PHB accumulation after exposure to high salt concentrations was observed (Arora et al., 2006). In *Aeromonas hydrophila* the production of a PHB-PHH copolymers results in increased resistance against a wide variety of abiotic stresses, including UV irradiation, hydrogen-peroxide, ethanol, heat and cold treatments and high osmotic pressure (Zhao et al., 2007). Interestingly, a study investigating *Pseudomonas oleovorans* showed that even the deletion of the PHA depolymyerase PhaZ was sufficient to increase the sensitivity towards hydrogen-peroxide and heat shock (Ruiz et al., 2004). This demonstrates that the entire PHB metabolism, including its mobilization, is important for providing stress tolerance to the PHB producing cells, rather than the sheer presence of the polymer (Castro-Sowinski et al., 2009). PHB was furthermore shown to increase the number of viable cells by protecting *C. necator* cells against cold stress (Nowroth et al., 2016). Additionally, in *Herbaspirillum seropedicae*, studies demonstrated that PHB reduces intracellular redoxstress, potentially by eliminate a surplus of reducing equivalents and thereby serving as an electron sink (Batista et al., 2018). In a similar way PHB is used in *Chromatium vinosum*, although here it rather serves as an electron storage than a sink. This anoxygenic phototrophic bacterium converts glycogen to PHB under dark, anaerobic conditions. This provides the strain with the advantage over other fermenting organisms, which commonly secrete their fermentation products and thereby loose carbon (van Gemerden, 1968). Another example of the role of PHB

can be found in *Bacillus cereus*: this bacterium produces most PHB just before the formation of spores and degrades it after sporulation, indicating the importance of PHB for surviving their dormant state (Valappil et al., 2007, Castro-Sowinski et al., 2009). Several studies also found an interconnection between PHB production and the formation of EPS (exopolysaccharides). Sometimes a mutant with impaired PHB production resulted in a higher EPS production (Wang et al., 2008), while in other strains, a lower PHB production correlated with lower EPS production (Kadouri et al., 2003b).In the latter case, the authors suggest that the increased EPS production is attributable to the intracellular mobilization of carbon sources (PHB).

Interestingly, PHB producing *Azospirillum brasilense* was able to endure long periods of starvation, but it also showed certain disadvantages compared to a PHB-free mutant, such as lower motility or impaired root adhesion and EPS production (Kadouri et al., 2002). This indicates that the ability to store PHB is not always an advantage, but has to be balanced based on the environmental conditions. In a similar manner, *Sinorhizobium* bacteria were shown to use a bet-hedging strategy to produce offspring with higher or lower amounts of PHB. These offspring are better adapted for long or short period starvation, respectively (Ratcliff and Denison, 2010).

Another interesting function of PHB could be the provision of nutrients to a microbial community (Prieto et al., 2016). When a PHB producer, which converts inorganic carbon to a condensed carbon polymer, is decomposed for example by predatory bacteria, it releases its PHB granules to the environment (Jendrossek and Handrick, 2002). Thereby, the energy rich carbon polymer is made available to the microbial community. This fits well to the observation, that most identified PHA depolymerases are those, which function extracellularly (Prieto et al., 2016). It was also shown, that predatory *Bdellovibrio* cells have a growth advantage when they were preying on PHA producing cells compared to a PHB-free mutant (Martínez et al., 2013). This further highlights the importance of PHB for the bacterial environment.

Additional physiological functions of PHB in bacteria are summarized and further described in recent reviews (Castro-Sowinski et al., 2009, Obruca et al., 2020).

PHB in Cyanobacteria

A large group of PHB producer are cyanobacteria. These bacteria grow photoautotrophically and are the only bacteria that perform oxygenic photosynthesis. This allows cyanobacteria to occupy almost all illuminated habitats. In a recent study, 137 different cyanobacterial strains were investigated for their ability to produce PHB. Out of these 137, 134 were PHB producers

(Kaewbai-Ngam et al., 2016). Interestingly, a phylogenetic analysis revealed, that the full set of functional *phaABC* genes appeared for the first time evolutionary in cyanobacteria, indicating its importance for cyanobacterial growth (Kalia et al., 2007). Although PHB appears to be very common in the phylum cyanobacteria, its physiological function is yet undiscovered. In recent years, several groups have tried to answer this question, for example by comparing a PHB-free Δ*phaEC* strain to a PHB-producing wildtype, the true function of PHB remains puzzling (Damrow et al., 2016, Koch et al., 2020a). Cyanobacteria produce PHB mostly under unbalanced growth conditions, for example when they are grown in a medium lacking either nitrogen, phosphate or potassium (Kaewbai-Ngam et al., 2016). Additional organic carbon sources, like acetate or fructose, can further increase the PHB production (Panda et al., 2006). PHB metabolism in cyanobacteria is best described during nitrogen starvation, which triggers a process called chlorosis (Koch et al., 2020a, Troschl et al., 2017). PHB slowly accumulates during the course of several weeks; depending on the cyanobacterial strain, up to 25 % PHB per cell-dry-weight can be accumulated (Kaewbai-Ngam et al., 2016). PHB is commonly stored in a few granules, which are located in the middle of the cell (Hauf et al., 2015). Compared to other PHB producers, only relatively little is known about the proteins, which are involved in PHB metabolism. Although recently two new proteins were found to play a role (the phasin PhaP as well as the regulator Slr0058) (Koch et al., 2020b, Hauf et al., 2015), more proteins, like for example PHB degrading enzymes, are to be discovered. Most studies were performed in the strain *Synechocystis sp*. PCC 6803 (hereafter *Synechocystis*), which serves as a well characterized model strain for cyanobacterial metabolism. In the following, the latest discoveries and hints towards PHB's physiological role are summarized.

The role of PHB during nutrient limitation

Cyanobacteria are known for producing a variety of different storage compounds, such as glycogen, cyanophycin or polyphosphate. In contrast to the unknown function of PHB, the polymers glycogen and cyanophycin can clearly be linked to carbon and nitrogen storage metabolism, respectively (Doello et al., 2018, Watzer and Forchhammer, 2018). As previous studies have shown, glycogen is the main carbon- and energy storage compound under conditions of nutrient limitation (Doello et al., 2018, Klotz et al., 2016) and its biosynthetic genes were found in all cyanobacterial genomes (Beck et al., 2012). It is remarkable that cyanobacteria produce two different carbon polymers, since most other microorganisms produce just one. This clearly indicates that the two carbon-polymers have different functions. Glycogen synthesis is extremely dynamic and is immediately induced when cells experience nitrogen-limitation. Since glycogen synthesis mutants are unable to survive nitrogen chlorosis, glycogen metabolism appears to be

pivotal for the acclimation to nitrogen deprivation (Klotz and Forchhammer, 2017, Doello et al., 2018). Mutants that are deficient in the major glycogen-degrading phosphorylase GlgP2 do not accumulate PHB during chlorosis. From these analysis, it could be concluded that glycogen is slowly degraded and converted into PHB during prolonged nitrogen starvation (Koch et al., 2019). The cyanobacterium *Synechocystis* PCC 6803 operates at least three parallel metabolic routes to degrade glycogen: the oxidative pentose phopshoate pathway (OPP), the Entner Doudoroff pathway (ED) and the Emden-Meyerhof-Parnas pathway (EMP) (Chen et al., 2016). Analysis of mutants, in which one or two of these pathways were disrupted showed that only the EMP pathway efficiently converts glycogen into PHB (Koch et al., 2019). The ED and the OPP pathway contributed to a much lesser degree to the PHB formation. This effect was even more pronounced when the cells were cultivated under light/dark regime (Koch et al., 2020a). Although *Synechocystis* normally accumulates more PHB under this condition, a mutant, which is unable to use the EMP pathway, produces almost no PHB. In contrast, the WT and a mutant unable to use neither the ED nor the OPP pathway (Δ*zwf*), produced ~15 % PHB / CDW.

A final glycolytic product of all three pathways is acetyl-CoA. The latter serves as the precursor for the subsequent PHB synthesis, while the formation of glycogen requires phosphorylated glucose residues. This further suggests a role of glycogen as a quick-response energy and carbon storage, since glucose-1P can directly be metabolized via any of the three pathways (ED, OPP, EMP) to provide energy for the cells anabolism. In contrast, acetyl-CoA rather serves as a building block for various anabolic reactions (e.g. in lipid metabolism) and anaplerotic reactions related to the TCA cycle. While glycogen quickly accumulates or degrades within just two days at the beginning or end of nitrogen chlorosis, respectively, the formation of PHB takes much longer, lasting for several weeks after the induction of nitrogen starvation (Koch et al., 2020b).

Remarkable differences between PHB and glycogen are that glycogen shows a higher solubility in water than PHB, and that PHB forms much larger granules than glycogen. In contrast, glycogen shows a more complex branching pattern, making it potentially able to be sterically more condensed. It was already hypothesized, that the relatively small glycogen granules could serve as a quick-response carbon storage, due their easier accessibility based on a larger surface to volume ratio, whereas the large PHB granules could instead form a long-term storage. However, under conditions of nitrogen limitation, no physiological differences were ever discovered between wildtype and a PHB-free Δ*phaEC* mutant strain (Damrow et al., 2016, Klotz et al., 2016). To test whether PHB can play a role in stress resistance, a recent study applied more than 30 different stresses to nitrogen starved *Synechocystis* cells, including all of those stresses, which are known for being relevant in other PHB producing bacteria (Koch et al., 2020a). However, in none

of the tested conditions, the ability to produce PHB gave the wildtype cells a growth advantage compare to a Δ*phaEC* mutant.

To better understand the metabolic role of PHB in *Synechocystis*, a recent study attempted to identify the so far unknown PHB depolymerase (Koch et al., 2020b). Sequence homology analysis indicated that the gene *slr0060* encodes for a putative esterase with a patatin-like domain, which is typical for intracellular PHB depolymerases. The respective deletion mutant Δ*slr0060* mutant produced slightly less PHB than a WT control but showed no further distinctive phenotype. Interestingly the same study revealed that when nitrogen was added to chlorotic cells to induce resuscitation to vegetatively growing cells, no net degradation of PHB in the cyanobacterial culture took place: The overall amount of PHB within a culture remained constant for several days (Koch et al., 2020b). Only through cell growth and division, the PHB level per cell decreased gradually. However, fluorescence-microscopic analysis investigating Nile red-stained PHB revealed that the granules disaggregated and were spread among diving daughter cells. The physiological function of this behaviour and why PHB does not get actively metabolized has yet to be explained. Possibly cultivation at laboratory conditions did not trigger the degradation of PHB and the required environmental conditions, which initiate PHB catabolism are still to be found. Therefore, to date it remains open whether cyanobacteria contain an intracellular PHB depolymerase as described for many other bacteria.

Potential role of PHB in controlling the redox state

Besides conditions of nutrient limitation, glycogen is the essential energy and carbon storage during dark phases, where no photosynthesis can take place. Excess of energy gets stored in the form of glycogen during the day, while during the night, it releases its energy and carbon to sustain the cyanobacterial metabolism. Although no studies so far have shown a PHB accumulation during conditions of balanced growth, there are several indicators that PHB might play a role during dark phases. Transcriptomic data from several studies have shown very clearly, that all PHB related genes are strongly upregulated at the beginning of the night and downregulated during the day (Saha et al., 2016, Kucho et al., 2005). It was furthermore shown, that PHB related genes are strictly controlled by the circadian clock (Köbler et al., 2018). Interestingly, the transcripts for PHB synthesis are countercyclically regulated to those of the glycogen metabolism. While the transcripts for glycogen synthesis are upregulated during the beginning of the day and downregulated during the beginning of the night, the PHB synthesizing genes are regulated in the exact opposite. This hints towards a conversion of both metabolites into each other, as it was already shown during nitrogen starvation (Koch et al., 2019). However, also during the night, a PHB free mutant shows no growth phenotype, while the growth of glycogen free mutants is

severely impaired (Damrow et al., 2016). Furthermore, under conditions of nitrogen limitation, growth at a dark/light regime increased the overall PHB accumulation in *Synechocystis* cells compared to growth at continuous light (Koch et al., 2020a). This further highlights the relevance of dark phases for the formation of PHB.

Fitting to these observations, PHB was already in the past considered to play a role as a potential electron sink, whereby PHB could store excess of electrons, since the formation of one PHB subunit requires one NADPH (De Philippis et al., 1992). This hypothesis, that PHB formation in cyanobacteria is involved in redox homeostasis, was further corroborated in studies by Schlebusch and Forchhammer (2010) and Hauf et al., (2013). A *Synechocystis* mutant, unable to accumulate PHB during nitrogen starvation was characterized in detail (Schlebusch and Forchhammer, 2010). In this mutant, the gene *sll0783,* which belongs to the most strongly induced genes during nitrogen starvation, was knocked out. This gene is the first gene of the Nit1C operon, a highly conversed gene cluster present in cyanobacteria and many other bacterial species (including proteobacteria and actinobacteria), enabling the utilization of cyanide (Jones et al., 2018). Many heterotrophic bacteria possessing this gene cluster are able to produce PHB and to fix nitrogen. Since the entire operon was highly upregulated in *Synechocystis* during nitrogen starvation, a role during nitrogen-chlorosis was suspected. Further analysis revealed, that the Δ*sll0783* mutant showed a strong decrease in its PHB synthase activity (Schlebusch and Forchhammer, 2010). Induction of expression of the PHB synthesis genes (*phaAB* and *phaEC*) was delayed as compared to the WT. However, in contrast to the expression of the *phaCE* genes, the activity of PHB synthase decayed in the mutant following an initial transient increase. Interestingly, the Δ*sll0783* mutant showed an impairment in its recovery from nitrogen starvation, which implied that that this could be due to decreased amounts of PHB in the sll0783 mutant. However, subsequent work showed that the ability to produce PHB *per se* is not relevant for resuscitation from nitrogen starvation (Klotz et al., 2016, Koch et al., 2020a). The inability of the Δ*sll0783* mutant to sustain PHB synthesis could finally be attributed to the redox-state of the cells: during nitrogen-starvation, the NADPH/$NADP^+$ ratio steadily increased in wild-type cells, whereas in the Δ*sll0783* mutant it remained constant. Treatment of the mutant cells with the protonophore CCCP or the ATPase inhibitor DCCD restored PHB synthase activity and PHB synthesis due to a compensatory increase in the NADPH/$NADP^+$ ratio (Hauf et al., 2013). Inhibition in ATP synthesis arrests anabolic reactions that consume NADPH. This highlights that the increased levels of NADPH trigger synthesis of PHB. In conclusion, these data suggested that PHB serves as a storage pool for excess reduction equivalents.

Hence, the formation of PHB would be particularly beneficial whenever a surplus of NADPH cannot be metabolized, for example because respiration is not possible and anaerobic processes are required. In this scenario, PHB would serve as an intracellular electron sink with the advantage to sustain all intracellular carbon, instead of secreting it like other fermentation products, such as acetate. As recent studies have shown, the Embden-Meyerhof-Parnas (EMP) pathway plays the central role for the formation of PHB (Koch et al., 2019, Koch et al., 2020a). The EMP pathway produces a relatively low NADPH/ATP ratio compared to other glycolytic routes, such as the OPP (oxidative-pentose-phosphate pathway) or ED (Entner-Doudoroff) pathway. This is advantageous under conditions of NADPH excess, such as anaerobic growth. A previous study has shown that the EMP pathway is also the most relevant during fermentation processes (Stal and Moezelaar, 1997).

Another role of PHB could be a storage to prevent intracellular acidification: it was shown that a PHB free *Cupriavidus necator* secretes pyruvate into its medium (Raberg et al., 2014). This fits to a previous observation, where *Synechocystis* mutants unable to synthesize glycogen secrete pyruvate and 2-oxoglutarate under conditions of carbon excess such as growth with addition glucose or nitrogen starvation (Grundel et al., 2012). Here the authors argue that it is extremely important for the cells to have a carbon sink to control their carbon homeostasis or to avoid energy spilling. Potentially PHB could here serve as an additional buffer for storing excess carbon, particularly because it is metabolically closer to pyruvate than glycogen. However, in contrast to the glycogen-deficient mutants, no studies have so far analyzed secreted organic acids in the supernatant of a PHB-free mutant. To further investigate this, future studies should investigate secreted metabolites under different growth conditions in a Δ*phaEC* mutant and compare it to a WT.

Cell Biology of PHB in *cyanobacteria*

The synthesis of PHB granules is tightly controlled. Based on sequence-homology to other PHB producing bacteria, several genes were identified, which encode for proteins that are putatively involved in the PHB metabolism. One of those genes is *slr0058*, which encodes for a protein that shows similarity to PhaF from *P. putida* (Koch et al., 2020b). A Δ*slr0058* mutant produces small amounts of PHB during vegetative growth (unlike the WT) and shows a growth deficiency compared to the WT. This growth deficiency was clearly coupled to the presence of PHB, since a variant of the *slr0058* mutant, which was unable to produce PHB (Δ*slr0058*-Δ*phaEC*), was recovering the initial phenotype. These results show that it is important for *Synechocystis* to ensure a tightly controlled PHB metabolism. The protein Slr0058 was furthermore shown to regulate the amount of PHB granules within the cell. While a WT possesses around 3 granules per

cell in average, the Δ*slr0058* mutant contained about twice as many. If a cell contains more granules, which are also smaller, the surface area of those is higher compared to fewer but larger granules. Hence, it can be hypothesized that a Δ*slr0058* mutant suffers from unintended interactions between the PHB surface and the cell's interior. How and why this negatively affects the cell growth has yet to be elucidated. Cell localization using fluorescent protein-tagged Slr0058 showed that it aggregated in distinct foci during vegetative growth and these foci dispersed during the course of chlorosis. This led to the hypothesis that Slr0058 could act as an initial aggregation point for the PHB synthase PhaEC to initiate PHB synthesis and dissociates from maturating PHB granules.

Another protein which was shown to regulate the number and size of PHB granules is PhaP (Ssl2501) (Hauf et al., 2015). Fluorescence microscopy showed that PhaP is directly located at the surface of PHB granules and hence considered a classical phasin. A PhaP deletion mutant showed half as many PHB granules as the WT. At the same time, the granules in the Δ*phaP* strain were larger than in the WT. The discovery of PhaP and Slr0058 shows, that the formation and maintenance of PHB granules in *Synechocystis* is tightly regulated. Decreased viability, for example in a Δ*slr0058* mutant strain, underlines the importance of this regulation. A summery of the current understanding of the PHB metabolism in *Synechocystis* is shown in Fig. ***4***.

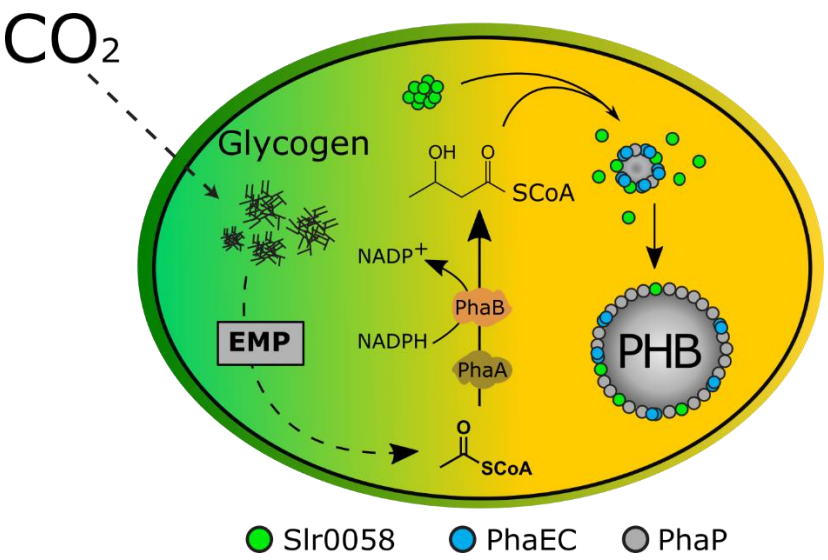

Fig. 4. Schematic overview of the current view of PHB metabolism in *Synechocystis*. After the induction of nitrogen starvation, cells fix anorganic CO_2 and store it in the form of glycogen. Throughout the course of chlorosis, glycogen is catabolized, mainly via the EMP pathway, to form acetyl-CoA, the building block of PHB. Next, PhaA and PhaB convert acetyl-CoA subunits to 3-hydroxybutyryl-CoA under the expense of one molecule NADPH, which gets oxidized to $NADP^+$. Slr0058 initiates the formation of PHB granules and detaches as the PHB granules mature. The elongation of 3-

hydroxybutyryl-CoA to the polymer PHB is catalysed by the enzyme PhaEC, while PhaP shields the surface of the PHB granule.

Interestingly, in a nitrogen-starved *Synechocystis* population, the distribution of PHB granules among the cells is quite heterogenous. A study addressing this apparent phenotypic heterogeneity showed that while a large population of cells contained only small- to medium amounts of PHB, a few cells accumulated larger quantities (Koch et al., 2020a). This indicates that the formation of PHB is not always beneficial, but rather a bet-hedging strategy of the cells to be prepared for different potential outcomes (Ratcliff and Denison, 2010). This highlights that the ability to possess PHB might be relevant under only very specific scenarios, hence making the physiological function hard to discover under laboratory conditions.

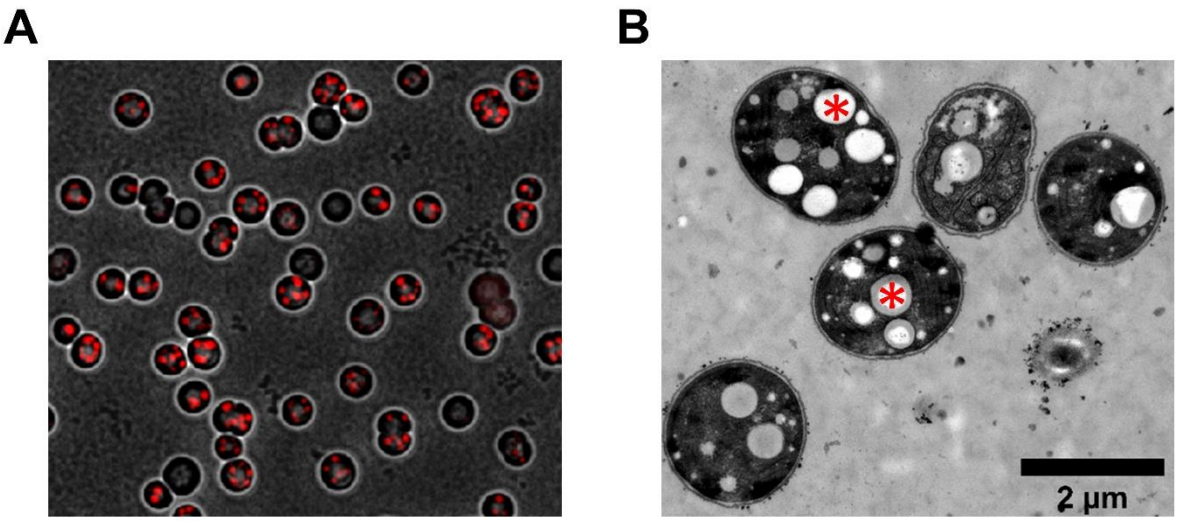

Fig. 5. Microscopic analysis of heterogeneity of PHB contents in WT cells. (A) Fluorescence microscopy of WT cells which were incubated for 14 days in nitrogen-free medium. Nile-red was used to visualize the PHB granules. (B) TEM picture of WT cells which were incubated for 17 days in nitrogen-free medium. Red asterisks indicate representative PHB granules in two different cells by. Figure modified from Koch et al., 2020.

Although several studies have tried to discover the conditions, where the ability of certain cyanobacteria to produce PHB is advantageous for the cells, no clear answer can so far be provided. To test whether PHB can play a role in stress resistance, a recent study applied more than 30 different stresses to nitrogen starved *Synechocystis* cells, including all of those stresses, which are known for being relevant in other PHB producing bacteria (Koch et al., 2020a). However, in none of the tested conditions, the ability to produce PHB gave the wildtype cells a growth advantage compare to a Δ*phaEC* mutant. Nevertheless, the fact that so many cyanobacterial species produce PHB in a highly regulated way indicates that PHB fulfils an important physiological function and provides an evolutionary advantage to cyanobacteria when

grown in their natural environment. These conditions could include, for example, the complex interactions with other microbes, which are difficult to mimic under laboratory conditions.

Conclusion and outlook

Despite the simple chemical structure of PHB, its granules are highly complex pseudo-organelles, with various different proteins involved in maintaining the correct function. Depending on the organism, PHB can serve numerous roles, from storage molecule to stress resistance and many more. Although the physiological function in cyanobacteria remain puzzling, the field of research is constantly expanding, thereby gaining deeper insights into its role. One of the most promising hypothesis is the role of PHB for the regulation of the intracellular redox balance. As an implication for biotechnological approaches this implies that when increased amounts of PHB are desired, cultivation conditions which favour high levels of reduction equivalents should be considered. Still, fundamental questions, such as a yet undiscovered PHB depolymerase, remain. Since cyanobacteria grow photoautotrophically, they could serve as a chassis for a carbon neutral, sustainable production of PHB. Further research in this field will hence be not only beneficial for basic research but may also provide knowledge of industrial relevance.

Conflict of Interest Statement

The authors have no conflicts of interest to declare.

Funding Sources

M. K. was funded by the Studienstiftung des Deutschen Volkes and the RTG 1708 “Molecular principles of bacterial survival strategies”. We acknowledge support by Open Access Publishing Fund of University of Tübingen.

Author Contributions

Conceptualization: K.F.; Writing-Original Draft Preparation: M. K.; Review and editing: M.K and K.F.

Figure Legends

Fig. 6. General structure of PHA. Depending on the side chain R, several different types of PHA are formed. In the case of PHB, the side chain corresponds to a methyl group.The monomeric units (n) of PHAs are linked via an ester bond between the hydroxy- and the carboxyl groups, forming the respective PHA.

Fig. 7. PHB synthesis pathway. Two units of acetyl-CoA are condensated to acetoacetyl-CoA via PhaA. Next, PhaB reduces it to 3-hydroxybutyryl-CoA. The latter serves as a monomer which gets polymerized to PHB by PhaC.

Fig. 8. PHA metabolism and different metabolic pathways (Koch and Forchhammer, 2020). Important enzymes are highlighted in red. Not shown is the PHA depolymerization, which is utilized by PhaZ.

Fig. 9. Schematic overview of the current view of PHB metabolism in *Synechocystis*. After the induction of nitrogen starvation, cells fix anorganic CO_2 and store it in the form of glycogen. Throughout the course of chlorosis, glycogen is catabolized, mainly via the EMP pathway, to form acetyl-CoA, the building block of PHB. Next, PhaA and PhaB convert acetyl-CoA subunits to 3-hydroxybutyryl-CoA under the expense of one molecule NADPH, which gets oxidized to $NADP^+$. Slr0058 initiates the formation of PHB granules and detaches as the PHB granules mature. The elongation of 3-hydroxybutyryl-CoA to the polymer PHB is catalysed by the enzyme PhaEC, while PhaP shields the surface of the PHB granule.

Fig. 10. Microscopic analysis of varying PHB contents in WT cells. (A) Fluorescence microscopy of WT cells after 14 days of nitrogen starvation. PHB granules are visualized by staining with Nile red. (B) TEM picture of WT cells after 17 days of nitrogen starvation. Representative PHB granules are indicated in two different cells by a red asterisks. Figure modified from (Koch et al., 2020a).

Reference list

AMARA, A. & MOAWAD, H. 2011. PhaC Synthases and PHA Depolymerases: The Enzymes that Produce and Degrade Plastic. *International Islamic University Malaysia Engineering Journal,* 12.

ANDERSON, A. J. & DAWES, E. A. 1990. Occurrence, Metabolism, Metabolic Role, and Industrial Uses of Bacterial Polyhydroxyalkanoates. *Microbiological Reviews,* 54**,** 450-472.

ARIAS, S., BASSAS-GALIA, M., MOLINARI, G. & TIMMIS, K. N. 2013. Tight coupling of polymerization and depolymerization of polyhydroxyalkanoates ensures efficient management of carbon resources in Pseudomonas putida. *Microbial Biotechnology,* 6**,** 551-563.

ARORA, N. K., SINGHAL, V. & MAHESHWARI, D. K. 2006. Salinity-induced accumulation of poly-β-hydroxybutyrate in rhizobia indicating its role in cell protection. *World Journal of Microbiology and Biotechnology,* 22**,** 603-606.

BATISTA, M. B., TEIXEIRA, C. S., SFEIR, M. Z. T., ALVES, L. P. S., VALDAMERI, G., PEDROSA, F. D., SASSAKI, G. L., STEFFENS, M. B. R., DE SOUZA, E. M., DIXON, R. & MULLER-SANTOS, M. 2018.

PHB Biosynthesis Counteracts Redox Stress in Herbaspirillum seropedicae. *Frontiers in Microbiology,* 9.
BECK, C., KNOOP, H., AXMANN, I. M. & STEUER, R. 2012. The diversity of cyanobacterial metabolism: genome analysis of multiple phototrophic microorganisms. *BMC genomics,* 13**,** 56-56.
BRESAN, S., SZNAJDER, A., HAUF, W., FORCHHAMMER, K., PFEIFFER, D. & JENDROSSEK, D. 2016. Polyhydroxyalkanoate (PHA) Granules Have no Phospholipids. *Sci Rep,* 6**,** 26612.
CASSURIAGA, A. P. A., FREITAS, B. C. B., MORAIS, M. G. & COSTA, J. A. V. 2018. Innovative polyhydroxybutyrate production by Chlorella fusca grown with pentoses. *Bioresour Technol,* 265**,** 456-463.
CASTRO-SOWINSKI, S., BURDMAN, S., MATAN, O. & OKON, Y. 2009. Natural Functions of Bacterial Polyhydroxyalkanoates.
CHEN, X., SCHREIBER, K., APPEL, J., MAKOWKA, A., FÄHNRICH, B., ROETTGER, M., HAJIREZAEI, M., SÖNNICHSEN, F., SCHÖNHEIT, P., MARTIN, W. & GUTEKUNST, K. 2016. The Entner–Doudoroff pathway is an overlooked glycolytic route in cyanobacteria and plants. *Proceedings of the National Academy of Sciences,* 113**,** 201521916.
DAMROW, R., MALDENER, I. & ZILLIGES, Y. 2016. The Multiple Functions of Common Microbial Carbon Polymers, Glycogen and PHB, during Stress Responses in the Non-Diazotrophic Cyanobacterium Synechocystis sp. PCC 6803. *Frontiers in microbiology,* 7**,** 966-966.
DE PHILIPPIS, R., ENA, A., GUASTIINI, M., SILI, C. & VINCENZINI, M. 1992. Factors affecting poly-β-hydroxybutyrate accumulation in cyanobacteria and in purple non-sulfur bacteria. *FEMS Microbiology Letters,* 103**,** 187-194.
DE SMET, M. J., EGGINK, G., WITHOLT, B., KINGMA, J. & WYNBERG, H. 1983. Characterization of intracellular inclusions formed by Pseudomonas oleovorans during growth on octane. *Journal of bacteriology,* 154**,** 870-878.
DOELLO, S., KLOTZ, A., MAKOWKA, A., GUTEKUNST, K. & FORCHHAMMER, K. 2018. A Specific Glycogen Mobilization Strategy Enables Rapid Awakening of Dormant Cyanobacteria from Chlorosis. *Plant Physiology,* 177**,** 594-603.
GRIEBEL, R., SMITH, Z. & MERRICK, J. M. 1968. Metabolism of poly(β-hydroxybutyrate). I. Purification, composition, and properties of native poly(β-hydroxybutyrate) granules from Bacillus megaterium. *Biochemistry,* 7**,** 3676-3681.
GRUNDEL, M., SCHEUNEMANN, R., LOCKAU, W. & ZILLIGES, Y. 2012. Impaired glycogen synthesis causes metabolic overflow reactions and affects stress responses in the cyanobacterium Synechocystis sp. PCC 6803. *Microbiology,* 158**,** 3032-3043.
HAUF, W., SCHLEBUSCH, M., HUGE, J., KOPKA, J., HAGEMANN, M. & FORCHHAMMER, K. 2013. Metabolic Changes in Synechocystis PCC6803 upon Nitrogen-Starvation: Excess NADPH Sustains Polyhydroxybutyrate Accumulation. *Metabolites,* 3**,** 101-18.
HAUF, W., WATZER, B., ROOS, N., KLOTZ, A. & FORCHHAMMER, K. 2015. Photoautotrophic Polyhydroxybutyrate Granule Formation Is Regulated by Cyanobacterial Phasin PhaP in Synechocystis sp. Strain PCC 6803. *Appl Environ Microbiol,* 81**,** 4411-22.
HAYWOOD, G., ANDERSON, A., WILLIAMS, D., DAWES, E. & EWING, D. 1991. Accumulation of a Poly(hydroxyalkanoate) copolymer containing primarily 3-hydroxyvalerate from simple carbohydrate substrates by Rhodococcus sp. NCIMB 40126. *International journal of biological macromolecules,* 13**,** 83-8.
ISHII-HYAKUTAKE, M., MIZUNO, S. & TSUGE, T. 2018. Biosynthesis and Characteristics of Aromatic Polyhydroxyalkanoates. *Polymers,* 10**,** 1267.
JENDROSSEK, D. 2009. Polyhydroxyalkanoate granules are complex subcellular organelles (carbonosomes). *J Bacteriol,* 191**,** 3195-202.
JENDROSSEK, D. & HANDRICK, R. 2002. Microbial degradation of polyhydroxyalkanoates. *Annu Rev Microbiol,* 56**,** 403-32.

JENDROSSEK, D. & PFEIFFER, D. 2014. New insights in the formation of polyhydroxyalkanoate granules (carbonosomes) and novel functions of poly(3-hydroxybutyrate). *Environmental Microbiology,* 16**,** 2357-2373.

JONES, L. B., GHOSH, P., LEE, J. H., CHOU, C. N. & KUNZ, D. A. 2018. Linkage of the Nit1C gene cluster to bacterial cyanide assimilation as a nitrogen source. *Microbiology,* 164**,** 956-968.

KADOURI, D., BURDMAN, S., JURKEVITCH, E. & OKON, Y. 2002. Identification and isolation of genes involved in poly(beta-hydroxybutyrate) biosynthesis in Azospirillum brasilense and characterization of a phbC mutant. *Appl Environ Microbiol,* 68**,** 2943-9.

KADOURI, D., JURKEVITCH, E. & OKON, Y. 2003a. Involvement of the reserve material poly-beta-hydroxybutyrate in Azospirillum brasilense stress endurance and root colonization. *Appl Environ Microbiol,* 69**,** 3244-50.

KADOURI, D., JURKEVITCH, E. & OKON, Y. 2003b. Poly β-hydroxybutyrate depolymerase (PhaZ) in Azospirillum brasilense and characterization of a phaZ mutant. *Archives of Microbiology,* 180**,** 309-318.

KAEWBAI-NGAM, A., INCHAROENSAKDI, A. & MONSHUPANEE, T. 2016. Increased accumulation of polyhydroxybutyrate in divergent cyanobacteria under nutrient-deprived photoautotrophy: An efficient conversion of solar energy and carbon dioxide to polyhydroxybutyrate by Calothrix scytonemicola TISTR 8095. *Bioresour Technol,* 212**,** 342-347.

KALIA, V. C., LAL, S. & CHEEMA, S. 2007. Insight in to the phylogeny of polyhydroxyalkanoate biosynthesis: horizontal gene transfer. *Gene,* 389**,** 19-26.

KAVITHA, G., KURINJIMALAR, C., SIVAKUMAR, K., PALANI, P. & RENGASAMY, R. 2016. Biosynthesis, purification and characterization of polyhydroxybutyrate from Botryococcus braunii kutz. *Int J Biol Macromol,* 89**,** 700-6.

KLOTZ, A. & FORCHHAMMER, K. 2017. Glycogen, a major player for bacterial survival and awakening from dormancy. *Future microbiology,* 12.

KLOTZ, A., GEORG, J., BUČINSKÁ, L., WATANABE, S., REIMANN, V., JANUSZEWSKI, W., SOBOTKA, R., JENDROSSEK, D., HESS, W. & FORCHHAMMER, K. 2016. Awakening of a dormant cyanobacterium: Resuscitation of chlorotic cells reveals a genetically determined program. *Curr Biol,* In Press.

KÖBLER, C., SCHULTZ, S.-J., KOPP, D., VOIGT, K. & WILDE, A. 2018. The role of the Synechocystis sp. PCC 6803 homolog of the circadian clock output regulator RpaA in day–night transitions. *Molecular Microbiology,* 110**,** 847-861.

KOCH, M., BERENDZEN, K. W. & FORCHHAMMER, A. K. 2020a. On the Role and Production of Polyhydroxybutyrate (PHB) in the Cyanobacterium Synechocystis sp. PCC 6803. *Life (Basel),* 10.

KOCH, M., DOELLO, S., GUTEKUNST, K. & FORCHHAMMER, K. 2019. PHB is Produced from Glycogen Turn-over during Nitrogen Starvation in Synechocystis sp. PCC 6803. *International journal of molecular sciences,* 20**,** 1942.

KOCH, M. & FORCHHAMMER, K. 2020. Storage polymers in cyanobacteria: friend or foe? . *Cyanobacteria biotechnology,* Wiley.

KOCH, M., ORTHWEIN, T., ALFORD, J. T. & FORCHHAMMER, K. 2020b. The Slr0058 Protein From Synechocystis sp. PCC 6803 Is a Novel Regulatory Protein Involved in PHB Granule Formation. *Frontiers in microbiology,* 11**,** 809-809.

KUCHO, K., OKAMOTO, K., TSUCHIYA, Y., NOMURA, S., NANGO, M., KANEHISA, M. & ISHIURA, M. 2005. Global analysis of circadian expression in the cyanobacterium Synechocystis sp. strain PCC 6803. *J Bacteriol,* 187**,** 2190-9.

LEMOIGNE, M. 1926. Produit de déshydratation et de polymérisation de l'acide b-oxybutyrique. *Bull. Soc. Chim. Biol.,* 8:770-782.

MARTÍNEZ, V., JURKEVITCH, E., GARCÍA, J. L. & PRIETO, M. A. 2013. Reward for Bdellovibrio bacteriovorus for preying on a polyhydroxyalkanoate producer. *Environmental Microbiology,* 15**,** 1204-1215.

MEZZINA, M. P. & PETTINARI, M. J. 2016. Phasins, Multifaceted Polyhydroxyalkanoate Granule-Associated Proteins. *Applied and Environmental Microbiology,* 82**,** 5060-5067.

MIYAKE, M., KATAOKA, K., SHIRAI, M. & ASADA, Y. 1997. Control of poly-beta-hydroxybutyrate synthase mediated by acetyl phosphate in cyanobacteria. *Journal of Bacteriology,* 179**,** 5009-5013.

NOWROTH, V., MARQUART, L. & JENDROSSEK, D. 2016. Low temperature-induced viable but not culturable state of Ralstonia eutropha and its relationship to accumulated polyhydroxybutyrate. *FEMS microbiology letters,* 363**,** fnw249.

OBRUCA, S., SEDLACEK, P., SLANINOVA, E., FRITZ, I., DAFFERT, C., MEIXNER, K., SEDRLOVA, Z. & KOLLER, M. 2020. Novel unexpected functions of PHA granules. *Appl Microbiol Biotechnol,* 104**,** 4795-4810.

PANDA, B., JAIN, P., SHARMA, L. & MALLICK, N. 2006. Optimization of cultural and nutritional conditions for accumulation of poly-beta-hydroxybutyrate in Synechocystis sp. PCC 6803. *Bioresour Technol,* 97**,** 1296-301.

PFEIFFER, D. & JENDROSSEK, D. 2014. PhaM Is the Physiological Activator of Poly(3-Hydroxybutyrate) (PHB) Synthase (PhaC1) in Ralstonia eutropha. *Applied and Environmental Microbiology,* 80**,** 555-563.

POHLMANN, A., FRICKE, W. F., REINECKE, F., KUSIAN, B., LIESEGANG, H., CRAMM, R., EITINGER, T., EWERING, C., PÖTTER, M., SCHWARTZ, E., STRITTMATTER, A., VOß, I., GOTTSCHALK, G., STEINBÜCHEL, A., FRIEDRICH, B. & BOWIEN, B. 2006. Genome sequence of the bioplastic-producing "Knallgas" bacterium Ralstonia eutropha H16. *Nature Biotechnology,* 24**,** 1257-1262.

PRIETO, A., DE EUGENIO, L., GALÁN, B., LUENGO, J. & WITHOLT, B. 2007. Synthesis and Degradation of Polyhydroxyalkanoates.

PRIETO, A., ESCAPA, I. F., MARTINEZ, V., DINJASKI, N., HERENCIAS, C., DE LA PENA, F., TARAZONA, N. & REVELLES, O. 2016. A holistic view of polyhydroxyalkanoate metabolism in Pseudomonas putida. *Environ Microbiol,* 18**,** 341-57.

RABERG, M., VOIGT, B., HECKER, M. & STEINBÜCHEL, A. 2014. A Closer Look on the Polyhydroxybutyrate- (PHB-) Negative Phenotype of Ralstonia eutropha PHB-4. *PLOS ONE,* 9**,** e95907.

RATCLIFF, W. C. & DENISON, R. F. 2010. Individual-level bet hedging in the bacterium Sinorhizobium meliloti. *Curr Biol,* 20**,** 1740-4.

RIVERA-BRISO, A. L. & SERRANO-AROCA, Á. 2018. Poly(3-Hydroxybutyrate-co-3-Hydroxyvalerate): Enhancement Strategies for Advanced Applications. *Polymers,* 10**,** 732.

RUIZ, J. A., LOPEZ, N. I. & MENDEZ, B. S. 2004. rpoS gene expression in carbon-starved cultures of the Polyhydroxyalkanoate-accumulating species Pseudomonas oleovorans. *Curr Microbiol,* 48**,** 396-400.

SAHA, R., LIU, D., HOYNES-O'CONNOR, A., LIBERTON, M., YU, J., BHATTACHARYYA-PAKRASI, M., BALASSY, A., ZHANG, F., MOON, T. S., MARANAS, C. D. & PAKRASI, H. B. 2016. Diurnal Regulation of Cellular Processes in the Cyanobacterium Synechocystis sp. Strain PCC 6803: Insights from Transcriptomic, Fluxomic, and Physiological Analyses. *mBio,* 7.

SCHEMBRI, M. A., WOODS, A. A., BAYLY, R. C. & DAVIES, J. K. 1995. Identification of a 13-kDa protein associated with the polyhydroxyalkanoic acid granules from Acinetobacter spp. *FEMS Microbiol Lett,* 133**,** 277-83.

SCHLEBUSCH, M. & FORCHHAMMER, K. 2010. Requirement of the nitrogen starvation-induced protein Sll0783 for polyhydroxybutyrate accumulation in Synechocystis sp. strain PCC 6803. *Appl Environ Microbiol,* 76**,** 6101-7.

STAL, L. J. & MOEZELAAR, R. 1997. Fermentation in cyanobacteria1. *FEMS Microbiology Reviews,* 21**,** 179-211.

TIMM, A. & STEINBÜCHEL, A. 1990. Formation of polyesters consisting of medium-chain-length 3-hydroxyalkanoic acids from gluconate by Pseudomonas aeruginosa and other fluorescent pseudomonads. *Applied and Environmental Microbiology,* 56**,** 3360-3367.

TROSCHL, C., MEIXNER, K. & DROSG, B. 2017. Cyanobacterial PHA Production-Review of Recent Advances and a Summary of Three Years' Working Experience Running a Pilot Plant. *Bioengineering (Basel, Switzerland),* 4**,** 26.

VALAPPIL, S. P., MISRA, S. K., BOCCACCINI, A. R., KESHAVARZ, T., BUCKE, C. & ROY, I. 2007. Large-scale production and efficient recovery of PHB with desirable material properties, from the newly characterised Bacillus cereus SPV. *J Biotechnol,* 132**,** 251-8.

VAN DER WALLE, G. A., DE KONING, G. J., WEUSTHUIS, R. A. & EGGINK, G. 2001. Properties, modifications and applications of biopolyesters. *Adv Biochem Eng Biotechnol,* 71**,** 263-91.

VAN GEMERDEN, H. 1968. On the ATP generation by Chromatium in darkness. *Arch Mikrobiol,* 64**,** 118-24.

WANG, C., SHENG, X., EQUI, R., TRAINER, M., CHARLES, T. & SOBRAL, B. 2008. Influence of the Poly-3-Hydroxybutyrate (PHB) Granule-Associated Proteins (PhaP1 and PhaP2) on PHB Accumulation and Symbiotic Nitrogen Fixation in Sinorhizobium meliloti Rm1021. *Journal of bacteriology,* 189**,** 9050-6.

WARD, P. G. & O'CONNOR, K. E. 2005. Bacterial synthesis of polyhydroxyalkanoates containing aromatic and aliphatic monomers by Pseudomonas putida CA-3. *Int J Biol Macromol,* 35**,** 127-33.

WATZER, B. & FORCHHAMMER, K. 2018. Cyanophycin Synthesis Optimizes Nitrogen Utilization in the Unicellular Cyanobacterium Synechocystis sp. Strain PCC 6803. *Appl Environ Microbiol,* 84.

WILDE, E. 1962. Untersuchungen über Wachstum und Speicherstoffsynthese von Hydrogenomonas. *Archiv für Mikrobiologie,* 43**,** 109-137.

YORK, G. M., STUBBE, J. & SINSKEY, A. J. 2001. New Insight into the Role of the PhaP Phasin of Ralstonia eutropha in Promoting Synthesis of Polyhydroxybutyrate. *Journal of Bacteriology,* 183**,** 2394-2397.

YORK, G. M., STUBBE, J. & SINSKEY, A. J. 2002. The Ralstonia eutropha PhaR Protein Couples Synthesis of the PhaP Phasin to the Presence of Polyhydroxybutyrate in Cells and Promotes Polyhydroxybutyrate Production. *Journal of Bacteriology,* 184**,** 59-66.

ZHANG, H., LIU, Y., YAO, C., CAO, X., TIAN, J. & XUE, S. 2017. FabG can function as PhaB for poly-3-hydroxybutyrate biosynthesis in photosynthetic cyanobacteria Synechocystis sp. PCC 6803. *Bioengineered,* 8**,** 707-715.

ZHAO, Y., LI, H., QIN, L., WANG, H. & CHEN, G.-Q. 2007. Disruption of the polyhydroxyalkanoate synthase gene in Aeromonas hydrophila reduces its survival ability under stress conditions. *FEMS microbiology letters,* 276**,** 34-41.

X. Acknowledgements

Dear friends and colleagues,

Receiving a doctoral degree was a long and emotional journey. Along the way I was supported by numerous people, who I would like to thank at this point.

Foremost, my doctoral-father, Karl Forchhammer. "Giving me the opportunity to work on this project" is particularly true in my case, since I initiated the research idea of my PhD myself without any assigned financial grant at the beginning. I highly appreciate this opportunity and the trust in me at this very early stage of my scientific career. Although there were several phases where my PhD was stressful and frustrating, I feel very fortunate how well it turned out in the end. This is largely due to the expertise, endurance and motivation of Karl Forchhammer, which was always a great inspiration to me. I feel very, very thankful for all your support throughout the years!

Then of course, my second supervisor, Dieter Jendrossek. It was a great coincidence that such an established expert in the field of PHB happened to live in Tübingen and happily supported me throughout my entire PhD. I still remember how we sat in your garden and discussed first projects ideas of my PhD. Thank you for your continuous support and your expertise whenever it was needed!

Next, someone, without all of this would not be possible: the Studienstiftung (including: all taxpayers). I feel very fortunate to live in a country where we have such institutions. Although many people were surprised that I wanted to get funded by a scholarship without any social security payments, I never regret this step. Meeting all those bright, inspiring people shaped me in many different ways. I feel very fortunate that I had the opportunity to spend four years of my life trying to investigate something I was truly fascinated about. This intellectual freedom would not have been possible without the Studienstiftung.

During my PhD I had the pleasure to supervise three motivated bachelor- and master students (some even twice). I would like to thank you, Tim, Janette and Anna-Lena, for your productive work, which even ended up in a publication. Furthermore, I would like to thank our technicians, especially Andi, Eva and Claudia, as well as Carmen and Mr. and Mrs. Lemaire for their help throughout the years. Also, Michaela for her positive attitude and her helpfulness with all sorts of bureaucratic problems.

Additionally, all lab members of the working group Forchhammer and Maldener (including the older generations) for their support whenever necessary. Especially: Niels, Sofia and Björn, who were a loyal company throughout the years. I would like to point out Björn for giving me advice for my thesis.

I also want to thank my previous mentors, who guided me through the sometimes confusing world of science: Aaron Kaplan for introducing me to the world of cyanobacteria, Jan Lüddecke for his expertise in molecular biology, as well as Paul Hudson for his curiosity to discover new concepts.

Thanks to all my friends in near and far for their support to ensure my mental and physical well-being.

Finally, my family, Trudi, Thomas, Jonas and Aaron, as well as Kathrin, for their long-lasting support enabling me to be in this fortunate situation in which I am today.

Danke!